8-2019

Isentropic Efficiency and Theoretical Analysis of the Planetary Rotor Expander

Joseph L. James
Utah State University

ISENTROPIC EFFICIENCY AND THEORETICAL ANALYSIS OF THE PLANETARY ROTOR EXPANDER

by

Joseph L. James

A thesis submitted in partial fulfillment
of the requirements for the degree

of

MASTER OF SCIENCE

in

Mechanical Engineering

Approved:

_____	_____
Geordie Richards, Ph.D. Major Professor	Stephen Whitmore, Ph.D. Committee Member
_____	_____
David Geller, Ph.D. Committee Member	Richard S. Inouye, Ph.D. Vice Provost for Graduate Studies

UTAH STATE UNIVERSITY
Logan, Utah

2019

ABSTRACT

Isentropic Efficiency and Theoretical Analysis of the Planetary Rotor Type Expander

by

Joseph L. James, Master of Science

Utah State University, 2019

Major Professor: Dr. Geordie Richards
Department: Mechanical and Aerospace Engineering

Expanders allow pressurized fluids to undergo a pressure reduction in a controlled volume to extract fluid energy. The energy is converted to mechanical work used to drive a generator. This thesis derives the isentropic efficiency of a planetary rotor expander (PRE), a century-old design undeveloped due to insufficient manufacturing capabilities (until recently). The PRE is advantageous in industrial applications where high pressures, large and mixed flows, and aggressive media is used. The PRE's design is intrinsically self-cleaning making it ideal for flows that leave deposits or ice during operation. These conditions are commonly found in the oil and gas, chemical, energy, and municipal markets, where it is difficult to implement a traditional volumetric expander such as a twin screw or scroll design. This thesis develops a theoretical model to compute the isentropic efficiency of the PRE as a function of its design variables for specific applications in these harsh environments. The independent design variables are the PRE rotor height, machine radius, rotor tip radius, and machine rotational frequency. A geometric analysis is completed to model the cavity mass flowrate, and leakage flowrate, in

order to calculate the PRE's isentropic efficiency. Calculations are performed using real gas analysis, which requires a multi-level iterative solver approach. In addition to modeling the PRE's efficiencies for different rotor sizes and speed, this thesis identifies design specifications capable of maximizing isentropic efficiency. The thesis presents two primary applications in industry where the calculation methods are different. The first application has a target power objective where the user seeks to match a required electrical load provided by the expander. For this application, the solution can be analytically solved, and we show that the optimal efficiency is achieved by minimizing the PRE mass flowrate. The second application is total energy recovery, where the user seeks to maximize power output of a flow while maintaining a mass flowrate driven by the flow requirements. The energy recovery application gives a mass flowrate as a constraint and cannot be solved analytically. An objective solver is developed along with the real gas iterative solver to converge to an optimized machine size and rotational speed.

(147 pages)

PUBLIC ABSTRACT

Isentropic Efficiency and Theoretical Analysis of the Planetary Rotor Type Expander

Joseph L. James

Expanders allow pressurized fluids to undergo a pressure decrease in a controlled environment via volumetric growth to extract fluid energy. There are many types of expanders, and the objective of this thesis is to model the efficiencies of the planetary rotor expander (PRE), a century-old design undeveloped due to insufficient manufacturing capabilities (until recently). Geometric relationships are derived and mathematical models are generated to determine the efficiency of the PRE as a function of design variables. Two industrially relevant case studies show that, to maximize isentropic efficiency, the planetary rotor expander (PRE) rotational frequency is maximized and rotor geometry optimized.

ACKNOWLEDGMENTS

I thank and dedicate this thesis to my wife Amy, and kids Bailey and Emmett for their patience. Thanks to Helidyne for inviting me to learn about such a unique machine. To Dr. Mikellides for employing the swim or die teaching method, where hard work was the only way not to drown. Finally, thanks to Dr. Geordie Richards, especially for supporting me when it was needed most.

Joseph L. James

CONTENTS

LIST OF FIGURES

Figure

LIST OF VARIABLES

$\dot{m}_{leak}$ = total leakage mass flowrate

$\dot{m}_{tot}$ = total system mass flowrate

$T^*_{helix}(h)$ = instantaneous number of helical twists

$\dot{V}_{cav.net}$ = net rotor cavity flowrate

$\dot{V}_{CSLeakage}$ = volumetric flowrate of the convex superellipse core leakage

$\dot{V}_{CynLeakage}$ = cylindrical core leakage flowrate

$\widetilde{V}_t$ = throat average velocity (Mach = 1 for choke conditions only)

$\dot{V}_{t.gapleak}$ = instantaneous gap leakage flowrate, time dependent

$\dot{V}_{tot.gapleak}$ = total PRE rotor gap leakage flowrate

$\dot{V}_{tot.leak}$ = total expander leakage

$\dot{w}_{exhaust}$ = power exiting the system

$\dot{w}_{shaft}$ = PRE shaft power

$\dot{w}_{system}$ = total available power (system power inlet, state 1)

$A_{Cav.sin}$ = maximum cavity cross sectional area minus the void area

A_{Core} = generic core area, either $A_{CylCore}$ or A_{CSCore}

A_{CSCore} = cross sectional area of a convex superellipse core

$A_{CSLeakage}$ = leakage cross sectional area when using a convex superellipse core

$A_{CylCore}$ = area of a cylindrical core

$A_{CynLeakage}$ =cross sectional leakage area when using a cylindrical core

A_D = area of a circle with a rotor diameter D

A_g = descriptive area used to calculate A_{CSCore}

$A_{gap}(t)$ = instantaneous total rotor gap area of all rotors

A_{gap} = total gap area between rotors

A_L = area of a square with a side length L

$A_{Sector\Delta}$ = descriptive area used to calculate A_{CSCore}

A_{Void} = total void area

A_y = descriptive area used to calculate A_{CSCore}

E_{mass} = expander mass efficiency (or mass flowrate efficiency)

E_{system} = system efficiency

h_1 = state 1 specific enthalpy

$h_{3,Isentropic}$ = state 3 isentropic specific enthalpy

J_1 = R1 junction width

J_2 = R1 junction length

L_{helix} = total gap coil length

M_t = Mach number at the throat

P_0 = cavity flow field stagnation pressure

P_2 = state 2 pressure

P_3 = state 3 pressure

P_t = throat fluid pressure

R_1 = rotor tip radius

R_2 = rotor girth radius

R_3 = rotor nose length

R_4 = rotor waist length

R_5 = machine center to rotor radius

R_g = process fluid specific gas constant

T_{helix} = number of twists contained within rotor height H (.5 for the PRE)

T_t = throat fluid temperature

$V_{cav.net}$ = net rotor cavity volume (total cavity volume minus the core volume)

$V_{cav.sin}$ = rotor cavity volume minus the void volume ($H \cdot A_{void}$)

$V_{cav.tot}$ = total rotor cavity volume

V_{Core} = generic core volume, either $V_{CylCore}$ or V_{CSCore} , same for $\dot{V}_{Core.Leakage}$

$V_{CSCore} = H \cdot A_{CSCore}$ = volume of a convex superellipse core in a full rotor cavity

$V_{cyl.gapleak}$ = total volume of fluid leaked during one cycle

$V_{CylCore} = H \cdot A_{CylCore}$ = volume of a cylindrical core within a full rotor cavity

γ_t = throat specific heat ratio

ρ_2 = state 2 density

ρ_t =throat density at leakage points

D = rotor diameter

E = machine radius

G = prescribed rotor gap clearance

h = instantaneous axial height of cycle

H = rotor height

ƒ = PRE frequency of rotation

L = rotor center to center length

S = R1 and R2 center radius

t = time

θ = angle of rotor twist

ACRONYMS/NOTATIONS

PRE – Planetary Rotor Expander

NG – Natural Gas

NGL – Natural Gas Liquid

STP – Standard Temperature and Pressure

CAD – Computer-aided Design

CSE – Convex Superellipse

MMSCFD – Million Standard Cubic Feet per Day

I. INTRODUCTION

1.1 DESCRIPTION OF EXPANDERS AND THE PRE

This thesis presents a theoretical isentropic efficiency analysis of the planetary rotor expander (PRE). It discusses the effects of rotor size and rotor speed on three different system states and determines system isentropic efficiency. The models also provide the optimization process for design towards specific applications. First, it is important to understand the general workings of expanders.

An expander is a mechanical device that reduces fluid pressure in a controlled environment to extract fluid energy. Pneumatic and hydraulic pressurized fluids contain energy typically used to transport energy or the fluid itself from one location to another. When an industrial process requires, fluid pressure is reduced by either a throttling valve or expander. Using a throttle valve is an isenthalpic process where fluid energy is not used [1]. This increases entropy and thus wastes energy. Throttling the pressure through an expander captures energy from the fluid increasing overall system efficiency. This is preferred as the desired exhaust pressure is still reached but converts energy from the pressure drop to available mechanical work. The dependent variable introduced when using an expander is downstream temperature, which will decrease as the expander extracts fluid energy from the flow.

A common example where an expander might be of use is a typical natural gas (NG) “wellhead to customer” process. Many pressure drops exist within the process where an expander can recover a percentage of the energy which would typically be wasted. The end of the process before the NG arrives to the customer is the city gate station (see Figure 1). These pressure drops have the potential to generate 100 to 500 kW of power [2], each enough to power

approximately 360 homes. Note that this is just an example of many types of industrial pressure drops that occur.

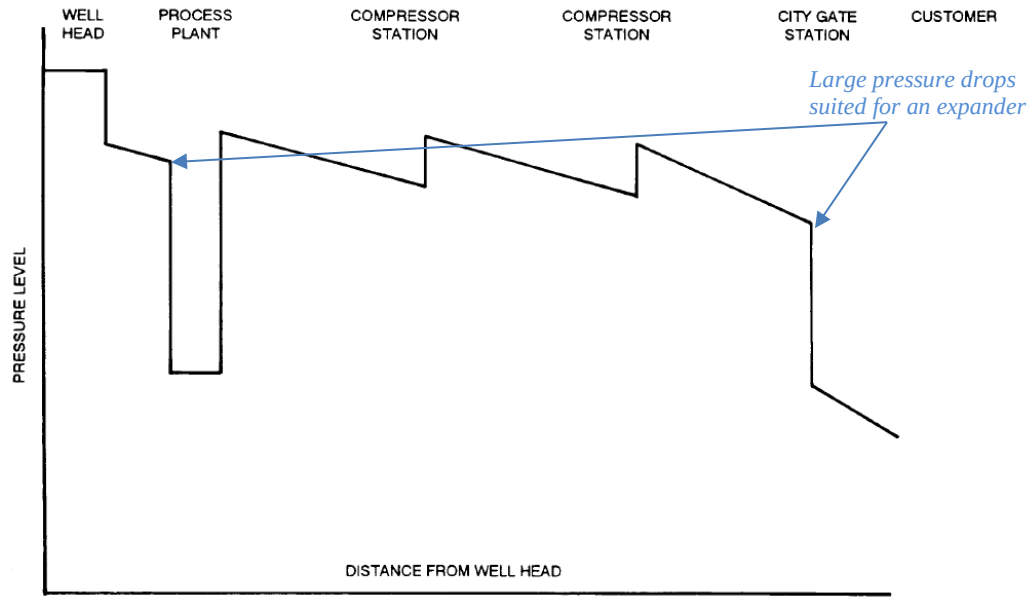

Figure 1: Natural Gas Process [2]

Expanders have two possible primary roles that depend on the application. First, the pressure reduction can be used to drive machinery via the available shaft power produced by an enthalpy reduction of the flow (i.e. electric generator, heater). Second, expanders can reduce the fluid's exhaust temperature lower than what the Joule-Thompson effect would supply. This is advantageous for industries requiring colder temperatures like refrigeration equipment or gas liquefaction of raw wellhead gas in the oil industry. Both roles seek to maximize the change in enthalpy but provide different by-products for the primary function. One application needs shaft power from a pressure let down of which the by-product is a colder downstream temperature, and the other needs a colder downstream temperature of which the by-product is shaft power. It is important to note that an expander does not need to be coupled to a generator, but some source

of resistance is needed for the enthalpy change to occur. An oil break, resistive gear box, or fan could be used as well.

Different types of expanders exist for various applications and are typically referred to as turbo-expanders. They can be separated into two major groups; turbines and volumetric expanders. Figure 2 shows the family tree of typical turbo-expanders. Many applications exist where the proper expander needs to be specified. No expander is suited for all applications [3]. Note that the PRE, if included in the family tree, would reside with the volumetric expanders.

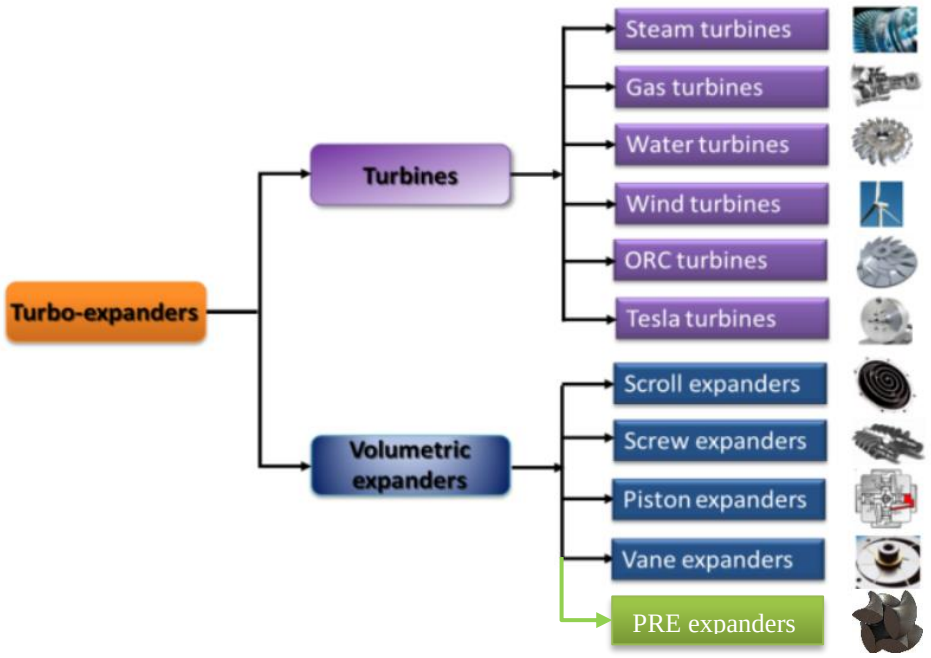

Figure 2: Turbo-expander types, adapted from [3]

Each expander type has its benefits and limitations. Turbines are generally the most efficient but require controlled conditions such as closed systems or clean working fluids. Also, the cost of turbines starts to become economically unviable under 500 kW [2]. A scroll and twin screw for example are low cost to manufacture and a proven design. However, due to their

geometry they have a maximum working pressure of 400-600 psi [4]. They are also prone to seizing if the fluid is not relatively clean. Reciprocating expanders can handle high pressures and flows, but malfunction when liquids are present in the process fluid [4].

The PRE expander falls under the volumetric expanders group and allows for expander use in industrial applications which requires a robust machine. Potentially, the PRE can handle pressure up to 2000+ psi, flows 10+ MMSCFD, mixed flows, and economical to manufacture for the intended use in industrial applications. Processing the fluid on the inside of the rotors allows for a robust rotor design to combat cyclic failure, one of the primary failure modes for expanders [5]. The PRE also has a self-cleaning behavior as each rotor sweeps past the adjacent rotor (each rotor spins the same direction) removing build up or debris.

This thesis analyzes system isentropic efficiency of the PRE, which has not been formally and publicly documented to date, in contrast to other type of expanders [6, 7, 8, 9, 10]. The PRE is a positive displacement expander with a one-to-one ratio, or with the installation of a metering valve can process a range of ratios determined solely on the timing of the valve. Note that this thesis does not consider the implementation of a metering valve (operation similar to a roots blower) to simplify the efficiency derivation. The mathematical models presented in this thesis should be proven out empirically, and after this is accomplished, one could apply a metering valve to achieve higher pressure ratios.

Rotors of the PRE (3 or 4 rotor configuration) are designed with a helical twist that meshes with an adjoining rotor when assembled together. The rotors turn the same direction, and as they do, a cavity inside the rotor mesh will grow and shrink through the rotation of the rotors. This passes a “packet” of fluid during operation, reducing its pressure and extracting energy. Figure 3 shows the geometry of the packet.

Figure 3 also shows a conceptual PRE design with a 4-rotor configuration and transparent containment vessel. The fluid enters through the top flange to be processed by the rotors. After fluid energy has been extracted from the fluid, it exhausts through the back side of the rotors an through the rotor windows out the bottom flange. All four rotors turn the drive assembly, and the drive assembly tranfers the power from the 4 rotors to a single ouput shaft coupled to a resistance device (i.e. generator via magnetic coupler).

During operation, the inlet of the rotors is always open to the gas source maintaining a constant cavity pressure. After turning half a cycle, the inlet starts to close. At the end of the cycle, the cavity completely encloses the fluid in the cavity. The rotors then open on the backside exhausting the fluid. As the leading packet of fluid is being exhausted, the following packet is entering on the front end creating two power cycles per rotor revolution.

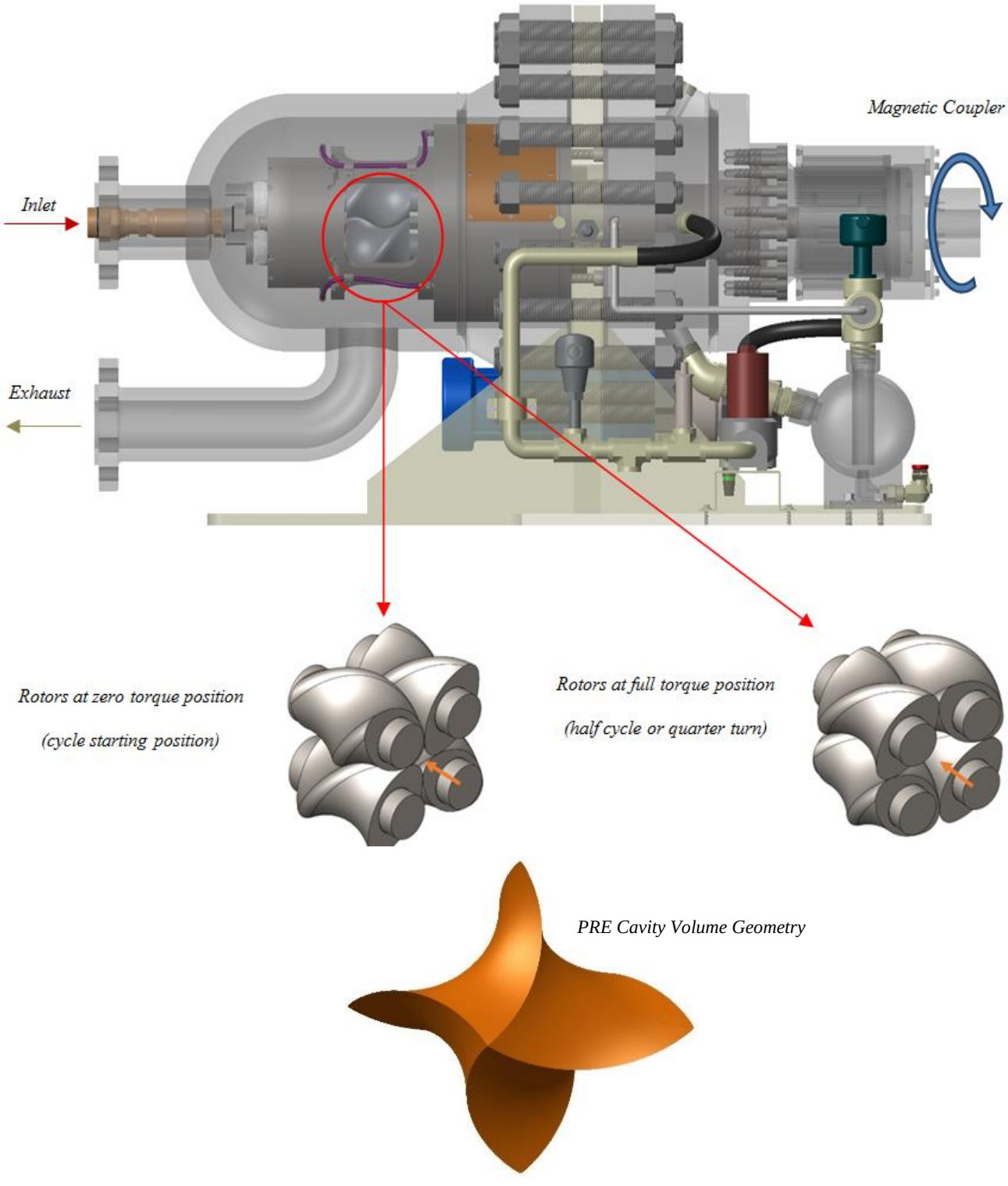

Figure 3: Packaged 4-rotor configured PRE design and cavity volume

1.2 HISTORY OF THE PRE

The PRE was first patented in 1902 by Thomas S. Colbourne (patent US710756A). His design consisted of 4 straight rotors and were linked using timing gears. In 1946, Rudolf D. Delamere designed a helical rotor and also conceived a 3 rotor configuration (patent DE102014001954A1). The 3 rotor PRE has a smaller cavity but larger rotors for the same machine envelope which is ideal for high pressure (2000 psi +) and low flows (larger rotor diameter for strength equals smaller cavity). Many patents were filed in the 20th century employing different configurations of the PRE including making it into an internal combustion engine, matrix array configuration, and multiple cavity rotors (see Figure 4). No prototype PRE has been reported to have been built until 2013 when a company called Helidyne constructed several 4-rotor PREs and tested them using various fluids. A preliminary analysis was performed by Jack Kerlin, co-founder of Helidyne, from 2008-2013 using ideal fluid computations. It is important to note that this thesis would not be possible without the groundwork laid by Helidyne. The cavity volume equation, rotor gap area, and preliminary rotor profile relationships were built by the Helidyne team. This thesis continues that analysis of the PRE by investigating results using real fluids computations, implementing true choked flow parameters (stagnation pressure analysis), deriving the core leakage equations, combining multiple process stages for total system efficiency computations, and finally optimizing isentropic efficiency from the derived equations.

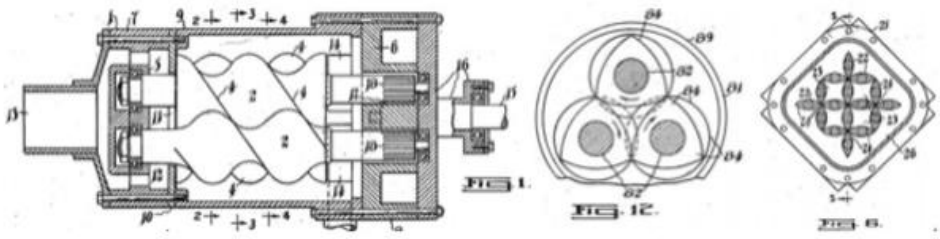

Figure 4: Patent designs of different theoretical improvements to the PRE

1.3 DESCRIPTION OF APPLICATIONS

This thesis optimizes rotor geometry and rotation frequency to maximize system efficiency, but system efficiency is dependent on the application which drives the selection of rotor geometry. Two different application types will be the focus of the optimization process, and case studies presented later (see chapter 3). These application types are paramount in analyzing rotor and system efficiency as they will determine machine size and speed.

The first application will be known as an "Energy Recovery" application. This type of system seeks to maximize power output of the expander by matching the mass flowrate required by the source. There are three fluid states in this application's system (see Figure 5 for a system description). State 1 is the upstream source where the pressure and temperature are known. State 2 is the inlet directly into the PRE and is also considered the state inside the rotor cavity. The changes from state 1 to state 2 are caused by the dynamic function of the PRE and upstream components (most applications implementing a control valve). A pressure drop will naturally occur in the piping network as the PRE operates and is dependent on plumbing geometry and flowrate of the expander. In this application, it is desired to minimize any upstream pressure drop as this increases state 2 fluid entropy and energy waste, but upstream expansion is expected depending on the flowrate of the PRE. State 3 exhausts into the downstream piping network of which the pressure is known. The temperature immediately downstream of the PRE is determined by PRE efficiency and is one of the dependent fluid process variables.

An example of this application is a large natural gas (NG) distribution company seeking to recover fluid energy from a letdown station. This is the case previously presented in section 1.1. High pressure networks (1000 psi+) are used to transport NG throughout the state. This pressure must be reduced to approximately 45 psi before entering an industrial use network

within a city. An Expander in place of a throttling valve would recover part of the energy used to charge the main distribution network and would follow an Energy Recovery model. Flow rate would be determined by the city's NG consumption, and the expander's size/speed would be optimized to match.

A similar application would be for oil wells seeking to increase the natural gas liquids (NGL) dropped out at the wellhead. Wellhead natural gas needs to remove the heavy hydrocarbons (C2 through C10) before it can be used as commercial grade NG. Decreasing the temperature changes the phase of the heavy constituents to a liquid mixture that can be separated from the gaseous NG. The colder the fluid temperature, the higher percentage of NGL is dropped out and less processing is needed later. A PRE in place of an expansion valve (which relies on the Joule-Thomson effect) in the refrigeration cycle would reduce the fluid temperature further with the byproduct being available shaft power. In this system, the PRE would be sized to match the wellhead NG flowrate. Peak system efficiency would be characterized as minimizing fluid power exiting the system and maximize PRE power output.

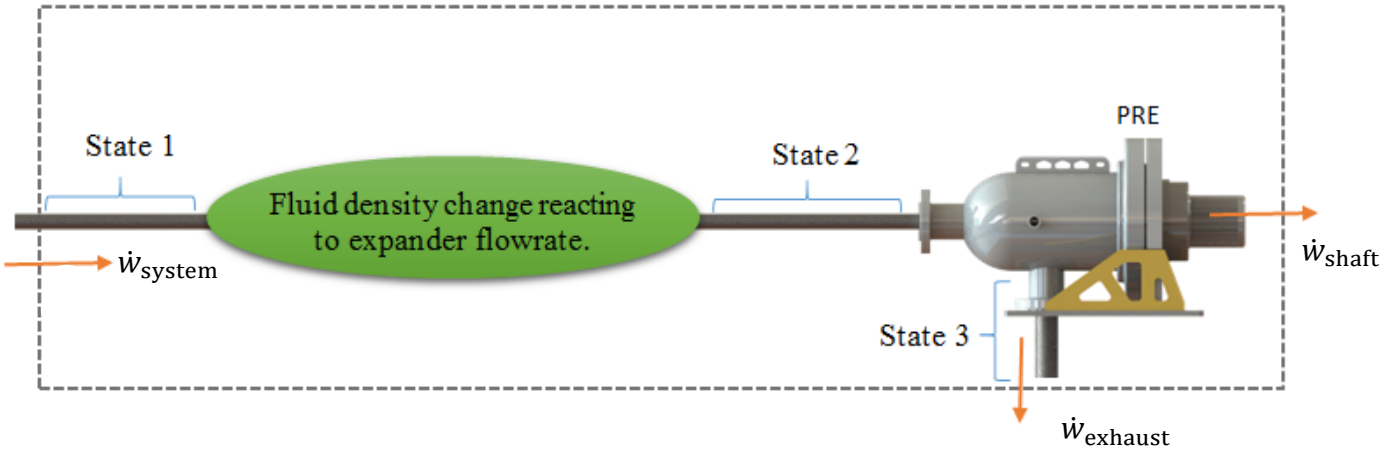

Figure 5: Energy Recovery System

$$\dot{w}_{\text{shaft}} = \dot{w}_{\text{system}} - \dot{w}_{\text{exhaust}} \quad (1)$$

Where:

$\dot{w}_{\text{exhaust}}$ = power exiting the system

$\dot{w}_{\text{system}}$ = total available power (system power inlet, state 1)

$\dot{w}_{\text{shaft}}$ = PRE shaft power

The second application type will be called a "Target Power" application. This system is designed to supply power dependent on a load requirement. There are three fluid states within this system type (see Figure 6 for a system description). State 1 is the upstream source where the upstream pressure and temperature are known. State 2 is the inlet directly into the PRE including the PRE cavity. State 2 is controlled by a control valve in-between state 1 and 2. This control valve regulates state 2's pressure to control the output shaft power of the PRE. State 3 exhausts into the downstream piping network of which the pressure is known. The temperature immediately downstream of the PRE is determined by PRE efficiency and control valve pressure drop.

An example of a Target Power application would be an offshore oil platform looking to replace diesel power generation sets. Using the high and low pressure ocean floor piping network previously installed (typically to run equipment and charged by an onshore turbine compressor), the PRE would utilize high pressure gas and exhaust into the low pressure pipe network to produce power. These platforms use a specific amount of power depending on which machines are in use and the PRE must have a power output to match (controlled by the control valve).

Maximum system efficiency for this application is characterized as minimizing the system mass flowrate while maintaining the required shaft power output.

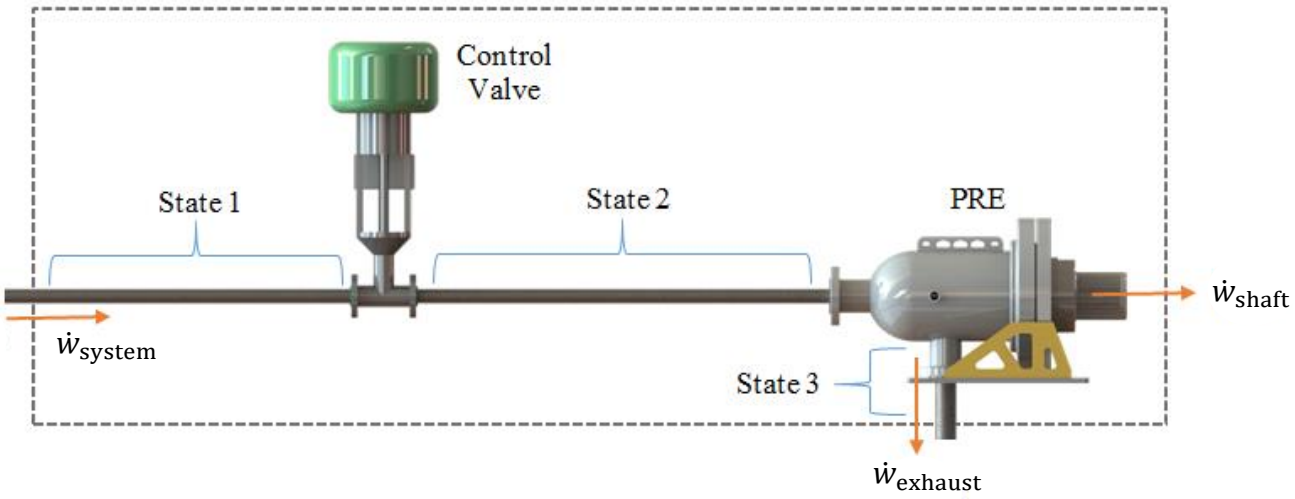

Figure 6: Target Power System

1.4 DERIVATION ASSUMPTIONS

This thesis isolates rotor geometry and rotor speed to provide a focused analysis of their effects on PRE isentropic efficiency. This study ignores parasitic losses within the system since they are either independent of rotor geometry and speed or have relatively negligible influence when assessing rotor geometry and speed. This is not to say that they are negligible to the system as these parasitic losses could consume a significant amount of power if not addressed. The following is a list of systems that would potentially alter overall system efficiency. These items are not included in this analysis, but their existence should be noted:

Ignored Parasitic Losses (for reference)

- Bearing oil pressure pumps
- Generator efficiency
- Instrumentation gas consumption
- Piping elevation change
- Bearing drag
- Auxiliary/Power electronics
- Transfer case efficiency
- Magnetic coupler/ Drivetrain
- Upstream Head loss

System Assumptions/Declarations

- Steady State $\left(\dot{m}_{system\ in} = \dot{m}_{system\ out}\right)$
- Adiabatic system $(0\ heat\ exchange\ with\ enviroment\ )$
- Fluid is non-compressible $(V < mach\ .3)$, except at leak points
- Convergence to leak point throats is isentropic
- Stagnation pressure and inside the cavity is assumed to equal the state 2 pressure.
- All pressures are in absolute and all flows are actual (opposed to standard).

EFFICIENCY DEFINITIONS

Mass efficiency will be defined as the cavity mass flowrate divided by total mass flowrate. Cavity mass flowrate is determined by cavity volume and rate of rotation combined with state 2 density. Total mass flowrate is the summation of cavity mass flowrate and cavity leakage mass flow rate (see equation 2). Mass efficiency is calculated in the case studies presented later, but is not needed to determine isentropic efficiency. It is simply noted to demonstrate maximized mass efficiency will not yield maximized isentropic efficiency. Note that leakage parameters are discussed in section 2.2,

$$E_{mass} = \frac{\dot{m}_{cav.net}}{\dot{m}_{tot}} = \frac{\dot{m}_{cav.net}}{\dot{m}_{cav.net} + \dot{m}_{leak}} = \frac{\rho_2 \cdot \dot{V}_{cav.net}}{\rho_2 \cdot \dot{V}_{cav.net} + \rho_t \cdot \dot{V}_{tot.leak}} \quad (2)$$

Where:

E_{mass} = expander mass efficiency (or mass flowrate efficiency)

$\dot{V}_{tot.leak}$ = total expander leakage

$\dot{V}_{cav.net}$ = net rotor cavity flowrate

ρ_2 = state 2 density

ρ_t =throat density at leakage points

$\dot{m}_{tot}$ = total system mass flowrate

$\dot{m}_{leak}$ = total leakage mass flowrate

System isentropic efficiency will be defined as the PRE shaft power (total expander extracted power) divided by total available power flowing into the system (ideal isentropic fluid power) [1],

$$E_{system} = \frac{\dot{w}_{shaft}}{\dot{w}_{system}}, \tag{3}$$

$$\dot{w}_{system} = \dot{m}_{tot}(h_1 - h_{3,Isentropic}), \tag{4}$$

where:

E_{system} = system efficiency

h_1 = state 1 specific enthalpy

$h_{3,Isentropic}$ = state 3 isentropic specific enthalpy

When assessing the two application types, equation 3 will change focus. In an energy recovery application, the system power is constant and the PRE shaft power alters when changing rotor geometry and speed. The opposite is true for a target power application where the PRE shaft power is held constant and changing rotor geometry and speed alters the system power. This difference in focus will drive a change in strategy when sizing a PRE for either application. This will be shown in the case studies.

As mentioned, the PRE analyzed in this thesis contains no metering valve into the rotor cavity. This allows a standard hydraulic power equation to be used to calculate shaft power using cavity pressure (state 2) and PRE flowrate. This is of course not ideal when using a process fluid in the gaseous state because expansive energy is not used in a hydraulic configuration. A metering valve creating higher pressure ratios involves another thermodynamic analysis that is

outside the scope of this thesis. When calculating shaft power of a one-to-one PRE, the following equation will be used [1],

$$\dot{w}_{shaft} = \dot{V}_{cav.net} \cdot (P_2 - P_3)\,, \tag{5}$$

where:

P_2 = state 2 pressure

P_3 = state 3 pressure

Equation 5 will be used to solve equations 3 and 4 according to the application being analyzed. For an energy recovery application, total mass flowrate $\dot{m}_{tot}$ is known and used to calculate state 2 pressure (and thus output power). However, this cannot be analytically solved due to the coupled nature of mass flowrate and state 2 pressure. An objective based solver is used to iterate the state 2 pressure until the total mass flowrate constraint is met. This is shown in the case studies. Output power is then used to calculate isentropic efficiency E_{system} (equation 3).

For a target power application, shaft power $\dot{w}_{shaft}$ is known, and rotor geometry/rotor speed will determine total mass flowrate $\dot{m}_{tot}$ in equation 4. This can be analytically solved because state 2 pressure is obtained directly from equation 5. Note that cavity volumetric flowrate $\dot{V}_{cav.net}$ is calculated by the product of cavity volume (packet volume) and PRE rotational speed. The final isentropic efficiency is calculated by using equations 3, 4, and 5 yielding

$$E_{system} = \frac{\dot{V}_{cav.net} \cdot (P_2 - P_3)}{\dot{m}_{tot}(h_1 - h_{3,Isentropic})}\,. \tag{6}$$

II. ISENTROPIC EFFICIENCY DERIVATION

The root of this thesis is a geometric analysis and optimization of the rotors so PRE performance can be predicted. The first task will be to map the rotor's geometry and derive geometric relationships. This reduces the geometric independent variables to three linear dimensions from which the entire rotor can be geometrically described.

After the rotors can be mathematically described, volumetric and mass flowrates are derived. This is completed by identifying all leak sources within the rotor mesh. After all leak flowrates have been identified, leak location densities are calculated to yield the mass flowrate at the leak points (using compressible flow analysis). The rotor cavity volume, density at state 2, and PRE rotational frequency yields the cavity mass flowrate. These two mass flowrates yield the total mass flowrate.

After the flowrates have been derived, several case studies are presented. These case studies use the derived isentropic efficiency equation to optimize PRE rotor size and speed in various scenarios. The system states 1 through 3 illustrated in Figure 5 and Figure 6 will be the systems used in these case studies and figures used for reference.

2.1 ROTOR GEOMETRY

A PRE rotor is constructed by taking the cross sectional rotor profile and helically extruding the profile through its height. There are three primary, independent variables from which all other rotor geometries are derived, which are machine radius E, tip radius R1, and rotor height H. Machine radius E represents the distance from the assembled machine centroid to outermost rotor tip but is also used as the basis for PRE radial size and an independent variable for all PRE geometry. Tip radius R1 is simply the radius of the rotor tip but affects rotor performance and strength. Rotor height H is as its description implies, the face to face distance of each rotor.

The PRE rotor profile is created by intersecting two circles each with a girth radius R2. The "lens" profile is created by rounding the tips with a tip radius R1 and 90 degree arc. Both circles with radii R1 and R2 are centered on a circle with center radius S (equally spaced, 90 degree interval), which itself is centered on the profile centroid. These three constraints fully define S, requiring only R1 and R2 to be known to generate the rotor profile. Note that girth radius R2 is a function of tip radius R1 and machine radius E (see Figure 7). After the rotor profile has been generated, it's then helically extruded through rotor height H. The pitch of a standard PRE rotor is equal to 0.5 revolutions per rotor height H.

Again, the rotor geometry uniquely processes the high pressure fluid on the inside of the rotors instead of outside like a conventional twin screw. This allows the rotors to flex without seizing in high pressure applications. The geometric relationships create continuous tangency from rotor to rotor maintaining a closed internal cavity volume as the rotors turn. This coupled with the rotors having the same direction of spin, creates relative motion rotor to rotor in close proximity. This allows the rotors to be self-cleaning against deposits and ice.

More variables identified with their specific uses are listed in equations 7 to 15. Figure 7 shows the rotor profile generation. Figure 8 shows a summary of the rotor's profile dimensions and assembled dimensions. Note these dimensions and this thesis only discuss a 2 lobed, 4 rotor PRE. Dimensions for a 3 lobed 3 rotor PRE are excluded.

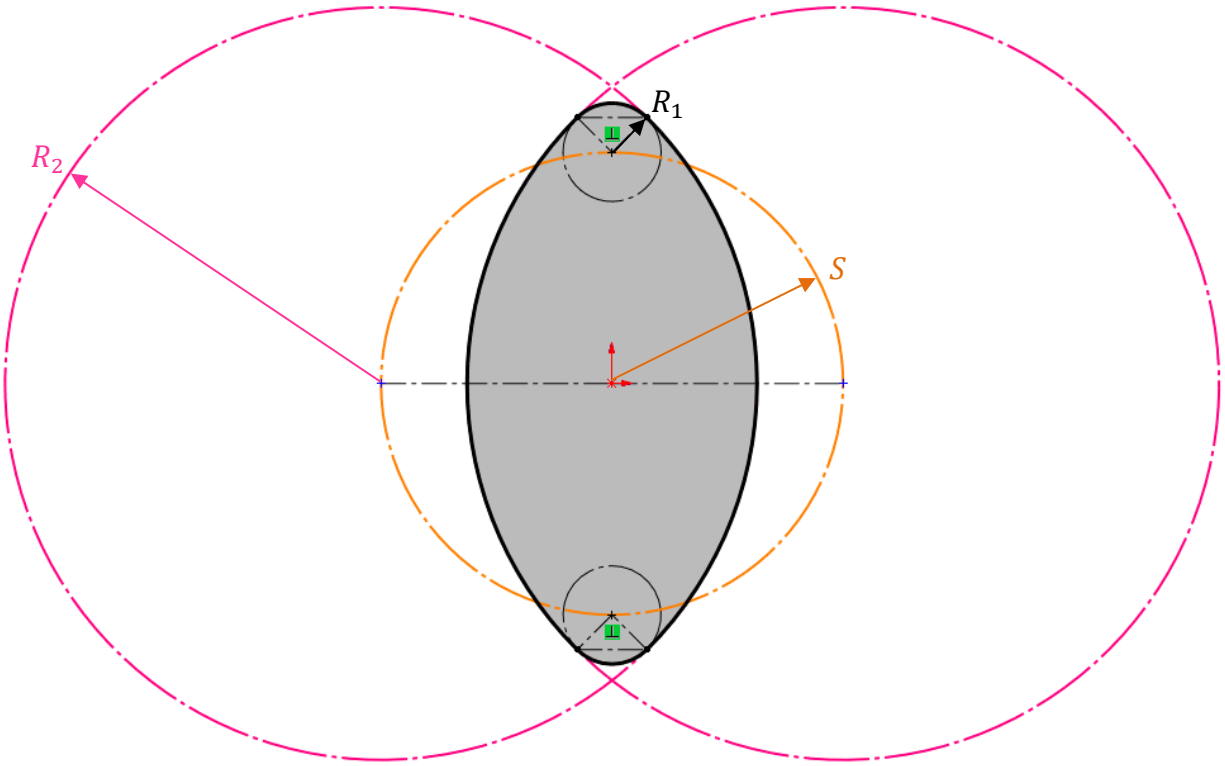

Figure 7: Rotor Profile

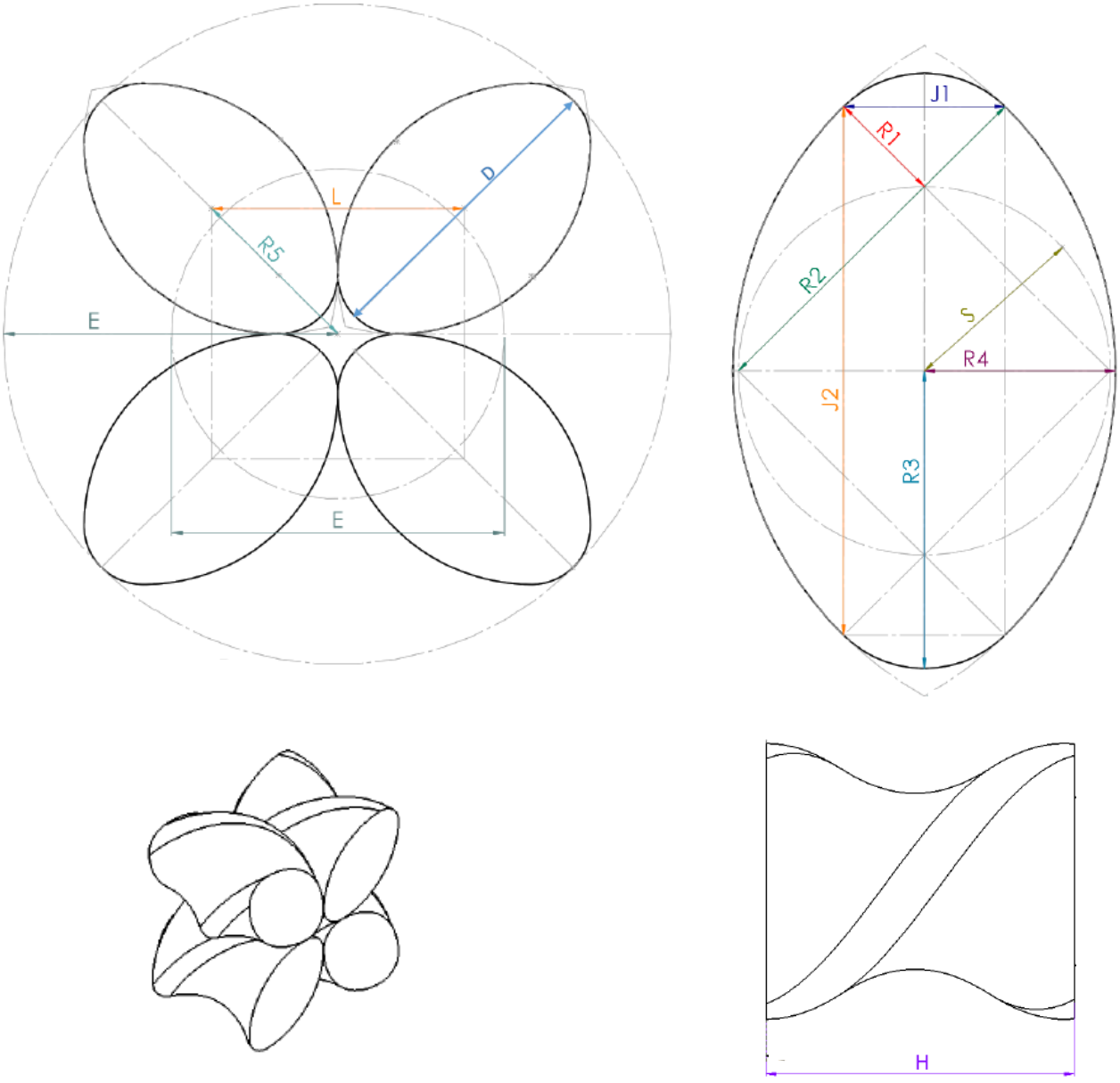

Figure 8: Rotor Dimensions

Machine Radius

Selected by user

$$E = \text{Independent Variable}$$

Tip Radius

Selected by user

$$R_1 = \text{Independent Variable}$$

Rotor Height

Selected by user

$$H = \text{Independent Variable}$$

Girth Radius

Used to generate rotor profile

$$R_2 = L - R_1 = \frac{E - R_1}{\sqrt{2}} \tag{7}$$

Nose Length

Used for radial load area, see appendices

$$R_3 = S + R_1 = \frac{E - R_1(\sqrt{2} - 1)}{2} \tag{8}$$

Waist Length

Used for radial load area, see appendices

$$R_4 = R_2 - S = \frac{E(\sqrt{2} - 1) + R_1}{2} \tag{9}$$

Machine Center to Rotor Center Radius

Center radius for 4 rotors equally spaced and assembled together

$$R_5 = \frac{L}{\sqrt{2}} = \frac{E + R_1(\sqrt{2} - 1)}{2} \tag{10}$$

R1 Junction Width

Used for radial load area, see appendices

$$J_1 = \sqrt{2}R_1 = R_1\sqrt{2} \tag{11}$$

R1 Junction Length

Used for radial load area, see appendices

$$J_2 = 2\left(S + \frac{R_1}{\sqrt{2}}\right) = E - R_1 \tag{12}$$

Rotor Center to Center length

Assembled rotor to rotor center distance, used to locate rotors and flowrate derivations

$$L = \frac{E + R_1(\sqrt{2} - 1)}{\sqrt{2}} = \frac{E + R_1(\sqrt{2} - 1)}{\sqrt{2}} \tag{13}$$

R2 and R1 center radius

Used to generate rotor profile

$$S = \sqrt{2}\left(\frac{L}{2} - R_1\right) = \frac{E - R_1(\sqrt{2} + 1)}{2} \tag{14}$$

Rotor Diameter

Used for all flowrate derivations

$$D = 2S + 2R_1 = 2R_3 = E + R_1(1 - \sqrt{2}) \tag{15}$$

2.2 LEAKAGE FLOWRATE

There are three areas where the PRE leaks the high-pressure fluid into the downstream exhaust. This leakage is a non-contributor to shaft power generation. The leak points are identified and mathematically described in this section which is needed in order to calculate expander isentropic efficiency.

All leak points are assumed to have the same bulk fluid velocity due to choked flow criteria. That is, bulk fluid velocity at the throats of each leakage point is then defined as the speed of sound according to the local fluid properties at the throat [11].

After the fluid velocity at the throat is determined, the cross-sectional areas at each leak point are derived and the volumetric flowrate leakage is calculated (using the choked flow fluid speed). The throat properties are known from the throat fluid velocity calculations previously discussed. These are used to calculate throat density, then leakage mass flowrate is finally calculated for each leak point.

2.2.1 CHOKED FLOW

The leak points in the PRE follow the conventional geometry of a convergent divergent nozzle. This allows a choked flow assumption to be used to determine fluid speed at the throat of all leakage points. Choked flow states that if the downstream pressure is lower than a calculated critical pressure, the flow's average velocity at the choke will be evaluated at Mach 1 according to the local fluid conditions (fluid, pressure, and temperature at the throat). This application uses compressible fluid analysis (Mach number >0.3) and it is important to note the fluid density at the choke will differ from the fluid density in the cavity.

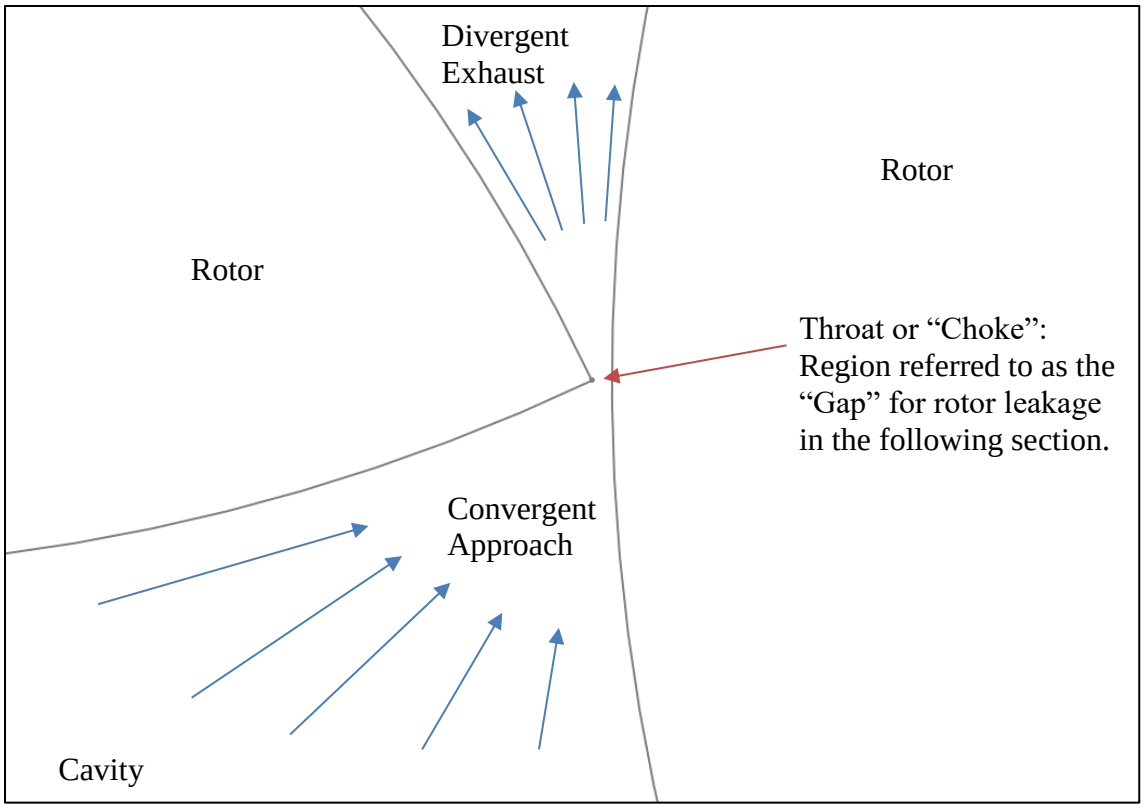

Figure 9: Gap Leakage Geometry (Rotor Gap)

As a reference, equation 17 shows the criteria for choked flow. As the rotor size grows, it is possible that the critical pressure requirement be reduced enough to make the throat velocity less than Mach 1 and should be checked. This is further discussed later in this section. For verified choked conditions, the throat velocity is equal to the speed of sound (Mach 1) according to the local fluid conditions and is used as the bulk fluid velocity at all leak points. The speed of sound is calculated as follows [11]:

$$\widetilde{V}_t = \sqrt{\gamma_t R_g T_t} \tag{16}$$

$$P_3 \leq P_0 \left(\frac{2}{\gamma_t + 1}\right)^{\frac{\gamma_t}{\gamma_t - 1}} = P_t \tag{17}$$

Where:

$\widetilde{V}_t$ = throat average velocity (Mach = 1 for choke conditions only)

γ_t = throat specific heat ratio

T_t = throat fluid temperature

P_t = throat fluid pressure

P_0 = cavity flow field stagnation pressure

R_g = process fluid specific gas constant

M_t = Mach number at the throat

If choked flow is assumed for the leak points, the choke temperature and pressure need to be calculated to determine throat fluid velocity (equation 16). This is accomplished by using the isentropic stagnation pressure and temperatures equations evaluated at Mach = 1 [11]:

$$T_t = \frac{T_0}{1 + \frac{\gamma_t - 1}{2} M_t^2} = \frac{T_2}{1 + \frac{\gamma_t - 1}{2}}, \tag{18}$$

$$P_t = \frac{P_0}{\left(1 + \frac{\gamma_t - 1}{2} M_t^2\right)^{\frac{\gamma_t}{\gamma_t - 1}}} = \frac{P_2}{\left(1 + \frac{\gamma_t - 1}{2}\right)^{\frac{\gamma_t}{\gamma_t - 1}}}. \tag{19}$$

The stagnation pressure and temperature are assumed to be the temperature and pressure at state 2 as the initial Mach number entering the cavity is relatively low for the regions of interest (< Mach .3) making $T_2 = T_0$ (units in Kelvin) and $P_2 = P_0$. Once the cavity cross sectional area is calculated and mass flowrate evaluated (and thus initial nozzle Mach number), this assumption can be tested, and error accounted for. Appendix A show tables for the case studies calculating this deviation and show it to be ~0% to 3%.

Since the throat specific heat ratio γ_t is dependent on the throat temperature and pressure, the above equations need to be iteratively calculated. The complexity comes from calculating the specific heat ratio. This was accomplished by using a NIST program called REFPROP which contains empirical parametric equations that yield fluid parameters (like specific heat ratio) as a function of two fluid states (for example pressure and temperature). The three way iterative solver for equations 18, 19, and specific heat ratio solves all three parameters coded into excel that queries REFPROP for each iteration. Initial, arbitrary values for throat pressure and throat temperature (1 psi and 250 K respectively) are used to calculate an initial value for throat specific heat ratio γ_t. The solver converges within a value of 0.001, and with an average specific heat ratio of 1.35 the relative error for this calculation is approximately 0.07%. The precision for

this iterative solver was selected as an optimization for computational costs. The objective GRG solver used to calculate state 2 pressure for an energy recovery application takes exponentially longer to compute due to this iterative throat parameter calculation. To calculate the isentropic efficiency of 400 different rotor sizes (20x20 grid analysis using machine radius E and rotor height H as free variables), the solver performs ~360,000 iterations to converge. This is because the solver queries the REFPROP data base to retrieve thermodynamic parameters for each iteration. A higher precision for the throat parameters would increase the computational time and have diminishing returns considering overall model accuracy (~ 5%).

Also, there is an important note to add concerning choked flow. The choked flow assumption is used because the industrial niche market where the PRE would be applied generally creates a choked flow scenario for optimized rotor configurations. State 1 pressure ideally ranges from 500 to 3000 psi, and state 3 pressure from 50 to 300 psi. These pressure ratios place an optimized rotor configuration in choked flow (at the leak points). The grid analyses shown in sections 3.1 to 3.5 possess rotor configurations where choked flow criteria is not satisfied. These configurations however are not the optimized rotor configurations. Maintaining the choked flow assumption even for these cases theoretically produces accurate results due to the state 1 to state 2 enthalpy loss becoming more dominant as state 2 pressure decreases (with increasing rotor size). In other words, as the difference between subcritical flow and choked flow becomes larger, the error produced by maintaining the choked flow assumption becomes less significant as the state 1 to state 2 enthalpy drop gets larger.

Appendix B uses the applications found in sections 3.1 and 3.3 and introduces a subcritical analysis. A flange tap configuration is used to determine an incompressible drag coefficient at the leak points [12]. The incompressible parameters are then used in combination

with subcritical flow analysis to determine the mass flowrate through the leak points [13] [14]. Note that a hydraulic diameter two times gap G (discussed further in 2.2.4) is used for the incompressible analysis instead of an upstream orifice diameter (PRE leak points have unconventional geometry for port analysis) [15]. It is shown for these applications, that ~2% error in isentropic efficiency exists along the choked/subcritical boundary, and asymptotically approaches 0% error even when the leakage flowrate becomes less choked.

If an application presents a rotor configuration where the choked/subcritical boundary is near the optimized rotor configuration, it is possible that a similar rotor configuration will have the same or better isentropic efficiency due to the reduced throat velocity of non-choked flow. This is unlikely under the intended applications for the PRE but should always be checked.

2.2.2 INTAKE PLATE LEAKAGE

The first leak point is between the head of the rotors and the intake plate. As the process gas enters the rotor cavity, the high-pressure gas is exposed to this junction. Leakage occurs because of the pressure difference between the intake/rotor cavity and the outside of the rotors. This leakage is considered constant and is independent of expander rotational speed. Because the rotors dynamically change the leakage cross section due to rotor rotation, it is difficult to predict this leakage, but can be obtained empirically. Various assembly techniques can be implemented to minimize the gap or reduce it to effectively zero. Since Standard machining practices would still produce a considerable gap due to tolerance stack up, a sacrificial coating can be applied to the intake plate and used to close the gap during assembly. The spinning rotors grind into the soft intake plate coating (i.e. nickel) reducing the gap to minimal clearance. To ensure clearance during operation, a diamond nickel matrix coating can be applied to the head of the rotors to prevent galling, especially during large temperature fluctuations. This thesis makes the assumption that these measures have been taken and head plate gap leakage has been reduced to a negligible amount. These same techniques cannot be used with rotor gap leakage or core leakage discussed in the following sections. The rotor geometry creates complications making it physically impractical and financially unreasonable. See Figure 10.

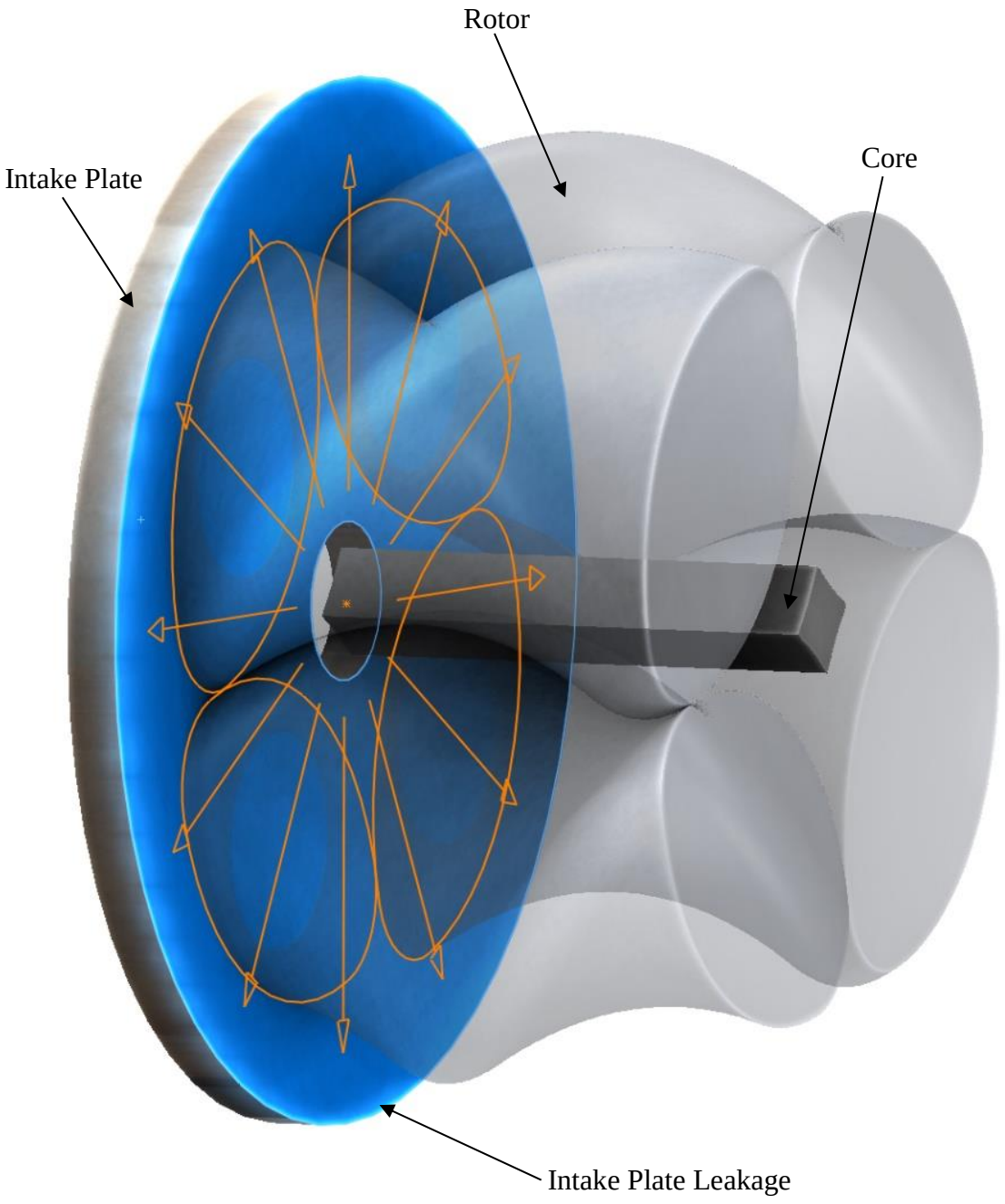

Figure 10: Intake Plate Leak Source

2.2.3 CORE LEAKAGE

The second leak source is located at the dynamic junction between the rotors and the core. Introducing a rounded rotor tip gives advantages such as larger rotor girth for strength, easier tip machinability, and larger fluid inlet ports. However, rounding the tips produces a void in the machine center. A core is needed to fill the void and reduce leakage out the exhaust end of the rotors (this also reduces the cavity volume for a given machine radius E and rotor height H). Two core profiles are generally considered depending on machine size; convex superellipse (CSE) and cylindrical. Both profiles still produce gaps at the machine center creating a leak path. This leakage is constant throughout the cycle of the rotors (the location of the leakage rotates around the core, but the leakage area remains constant). Because of the dynamic motion of the rotors entering and exiting the adjacent rotor's envelope, a core will not be able to remove core leakage completely but only minimize it. A pointed tip, knife edge rotor design could theoretically remove core leakage, but is unfeasible due to the machinability and operational limitations (knife tips bend and wear).

As shown by Figure 11, the convex superellipse core profile reduces the leakage area noticeably more than the cylindrical core profile and is optimal if it can be used. However, due to its manufacturability, the convex superellipse profile has size limitations where a cylindrical core can be manufactured to a relatively smaller diameter more accurately. This is discussed further in this section.

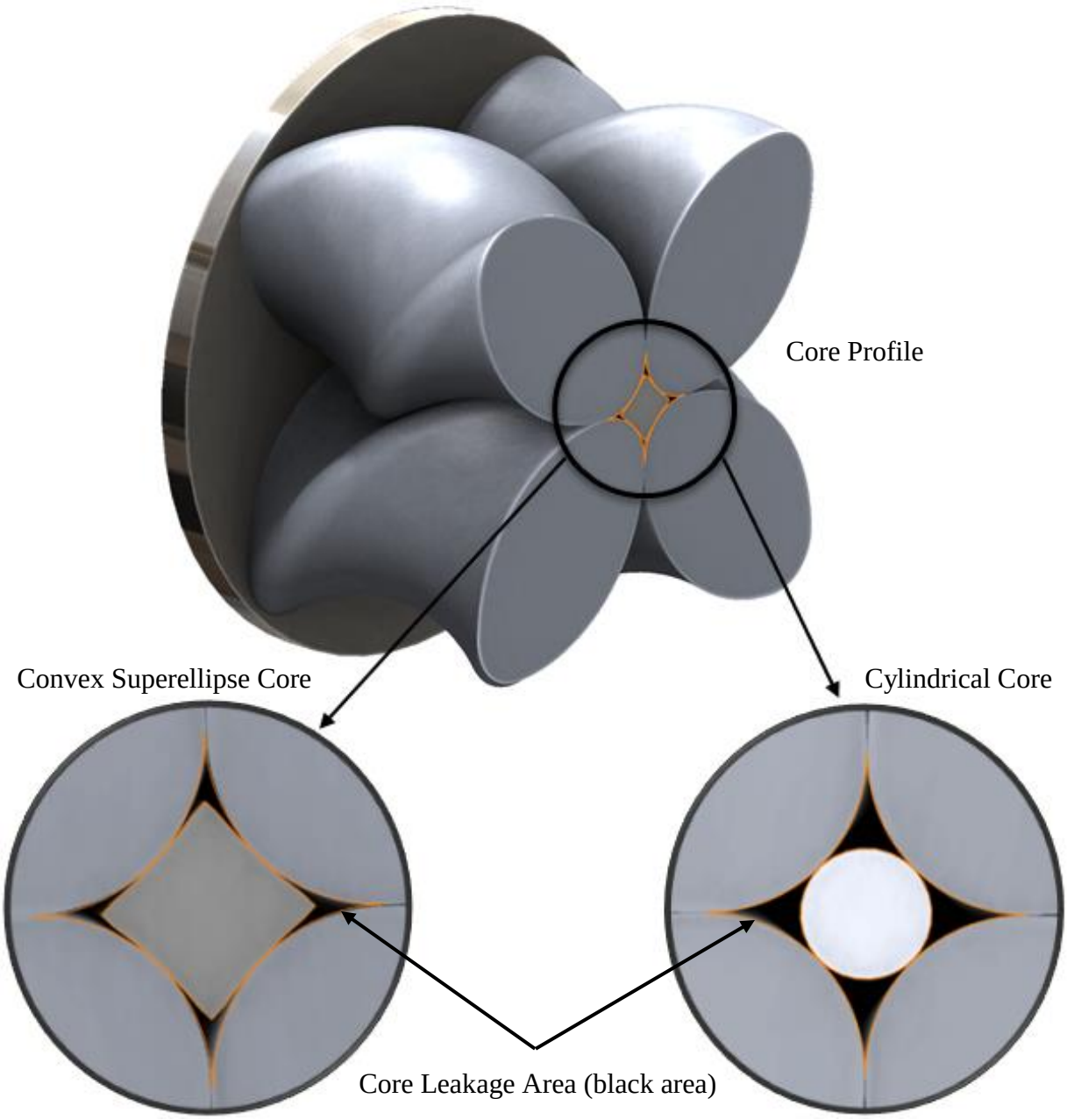

Figure 11: Illustration of Core Profiles

First, the area of the void created by the rounded tips is calculated:

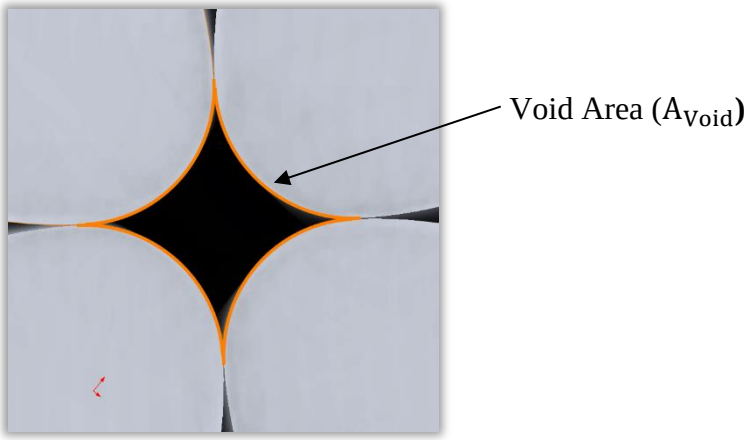

Figure 12: Core Void Area Illustration

The area of the void created by the core is mathematically driven by the tip radius R_1. Figure 13 shows that R_1 spans a 90 degree arc length. This creates a square with sides equal to two times R_1. Subtracting the rotor area from this square yields the void area,

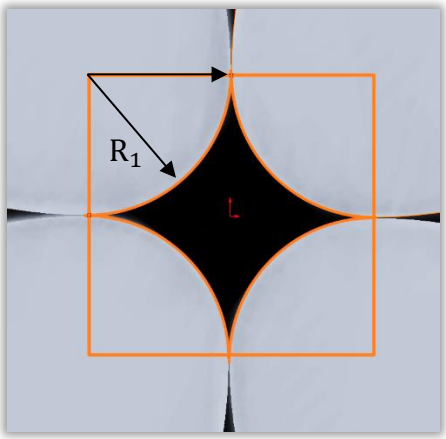

Figure 13: Core Void Area Calculation

$$A_{Void} = 4R_1^2 - \pi R_1^2 = R_1^2(4 - \pi). \quad (20)$$

Next, the core's cross-sectional area is calculated and subtracted from the void area to give the core leakage area. There are 2 basic shapes for a core. The first core type is a convex superellipse as shown in Figure 11 which minimizes the core area leakage. The second core type is a cylindrical core which will produce a greater core leakage area. Due to the high tolerance needed for a core design, limitations in manufacturing a small convex superellipse core might force the design to use a cylindrical core.

The cylindrical core area (A_{CynCore}) is calculated by taking the area of a circle created by two rotor diameters inside the machine radius:

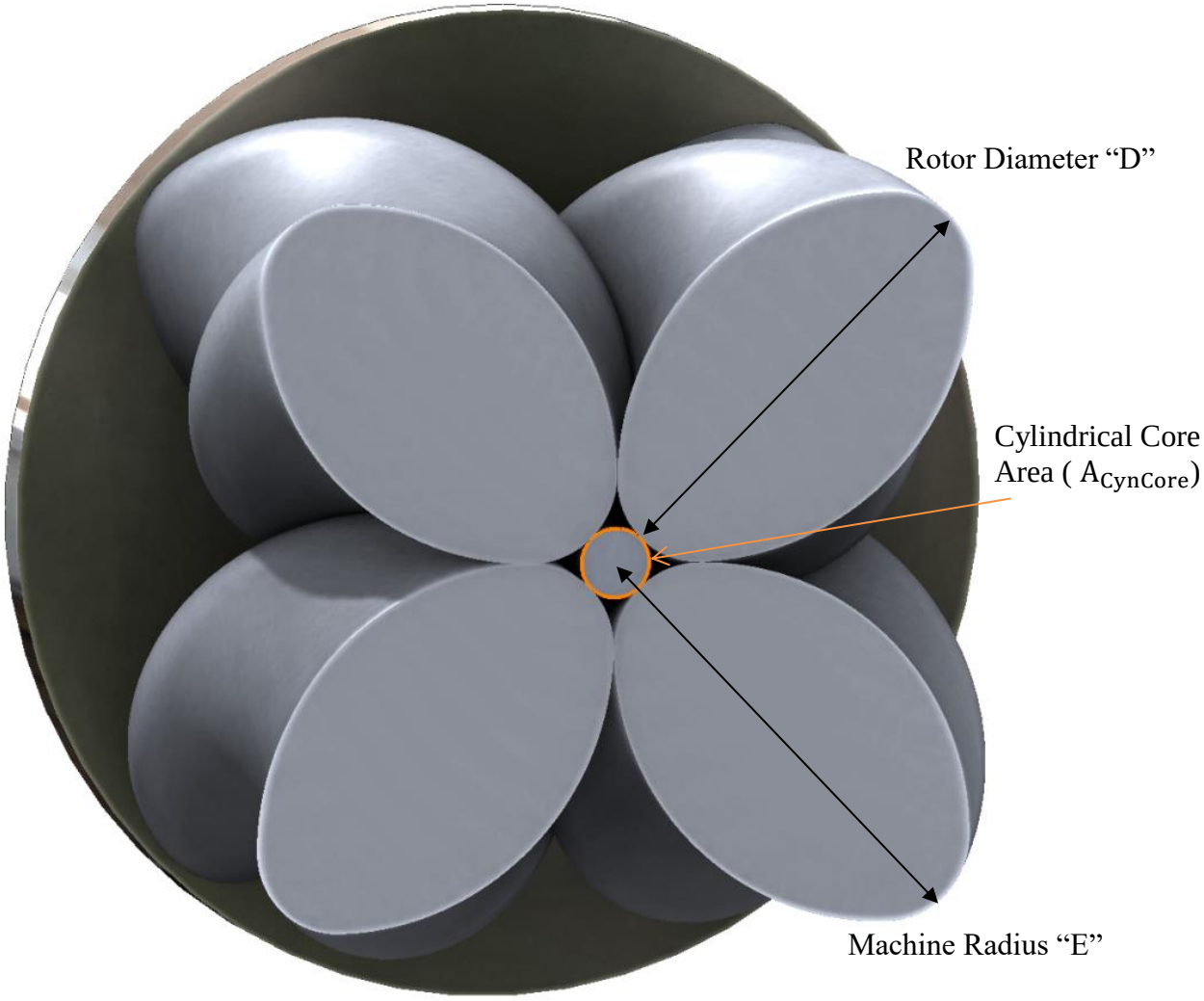

Figure 14: Cylindrical Core Geometry

$$A_{CylCore} = \pi(E - D)^2 \,, \tag{21}$$

$$A_{CylCore} = \pi R_1^2 \left(1 - \sqrt{2}\right)^2 \,. \tag{22}$$

The core leakage area ($A_{CynLeakage}$) when using a cylindrical core is calculated by

$$A_{CynLeakage} = A_{Void} - A_{CylCore} \,, \tag{23}$$

$$A_{CynLeakage} = R_1^2(4 - \pi) - \pi R_1^2 \left(1 - \sqrt{2}\right)^2 \,, \tag{24}$$

$$A_{CynLeakage} = R_1^2 \left[4 - \pi - \pi\left(1 - \sqrt{2}\right)^2\right] \approx .319 R_1^2 \,. \tag{25}$$

Multiplying equation 25 by equation 16 yields cylindrical core volumetric flowrate leakage,

$$\dot{V}_{CynLeakage} = R_1^2 \left[4 - \pi - \pi\left(1 - \sqrt{2}\right)^2\right] \cdot \widetilde{V}_t \,, \tag{26}$$

$$\dot{V}_{CynLeakage} = R_1^2 \left[4 - \pi - \pi\left(1 - \sqrt{2}\right)^2\right] \cdot \sqrt{\gamma_t R_g T_t} \,, \tag{27}$$

where

A_{Void} = total void area,

$A_{CylCore}$ = cylindrical core cross sectional area,

$A_{CynLeakage}$ =cross sectional leakage area when using a cylindrical core,

$\dot{V}_{CynLeakage}$ = cylindrical core leakage flowrate.

The convex superellipse shaped core minimizes core leakage to increase efficiency for PREs with rounded tip rotors. Similarly, with a cylindrical core, the core leakage area is calculated by subtracting the superellipse core area from the area of the void created by having rounded tip rotors (see Figure 15). Core leakage area cannot be reduced any further than a convex superellipse design when using a static core. A dynamic helical core that rotates in sync with the rotors could close the gap and act as a 5^{th} rotor in a 4 rotor configuration. This poses design challenges with rotor indexing, and for simplification, a static core will be used in this analysis.

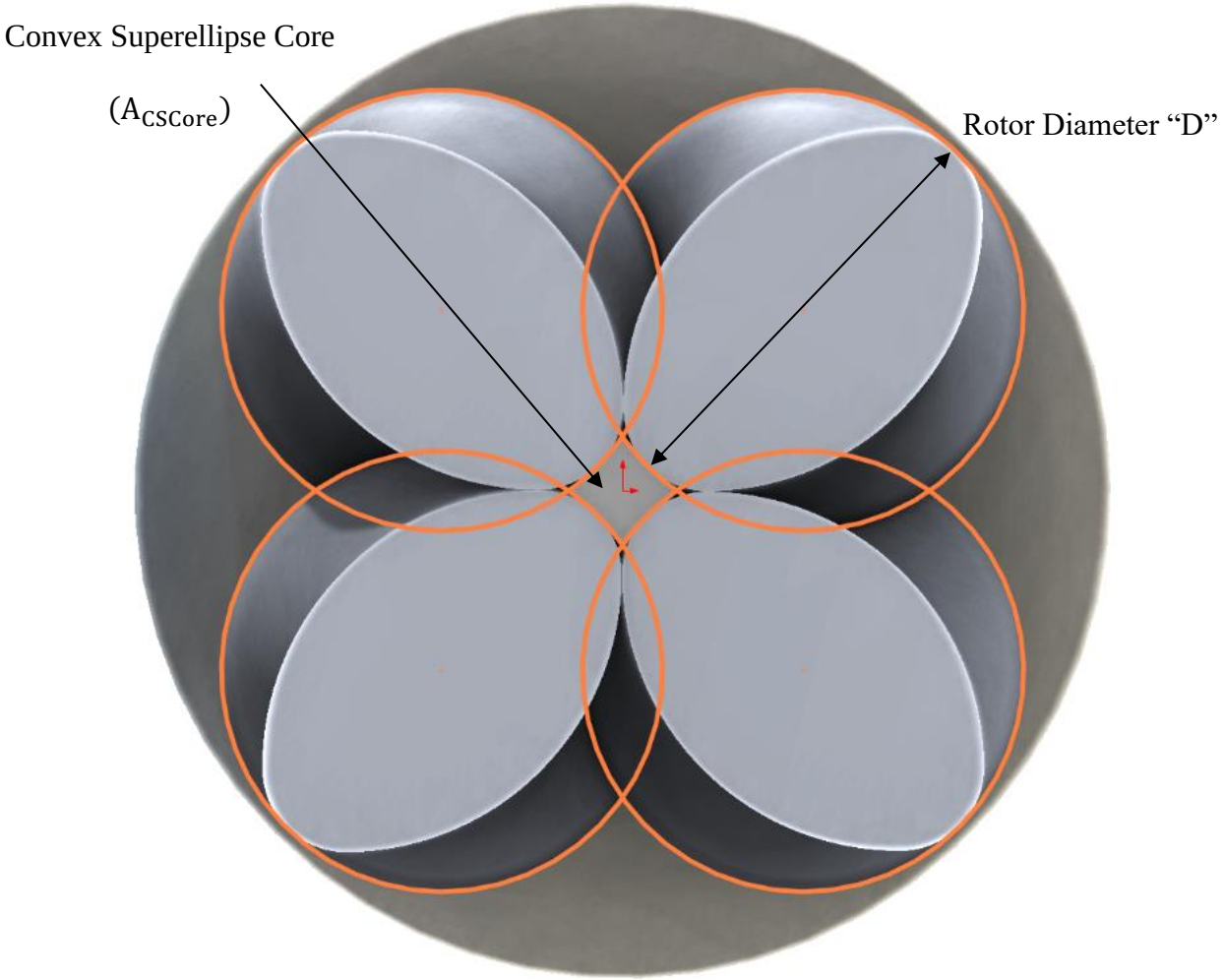

Figure 15: Rotor Tip Intersection

The superellipse shaped core is created by the continuation of the rotor tip arc until it intersects with the adjacent rotor tip's path. By calculating the area of the square formed by the rotor center to center dimension L and subtracting the formed areas inside of that square, the area of the superellipse core remains. Two different areas emerge inside square L: the green area labeled as A_g and the yellow area as A_Y. See Figure 16.

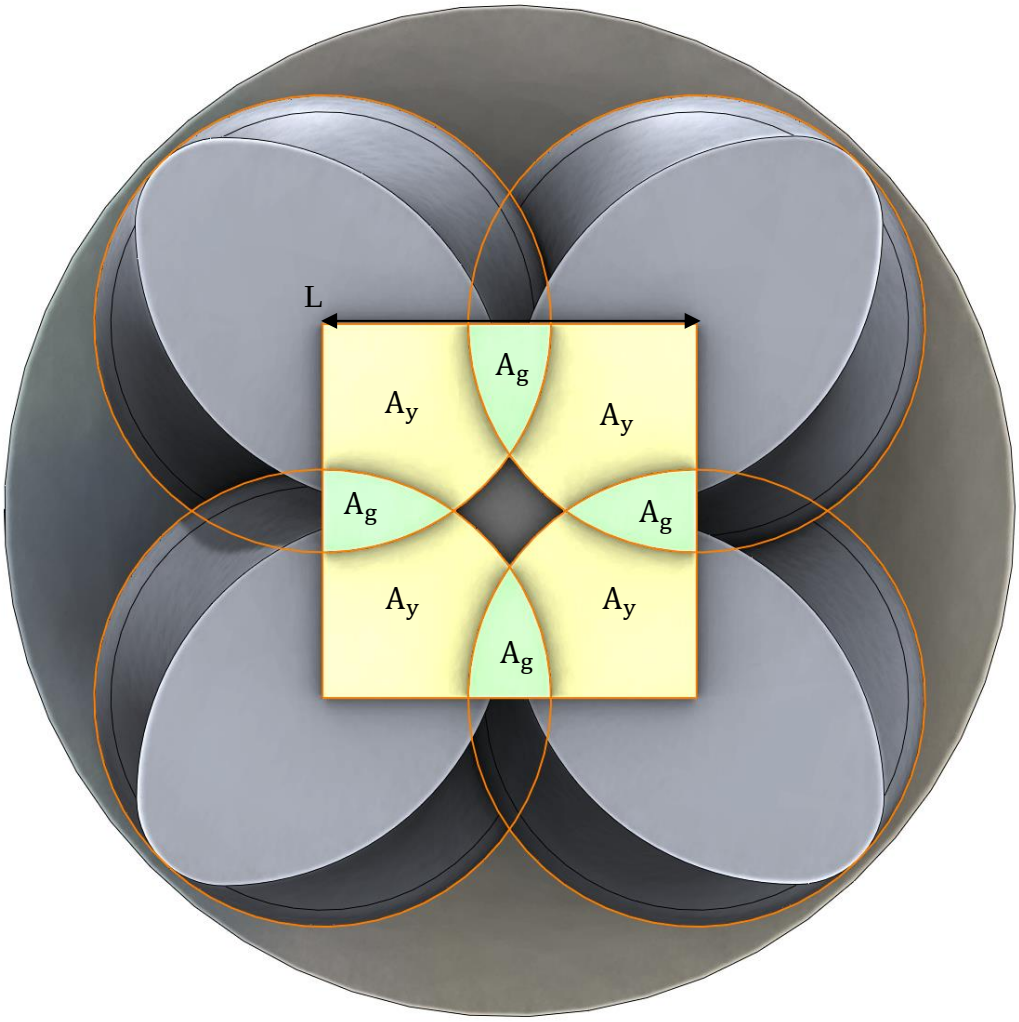

Figure 16: Convex Superellipse Core Area Analysis

The area of the square A_L enclosed by dimension L:

$$A_L = L^2. \tag{28}$$

Area A_y is calculated by subtracting $2A_g$ from one quarter of the area of the circle made by rotor diameter D. Area A_g is half the area of two overlapping circles. First, A_g is calculated by breaking down the sector created by rotor diameter D and subtracting the segment triangle formed by dimension L. Note that angles are in radians.

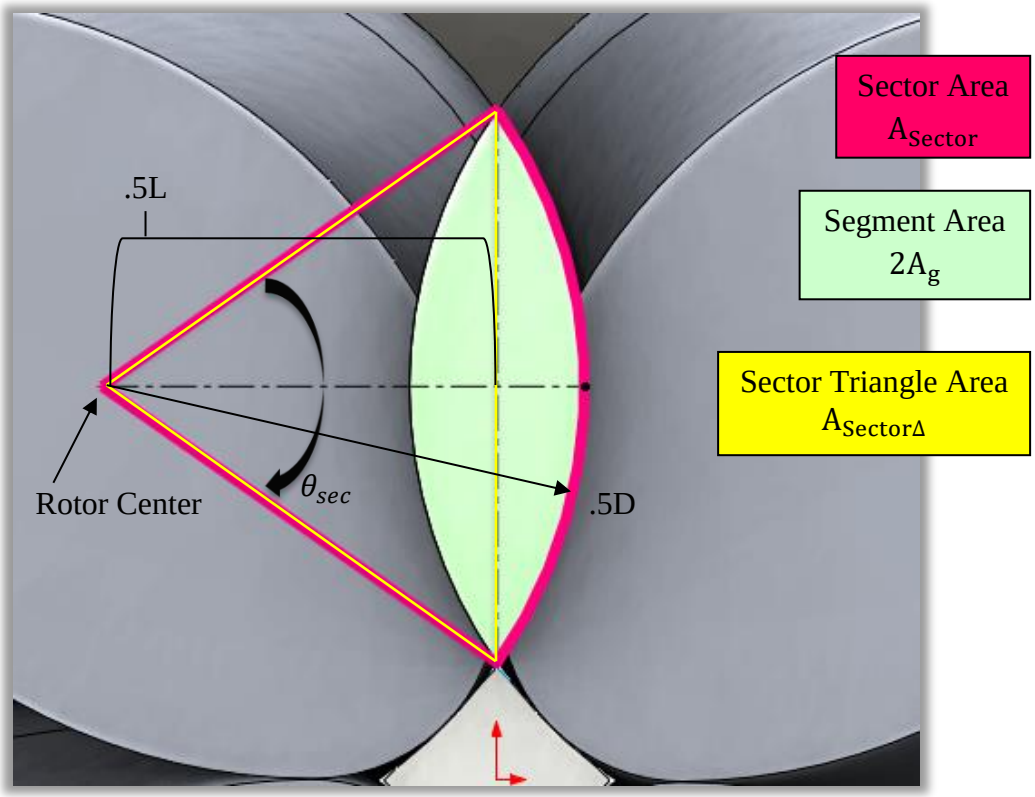

Figure 17: Convex Superellipse Segment Drawing

Sector Angle:

$$\cos\left(\frac{\theta_{sec}}{2}\right) = \frac{L}{D}, \tag{29}$$

$$\theta_{sec} = 2\cos^{-1}\left(\frac{L}{D}\right). \tag{30}$$

Sector Area:

$$A_{Sector} = \frac{\pi D^2}{4} \cdot \frac{\theta_{sec}}{2\pi}, \tag{31}$$

$$A_{Sector} = \frac{\pi D^2}{4} \cdot \frac{2\cos^{-1}\left(\frac{L}{D}\right)}{2\pi}, \tag{32}$$

$$A_{Sector} = \frac{D^2\cos^{-1}\left(\frac{L}{D}\right)}{4}. \tag{33}$$

Sector Triangle Area:

$$A_{Sector\Delta} = \frac{L\sqrt{\left(\frac{D}{2}\right)^2 - \left(\frac{L}{2}\right)^2}}{2}, \tag{34}$$

$$A_{Sector\Delta} = \frac{L\sqrt{D^2 - L^2}}{4}. \tag{35}$$

Calculating A_g:

$$A_g = A_{Sector} - A_{Sector\Delta}, \tag{36}$$

$$A_g = \frac{D^2\cos^{-1}\left(\frac{L}{D}\right) - L\sqrt{D^2 - L^2}}{4}. \tag{37}$$

To calculate the area A_y, subtract $2A_g$ from ¼ of the rotor diameter area A_D yielding

$$A_D = \frac{\pi D^2}{4}, \tag{38}$$

$$\mathrm{A_y} = \frac{\mathrm{A_D}}{4} - 2\mathrm{A_g}\,. \tag{39}$$

The area of a convex superellipse core $\mathrm{A_{CS\,Core}}$ is:

$$\mathrm{A_{CSCore}} = A_L - 4A_y - 4A_g\,, \tag{40}$$

$$\mathrm{A_{CSCore}} = A_L - 4\left(\frac{\mathrm{A_D}}{4} - 2\mathrm{A_g}\right) - 4A_g\,, \tag{41}$$

$$\mathrm{A_{CSCore}} = A_L - \mathrm{A_D} + 4\mathrm{A_g}\,, \tag{42}$$

$$\mathrm{A_{CSCore}} = \mathrm{L^2} - \frac{\pi \mathrm{D^2}}{4} + \left[\mathrm{D^2 cos^{-1}}\left(\frac{\mathrm{L}}{\mathrm{D}}\right) - \mathrm{L}\sqrt{\mathrm{D^2 - L^2}}\right], \tag{43}$$

where:

$\mathrm{A_{CSCore}}$ = cross sectional area of a convex superellipse core (see equation 42),

$\mathrm{A_g}$ = descriptive area used to calculate $\mathrm{A_{CSCore}}$ (see Figure 16),

$\mathrm{A_y}$ = descriptive area used to calculate $\mathrm{A_{CSCore}}$ (see Figure 16),

$\mathrm{A_L}$ = area of a square with a side length L (see Figure 16),

$\mathrm{A_{Sector\Delta}}$ = descriptive area used to calculate $\mathrm{A_{CSCore}}$ (see Figure 17),

$\mathrm{A_D}$ = area of a circle with a rotor diameter D.

To find the leakage area when a convex superellipse core $A_{\mathrm{CSLeakage}}$ is used, the superellipse core area is subtracted from the core void area $\mathrm{A_{Void}}$ found in equation 20,

$$\mathrm{A_{CSLeakage}} = \mathrm{A_{Void}} - \mathrm{A_{CSCore}}\,, \tag{44}$$

$$A_{CSLeakage} = R_1^2(4-\pi) - \left[L^2 - \frac{\pi D^2}{4} + \left(D^2\cos^{-1}\left(\frac{L}{D}\right) - L\sqrt{D^2 - L^2}\right)\right]. \quad (45)$$

Convex superellipse core leakage is calculated by multiplying the superellipse leakage area with the speed of sound in the working fluid as defined by choked flow in equation 16:

$$\dot{V}_{CSLeakage} = A_{CSLeakage} \cdot \tilde{V}_t\,, \quad (46)$$

$$\dot{V}_{CSLeakage} = \left[R_1^2(4-\pi) - L^2 + \frac{\pi D^2}{4} - \left(D^2\cos^{-1}\left(\frac{L}{D}\right) - L\sqrt{D^2 - L^2}\right)\right] \cdot \sqrt{\gamma_t R_g T_t}\,, \quad (47)$$

where:

$A_{CSLeakage}$ = leakage cross sectional area when using a convex superellipse core,

$\dot{V}_{CSLeakage}$ = volumetric flowrate of the convex superellipse core leakage.

Note that equation 47 uses dimension L, which is not one of the three primary variables noted in the rotor geometry section. This is to keep these equations manageable with upcoming derivations.

Where:

A_{Core} = generic core area, either $A_{CylCore}$ or A_{CSCore},

$V_{CylCore} = H \cdot A_{CylCore}$ = volume of a cylindrical core within a full rotor cavity,

$V_{CSCore} = H \cdot A_{CSCore}$ = volume of a convex superellipse core in a full rotor cavity,

V_{Core} = generic core volume, either $V_{CylCore}$ or V_{CSCore} , same for $\dot{V}_{Core.Leakage}$.

A comparison between these two types of cores can be made to show the magnitude difference between them. A convex superellipse core minimizes the core leakage area in a 4-rotor configuration with an R_1 greater than zero. The cylindrical core yields a larger core leakage

area but can be reliably manufactured much smaller (for a smaller R_1) and cheaper. Below compares the core leakage area of both types are compared to provide insight for core selection.

First, the cylindrical core leakage area is calculated for a range of applicable primary variables. Using equation 25, $A_{CynLeakage}$ (only a function of R_1):

$A_{CynLeakage}$ (in^2)

R1 (in.)																	
0.100	0.125	0.150	0.175	0.200	0.225	0.250	0.275	0.300	0.325	0.350	0.375	0.400	0.425	0.450	0.475	0.500
0.003	0.005	0.007	0.010	0.013	0.016	0.020	0.024	0.029	0.034	0.039	0.045	0.051	0.058	0.065	0.072	0.080

$$A_{CynLeakage} = R_1^2\left[4 - \pi - \pi\left(1 - \sqrt{2}\right)^2\right] \approx .319R_1^2 .$$

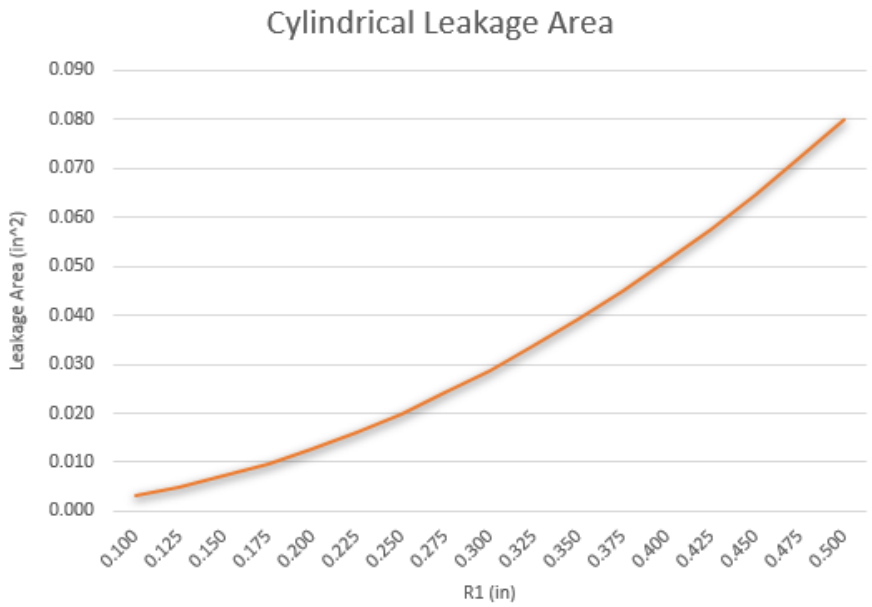

Figure 18: Cylindrical Core Leakage Area Graph

The convex superellipse core's area is dependent on both tip radius R_1 and machine radius E. The graph for calculating the convex superellipse core can be found below modeled after equation 45:

$$A_{CSLeakage}(in^2)$$

E (in.) \ R1 (in.)	0.100	0.125	0.150	0.175	0.200	0.225	0.250	0.275	0.300	0.325	0.350	0.375	0.400	0.425	0.450	0.475	0.500
2.0	0.002	0.002	0.004	0.005	0.006	0.007	0.009	0.011	0.012	0.014	0.016	0.018	0.020	0.022	0.023	0.025	0.027
2.5	0.002	0.003	0.004	0.005	0.006	0.008	0.009	0.011	0.013	0.015	0.017	0.019	0.022	0.024	0.026	0.029	0.031
3.0	0.002	0.003	0.004	0.005	0.006	0.008	0.010	0.012	0.014	0.016	0.018	0.020	0.023	0.025	0.028	0.031	0.033
3.5	0.002	0.003	0.004	0.005	0.006	0.008	0.010	0.012	0.014	0.016	0.018	0.021	0.024	0.026	0.029	0.032	0.035
4.0	0.002	0.003	0.004	0.005	0.006	0.008	0.010	0.012	0.014	0.016	0.019	0.021	0.024	0.027	0.030	0.033	0.036
4.5	0.002	0.003	0.004	0.005	0.007	0.008	0.010	0.012	0.014	0.017	0.019	0.022	0.025	0.027	0.031	0.034	0.037
5.0	0.002	0.003	0.004	0.005	0.007	0.008	0.010	0.012	0.014	0.017	0.019	0.022	0.025	0.028	0.031	0.034	0.038
5.5	0.002	0.003	0.004	0.005	0.007	0.008	0.010	0.012	0.015	0.017	0.020	0.022	0.025	0.028	0.031	0.035	0.038
6.0	0.002	0.003	0.004	0.005	0.007	0.008	0.010	0.012	0.015	0.017	0.020	0.022	0.025	0.028	0.032	0.035	0.039
6.5	0.002	0.003	0.004	0.005	0.007	0.008	0.010	0.012	0.015	0.017	0.020	0.023	0.026	0.029	0.032	0.035	0.039
7.0	0.002	0.003	0.004	0.005	0.007	0.008	0.010	0.012	0.015	0.017	0.020	0.023	0.026	0.029	0.032	0.036	0.039
7.5	0.002	0.003	0.004	0.005	0.007	0.008	0.010	0.012	0.015	0.017	0.020	0.023	0.026	0.029	0.032	0.036	0.040
8.0	0.002	0.003	0.004	0.005	0.007	0.008	0.010	0.013	0.015	0.017	0.020	0.023	0.026	0.029	0.033	0.036	0.040

$$A_{CSLeakage} = R_1^2(4-\pi) - \left[L^2 - \frac{\pi D^2}{4} + \left(D^2\cos^{-1}\left(\frac{L}{D}\right) - L\sqrt{D^2 - L^2}\right)\right].$$

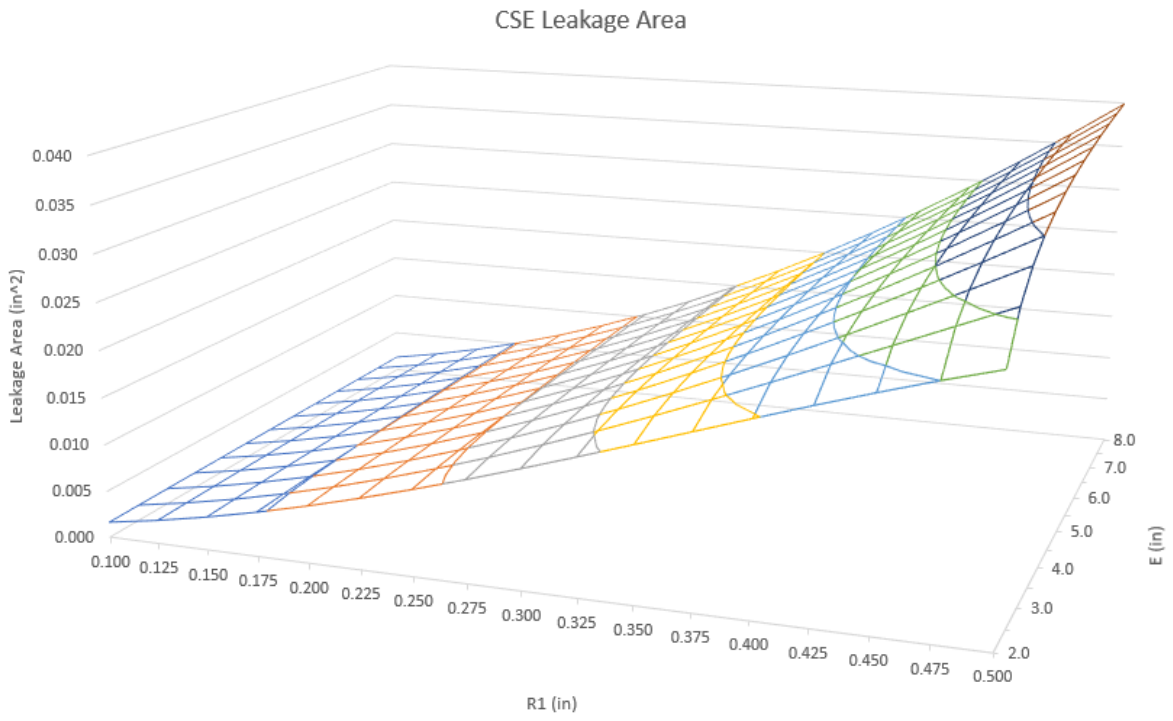

Figure 19: Convex Superellipse Core Leakage Area Graph

The CSE core varies slightly with changes in machine size but comparing leakage areas from both core types yields a comparative ratio showing the difference in area. Figure 20 shows

that the cylindrical core has an average of two times the leakage area than a CSE core for plausible machine sizes (this ratio rapidly increases as R_1 increases because cylindrical core leakage area increases exponentially with R_1). Since both cases would have the same bulk velocity as defined by choked flow, the same ratio applies for core volumetric leak rate.

$$\frac{A_{CynLeakage}}{A_{CSLeakage}}$$

	R1 (in.)																
E (in.)	0.100	0.125	0.150	0.175	0.200	0.225	0.250	0.275	0.300	0.325	0.350	0.375	0.400	0.425	0.450	0.475	0.500
2.0	2.0	2.0	2.0	2.1	2.1	2.2	2.2	2.3	2.3	2.4	2.4	2.5	2.6	2.7	2.8	2.9	3.0
2.5	1.9	2.0	2.0	2.0	2.1	2.1	2.1	2.2	2.2	2.2	2.3	2.3	2.4	2.4	2.5	2.5	2.6
3.0	1.9	1.9	2.0	2.0	2.0	2.0	2.1	2.1	2.1	2.1	2.2	2.2	2.2	2.3	2.3	2.4	2.4
3.5	1.9	1.9	2.0	2.0	2.0	2.0	2.0	2.0	2.1	2.1	2.1	2.1	2.2	2.2	2.2	2.2	2.3
4.0	1.9	1.9	1.9	2.0	2.0	2.0	2.0	2.0	2.0	2.1	2.1	2.1	2.1	2.1	2.2	2.2	2.2
4.5	1.9	1.9	1.9	1.9	2.0	2.0	2.0	2.0	2.0	2.0	2.0	2.1	2.1	2.1	2.1	2.1	2.2
5.0	1.9	1.9	1.9	1.9	1.9	2.0	2.0	2.0	2.0	2.0	2.0	2.0	2.1	2.1	2.1	2.1	2.1
5.5	1.9	1.9	1.9	1.9	1.9	1.9	2.0	2.0	2.0	2.0	2.0	2.0	2.0	2.0	2.1	2.1	2.1
6.0	1.9	1.9	1.9	1.9	1.9	1.9	1.9	2.0	2.0	2.0	2.0	2.0	2.0	2.0	2.0	2.1	2.1
6.5	1.9	1.9	1.9	1.9	1.9	1.9	1.9	2.0	2.0	2.0	2.0	2.0	2.0	2.0	2.0	2.0	2.0
7.0	1.9	1.9	1.9	1.9	1.9	1.9	1.9	1.9	2.0	2.0	2.0	2.0	2.0	2.0	2.0	2.0	2.0
7.5	1.9	1.9	1.9	1.9	1.9	1.9	1.9	1.9	1.9	2.0	2.0	2.0	2.0	2.0	2.0	2.0	2.0
8.0	1.9	1.9	1.9	1.9	1.9	1.9	1.9	1.9	1.9	1.9	2.0	2.0	2.0	2.0	2.0	2.0	2.0

Figure 20: Convex Superellipse Core Leakage Area Graph

Consideration when selecting a core would include core cost, rotor tip wear, cavity volume, and cavity leak rate. Smaller R1 values yield larger cavity volumes and smaller leak rates for both core types. However, smaller R1 values increase rotor tip wear, decrease cavity inlet area, and increase core manufacturing costs. Core selection is a multi-variable optimization not included in this thesis. For the case studies found in Chapter 3, a cylindrical core with a tip radius of R1 will be used.

2.2.4 ROTOR GAP LEAKAGE

The third leak source occurs between adjoining rotors. High precision rotor bearing housings can prescribe a gap between rotors, as planetary rotors have relative motion between them and cannot touch. This gap is a non-trivial leak point and should be minimized in order to increase efficiency. Before analyzing the rotor gap leakage, three gap behaviors need to be understood.

The first gap behavior is as Figure 21 shows; the gap twist reverses direction halfway through the cycle. Even though the gap's helical path changes direction of rotation, its pitch remains constant.

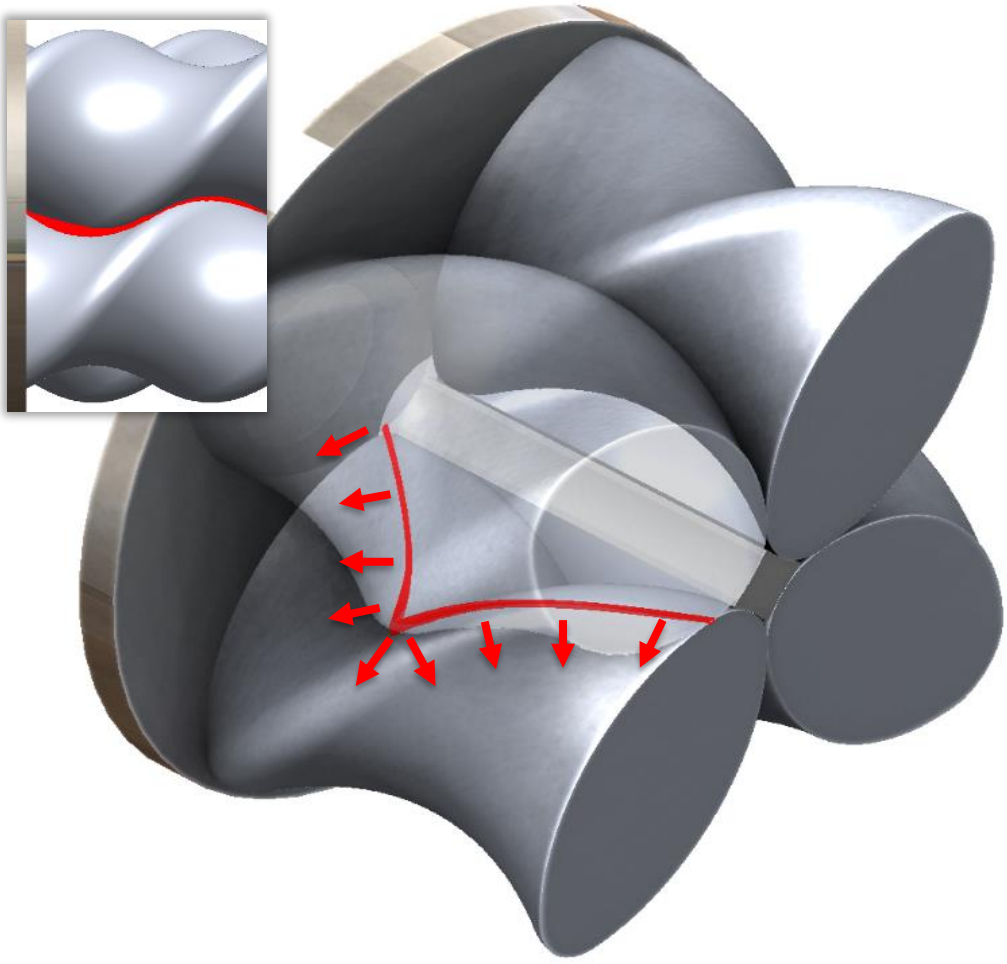

Figure 21: Gap Behavior 1, Gap Choke Twist Reversal

The second gap behavior is as the rotors twist, the gap created between the rotors travels radially. The lower and upper bounds for its radial travel are the distance between the R_1 junction (where R_1 merges with R_2, see Figure 8) and R_1 tip (or rotor tip). For the analysis, a radial height is needed to calculate the gap arc length and so an average will be used since the girth and tip radius R1 and R2 are constant radii. Note the gap's radial travel will complete two "junction to tip" radial cycles for one rotor cycle. Note as R_1 reduces to zero, the radial travel also reduces to zero.

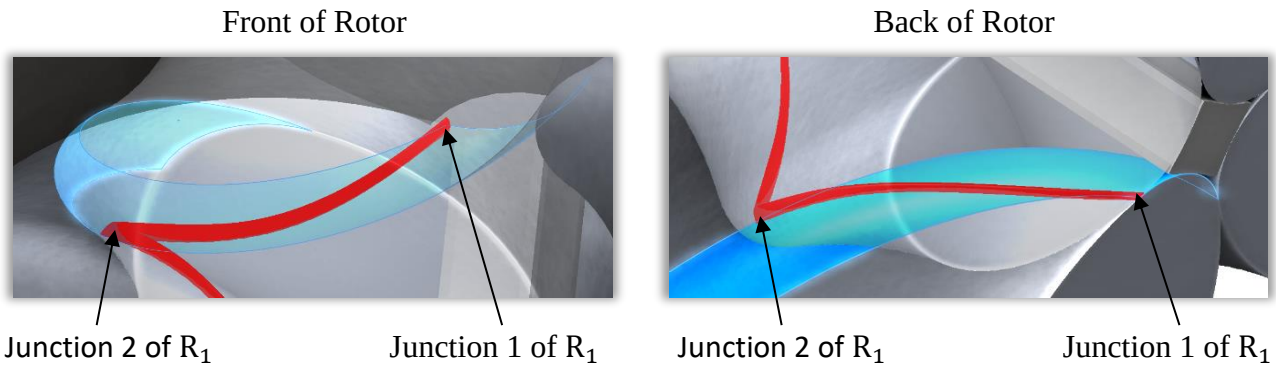

Figure 22: Gap Behavior 2, Tip Radius Cross Over

The third gap behavior is that the gap length grows as the rotors progress through their cycle. Meaning at the beginning of each cycle, the rotor gap length is effectively zero and grows at a rate that is a function of expander rotational speed. As the rotors are only partly through its cycle, this creates a shorter gap length than the figures above. Gap thickness is constant through the cycle. Note with each new cycle, the gap length returns to zero and regrows.

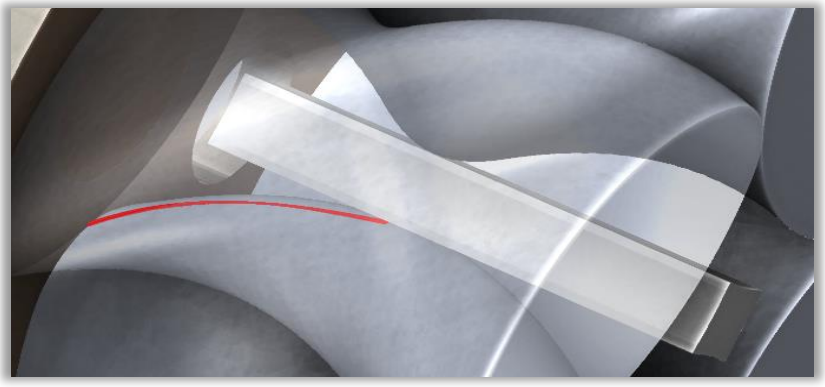

Figure 23: Gap Behavior 3, Gap Length Growth

To calculate the rotor gap leakage, the length of the rotor gap needs to be mathematically modeled. The length grows along a helical path with a constant pitch (even though it reverses direction halfway through the cycle), and with a varying radius as shown by behavior two. For model simplicity, rotor diameter is used as the helix diameter. This is true as R_1 approaches zero making rotor diameter D an approximation for the helix diameter for a small tip radius R_1. Heuristic analysis shows that isentropic efficiency error induced by assuming the helix diameter to be rotor diameter D is less than .05% for rotor sizes that have a tip radius R_1 to machine radius E ratio less than .07. Appendix G contains derivations of the varying helix diameter for reference. The gap length L_{helix} is modeled the standard length of a helix,

$$L_{helix} = \sqrt{[\pi T_{helix} D]^2 + H^2}\,, \tag{48}$$

where:

L_{helix} = total gap coil length,

T_{helix} = number of twists contained within rotor height H (.5 for the PRE).

To calculate the gap length as the rotors rotate, number of rotor twist T_{helix} is expressed in terms of time to represent the transient nature of the gap growth. First, the number of helical twists is expressed in terms of instantaneous axial position:

$$T^*_{helix}(h) = T_{helix}\frac{h}{H}, \tag{49}$$

where:

$T^*_{helix}(h)$ = instantaneous number of helical twists,

h = instantaneous axial height of cycle (see Figure 23).

The instantaneous axial height can be expressed in terms of time:

$$h(t) = 2ƒHt\,, \tag{50}$$

where:

$ƒ =$ PRE frequency of rotation,

$t =$ time.

Substituting equation 50 into equation 49:

$$T^*_{helix}(t) = T_{helix}\frac{2ƒHt}{H}, \tag{51}$$

$$T^*_{helix}(t) = T_{helix}2ƒt\,. \tag{52}$$

To model the gap leakage coil length in terms of time, substitute equations 50 and 52 into equation 48:

$$L_{helix}(t) = \sqrt{[\pi T^*_{helix}(t)D]^2 + \big(h(t)\big)^2}, \tag{53}$$

$$L_{helix}(t) = 2ƒt\sqrt{[\pi T_{helix}D]^2 + H^2}\,. \tag{54}$$

The rotor gap leakage area is the gap length multiplied by the constant gap thickness G This gap thickness is given as it is driven by tolerance stack up of the PRE assembly. The gap area is multiplied by 4 because a 4 rotor machine has 4 rotor gaps and equations yield:

$$A_{gap}(t) = (4G)2ƒt\sqrt{[\pi T_{helix}D]^2 + H^2}, \tag{55}$$

$$A_{gap}(t) = 8Gƒt\sqrt{[\pi T_{helix}D]^2 + H^2}\,, \tag{56}$$

where:

$A_{gap}(t)$ = instantaneous total rotor gap area of all rotors,

G = prescribed rotor gap clearance.

Rotor gap leakage $\dot{V}_{t-gapleak}$ is calculated by multiplying total gap area by gap choke speed found from equation 16:

$$\dot{V}_{t.gapleak} = \tilde{V}_t \cdot A_{gap}(t), \tag{57}$$

$$\dot{V}_{t.gapleak}(t) = \sqrt{\gamma_t R_g T_t} \cdot 8Gft\sqrt{[\pi T_{helix} D]^2 + H^2}. \tag{58}$$

Equation 58 gives the instantaneous leakage dependent on time and PRE rotational speed. Integrating equation 58 from zero to the length of time to complete one cycle will give the volume of fluid leaked during one complete cycle. Using equation 50 to determine time t to complete one cycle (h=H):

$$h(t) = H = 2fHt\,, \tag{59}$$

$$t = \frac{1}{2f}. \tag{60}$$

Integral equation defining total gap leakage flowrate during one cycle:

$$\dot{V}_{t.gapleak} = \frac{dV}{dt}\,. \tag{61}$$

Integrating equation 61 using equation 60 as the upper bounds yields the volume of fluid leaked during one cycle $V_{cyl-gapleak}$:

$$\frac{dV}{dt} = \sqrt{\gamma_t R_g T_t} \cdot 8G\mathfrak{f}t\sqrt{[\pi T_{helix} D]^2 + H^2}\,, \tag{62}$$

$$\int_0^{V_{cyl.gapleak}} dV = \int_0^{\frac{1}{2\mathfrak{f}}} \left(\sqrt{\gamma_t R_g T_t} \cdot 8G\mathfrak{f}t\sqrt{[\pi T_{helix} D]^2 + H^2}\right) dt\,, \tag{63}$$

$$V_{cyl.gapleak} = \sqrt{\gamma_t R_g T_t} \cdot 8G\mathfrak{f}\frac{t^2}{2}\sqrt{[\pi T_{helix} D]^2 + H^2}\,\Bigg|_0^{\frac{1}{2\mathfrak{f}}}, \tag{64}$$

$$V_{cyl.gapleak} = \sqrt{\gamma_t R_g T_t} \cdot 8G\mathfrak{f}\frac{\left(\frac{1}{2\mathfrak{f}}\right)^2}{2}\sqrt{[\pi T_{helix} D]^2 + H^2}\,, \tag{65}$$

$$V_{cyl.gapleak} = \frac{G\sqrt{\gamma_t R_g T_t}}{\mathfrak{f}}\sqrt{[\pi T_{helix} D\,]^2 + H^2}\,. \tag{66}$$

Notice in equation 66 the volume of fluid leaked during one cycle is inversely proportional to the rotational frequency of the PRE. To calculate the total gap leakage volumetric flowrate $\dot{V}_{tot.gapleak}$, multiply equation 66 by two (number of cycles per expander revolution) and the expander frequency:

$$\dot{V}_{tot.gapleak} = (2\mathfrak{f})\frac{G\sqrt{\gamma_t R_g T_t}}{\mathfrak{f}}\sqrt{[\pi T_{helix} D]^2 + H^2}, \tag{67}$$

$$\dot{V}_{tot.gapleak} = 2G\sqrt{\gamma_t R_g T_t}\sqrt{[\pi T_{helix} D]^2 + H^2}\,, \tag{68}$$

where:

$\dot{V}_{t.gapleak}$ = instantaneous gap leakage flowrate, time dependent,

$V_{cyl.gapleak}$ = total volume of fluid leaked during one cycle,

$\dot{V}_{tot.gapleak}$ = total PRE rotor gap leakage flowrate.

Equation 68 calculates a steady state flowrate on a macro level. Equation 58 shows that gap flowrate is transient and repeats every cycle. Since normal operation of the PRE is between 10 and 80 Hz and the gap leakage cycle occurs twice per rotor revolution, considering gap leakage steady state is acceptable. This makes the gap leakage flowrate independent of time and PRE rotational speed. Equation 68 also makes it possible to redefine the rotor gap area without the time dependency since area is simply volumetric flowrate (equation 68) divided by the average cross sectional fluid velocity ($\widetilde{\mathrm{V}}_{\mathrm{t}}$), and substituting rotor diameter D for the primary variables:

$$A_{gap} = 2G\sqrt{\left[\pi T_{helix}\left(\mathrm{E} + \mathrm{R}_1\left(1-\sqrt{2}\right)\right)\right]^2 + H^2}, \tag{69}$$

where:

$\mathrm{A}_{\mathrm{gap}}$ = total gap area between rotors.

2.3 CAVITY FLOWRATE

Cavity flowrate is determined by multiplying expander frequency by 2 times the cavity volume (2 cycles per revolution for a 4x4 rotor). Much like how gap leakage is transient in a micro time scale but static in a macro timescale, so is expander flowrate. The flowrate measurement is isolated to how many cycles are completed each second. The task is then to calculate cavity volume. This volume (see Figure 24: is confined by 4 rotors meshing together with a 90 degrees offset. The cavity is largest when the rotors are in the 0-torque position (or the start of a cycle or 0 degrees angle of twist).

The cavity volume is complex to construct as it is the internal volume of the combined subassembly. Several processes will be shown and verified on how to achieve an analytical cavity volume equation dependent on machine radius E, tip radius R1, and rotor height H.

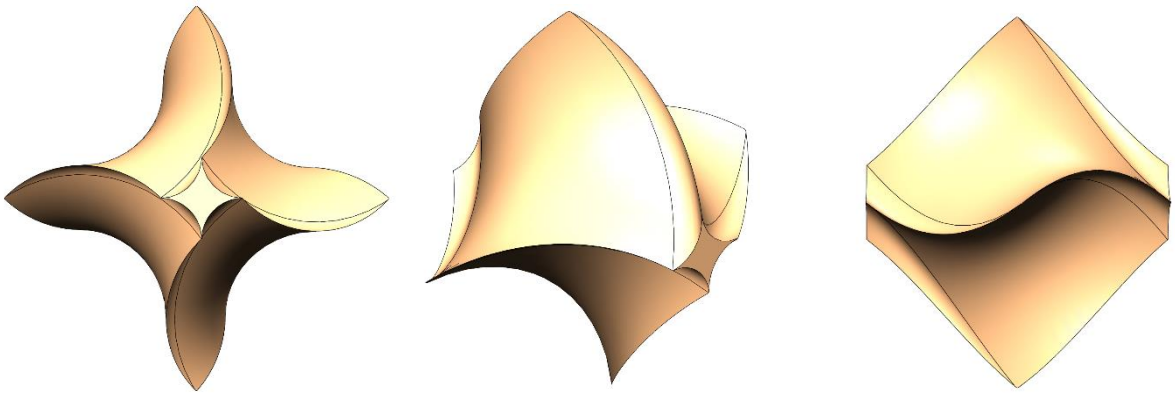

Front View
(machine center axis)

Isometric View

Side View

Figure 24: PRE Cavity Volume (shown: E=4, H=4, R1=.5)

First, the cavity volume is calculated without a core. After the core type has been selected, the core volume will be subtracted from the total cavity volume to yield the net cavity volume. If the cavity cross sectional area is viewed without the void area A_{Void}, it can be shown to increase at the rate of sine squared as the angle of rotor rotation increases. A design study using SolidWorks was used to create the cavity volume cross sectional area according to rotation angle, where 90 degrees occupies half of a cycle (note that rotation angle theta is analogous to axial position h as the rotors have a constant pitch). This design study calculates the cross-sectional area from 0 degrees to 90 degrees of rotation with .1-degree increments.

Figure 25 plots the results from the design study using two rotor configurations: a 4 inch machine radius E, 4 inch rotor height H, with a .5 inch and .002 inch tip radius R1. The results are shown as a ratio of the maximum area, then compared with the progression of sin-squared law. This shows the sin-squared law can be used to integrate the cross-sectional area to calculate total cavity volume.

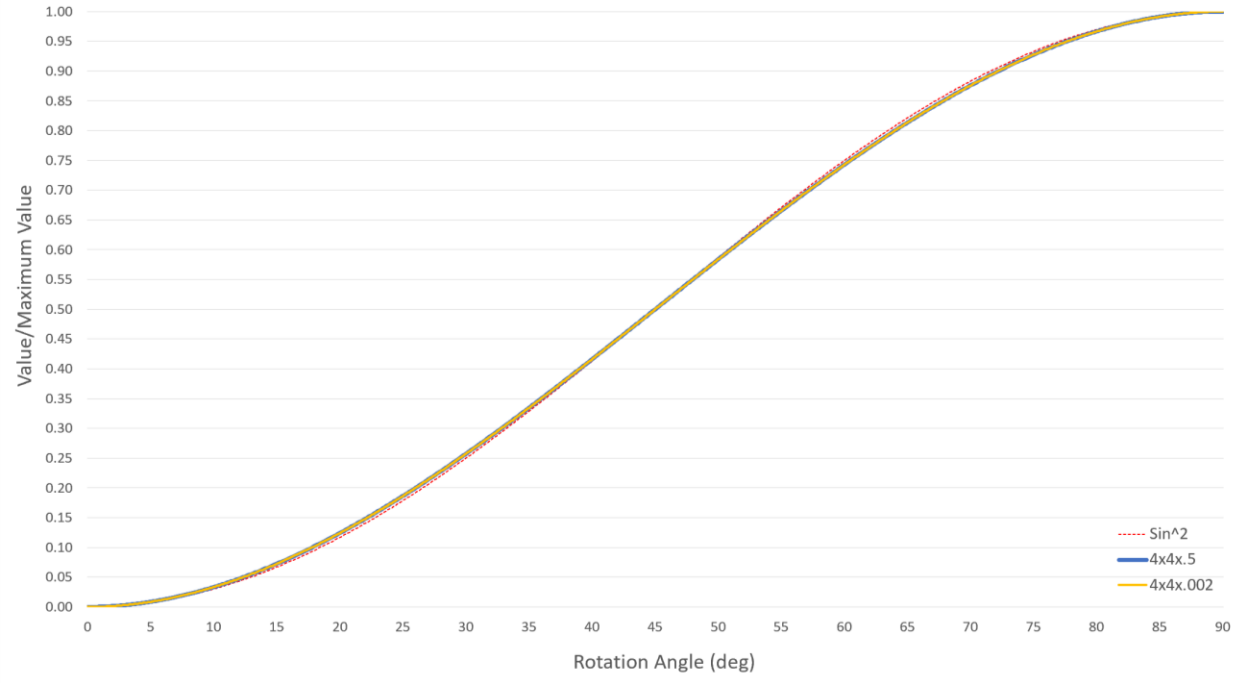

Figure 25: PRE Cavity Cross Sectional Areas Growth Compared To the Sin-squared Law

Figure 26 shows how the cross-sectional area is formed as the rotors rotate through a cycle. The blue cross-sectional plane shows the location of the area relative to the full cavity volume.

Angle Rotation (degrees)	Cross Sectional Plane	Cross Sectional Area
0	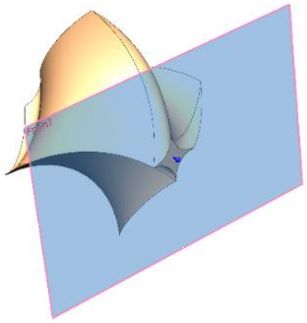	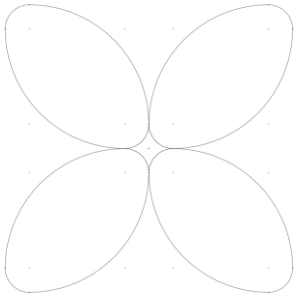
15	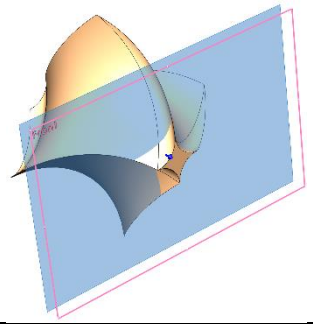	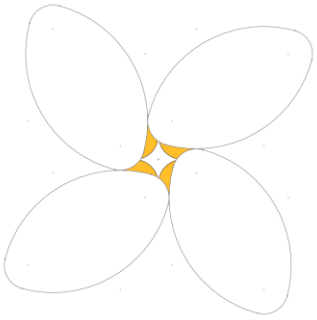
30	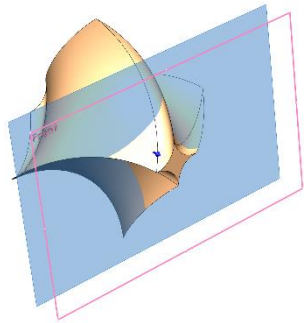	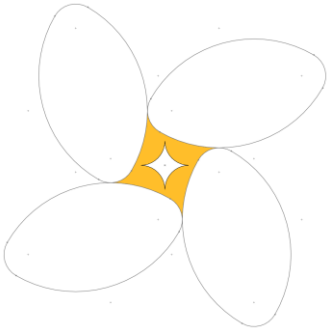

45	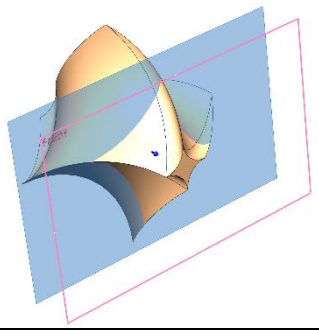	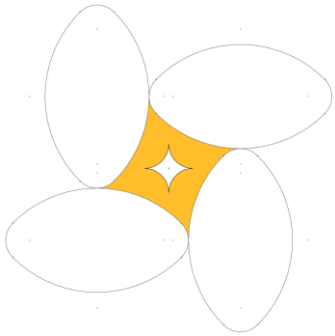
60	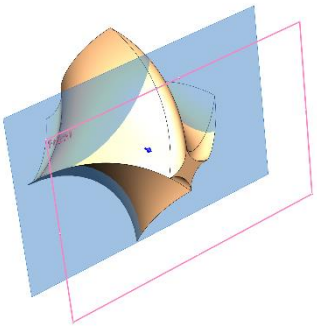	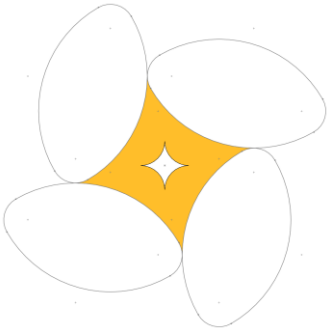
75	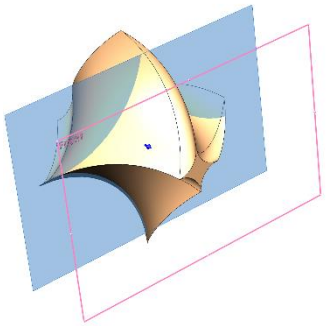	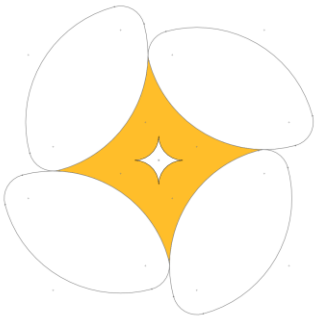
90	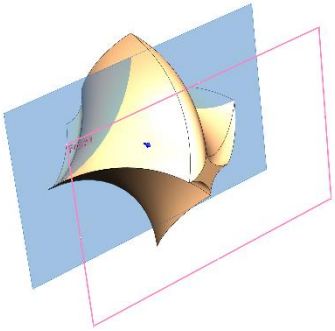	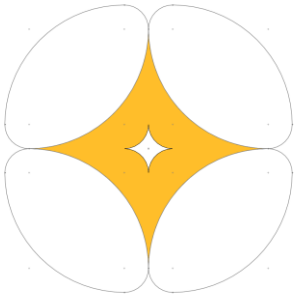

Figure 26: PRE Cavity Cross Sectional Areas for Different Angles of Rotation

(shown: E=4, H=4, R1=.5)

The maximum cross-sectional area without the void area is used to calculate total cavity volume due to the position creating an easy to calculate geometry using already predefined variables. This area becomes difficult to analytically calculate when deviating from this position because the geometry becomes somewhat contorted as shown by Figure 26. This area is located at half the rotor height H, or rotor rotation of 90 degrees (this is also when the rotors produce the maximum torque). This area reduces by the sin-squared law as the rotation angle reduces to 0 as shown by Figure 25.

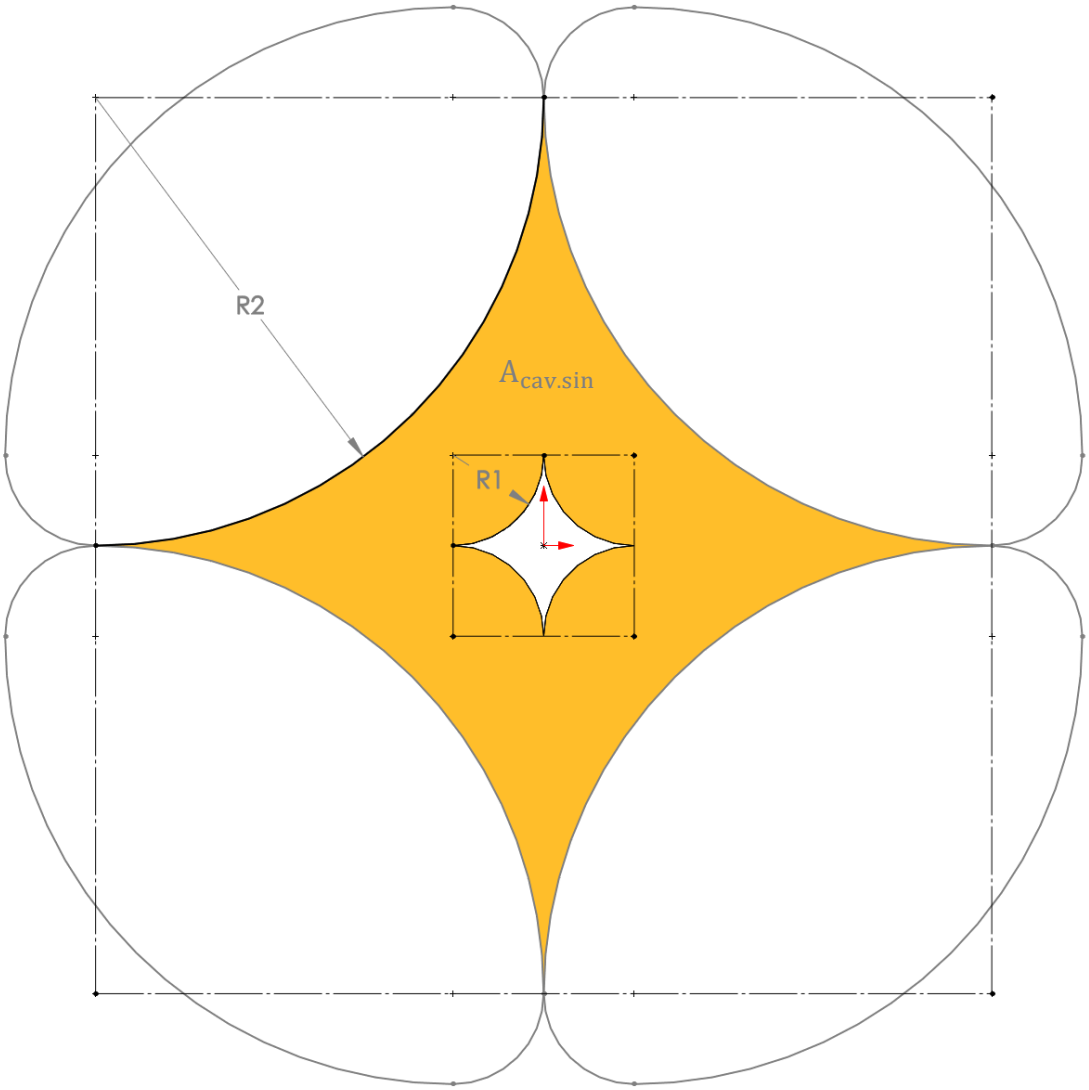

Figure 27: PRE Cavity Max Cross Sectional Area with the Void Area Removed

The maximum cavity area without the void area in Figure 27 is calculated by:

$$A_{cav.sin} = (2R_2)^2 - \pi R_2^2 - A_{void} \, . \tag{70}$$

Substituting R_2 for primary variables machine radius E and tip radius R_1, and using equation 20 for the void area:

$$A_{cav.sin} = \left(\frac{E - R_1}{\sqrt{2}}\right)^2 (4 - \pi) - R_1^2(4 - \pi) \, , \tag{71}$$

$$A_{cav.sin} = (4 - \pi)\left[\frac{(E - R_1)^2}{2} - R_1^2\right], \tag{72}$$

$$A_{cav.sin} = \frac{(4 - \pi)}{2}(E^2 - 2ER_1 - R_1^2) \, , \tag{73}$$

where:

$A_{Cav.sin}$ = maximum cavity cross sectional area minus the void area.

As previously shown, the cross-sectional area reduces through the rotor rotation according to the sine squared law. Thus, the change in volume with a change in height is:

$$dV_{cav.sin} = A_{cav.sin} \cdot \sin^2\theta \cdot dH \, , \tag{74}$$

where:

θ = angle of rotor twist.

Equation 74 can be expressed in terms of a change in angle theta instead of a change in rotor height H as the rotors have a constant pitch. The rotors occupy a 180° twist along rotor height H (180° = π rads) and so dH can be rewritten as:

$$dH = H\frac{d\theta}{\pi}. \tag{75}$$

Equation 74 becomes:

$$dV_{cav.sin} = A_{cav.sin} \cdot \sin^2\theta \cdot H\frac{d\theta}{\pi}, \tag{76}$$

$$V_{cav.sin} = \frac{H \cdot A_{cav.sin}}{\pi}\int_0^{\pi} \sin^2\theta \, d\theta = \frac{H \cdot A_{cav.sin}\left(\frac{\theta}{2} - \frac{\sin 2\theta}{4}\right)}{\pi}\Bigg|_0^{\pi}, \tag{77}$$

$$V_{cav.sin} = \frac{H \cdot A_{cav.sin}}{2}. \tag{78}$$

Substituting equation 73 into equation 78:

$$V_{cav.sin} = \frac{H(4-\pi)}{4}(E^2 - 2ER_1 - R_1^2), \tag{79}$$

where:

$V_{cav.sin}$ = rotor cavity volume minus the void volume ($H \cdot A_{void}$).

Total cavity volume is equal to the sin rotor volume $V_{cav.sin}$ plus the void volume:

$$V_{cav.tot} = \frac{H(4-\pi)}{4}(E^2 - 2ER_1 - R_1^2) + A_{void}H, \tag{80}$$

$$V_{cav.tot} = \frac{H(4-\pi)}{4}(E^2 - 2ER_1 - R_1^2) + R_1^2(4-\pi)H, \tag{81}$$

$$V_{cav.tot} = H(4-\pi)\left[\frac{E^2 - 2ER_1 + 3R_1^2}{4}\right], \tag{82}$$

where:

$V_{cav.tot}$ = total rotor cavity volume.

Because of the presence of a core, a net cavity volume is needed. The net cavity volume is equal to the total cavity volume minus the core volume:

$$V_{cav.net} = H\left[(4-\pi)\left(\frac{E^2 - 2ER_1 + 3R_1^2}{4}\right) - A_{Core}\right], \tag{83}$$

where:

$V_{cav.net}$ = net rotor cavity volume (total cavity volume minus the core volume).

Net rotor cavity flowrate is calculated by multiplying true cavity volume by 2 times the expander rotational frequency (two cycles per revolution):

$$\dot{V}_{cav.net} = 2ƒH\left[(4-\pi)\left(\frac{E^2 - 2ER_1 + 3R_1^2}{4}\right) - A_{Core}\right]. \tag{84}$$

The sin-squared law used for the cavity volume derivation is based on the characteristic trait of a single rotor configuration (4x4x.5). It is important than to verify equation 84 with multiple rotor configurations to ensure the model holds true. This can be verified using a design study in SolidWorks CAD. The CAD model uses four discrete rotor parts that are meshed together with a gap G value of 0. The rotors are oriented at 0 degrees of rotation creating the maximum cavity volume. The CAD intersect tool fills the volume from axial entrance to exit. This volume is measured as the rotors change in machine radius E (varies from 2.5 to 10 inches) and tip radius R1 (varies from 0 to 1 inches). Rotor height H is held static at 4 inches (since equation 84 shows that rotor height H is proportional to cavity flowrate) and the core area A_{Core} is equal to 0.

As Figure 28 shows, equation 84 has ±.15% error (average error = .05%) when compared with CAD generated volume values. Since CAD models use a tetrahedral mesh to form volumes,

there is an inherent estimation when calculating volume using CAD. It would be ideal to derive the cavity volume directly from geometric relationships, but due to its complexity, this is not in the scope of this thesis. Since equation 84 shows to have an error < .2%, it will suffice that the sin-squared law be used as an adequate approximation to determine cavity flowrate.

Figure 29 shows the cavity volumes using the maximum and minimum machine radius E and tip radius R1 from the design study. This visually shows the magnitude of volume change when E and R1 vary. Note again that these volumes are formed without a core as they are added later depending on the selected core type.

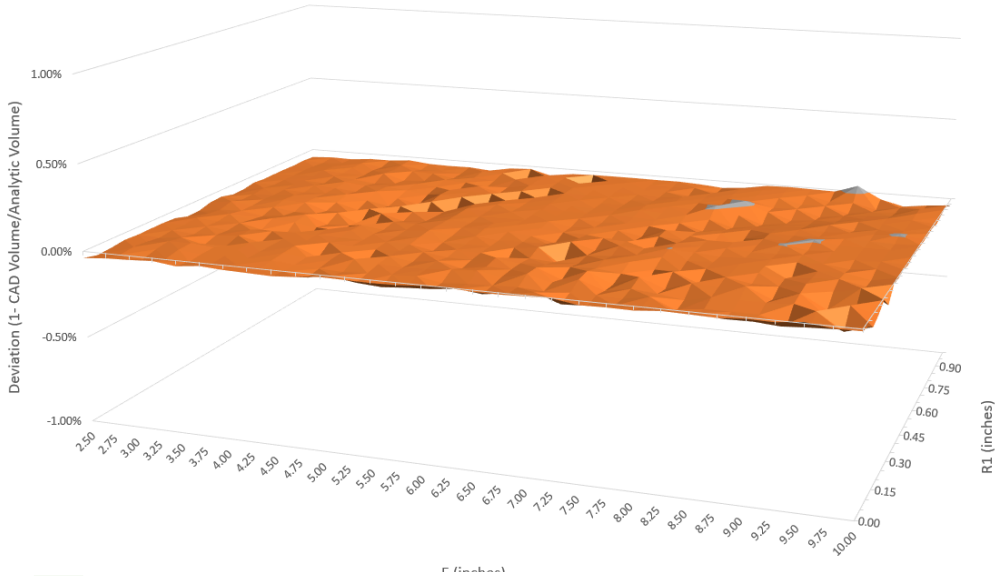

	R1																				
E	0.00	0.05	0.10	0.15	0.20	0.25	0.30	0.35	0.40	0.45	0.50	0.55	0.60	0.65	0.70	0.75	0.80	0.85	0.90	0.95	1.00
2.50	-0.04%	-0.06%	-0.05%	-0.04%	-0.05%	-0.04%	-0.04%	-0.05%	-0.07%	-0.07%	-0.05%	-0.04%	-0.06%	-0.06%	-0.05%	-0.05%	-0.05%	-0.05%	-0.05%	-0.05%	-0.05%
2.75	-0.03%	-0.04%	-0.03%	-0.04%	-0.05%	-0.04%	-0.04%	-0.03%	-0.04%	-0.05%	-0.03%	-0.05%	-0.05%	-0.04%	-0.05%	-0.05%	-0.05%	-0.04%	-0.05%	-0.05%	-0.04%
3.00	-0.02%	-0.06%	-0.03%	-0.02%	-0.04%	-0.05%	-0.04%	-0.04%	-0.03%	-0.04%	-0.05%	-0.04%	-0.04%	-0.04%	-0.04%	-0.04%	-0.04%	-0.03%	-0.04%	-0.04%	-0.05%
3.25	-0.02%	-0.04%	-0.02%	-0.02%	-0.07%	-0.04%	-0.05%	-0.04%	-0.05%	-0.07%	-0.04%	-0.03%	-0.03%	-0.04%	-0.03%	-0.05%	-0.03%	-0.04%	-0.03%	-0.03%	-0.03%
3.50	-0.03%	-0.05%	-0.04%	-0.03%	-0.06%	-0.03%	-0.03%	-0.07%	-0.03%	-0.05%	-0.06%	-0.03%	-0.04%	-0.04%	-0.04%	-0.03%	-0.04%	-0.05%	-0.04%	-0.05%	-0.03%
3.75	-0.02%	-0.04%	-0.04%	-0.03%	-0.03%	-0.06%	-0.03%	-0.10%	-0.04%	-0.03%	-0.06%	-0.08%	-0.05%	-0.03%	-0.05%	-0.04%	-0.06%	-0.02%	-0.03%	-0.03%	-0.02%
4.00	-0.03%	-0.03%	-0.03%	-0.03%	-0.03%	-0.03%	-0.03%	-0.11%	-0.06%	-0.08%	-0.04%	-0.07%	-0.09%	-0.06%	-0.03%	-0.04%	-0.05%	-0.06%	-0.03%	-0.05%	-0.04%
4.25	-0.03%	-0.04%	-0.03%	-0.03%	-0.02%	-0.03%	-0.03%	-0.03%	-0.10%	-0.08%	-0.11%	-0.04%	-0.07%	-0.09%	-0.07%	-0.05%	-0.04%	-0.05%	-0.03%	-0.04%	-0.04%
4.50	-0.03%	-0.05%	-0.05%	-0.04%	-0.08%	-0.02%	-0.03%	-0.02%	-0.03%	-0.11%	-0.02%	-0.12%	-0.04%	-0.08%	-0.10%	-0.07%	-0.05%	-0.03%	-0.05%	-0.05%	-0.04%
4.75	-0.03%	-0.07%	-0.05%	-0.04%	-0.03%	-0.03%	-0.03%	-0.03%	-0.04%	-0.03%	-0.06%	-0.03%	-0.14%	-0.04%	-0.02%	-0.03%	-0.07%	-0.04%	-0.04%	-0.03%	-0.05%
5.00	-0.01%	-0.04%	-0.06%	-0.02%	-0.09%	-0.04%	-0.03%	-0.04%	-0.03%	-0.03%	-0.05%	-0.05%	-0.05%	-0.13%	-0.03%	-0.03%	-0.02%	-0.06%	-0.04%	-0.03%	-0.03%
5.25	-0.01%	-0.07%	-0.05%	-0.04%	-0.03%	-0.04%	-0.03%	-0.02%	-0.02%	-0.02%	-0.02%	-0.03%	-0.02%	-0.03%	-0.14%	-0.03%	-0.05%	-0.05%	-0.03%	-0.12%	-0.02%
5.50	-0.02%	-0.08%	-0.05%	-0.05%	-0.05%	-0.03%	-0.06%	-0.04%	-0.04%	-0.03%	-0.03%	-0.03%	-0.03%	-0.02%	-0.03%	-0.13%	-0.03%	-0.02%	-0.02%	-0.02%	-0.05%
5.75	-0.01%	-0.07%	-0.04%	-0.04%	-0.03%	-0.05%	-0.04%	-0.04%	-0.03%	-0.02%	-0.02%	-0.02%	-0.02%	-0.03%	-0.03%	-0.03%	-0.12%	-0.03%	-0.02%	-0.02%	-0.03%
6.00	0.00%	-0.06%	-0.07%	-0.03%	-0.06%	-0.05%	-0.04%	-0.04%	-0.04%	-0.03%	-0.02%	-0.02%	-0.02%	-0.02%	-0.02%	-0.02%	-0.02%	-0.02%	-0.02%	-0.18%	-0.03%
6.25	0.00%	-0.05%	-0.06%	-0.02%	-0.04%	-0.02%	-0.10%	-0.04%	-0.04%	-0.04%	-0.03%	-0.02%	-0.02%	-0.03%	-0.03%	-0.02%	-0.02%	-0.02%	-0.02%	-0.02%	-0.03%
6.75	-0.01%	-0.04%	-0.05%	-0.01%	-0.01%	-0.04%	-0.06%	-0.12%	-0.01%	-0.03%	-0.04%	-0.03%	-0.04%	-0.02%	-0.02%	-0.03%	-0.03%	-0.03%	-0.03%	-0.03%	-0.03%
7.00	0.00%	-0.02%	-0.06%	-0.04%	-0.07%	-0.04%	-0.05%	-0.04%	-0.05%	-0.01%	-0.06%	-0.04%	-0.03%	-0.03%	-0.01%	-0.01%	-0.02%	-0.03%	-0.03%	-0.03%	-0.03%
7.25	0.00%	-0.07%	-0.05%	-0.02%	-0.01%	-0.03%	-0.02%	-0.03%	-0.01%	-0.02%	-0.05%	-0.06%	-0.03%	-0.03%	-0.02%	-0.01%	-0.01%	-0.02%	-0.05%	-0.02%	-0.03%
7.50	-0.02%	-0.07%	-0.05%	-0.07%	-0.07%	-0.05%	-0.02%	-0.02%	-0.01%	-0.07%	-0.01%	-0.01%	-0.08%	-0.04%	-0.02%	-0.02%	-0.01%	-0.01%	-0.02%	-0.05%	-0.04%
7.75	-0.02%	-0.05%	-0.05%	-0.04%	-0.01%	-0.10%	-0.05%	-0.01%	0.00%	-0.01%	-0.03%	-0.03%	-0.05%	-0.08%	-0.04%	0.01%	-0.01%	-0.01%	-0.01%	-0.01%	-0.03%
8.00	-0.02%	-0.05%	-0.03%	-0.05%	-0.07%	-0.01%	-0.04%	-0.02%	-0.01%	-0.01%	-0.01%	-0.06%	-0.04%	-0.05%	-0.08%	-0.03%	0.02%	-0.01%	-0.01%	0.00%	-0.01%
8.25	-0.01%	-0.04%	-0.09%	-0.07%	-0.02%	-0.06%	-0.02%	-0.02%	-0.02%	-0.01%	-0.01%	-0.08%	-0.06%	-0.04%	-0.06%	-0.08%	-0.03%	-0.04%	-0.01%	-0.01%	-0.01%
8.50	-0.01%	-0.05%	-0.07%	-0.04%	-0.03%	-0.01%	-0.01%	-0.01%	-0.02%	-0.02%	-0.01%	-0.01%	-0.02%	-0.03%	-0.05%	-0.06%	-0.08%	-0.04%	-0.04%	-0.02%	-0.01%
8.75	-0.02%	-0.06%	-0.07%	-0.04%	-0.01%	-0.04%	-0.01%	-0.01%	-0.01%	-0.02%	0.00%	-0.01%	-0.02%	-0.02%	-0.04%	-0.05%	-0.06%	-0.08%	-0.04%	-0.04%	-0.01%
9.00	-0.01%	-0.06%	-0.07%	-0.05%	-0.07%	-0.04%	-0.03%	-0.08%	-0.01%	-0.01%	-0.02%	0.01%	-0.01%	-0.02%	-0.01%	-0.03%	-0.05%	-0.06%	-0.08%	-0.04%	0.04%
9.25	-0.01%	-0.07%	-0.11%	-0.04%	-0.02%	-0.01%	-0.01%	-0.01%	-0.01%	-0.01%	-0.01%	-0.01%	-0.01%	-0.01%	-0.04%	-0.01%	-0.03%	-0.04%	-0.05%	-0.07%	-0.04%
9.50	0.01%	-0.06%	-0.02%	-0.07%	-0.10%	-0.03%	-0.01%	-0.01%	-0.03%	-0.01%	-0.01%	-0.01%	-0.01%	-0.01%	-0.01%	-0.01%	-0.01%	-0.03%	-0.05%	-0.05%	-0.07%
9.75	-0.01%	-0.06%	-0.11%	-0.02%	-0.08%	0.00%	-0.04%	-0.04%	-0.01%	-0.01%	-0.01%	-0.01%	-0.02%	0.00%	-0.01%	-0.01%	-0.01%	-0.01%	-0.01%	-0.05%	-0.05%
10.00	-0.01%	-0.03%	-0.07%	-0.05%	-0.01%	-0.08%	-0.01%	-0.01%	0.00%	-0.02%	-0.01%	-0.01%	-0.01%	-0.01%	-0.01%	-0.01%	-0.02%	-0.01%	0.00%	-0.01%	-0.05%

Figure 28: Deviation of analytic volume (equation 84) from the calculated CAD volume

E x H x R1	Cavity Volume
2.5 x 4 x 0	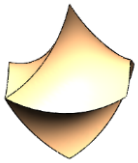
2.5 x 4 x 1	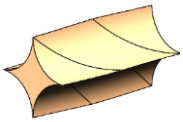
10 x 4 x 1	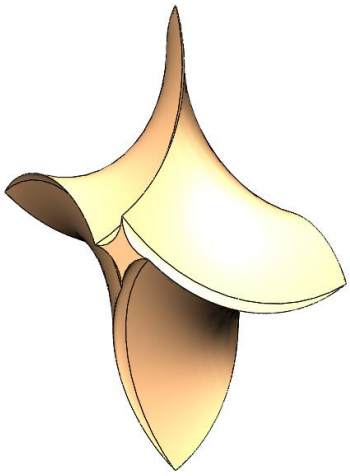
10 x 4 x 0	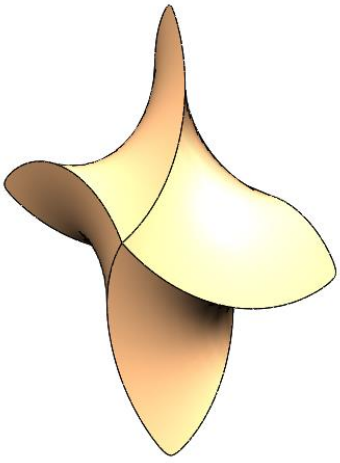

Figure 29: Max. and Min. E Machine Radius E and Tip Radius R1 Used in the Design Study

2.4 ISENTROPIC EFFICIENCY

Total mass flowrate through the PRE is required to evaluate isentropic efficiency. The volumetric flowrates are multiplied by the densities found in the cavity and throat. Note, a single throat density is used for both leakage areas as they share a stagnation pressure and temperature:

$$\dot{m}_{tot} = \rho_2 \dot{V}_{cav.net} + \rho_t \left(\dot{V}_{tot.gapleak} + \dot{V}_{Core.Leakage} \right), \tag{85}$$

$$\begin{aligned} \dot{m}_{tot} = \rho_2 H \int \left[(4 - \pi) \left(\frac{E^2 - 2ER_1 + 3R_1^2}{4} \right) - A_{Core} \right] \\ + \rho_t \left[2G \sqrt{\gamma_t R_g T_t} \sqrt{\left[\pi T_{helix} \left(E + R_1 \left(1 - \sqrt{2} \right) \right) \right]^2 + H^2} + \dot{V}_{Core.Leakage} \right] \end{aligned} \tag{86}$$

Using equations 68 and 84 with core leakage to substitute into equation 2 yields the mass efficiency. This efficiency will give insight when optimizing rotor geometries with different applications. This is discussed more in the case studies.

$$E_{mass} = \frac{\dot{m}_{cav.net}}{\dot{m}_{tot}} = \frac{\rho_2 \dot{V}_{cav.net}}{\rho_2 \dot{V}_{cav.net} + \rho_t \left(\dot{V}_{tot.gapleak} + \dot{V}_{Core.Leakage} \right)}. \tag{87}$$

Finally, isentropic efficiency is calculated using equations 6, 84, and 86 separated into two equations showing a cylindrical core and convex superellipse core.

PRE Isentropic Efficiency (cylindrical core)

$$E_{system} = \frac{\dot{V}_{cav.net} \cdot (P_2 - P_3)}{\dot{m}_{tot}(h_1 - h_{3,Isentropic})} = \frac{\dot{w}_{shaft}}{\dot{m}_{tot}(h_1 - h_{3,Isentropic})}, \quad (88)$$

where:

$$\dot{w}_{shaft} = 2ƒH\left[(4-\pi)\left(\frac{E^2 - 2ER_1 + 3R_1^2}{4}\right) - \pi R_1^2\left(1-\sqrt{2}\right)^2\right] \cdot (P_2 - P_3),$$

$$\dot{m}_{tot} = \dot{m}_{cavity} + \dot{m}_{leakage},$$

and:

$$\dot{m}_{cavity} = \rho_2 2ƒH\left[(4-\pi)\left(\frac{E^2 - 2ER_1 + 3R_1^2}{4}\right) - \pi R_1^2\left(1-\sqrt{2}\right)^2\right],$$

$$\dot{m}_{leakage} = \rho_t\sqrt{\gamma_t R_g T_t}\left(2G\sqrt{\left[\pi T_{helix}\left(E + R_1\left(1-\sqrt{2}\right)\right)\right]^2 + H^2} + R_1^2\left[4 - \pi - \pi\left(1-\sqrt{2}\right)^2\right]\right).$$

PRE Isentropic Efficiency (CSE core)

$$E_{system} = \frac{\dot{V}_{cav.net} \cdot (P_2 - P_3)}{\dot{m}_{tot}(h_1 - h_{3,Isentropic})} = \frac{\dot{w}_{shaft}}{\dot{m}_{tot}(h_1 - h_{3,Isentropic})}, \quad (89)$$

where:

$$\dot{w}_{shaft} = 2ƒH\left((4-\pi)\left(\frac{E^2 - 2ER_1 + 3R_1^2}{4}\right) - \left[L^2 - \frac{\pi D^2}{4} + \left(D^2\cos^{-1}\left(\frac{L}{D}\right) - L\sqrt{D^2 - L^2}\right)\right]\right) \cdot (P_2 - P_3)$$

$$\dot{m}_{tot} = \dot{m}_{cavity} + \dot{m}_{leakage.}$$

and:

$$\dot{m}_{cavity} = \rho_2 2ƒH\left[(4-\pi)\left(\frac{E^2 - 2ER_1 + 3R_1^2}{4}\right) - \left[L^2 - \frac{\pi D^2}{4} + \left[D^2\cos^{-1}\left(\frac{L}{D}\right) - L\sqrt{D^2 - L^2}\right]\right]\right],$$

$$\dot{m}_{leakage} = \rho_t\sqrt{\gamma_t R_g T_t}\left(2G\sqrt{\left[\pi T_{helix}\left(E + R_1\left(1-\sqrt{2}\right)\right)\right]^2 + H^2}\right.$$

$$\left. + \left[R_1^2(4-\pi) - L^2 + \frac{\pi D^2}{4} - \left(D^2\cos^{-1}\left(\frac{L}{D}\right) - L\sqrt{D^2 - L^2}\right)\right]\right).$$

Again, note that the throat variables in the leakage mass flowrate term are iteratively calculated. State 2 pressure P_2 is the calculated variable either through further iteration in an energy recovery application, or from equation 5 in a target power application.

III. CASE STUDIES

Chapter 3 calculates isentropic efficiency using equation 88 in various applications. The strategy for calculating isentropic efficiency is different depending on the application. As previously mentioned, two primary applications exist for the PRE: target power and energy recovery. For both applications, a sequential approach is used to obtain the independent variables required for evaluating equation 88.

Three fluid states exist for both applications as shown with Figure 5 and Figure 6. State 1 properties are known for both applications along with state 3 pressure. All other properties are evaluated using the given application. The primary difference between calculating isentropic efficiency of an energy recovery and target power application is calculating state 2 pressure (cavity pressure). Energy recovery requires that total mass flow rate remains constant. This requires an iterative process to determine state 2 cavity pressure. Target power requires that power output remain constant and uses Equation 5 to determine state 2 cavity pressure based on the application's load requirement.

Both applications will be analyzed separately fixing rotational speed and rotor size, yielding four studies. These studies serve two purposes. One, to demonstrate the behavior and influence the free variables possess. The second is that packaging a PRE employs other constraints due to auxiliary equipment. For example, an application might require a 60 Hz frequency generator. This holds the PRE to a set rotational speed. Another example is that a built PRE could be used in different applications keeping rotor geometries fixed, and if possible, the speed can be altered to optimize efficiency. Study 5 optimizes rotor geometry and rotor speed of the PRE for both energy recovery and target power.

All studies employ a grid analysis using Excel, which was chosen because of its integration with REFPROP, a NIST based thermodynamic data base. All thermodynamic state parameters are calculated using REFPROP through excel allowing the state parameters like temperature, specific heat ratio, and density to be calculated directly. This is especially advantageous in study 1 and study 2 where an energy recovery application is investigated. As mentioned, energy recovery requires an iterative process to determine state 2 pressure P_2. REFPROP through excel allows the thermodynamic variables to be calculated live with the iterative solver in these studies. REFPROP in excel also allows throat properties to be iteratively solved (see section 2.2.1) automatically using Excel's circular reference iterator. Note that energy recovery requires 2 iterative functions; iterating state 2 pressure P_2, and iterating throat properties for every state 2 pressure iteration. A target power application only requires iterating throat properties from section 2.2.1.

3.1 STUDY 1 – ENERGY RECOVERY VARIABLE ROTOR SIZE

This study calculates equation 88 step by step to yield the isentropic efficiencies of 400 possible rotor height H and machine radius E combinations (grid analysis) for an energy recovery application. The rotational frequency ƒ is held at a constant value typically found in industry, and other given parameters for this study are below. Study 1 demonstrates how rotor geometry influences isentropic efficiency and shows how to optimize a PRE when a constant rotational speed is required by the application. Figure 30 shows the calculation process for evaluating an energy recovery process. Each step of this process is shown in study 1 below.

Process Fluid	Methane	State 1 Pressure	1200 psi
Molecular Weight	16.04 kg/kmol	State 1 Temperature	100 °F
Specific Gas Constant	518.27 kJ/kg°K	State 1 Enthalpy (reference)	863.1 kJ/kg
Expander Frequency	60 Hz	State 1 Entropy(reference)	4.3 kJ/kg°K
Tip Radius R_1	.125''	State 3 Pressure	200 psi
Rotor Gap G	.005''	State 3 Isentropic Enthalpy $h_{3,Isentropic}$	658.2 kJ/kg
System Mass Flowrate	1 kg/s		

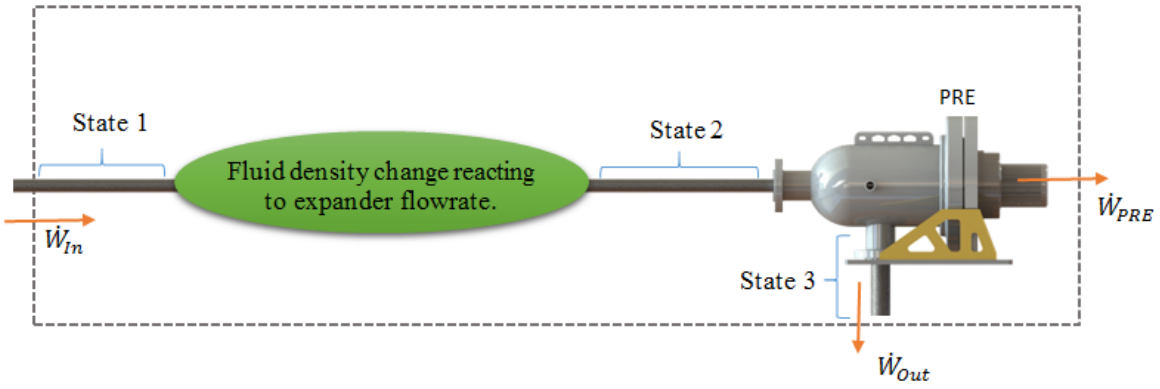

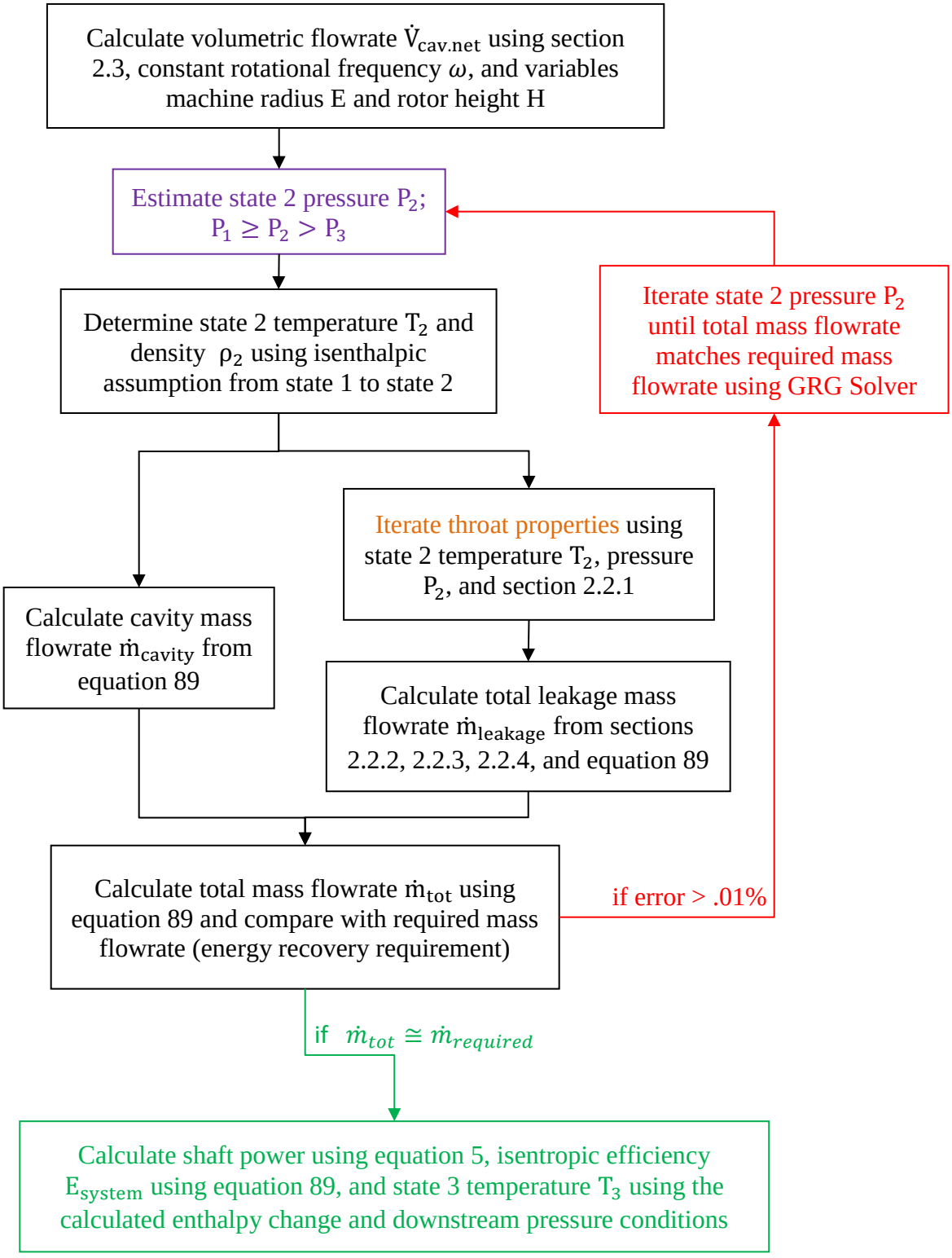

Figure 30: Study 1 Energy Recovery Calculation Process

The primary focus when calculating equation 88 is determining state 2 pressure for each rotor size configuration (pressure inside the cavity). State 2 pressure drives the mass flowrate calculation in the cavity and the leakage points (see section 2.2.1). Since total mass flowrate is coupled to state 2 pressure via the sum of cavity and leakage flowrates, an iterative solver is required to calculate equation 88. The state 2 pressure P_2 iterative solver used for this study was performed using the GRG nonlinear method in Excel. Since an energy recovery application gives the required mass flowrate, it is set as the objective variable (i.e. all required inputs for state 2 pressure must yield 1 kg/s total mass flowrate). The state 2 pressure is the free variable and has upper and lower bounds set by state 1 and state 3 pressures. The solver has a tolerance of .01%.

First, the cavity volumetric flowrate is calculated using the net cavity flowrate equation 84, and due to using a circular core, equation 22 is used to calculate core area. Note that machine radius E and rotor height H are given in inches.

Table 1: Study 1 Net Cavity Flowrate $\dot{V}_{cav.net}\left(\frac{ft.^3}{min.}\right)$

	H (in.)																			
E (in.)	0.5	1.0	1.5	2.0	2.5	3.0	3.5	4.0	4.5	5.0	5.5	6.0	6.5	7.0	7.5	8.0	8.5	9.0	9.5	10.0
0.5	0.1	0.1	0.2	0.2	0.3	0.4	0.4	0.5	0.5	0.6	0.7	0.7	0.8	0.8	0.9	0.9	1.0	1.1	1.1	1.2
1.0	0.3	0.7	1.0	1.4	1.7	2.0	2.4	2.7	3.0	3.4	3.7	4.1	4.4	4.7	5.1	5.4	5.8	6.1	6.4	6.8
1.5	0.8	1.7	2.5	3.4	4.2	5.0	5.9	6.7	7.6	8.4	9.3	10.1	10.9	11.8	12.6	13.5	14.3	15.1	16.0	16.8
2.0	1.6	3.1	4.7	6.3	7.8	9.4	11.0	12.5	14.1	15.7	17.2	18.8	20.4	21.9	23.5	25.1	26.6	28.2	29.8	31.3
2.5	2.5	5.0	7.5	10.1	12.6	15.1	17.6	20.1	22.6	25.2	27.7	30.2	32.7	35.2	37.7	40.3	42.8	45.3	47.8	50.3
3.0	3.7	7.4	11.1	14.8	18.4	22.1	25.8	29.5	33.2	36.9	40.6	44.3	48.0	51.7	55.3	59.0	62.7	66.4	70.1	73.8
3.5	5.1	10.2	15.3	20.3	25.4	30.5	35.6	40.7	45.8	50.9	55.9	61.0	66.1	71.2	76.3	81.4	86.5	91.5	96.6	101.7
4.0	6.7	13.4	20.1	26.8	33.5	40.2	46.9	53.6	60.3	67.1	73.8	80.5	87.2	93.9	100.6	107.3	114.0	120.7	127.4	134.1
4.5	8.5	17.1	25.6	34.2	42.7	51.3	59.8	68.4	76.9	85.5	94.0	102.6	111.1	119.7	128.2	136.8	145.3	153.9	162.4	171.0
5.0	10.6	21.2	31.8	42.5	53.1	63.7	74.3	84.9	95.5	106.1	116.8	127.4	138.0	148.6	159.2	169.8	180.5	191.1	201.7	212.3
5.5	12.9	25.8	38.7	51.6	64.5	77.4	90.3	103.2	116.1	129.0	142.0	154.9	167.8	180.7	193.6	206.5	219.4	232.3	245.2	258.1
6.0	15.4	30.8	46.3	61.7	77.1	92.5	107.9	123.3	138.8	154.2	169.6	185.0	200.4	215.9	231.3	246.7	262.1	277.5	292.9	308.4
6.5	18.2	36.3	54.5	72.6	90.8	108.9	127.1	145.2	163.4	181.5	199.7	217.9	236.0	254.2	272.3	290.5	308.6	326.8	344.9	363.1
7.0	21.1	42.2	63.3	84.5	105.6	126.7	147.8	168.9	190.0	211.1	232.3	253.4	274.5	295.6	316.7	337.8	359.0	380.1	401.2	422.3
7.5	24.3	48.6	72.9	97.2	121.5	145.8	170.1	194.4	218.7	243.0	267.3	291.6	315.9	340.2	364.5	388.8	413.1	437.4	461.7	486.0
8.0	27.7	55.4	83.1	110.8	138.5	166.2	193.9	221.6	249.3	277.1	304.8	332.5	360.2	387.9	415.6	443.3	471.0	498.7	526.4	554.1
8.5	31.3	62.7	94.0	125.3	156.7	188.0	219.3	250.7	282.0	313.4	344.7	376.0	407.4	438.7	470.0	501.4	532.7	564.0	595.4	626.7
9.0	35.2	70.4	105.6	140.8	175.9	211.1	246.3	281.5	316.7	351.9	387.1	422.3	457.5	492.6	527.8	563.0	598.2	633.4	668.6	703.8
9.5	39.3	78.5	117.8	157.1	196.3	235.6	274.9	314.1	353.4	392.7	431.9	471.2	510.5	549.7	589.0	628.3	667.5	706.8	746.1	785.3
10.0	43.6	87.1	130.7	174.3	217.8	261.4	305.0	348.5	392.1	435.7	479.2	522.8	566.4	609.9	653.5	697.1	740.6	784.2	827.8	871.3

Equation 84 $$\dot{V}_{cav.net} = 2ʃH\left[(4-\pi)\left(\frac{E^2 - 2ER_1 + 3R_1^2}{4}\right) - A_{Core}\right]$$

Equation 22 $$A_{CylCore} = \pi R_1^2\left(1-\sqrt{2}\right)^2$$

Next, state 2 pressure P_2 is estimated to progress the calculation through the process in Figure 30. Table 1, equation 86, and iterating the system to state 2 pressure allow for mass flowrates to be calculated. Table 2 shows the converged values of the solver. Dashes in the table indicate an impossible scenario where the rotor size combination would result in a cavity pressure higher than state 1 or lower than state 3.

Table 2: Study 1 State 2 Pressure (cavity pressure)

$$P_2 \left(\frac{\text{lbs}}{\text{in.}^2}\right)$$

E (in.) \ H (in.)	0.5	1.0	1.5	2.0	2.5	3.0	3.5	4.0	4.5	5.0	5.5	6.0	6.5	7.0	7.5	8.0	8.5	9.0	9.5	10.0
0.5	-	-	-	-	-	-	-	-	-	-	-	-	-	-	-	1190	1142	1095	1051	1010
1.0	-	-	-	-	-	-	-	-	-	-	-	-	-	1188	1133	1080	1031	985	943	905
1.5	-	-	-	-	-	-	-	-	-	-	-	1134	1070	1012	959	912	867	827	790	756
2.0	-	-	-	-	-	-	-	-	1135	1058	989	927	870	820	775	734	698	664	633	605
2.5	-	-	-	-	-	1171	1075	991	916	849	790	739	693	652	615	582	552	526	501	478
3.0	-	-	-	1162	1051	954	869	796	733	678	630	588	551	518	489	462	438	416	397	379
3.5	-	-	1090	969	865	779	706	645	591	547	508	473	443	416	392	371	351	334	318	304
4.0	-	1070	928	813	719	643	580	529	484	446	414	385	360	338	319	301	286	271	258	247
4.5	1113	935	795	688	605	538	484	439	402	370	342	319	298	279	263	248	235	224	213	203
5.0	1001	820	687	589	515	456	409	370	338	310	287	267	249	234	220	208	-	-	-	-
5.5	904	724	599	510	442	390	349	315	287	264	244	226	211	-	-	-	-	-	-	-
6.0	818	643	527	445	384	338	301	271	247	226	209	-	-	-	-	-	-	-	-	-
6.5	745	575	466	391	336	295	262	236	214	-	-	-	-	-	-	-	-	-	-	-
7.0	681	518	416	347	297	260	230	207	-	-	-	-	-	-	-	-	-	-	-	-
7.5	625	468	373	309	264	230	204	-	-	-	-	-	-	-	-	-	-	-	-	-
8.0	575	425	336	278	236	205	-	-	-	-	-	-	-	-	-	-	-	-	-	-
8.5	532	388	305	251	213	-	-	-	-	-	-	-	-	-	-	-	-	-	-	-
9.0	493	356	278	227	-	-	-	-	-	-	-	-	-	-	-	-	-	-	-	-
9.5	458	327	254	207	-	-	-	-	-	-	-	-	-	-	-	-	-	-	-	-
10.0	427	302	233	-	-	-	-	-	-	-	-	-	-	-	-	-	-	-	-	-

SOLVER $P_2(\dot{m}_{tot})$ Iteratively solved using objective solver

Note the dark purple values in the above table require the lowest pressure drop when moving from the state 1 reservoir to the state 2 cavity. Initially this would lead to the expectation that those machine sizes would yield the highest isentropic efficiency (lowest increase in entropy). These machine sizes will be compared with the final calculations to test the validity of this assumption.

State 2 temperature and density can be determined by assuming an isenthalpic process from state 1 to state 2 (h1=h2). Having two state variables, state 2 pressure from Table 2 and

state 1 enthalpy, state 2 temperature and density are calculated using NIST REFPROP. State 2 temperature and density are required when determining cavity and leakage mass flowrates.

Table 3: Study 1 State 2 Temperature T_2 (°F)

E (in.) \ H (in.)	0.5	1.0	1.5	2.0	2.5	3.0	3.5	4.0	4.5	5.0	5.5	6.0	6.5	7.0	7.5	8.0	8.5	9.0	9.5	10.0
0.5	-	-	-	-	-	-	-	-	-	-	-	-	-	-	-	99.6	97.6	95.6	93.8	92.0
1.0	-	-	-	-	-	-	-	-	-	-	-	-	-	99.5	97.2	95.0	92.9	90.8	89.0	87.2
1.5	-	-	-	-	-	-	-	-	-	-	-	97.3	94.6	92.0	89.7	87.5	85.5	83.6	81.8	80.2
2.0	-	-	-	-	-	-	-	-	97.3	94.1	91.0	88.2	85.6	83.3	81.1	79.1	77.3	75.6	74.1	72.6
2.5	-	-	-	-	-	98.8	94.8	91.1	87.7	84.6	81.8	79.3	77.1	75.0	73.1	71.4	69.9	68.5	67.2	65.9
3.0	-	-	-	98.4	93.7	89.5	85.5	82.1	79.1	76.3	73.9	71.7	69.8	68.1	66.5	65.1	63.7	62.6	61.5	60.5
3.5	-	-	95.4	90.2	85.4	81.3	77.7	74.7	71.9	69.6	67.5	65.7	64.0	62.5	61.2	60.0	58.9	57.9	57.0	56.2
4.0	-	94.6	88.3	82.9	78.4	74.6	71.4	68.6	66.3	64.2	62.4	60.8	59.4	58.2	57.1	56.1	55.2	54.3	53.6	52.9
4.5	96.4	88.6	82.1	76.9	72.6	69.1	66.3	63.8	61.7	60.0	58.4	57.1	55.9	54.8	53.9	53.0	52.2	51.6	50.9	50.3
5.0	91.5	83.2	76.8	71.8	67.9	64.7	62.1	60.0	58.2	56.6	55.3	54.1	53.1	52.1	51.3	50.6	-	-	-	-
5.5	87.2	78.6	72.3	67.6	64.0	61.1	58.8	56.9	55.3	53.9	52.7	51.7	50.8	-	-	-	-	-	-	-
6.0	83.2	74.6	68.5	64.1	60.8	58.2	56.1	54.4	52.9	51.7	50.7	-	-	-	-	-	-	-	-	-
6.5	79.7	71.1	65.3	61.2	58.1	55.7	53.8	52.3	51.0	-	-	-	-	-	-	-	-	-	-	-
7.0	76.5	68.1	62.5	58.7	55.8	53.7	52.0	50.6	-	-	-	-	-	-	-	-	-	-	-	-
7.5	73.6	65.4	60.1	56.5	53.9	51.9	50.4	-	-	-	-	-	-	-	-	-	-	-	-	-
8.0	71.1	63.0	58.1	54.7	52.3	50.5	-	-	-	-	-	-	-	-	-	-	-	-	-	-
8.5	68.8	61.0	56.3	53.1	50.9	-	-	-	-	-	-	-	-	-	-	-	-	-	-	-
9.0	66.7	59.2	54.7	51.8	-	-	-	-	-	-	-	-	-	-	-	-	-	-	-	-
9.5	64.9	57.6	53.3	50.6	-	-	-	-	-	-	-	-	-	-	-	-	-	-	-	-
10.0	63.2	56.1	52.1	-	-	-	-	-	-	-	-	-	-	-	-	-	-	-	-	-

Table 4: Study 1 State 2 Density ρ_2 $\left(\frac{kg}{m^3}\right)$

E (in.) \ H (in.)	0.5	1.0	1.5	2.0	2.5	3.0	3.5	4.0	4.5	5.0	5.5	6.0	6.5	7.0	7.5	8.0	8.5	9.0	9.5	10.0
0.5	-	-	-	-	-	-	-	-	-	-	-	-	-	-	-	57.1	54.8	52.7	50.6	48.7
1.0	-	-	-	-	-	-	-	-	-	-	-	-	-	57.0	54.4	51.9	49.6	47.5	45.5	43.7
1.5	-	-	-	-	-	-	-	-	-	-	-	54.5	51.5	48.8	46.3	44.0	41.9	40.0	38.2	36.6
2.0	-	-	-	-	-	-	-	-	54.5	50.9	47.7	44.7	42.1	39.7	37.5	35.6	33.8	32.2	30.7	29.3
2.5	-	-	-	-	-	56.2	51.7	47.8	44.2	41.0	38.2	35.8	33.5	31.6	29.8	28.2	26.8	25.5	24.3	23.2
3.0	-	-	-	55.7	50.6	46.0	42.0	38.5	35.5	32.9	30.5	28.5	26.7	25.1	23.7	22.4	21.2	20.2	19.2	18.4
3.5	-	-	52.4	46.8	41.8	37.7	34.2	31.2	28.7	26.5	24.6	22.9	21.5	20.2	19.0	18.0	17.0	16.2	15.4	14.7
4.0	-	51.5	44.8	39.3	34.8	31.2	28.1	25.6	23.5	21.6	20.1	18.7	17.4	16.4	15.4	14.6	13.8	13.1	12.5	11.9
4.5	53.5	45.1	38.5	33.3	29.3	26.1	23.5	21.3	19.5	17.9	16.6	15.4	14.4	13.5	12.7	12.0	11.4	10.8	10.3	9.8
5.0	48.2	39.6	33.3	28.6	25.0	22.1	19.8	17.9	16.4	15.0	13.9	12.9	12.1	11.3	10.6	10.0	-	-	-	-
5.5	43.7	35.1	29.0	24.7	21.4	18.9	16.9	15.3	13.9	12.8	11.8	10.9	10.2	-	-	-	-	-	-	-
6.0	39.6	31.2	25.5	21.6	18.6	16.4	14.6	13.1	12.0	11.0	10.1	-	-	-	-	-	-	-	-	-
6.5	36.1	27.9	22.6	19.0	16.3	14.3	12.7	11.4	10.4	-	-	-	-	-	-	-	-	-	-	-
7.0	33.0	25.1	20.1	16.8	14.4	12.6	11.1	10.0	-	-	-	-	-	-	-	-	-	-	-	-
7.5	30.3	22.7	18.1	15.0	12.8	11.1	9.9	-	-	-	-	-	-	-	-	-	-	-	-	-
8.0	27.9	20.6	16.3	13.4	11.4	9.9	-	-	-	-	-	-	-	-	-	-	-	-	-	-
8.5	25.8	18.8	14.8	12.1	10.3	-	-	-	-	-	-	-	-	-	-	-	-	-	-	-
9.0	23.9	17.2	13.4	11.0	-	-	-	-	-	-	-	-	-	-	-	-	-	-	-	-
9.5	22.2	15.8	12.3	10.0	-	-	-	-	-	-	-	-	-	-	-	-	-	-	-	-
10.0	20.7	14.6	11.3	-	-	-	-	-	-	-	-	-	-	-	-	-	-	-	-	-

NIST REFPROP $T_2(P_2, h_1)$ isenthalpic

NIST REFPROP $\rho_2(P_2, T_2)$

Cavity mass flowrate can be calculated using Table 1 and Table 4, and is the product of volumetric flowrate and density (see equation 2).

Table 5: Study 1 Cavity Mass Flowrate $\dot{m}_{cav.net}\left(\frac{kg}{s}\right)$

E (in.) \ H (in.)	0.5	1.0	1.5	2.0	2.5	3.0	3.5	4.0	4.5	5.0	5.5	6.0	6.5	7.0	7.5	8.0	8.5	9.0	9.5	10.0
0.5	-	-	-	-	-	-	-	-	-	-	-	-	-	-	-	1.00	1.00	1.00	1.00	1.00
1.0	-	-	-	-	-	-	-	-	-	-	-	-	-	1.00	1.00	1.00	1.00	1.00	1.00	1.00
1.5	-	-	-	-	-	-	-	-	-	-	-	1.00	1.00	1.00	1.00	1.00	1.00	1.00	1.00	1.00
2.0	-	-	-	-	-	-	-	-	1.00	1.00	1.00	1.00	1.00	1.00	1.00	1.00	1.00	1.00	1.00	1.00
2.5	-	-	-	-	-	1.00	1.00	1.00	1.00	1.00	1.00	1.00	1.00	1.00	1.00	1.00	1.00	1.00	1.00	1.00
3.0	-	-	-	1.00	1.00	1.00	1.00	1.00	1.00	1.00	1.00	1.00	1.00	1.00	1.00	1.00	1.00	1.00	1.00	1.00
3.5	-	-	1.00	1.00	1.00	1.00	1.00	1.00	1.00	1.00	1.00	1.00	1.00	1.00	1.00	1.00	1.00	1.00	1.00	1.00
4.0	-	1.00	1.00	1.00	1.00	1.00	1.00	1.00	1.00	1.00	1.00	1.00	1.00	1.00	1.00	1.00	1.00	1.00	1.00	1.00
4.5	1.00	1.00	1.00	1.00	1.00	1.00	1.00	1.00	1.00	1.00	1.00	1.00	1.00	1.00	1.00	1.00	1.00	1.00	1.00	1.00
5.0	1.00	1.00	1.00	1.00	1.00	1.00	1.00	1.00	1.00	1.00	1.00	1.00	1.00	1.00	1.00	1.00	-	-	-	-
5.5	1.00	1.00	1.00	1.00	1.00	1.00	1.00	1.00	1.00	1.00	1.00	1.00	1.00	-	-	-	-	-	-	-
6.0	1.00	1.00	1.00	1.00	1.00	1.00	1.00	1.00	1.00	1.00	1.00	-	-	-	-	-	-	-	-	-
6.5	1.00	1.00	1.00	1.00	1.00	1.00	1.00	1.00	1.00	-	-	-	-	-	-	-	-	-	-	-
7.0	1.00	1.00	1.00	1.00	1.00	1.00	1.00	1.00	-	-	-	-	-	-	-	-	-	-	-	-
7.5	1.00	1.00	1.00	1.00	1.00	1.00	1.00	-	-	-	-	-	-	-	-	-	-	-	-	-
8.0	1.00	1.00	1.00	1.00	1.00	1.00	-	-	-	-	-	-	-	-	-	-	-	-	-	-
8.5	1.00	1.00	1.00	1.00	1.00	-	-	-	-	-	-	-	-	-	-	-	-	-	-	-
9.0	1.00	1.00	1.00	1.00	-	-	-	-	-	-	-	-	-	-	-	-	-	-	-	-
9.5	1.00	1.00	1.00	1.00	-	-	-	-	-	-	-	-	-	-	-	-	-	-	-	-
10.0	1.00	1.00	1.00	-	-	-	-	-	-	-	-	-	-	-	-	-	-	-	-	-

Equation 2 $\dot{m}_{cav.net} = \rho_2 \cdot \dot{V}_{cav.net}$

Total leakage flowrate is the sum of all leak points and is required to determine isentropic efficiency. This is done by evaluating the general states at leakage throat points using equations 18 and 19 with an iterative process involving the throat specific heat ratio (see section 2.2.1). Note the values in red on Table 7 indicate nonchoked configurations. This is for reference (see appendix B for details). Table 7: Study 1 Throat Pressure $P_t\left(\frac{lbs}{in.^2}\right)$This iterative process yields the following:

Equation 18 $$T_t = \frac{T_2}{1 + \frac{\gamma_t - 1}{2}}$$

Equation 19 $$P_t = \frac{P_2}{\left(1 + \frac{\gamma_t - 1}{2}\right)^{\frac{\gamma_t}{\gamma_t - 1}}}$$

NIST REFPROP $\gamma_t\,(T_t, P_t)$

Table 6: Study 1 Throat Temperature T_t (°F)

E (in.) \ H (in.)	0.5	1.0	1.5	2.0	2.5	3.0	3.5	4.0	4.5	5.0	5.5	6.0	6.5	7.0	7.5	8.0	8.5	9.0	9.5	10.0
0.5	-	-	-	-	-	-	-	-	-	-	-	-	-	-	-	-36.1	-33.7	-31.7	-30.2	-29.0
1.0	-	-	-	-	-	-	-	-	-	-	-	-	-	-36.0	-33.3	-31.2	-29.6	-28.3	-27.4	-26.7
1.5	-	-	-	-	-	-	-	-	-	-	-	-33.3	-30.8	-29.1	-27.7	-26.8	-26.0	-25.5	-25.1	-24.8
2.0	-	-	-	-	-	-	-	-	-33.4	-30.4	-28.4	-27.1	-26.1	-25.4	-25.0	-24.6	-24.4	-24.3	-24.2	-24.2
2.5	-	-	-	-	-	-35.1	-31.0	-28.5	-26.9	-25.8	-25.1	-24.7	-24.4	-24.3	-24.2	-24.2	-24.3	-24.3	-24.4	-24.6
3.0	-	-	-	-34.6	-30.2	-27.6	-26.1	-25.2	-24.6	-24.4	-24.2	-24.2	-24.3	-24.4	-24.5	-24.7	-24.8	-25.0	-25.1	-25.3
3.5	-	-	-31.6	-28.0	-26.0	-25.0	-24.5	-24.3	-24.2	-24.3	-24.4	-24.6	-24.8	-25.0	-25.2	-25.4	-25.6	-25.8	-25.9	-26.1
4.0	-	-30.8	-27.1	-25.3	-24.5	-24.3	-24.2	-24.3	-24.5	-24.8	-25.0	-25.2	-25.5	-25.7	-25.9	-26.1	-26.3	-26.5	-26.7	-26.9
4.5	-32.4	-27.2	-25.1	-24.4	-24.2	-24.3	-24.5	-24.8	-25.1	-25.4	-25.7	-25.9	-26.2	-26.4	-26.6	-26.8	-27.0	-27.2	-27.4	-27.5
5.0	-28.8	-25.4	-24.4	-24.2	-24.4	-24.7	-25.0	-25.4	-25.7	-26.0	-26.3	-26.6	-26.8	-27.0	-27.2	-27.4	-	-	-	-
5.5	-26.7	-24.6	-24.2	-24.4	-24.8	-25.2	-25.6	-26.0	-26.3	-26.6	-26.9	-27.2	-27.4	-	-	-	-	-	-	-
6.0	-25.4	-24.3	-24.3	-24.8	-25.2	-25.7	-26.1	-26.5	-26.9	-27.2	-27.4	-	-	-	-	-	-	-	-	-
6.5	-24.7	-24.2	-24.6	-25.2	-25.7	-26.2	-26.6	-27.0	-27.3	-	-	-	-	-	-	-	-	-	-	-
7.0	-24.4	-24.4	-25.0	-25.6	-26.2	-26.7	-27.1	-27.4	-	-	-	-	-	-	-	-	-	-	-	-
7.5	-24.2	-24.6	-25.4	-26.0	-26.6	-27.1	-27.5	-	-	-	-	-	-	-	-	-	-	-	-	-
8.0	-24.2	-24.9	-25.7	-26.4	-27.0	-27.5	-	-	-	-	-	-	-	-	-	-	-	-	-	-
8.5	-24.3	-25.2	-26.1	-26.8	-27.4	-	-	-	-	-	-	-	-	-	-	-	-	-	-	-
9.0	-24.5	-25.5	-26.4	-27.1	-	-	-	-	-	-	-	-	-	-	-	-	-	-	-	-
9.5	-24.7	-25.8	-26.8	-27.4	-	-	-	-	-	-	-	-	-	-	-	-	-	-	-	-
10.0	-24.9	-26.1	-27.1	-	-	-	-	-	-	-	-	-	-	-	-	-	-	-	-	-

Table 7: Study 1 Throat Pressure P_t $\left(\frac{\text{lbs}}{\text{in.}^2}\right)$

E (in.) \ H (in.)	0.5	1.0	1.5	2.0	2.5	3.0	3.5	4.0	4.5	5.0	5.5	6.0	6.5	7.0	7.5	8.0	8.5	9.0	9.5	10.0
0.5	-	-	-	-	-	-	-	-	-	-	-	-	-	-	-	584	565	545	526	508
1.0	-	-	-	-	-	-	-	-	-	-	-	-	-	583	561	538	517	496	477	459
1.5	-	-	-	-	-	-	-	-	-	-	-	561	534	508	484	463	442	423	405	389
2.0	-	-	-	-	-	-	-	-	562	529	498	470	444	420	398	379	361	344	329	315
2.5	-	-	-	-	-	576	536	499	465	434	405	381	358	338	320	304	289	275	263	251
3.0	-	-	-	573	526	482	443	408	378	351	328	306	288	272	257	243	231	220	210	201
3.5	-	-	543	489	441	400	365	335	308	286	266	249	233	219	207	196	186	177	169	161
4.0	-	534	471	416	371	334	303	277	255	235	218	204	191	180	169	160	152	145	138	132
4.5	552	473	408	356	315	282	254	231	212	196	182	169	158	149	140	133	126	119	114	109
5.0	503	420	356	307	270	240	216	196	179	165	153	142	133	125	118	111	-	-	-	-
5.5	459	374	312	267	233	206	185	167	153	141	130	121	113	-	-	-	-	-	-	-
6.0	419	334	276	234	203	179	160	145	132	121	112	-	-	-	-	-	-	-	-	-
6.5	384	300	245	207	179	157	140	126	115	-	-	-	-	-	-	-	-	-	-	-
7.0	353	272	219	184	158	138	123	111	-	-	-	-	-	-	-	-	-	-	-	-
7.5	325	246	197	164	141	123	109	-	-	-	-	-	-	-	-	-	-	-	-	-
8.0	300	224	178	148	126	110	-	-	-	-	-	-	-	-	-	-	-	-	-	-
8.5	279	205	162	134	114	-	-	-	-	-	-	-	-	-	-	-	-	-	-	-
9.0	259	189	148	121	-	-	-	-	-	-	-	-	-	-	-	-	-	-	-	-
9.5	241	174	135	111	-	-	-	-	-	-	-	-	-	-	-	-	-	-	-	-
10.0	225	161	124	-	-	-	-	-	-	-	-	-	-	-	-	-	-	-	-	-

Table 8: Study 1 Throat Specific Heat Ratio γ_t

E (in.) \ H (in.)	0.5	1.0	1.5	2.0	2.5	3.0	3.5	4.0	4.5	5.0	5.5	6.0	6.5	7.0	7.5	8.0	8.5	9.0	9.5	10.0
0.5	-	-	-	-	-	-	-	-	-	-	-	-	-	-	-	1.64	1.62	1.60	1.58	1.56
1.0	-	-	-	-	-	-	-	-	-	-	-	-	-	1.64	1.61	1.59	1.57	1.55	1.54	1.53
1.5	-	-	-	-	-	-	-	-	-	-	-	1.61	1.58	1.56	1.54	1.53	1.51	1.50	1.49	1.48
2.0	-	-	-	-	-	-	-	-	1.61	1.58	1.55	1.53	1.52	1.50	1.49	1.48	1.47	1.46	1.45	1.44
2.5	-	-	-	-	-	1.63	1.59	1.56	1.53	1.51	1.49	1.48	1.47	1.46	1.45	1.44	1.43	1.43	1.42	1.42
3.0	-	-	-	1.63	1.58	1.54	1.51	1.49	1.48	1.46	1.45	1.44	1.43	1.42	1.42	1.41	1.41	1.40	1.40	1.39
3.5	-	-	1.59	1.55	1.51	1.49	1.47	1.45	1.44	1.43	1.42	1.41	1.41	1.40	1.40	1.39	1.39	1.39	1.38	1.38
4.0	-	1.58	1.53	1.50	1.47	1.45	1.44	1.43	1.42	1.41	1.40	1.40	1.39	1.39	1.38	1.38	1.38	1.37	1.37	1.37
4.5	1.60	1.54	1.49	1.47	1.44	1.43	1.42	1.41	1.40	1.39	1.39	1.38	1.38	1.37	1.37	1.37	1.37	1.36	1.36	1.36
5.0	1.56	1.50	1.46	1.44	1.42	1.41	1.40	1.39	1.39	1.38	1.38	1.37	1.37	1.37	1.36	1.36	-	-	-	-
5.5	1.53	1.47	1.44	1.42	1.41	1.40	1.39	1.38	1.38	1.37	1.37	1.36	1.36	-	-	-	-	-	-	-
6.0	1.50	1.45	1.43	1.41	1.40	1.39	1.38	1.37	1.37	1.36	1.36	-	-	-	-	-	-	-	-	-
6.5	1.48	1.44	1.41	1.40	1.39	1.38	1.37	1.37	1.36	-	-	-	-	-	-	-	-	-	-	-
7.0	1.46	1.42	1.40	1.39	1.38	1.37	1.37	1.36	-	-	-	-	-	-	-	-	-	-	-	-
7.5	1.45	1.41	1.39	1.38	1.37	1.37	1.36	-	-	-	-	-	-	-	-	-	-	-	-	-
8.0	1.44	1.40	1.39	1.37	1.37	1.36	-	-	-	-	-	-	-	-	-	-	-	-	-	-
8.5	1.43	1.40	1.38	1.37	1.36	-	-	-	-	-	-	-	-	-	-	-	-	-	-	-
9.0	1.42	1.39	1.37	1.36	-	-	-	-	-	-	-	-	-	-	-	-	-	-	-	-
9.5	1.41	1.38	1.37	1.36	-	-	-	-	-	-	-	-	-	-	-	-	-	-	-	-
10.0	1.41	1.38	1.37	-	-	-	-	-	-	-	-	-	-	-	-	-	-	-	-	-

The throat density and local speed of sound can be calculated using

Table 6, Table 7, and Table 8 which will be used to calculate leakage mass flowrate.

Table 9: Study 1 Throat Density $\rho_t \left(\frac{kg}{m^3}\right)$

E (in.) \ H (in.)	0.5	1.0	1.5	2.0	2.5	3.0	3.5	4.0	4.5	5.0	5.5	6.0	6.5	7.0	7.5	8.0	8.5	9.0	9.5	10.0
0.5	-	-	-	-	-	-	-	-	-	-	-	-	-	-	-	39.56	37.59	35.76	34.09	32.57
1.0	-	-	-	-	-	-	-	-	-	-	-	-	-	39.47	37.22	35.17	33.34	31.65	30.16	28.81
1.5	-	-	-	-	-	-	-	-	-	-	-	37.27	34.80	32.64	30.73	29.06	27.51	26.13	24.88	23.74
2.0	-	-	-	-	-	-	-	-	37.33	34.35	31.79	29.59	27.63	25.91	24.39	23.03	21.82	20.72	19.72	18.82
2.5	-	-	-	-	-	38.76	35.01	31.90	29.20	26.89	24.88	23.17	21.65	20.31	19.12	18.06	17.10	16.25	15.47	14.75
3.0	-	-	-	38.39	34.08	30.56	27.56	25.09	22.99	21.18	19.62	18.24	17.06	16.02	15.08	14.24	13.49	12.81	12.19	11.63
3.5	-	-	35.56	31.10	27.44	24.51	22.11	20.09	18.37	16.93	15.68	14.59	13.63	12.79	12.04	11.37	10.77	10.23	9.74	9.29
4.0	-	34.81	29.65	25.65	22.54	20.05	18.01	16.36	14.95	13.75	12.73	11.84	11.04	10.37	9.76	9.22	8.73	8.29	7.89	7.53
4.5	36.44	29.87	25.05	21.52	18.80	16.66	14.94	13.52	12.35	11.35	10.49	9.75	9.11	8.54	8.04	7.59	7.18	6.82	6.49	6.19
5.0	32.23	25.89	21.48	18.29	15.91	14.04	12.56	11.35	10.35	9.50	8.78	8.15	7.61	7.13	6.71	6.33	-	-	-	-
5.5	28.79	22.68	18.62	15.76	13.62	11.99	10.70	9.65	8.78	8.05	7.44	6.90	6.44	-	-	-	-	-	-	-
6.0	25.85	20.05	16.30	13.69	11.79	10.35	9.21	8.29	7.54	6.91	6.37	-	-	-	-	-	-	-	-	-
6.5	23.39	17.85	14.38	12.02	10.31	9.02	8.01	7.20	6.54	-	-	-	-	-	-	-	-	-	-	-
7.0	21.28	16.02	12.78	10.63	9.09	7.93	7.03	6.31	-	-	-	-	-	-	-	-	-	-	-	-
7.5	19.45	14.43	11.45	9.47	8.07	7.02	6.21	-	-	-	-	-	-	-	-	-	-	-	-	-
8.0	17.85	13.08	10.31	8.49	7.21	6.26	-	-	-	-	-	-	-	-	-	-	-	-	-	-
8.5	16.46	11.92	9.33	7.65	6.48	-	-	-	-	-	-	-	-	-	-	-	-	-	-	-
9.0	15.23	10.91	8.48	6.93	-	-	-	-	-	-	-	-	-	-	-	-	-	-	-	-
9.5	14.13	10.02	7.75	6.31	-	-	-	-	-	-	-	-	-	-	-	-	-	-	-	-
10.0	13.15	9.24	7.10	-	-	-	-	-	-	-	-	-	-	-	-	-	-	-	-	-

NIST REPROP $\rho_t (T_t, P_t)$

Table 10: Study 1 Throat Average Velocity $\widetilde{V}_t \left(\frac{m}{s}\right)$

E (in.) \ H (in.)	0.5	1.0	1.5	2.0	2.5	3.0	3.5	4.0	4.5	5.0	5.5	6.0	6.5	7.0	7.5	8.0	8.5	9.0	9.5	10.0
0.5	-	-	-	-	-	-	-	-	-	-	-	-	-	-	-	447.3	445.3	443.4	441.6	440.1
1.0	-	-	-	-	-	-	-	-	-	-	-	-	-	447.2	444.9	442.8	440.9	439.1	437.6	436.2
1.5	-	-	-	-	-	-	-	-	-	-	-	444.9	442.4	440.1	438.2	436.4	434.8	433.4	432.1	430.9
2.0	-	-	-	-	-	-	-	-	445.0	441.9	439.3	437.0	435.0	433.2	431.6	430.1	428.8	427.7	426.6	425.6
2.5	-	-	-	-	-	446.5	442.6	439.4	436.6	434.2	432.1	430.3	428.7	427.2	426.0	424.8	423.8	422.8	422.0	421.2
3.0	-	-	-	446.1	441.6	438.0	434.9	432.3	430.1	428.2	426.5	425.0	423.7	422.6	421.5	420.6	419.8	419.0	418.3	417.7
3.5	-	-	443.2	438.5	434.8	431.7	429.2	427.0	425.1	423.6	422.2	421.0	419.9	419.0	418.1	417.4	416.7	416.1	415.5	415.0
4.0	-	442.4	437.0	432.9	429.6	427.0	424.8	422.9	421.4	420.1	418.9	417.9	417.0	416.3	415.6	414.9	414.4	413.9	413.4	413.0
4.5	444.1	437.3	432.3	428.5	425.6	423.3	421.4	419.8	418.5	417.4	416.4	415.5	414.8	414.1	413.6	413.0	412.6	412.2	411.8	411.4
5.0	439.7	433.1	428.5	425.1	422.5	420.4	418.7	417.4	416.2	415.3	414.4	413.7	413.1	412.5	412.0	411.6	-	-	-	-
5.5	436.2	429.8	425.4	422.3	419.9	418.1	416.6	415.4	414.4	413.6	412.9	412.2	411.7	-	-	-	-	-	-	-
6.0	433.1	426.9	422.9	420.0	417.9	416.2	414.9	413.9	413.0	412.3	411.6	-	-	-	-	-	-	-	-	-
6.5	430.5	424.6	420.8	418.1	416.2	414.7	413.5	412.6	411.8	-	-	-	-	-	-	-	-	-	-	-
7.0	428.3	422.6	419.0	416.5	414.8	413.4	412.4	411.6	-	-	-	-	-	-	-	-	-	-	-	-
7.5	426.3	420.8	417.5	415.2	413.6	412.4	411.4	-	-	-	-	-	-	-	-	-	-	-	-	-
8.0	424.6	419.3	416.2	414.1	412.6	411.5	-	-	-	-	-	-	-	-	-	-	-	-	-	-
8.5	423.1	418.0	415.1	413.1	411.8	-	-	-	-	-	-	-	-	-	-	-	-	-	-	-
9.0	421.7	416.9	414.1	412.3	-	-	-	-	-	-	-	-	-	-	-	-	-	-	-	-
9.5	420.5	415.9	413.2	411.6	-	-	-	-	-	-	-	-	-	-	-	-	-	-	-	-
10.0	419.4	415.0	412.5	-	-	-	-	-	-	-	-	-	-	-	-	-	-	-	-	-

Equation 16 $$\widetilde{V}_t = \sqrt{\gamma_t R_g T_t}$$

Next, the leak points cross sectional areas are calculated. Core leakage area using a cylindrical core is static as it is only dependent on R_1.

Table 11: Study 1 Core Leakage Area (cylindrical core)

$A_{CynLeakage}$ (in.^{2})

E (in.) \ H (in.)	0.5	1.0	1.5	2.0	2.5	3.0	3.5	4.0	4.5	5.0	5.5	6.0	6.5	7.0	7.5	8.0	8.5	9.0	9.5	10.0
0.5	.00499 in.^{2}																			
1.0																				
1.5																				
2.0																				
2.5																				
3.0																				
3.5																				
4.0																				
4.5																				
5.0																				
5.5																				
6.0																				
6.5																				
7.0																				
7.5																				
8.0																				
8.5																				
9.0																				
9.5																				
10.0																				

Equation 25 $$A_{CynLeakage} = R_1^2\left[4 - \pi - \pi\left(1 - \sqrt{2}\right)^2\right] \cong .319R_1^2$$

Table 12: Study 1 Rotor Gap Leakage Area

A_{gap} (in.^{2})

E (in.) \ H (in.)	0.5	1.0	1.5	2.0	2.5	3.0	3.5	4.0	4.5	5.0	5.5	6.0	6.5	7.0	7.5	8.0	8.5	9.0	9.5	10.0
0.5	0.009	0.012	0.017	0.021	0.026	0.031	0.036	0.041	0.046	0.050	0.055	0.060	0.065	0.070	0.075	0.080	0.085	0.090	0.095	0.100
1.0	0.016	0.018	0.021	0.025	0.029	0.033	0.038	0.043	0.047	0.052	0.057	0.062	0.067	0.072	0.076	0.081	0.086	0.091	0.096	0.101
1.5	0.023	0.025	0.027	0.030	0.034	0.038	0.042	0.046	0.050	0.055	0.060	0.064	0.069	0.074	0.078	0.083	0.088	0.093	0.098	0.103
2.0	0.031	0.032	0.034	0.037	0.040	0.043	0.046	0.050	0.054	0.059	0.063	0.067	0.072	0.076	0.081	0.086	0.090	0.095	0.100	0.105
2.5	0.039	0.040	0.041	0.043	0.046	0.049	0.052	0.055	0.059	0.063	0.067	0.071	0.076	0.080	0.084	0.089	0.093	0.098	0.102	0.107
3.0	0.047	0.047	0.049	0.050	0.053	0.055	0.058	0.061	0.065	0.068	0.072	0.076	0.080	0.084	0.088	0.092	0.097	0.101	0.106	0.110
3.5	0.054	0.055	0.056	0.058	0.060	0.062	0.064	0.067	0.070	0.074	0.077	0.081	0.085	0.089	0.093	0.097	0.101	0.105	0.109	0.114
4.0	0.062	0.063	0.064	0.065	0.067	0.069	0.071	0.074	0.077	0.080	0.083	0.086	0.090	0.094	0.097	0.101	0.105	0.109	0.113	0.118
4.5	0.070	0.071	0.071	0.073	0.074	0.076	0.078	0.081	0.083	0.086	0.089	0.092	0.095	0.099	0.103	0.106	0.110	0.114	0.118	0.122
5.0	0.078	0.078	0.079	0.080	0.082	0.083	0.085	0.087	0.090	0.092	0.095	0.098	0.101	0.105	0.108	0.112	0.115	0.119	0.123	0.127
5.5	0.086	0.086	0.087	0.088	0.089	0.091	0.092	0.094	0.097	0.099	0.102	0.105	0.107	0.111	0.114	0.117	0.121	0.124	0.128	0.132
6.0	0.094	0.094	0.095	0.096	0.097	0.098	0.100	0.102	0.104	0.106	0.108	0.111	0.114	0.117	0.120	0.123	0.126	0.130	0.133	0.137
6.5	0.101	0.102	0.102	0.103	0.104	0.106	0.107	0.109	0.111	0.113	0.115	0.118	0.120	0.123	0.126	0.129	0.132	0.135	0.139	0.142
7.0	0.109	0.110	0.110	0.111	0.112	0.113	0.115	0.116	0.118	0.120	0.122	0.125	0.127	0.130	0.132	0.135	0.138	0.141	0.145	0.148
7.5	0.117	0.117	0.118	0.119	0.120	0.121	0.122	0.124	0.125	0.127	0.129	0.131	0.134	0.136	0.139	0.142	0.145	0.148	0.151	0.154
8.0	0.125	0.125	0.126	0.126	0.127	0.128	0.130	0.131	0.133	0.134	0.136	0.139	0.141	0.143	0.146	0.148	0.151	0.154	0.157	0.160
8.5	0.133	0.133	0.134	0.134	0.135	0.136	0.137	0.139	0.140	0.142	0.144	0.146	0.148	0.150	0.152	0.155	0.158	0.160	0.163	0.166
9.0	0.141	0.141	0.141	0.142	0.143	0.144	0.145	0.146	0.148	0.149	0.151	0.153	0.155	0.157	0.159	0.162	0.164	0.167	0.170	0.173
9.5	0.148	0.149	0.149	0.150	0.151	0.151	0.152	0.154	0.155	0.157	0.158	0.160	0.162	0.164	0.166	0.169	0.171	0.174	0.176	0.179
10.0	0.156	0.157	0.157	0.158	0.158	0.159	0.160	0.161	0.163	0.164	0.166	0.167	0.169	0.171	0.173	0.176	0.178	0.180	0.183	0.186

Equation 69 $$A_{gap} = 2G\sqrt{[\pi T_{helix} D]^2 + H^2}$$

Using Table 9, Table 10, Table 11, and Table 12, the total leakage mass flowrate is:

Table 13: Study 1 Total Leakage Mass Flowrate $\dot{m}_{leak}\left(\frac{kg}{s}\right)$

E (in.) \ H (in.)	0.5	1.0	1.5	2.0	2.5	3.0	3.5	4.0	4.5	5.0	5.5	6.0	6.5	7.0	7.5	8.0	8.5	9.0	9.5	10.0
0.5	-	-	-	-	-	-	-	-	-	-	-	-	-	-	-	0.974	0.975	0.974	0.974	0.973
1.0	-	-	-	-	-	-	-	-	-	-	-	-	-	0.872	0.870	0.868	0.866	0.863	0.861	0.860
1.5	-	-	-	-	-	-	-	-	-	-	-	0.740	0.734	0.728	0.724	0.721	0.718	0.715	0.712	0.710
2.0	-	-	-	-	-	-	-	-	0.637	0.623	0.612	0.604	0.596	0.589	0.584	0.579	0.575	0.572	0.569	0.566
2.5	-	-	-	-	-	0.600	0.570	0.547	0.528	0.513	0.500	0.490	0.482	0.475	0.469	0.464	0.459	0.456	0.453	0.450
3.0	-	-	-	0.612	0.559	0.520	0.488	0.463	0.444	0.428	0.415	0.404	0.396	0.388	0.382	0.376	0.372	0.368	0.364	0.361
3.5	-	-	0.622	0.552	0.498	0.457	0.425	0.400	0.380	0.364	0.351	0.340	0.331	0.323	0.317	0.311	0.306	0.302	0.298	0.295
4.0	-	0.674	0.575	0.503	0.449	0.408	0.376	0.352	0.332	0.315	0.302	0.291	0.282	0.274	0.268	0.262	0.257	0.253	0.249	0.246
4.5	0.783	0.637	0.534	0.462	0.409	0.369	0.338	0.313	0.294	0.278	0.265	0.254	0.245	0.237	0.230	0.225	0.220	0.216	0.212	0.209
5.0	0.758	0.603	0.500	0.428	0.376	0.336	0.306	0.282	0.263	0.248	0.235	0.225	0.216	0.208	0.202	0.196	-	-	-	-
5.5	0.735	0.573	0.469	0.399	0.347	0.309	0.280	0.257	0.239	0.224	0.211	0.201	0.192	-	-	-	-	-	-	-
6.0	0.712	0.546	0.443	0.373	0.323	0.287	0.258	0.236	0.218	0.204	0.192	-	-	-	-	-	-	-	-	-
6.5	0.691	0.522	0.419	0.351	0.303	0.267	0.240	0.218	0.201	-	-	-	-	-	-	-	-	-	-	-
7.0	0.672	0.500	0.398	0.331	0.284	0.250	0.224	0.203	-	-	-	-	-	-	-	-	-	-	-	-
7.5	0.653	0.480	0.379	0.314	0.268	0.235	0.210	-	-	-	-	-	-	-	-	-	-	-	-	-
8.0	0.635	0.461	0.362	0.298	0.254	0.222	-	-	-	-	-	-	-	-	-	-	-	-	-	-
8.5	0.619	0.444	0.346	0.284	0.241	-	-	-	-	-	-	-	-	-	-	-	-	-	-	-
9.0	0.603	0.428	0.332	0.271	-	-	-	-	-	-	-	-	-	-	-	-	-	-	-	-
9.5	0.588	0.413	0.318	0.259	-	-	-	-	-	-	-	-	-	-	-	-	-	-	-	-
10.0	0.574	0.400	0.306	-	-	-	-	-	-	-	-	-	-	-	-	-	-	-	-	-

Equation 2 $$\dot{m}_{leak} = \rho_t \cdot \dot{V}_{tot.leak} = \rho_t \tilde{V}_t \left(A_{gap} + A_{CynLeakage}\right)$$

Summing Table 5 and Table 13 yields the total mass flowrate through the PRE for each machine radius E and rotor height H combination. This verifies the solvers results (color discrepancy found in Table 14 due to solver accuracy criteria of .01%)

Table 14: Study 1 Total PRE Mass Flowrate $\dot{m}_{tot}\left(\frac{kg}{s}\right)$

E (in.) \ H (in.)	0.5	1.0	1.5	2.0	2.5	3.0	3.5	4.0	4.5	5.0	5.5	6.0	6.5	7.0	7.5	8.0	8.5	9.0	9.5	10.0
0.5	-	-	-	-	-	-	-	-	-	-	-	-	-	-	-	1.00	1.00	1.00	1.00	1.00
1.0	-	-	-	-	-	-	-	-	-	-	-	-	-	1.00	1.00	1.00	1.00	1.00	1.00	1.00
1.5	-	-	-	-	-	-	-	-	-	-	-	1.00	1.00	1.00	1.00	1.00	1.00	1.00	1.00	1.00
2.0	-	-	-	-	-	-	-	-	1.00	1.00	1.00	1.00	1.00	1.00	1.00	1.00	1.00	1.00	1.00	1.00
2.5	-	-	-	-	-	1.00	1.00	1.00	1.00	1.00	1.00	1.00	1.00	1.00	1.00	1.00	1.00	1.00	1.00	1.00
3.0	-	-	-	1.00	1.00	1.00	1.00	1.00	1.00	1.00	1.00	1.00	1.00	1.00	1.00	1.00	1.00	1.00	1.00	1.00
3.5	-	-	1.00	1.00	1.00	1.00	1.00	1.00	1.00	1.00	1.00	1.00	1.00	1.00	1.00	1.00	1.00	1.00	1.00	1.00
4.0	-	1.00	1.00	1.00	1.00	1.00	1.00	1.00	1.00	1.00	1.00	1.00	1.00	1.00	1.00	1.00	1.00	1.00	1.00	1.00
4.5	1.00	1.00	1.00	1.00	1.00	1.00	1.00	1.00	1.00	1.00	1.00	1.00	1.00	1.00	1.00	1.00	1.00	1.00	1.00	1.00
5.0	1.00	1.00	1.00	1.00	1.00	1.00	1.00	1.00	1.00	1.00	1.00	1.00	1.00	1.00	1.00	1.00	-	-	-	-
5.5	1.00	1.00	1.00	1.00	1.00	1.00	1.00	1.00	1.00	1.00	1.00	1.00	1.00	-	-	-	-	-	-	-
6.0	1.00	1.00	1.00	1.00	1.00	1.00	1.00	1.00	1.00	1.00	1.00	-	-	-	-	-	-	-	-	-
6.5	1.00	1.00	1.00	1.00	1.00	1.00	1.00	1.00	1.00	-	-	-	-	-	-	-	-	-	-	-
7.0	1.00	1.00	1.00	1.00	1.00	1.00	1.00	1.00	-	-	-	-	-	-	-	-	-	-	-	-
7.5	1.00	1.00	1.00	1.00	1.00	1.00	1.00	-	-	-	-	-	-	-	-	-	-	-	-	-
8.0	1.00	1.00	1.00	1.00	1.00	1.00	-	-	-	-	-	-	-	-	-	-	-	-	-	-
8.5	1.00	1.00	1.00	1.00	1.00	-	-	-	-	-	-	-	-	-	-	-	-	-	-	-
9.0	1.00	1.00	1.00	1.00	-	-	-	-	-	-	-	-	-	-	-	-	-	-	-	-
9.5	1.00	1.00	1.00	1.00	-	-	-	-	-	-	-	-	-	-	-	-	-	-	-	-
10.0	1.00	1.00	1.00	-	-	-	-	-	-	-	-	-	-	-	-	-	-	-	-	-

Since state 2 pressure P_2 has been successfully converged to produce total mass flowrates $\dot{m}_{tot}$ equal to 1 kg/s, the applications performance can be evaluated. This includes mass efficiency, isentropic efficiency, power generated, and state 3 temperature.

Mass efficiency as stated by equation 2 is shown in Table 15 using cavity mass flowrate from Table 5 and total mass flowrate from Table 14.

Table 15: Study 1 Mass Efficiency

E_{mass}

E (in.) \ H (in.)	0.5	1.0	1.5	2.0	2.5	3.0	3.5	4.0	4.5	5.0	5.5	6.0	6.5	7.0	7.5	8.0	8.5	9.0	9.5	10.0
0.5	-	-	-	-	-	-	-	-	-	-	-	-	-	-	-	3%	3%	3%	3%	3%
1.0	-	-	-	-	-	-	-	-	-	-	-	-	-	13%	13%	13%	13%	14%	14%	14%
1.5	-	-	-	-	-	-	-	-	-	-	-	26%	27%	27%	28%	28%	28%	29%	29%	29%
2.0	-	-	-	-	-	-	-	-	36%	38%	39%	40%	40%	41%	42%	42%	42%	43%	43%	43%
2.5	-	-	-	-	-	40%	43%	45%	47%	49%	50%	51%	52%	52%	53%	54%	54%	54%	55%	55%
3.0	-	-	-	39%	44%	48%	51%	54%	56%	57%	58%	60%	60%	61%	62%	62%	63%	63%	64%	64%
3.5	-	-	38%	45%	50%	54%	57%	60%	62%	64%	65%	66%	67%	68%	68%	69%	69%	70%	70%	71%
4.0	-	33%	43%	50%	55%	59%	62%	65%	67%	68%	70%	71%	72%	73%	73%	74%	74%	75%	75%	75%
4.5	22%	36%	47%	54%	59%	63%	66%	69%	71%	72%	74%	75%	76%	76%	77%	78%	78%	78%	79%	79%
5.0	24%	40%	50%	57%	62%	66%	69%	72%	74%	75%	77%	78%	78%	79%	80%	80%	-	-	-	-
5.5	27%	43%	53%	60%	65%	69%	72%	74%	76%	78%	79%	80%	81%	-	-	-	-	-	-	-
6.0	29%	45%	56%	63%	68%	71%	74%	76%	78%	80%	81%	-	-	-	-	-	-	-	-	-
6.5	31%	48%	58%	65%	70%	73%	76%	78%	80%	-	-	-	-	-	-	-	-	-	-	-
7.0	33%	50%	60%	67%	72%	75%	78%	80%	-	-	-	-	-	-	-	-	-	-	-	-
7.5	35%	52%	62%	69%	73%	77%	79%	-	-	-	-	-	-	-	-	-	-	-	-	-
8.0	36%	54%	64%	70%	75%	78%	-	-	-	-	-	-	-	-	-	-	-	-	-	-
8.5	38%	56%	65%	72%	76%	-	-	-	-	-	-	-	-	-	-	-	-	-	-	-
9.0	40%	57%	67%	73%	-	-	-	-	-	-	-	-	-	-	-	-	-	-	-	-
9.5	41%	59%	68%	74%	-	-	-	-	-	-	-	-	-	-	-	-	-	-	-	-
10.0	43%	60%	69%	-	-	-	-	-	-	-	-	-	-	-	-	-	-	-	-	-

Equation 2 $$E_{mass} = \frac{\dot{m}_{cav.net}}{\dot{m}_{tot}}$$

Table 15 shows as machine size increases, so does the mass efficiency. Values in red show the top 10% configurations with the highest mass efficiencies. Isentropic efficiency calculation shows the importance of performing a system analysis as high mass efficiency does not equal high isentropic efficiency.

Table 16 is the calculated result of equation 88, which can be used to optimize a PRE with varying machine radius E and rotor height H. It shows a 3.5 inch machine radius E and 4 inch rotor height H configuration yields the most efficient PRE design with the given application. It is important to reiterate that the presented PRE design does not incorporate a metering valve and runs "hydraulically". Implementation of a metering valve if tuned to the optimized pressure ratios could yield isentropic efficiencies upwards of 50 to 60%.

Table 16: Study 1 Isentropic Efficiency E_{system}

E (in.) \ H (in.)	0.5	1.0	1.5	2.0	2.5	3.0	3.5	4.0	4.5	5.0	5.5	6.0	6.5	7.0	7.5	8.0	8.5	9.0	9.5	10.0
0.5	-	-	-	-	-	-	-	-	-	-	-	-	-	-	-	1.5%	1.5%	1.5%	1.5%	1.5%
1.0	-	-	-	-	-	-	-	-	-	-	-	-	-	7.4%	7.5%	7.6%	7.6%	7.6%	7.6%	7.6%
1.5	-	-	-	-	-	-	-	-	-	-	-	15.0%	15.1%	15.2%	15.2%	15.2%	15.1%	15.1%	15.0%	14.8%
2.0	-	-	-	-	-	-	-	-	21.0%	21.4%	21.6%	21.7%	21.7%	21.6%	21.5%	21.3%	21.1%	20.8%	20.5%	20.2%
2.5	-	-	-	-	-	23.3%	24.5%	25.3%	25.7%	25.9%	26.0%	25.8%	25.6%	25.3%	24.9%	24.4%	23.9%	23.4%	22.8%	22.2%
3.0	-	-	-	22.5%	24.9%	26.5%	27.5%	28.0%	28.1%	28.0%	27.7%	27.3%	26.7%	26.1%	25.4%	24.6%	23.7%	22.8%	21.9%	21.0%
3.5	-	-	21.6%	24.8%	26.9%	28.1%	28.6%	28.7%	28.5%	28.0%	27.3%	26.5%	25.5%	24.4%	23.2%	22.0%	20.8%	19.5%	18.1%	16.7%
4.0	-	18.5%	23.3%	26.1%	27.7%	28.3%	28.4%	28.0%	27.3%	26.2%	25.0%	23.7%	22.2%	20.6%	19.0%	17.3%	15.5%	13.7%	11.8%	9.9%
4.5	12.4%	19.9%	24.2%	26.5%	27.5%	27.6%	27.0%	26.0%	24.6%	23.0%	21.3%	19.3%	17.2%	15.1%	12.8%	10.5%	8.2%	5.8%	3.3%	0.8%
5.0	13.5%	20.9%	24.6%	26.3%	26.5%	25.9%	24.6%	22.9%	20.9%	18.6%	16.1%	13.5%	10.8%	8.0%	5.0%	2.1%	-	-	-	-
5.5	14.4%	21.5%	24.5%	25.4%	24.8%	23.4%	21.4%	18.9%	16.1%	13.0%	9.8%	6.5%	3.0%	-	-	-	-	-	-	-
6.0	15.1%	21.7%	24.0%	24.0%	22.5%	20.2%	17.3%	14.0%	10.3%	6.5%	2.4%	-	-	-	-	-	-	-	-	-
6.5	15.7%	21.7%	23.0%	22.0%	19.7%	16.4%	12.6%	8.3%	3.7%	-	-	-	-	-	-	-	-	-	-	-
7.0	16.1%	21.3%	21.7%	19.7%	16.3%	12.0%	7.1%	1.9%	-	-	-	-	-	-	-	-	-	-	-	-
7.5	16.4%	20.7%	20.0%	16.9%	12.3%	7.0%	1.0%	-	-	-	-	-	-	-	-	-	-	-	-	-
8.0	16.5%	19.8%	18.0%	13.7%	8.0%	1.4%	-	-	-	-	-	-	-	-	-	-	-	-	-	-
8.5	16.5%	18.7%	15.6%	10.1%	3.1%	-	-	-	-	-	-	-	-	-	-	-	-	-	-	-
9.0	16.4%	17.4%	13.0%	6.1%	-	-	-	-	-	-	-	-	-	-	-	-	-	-	-	-
9.5	16.1%	15.9%	10.0%	1.7%	-	-	-	-	-	-	-	-	-	-	-	-	-	-	-	-
10.0	15.7%	14.1%	6.8%	-	-	-	-	-	-	-	-	-	-	-	-	-	-	-	-	-

Equation 6 $$E_{system} = \frac{\dot{V}_{cav.net} \cdot (P_2 - P_3)}{\dot{m}_{tot}(h_1 - h_{3,Isentropic})} = \frac{\dot{w}_{shaft}}{\dot{m}_{tot}(h_1 - h_{3,Isentropic})}$$

NIST REFPROP $h_1(P_1, T_1)$

NIST REFPROP $h_{3,isentropic}(P_3, s_1)$

The first byproduct of using a PRE is generated shaft power. Using equation 5, Table 1, and Table 2, shaft power generated is calculated in Table 17.

Table 17: Study 1 Shaft Power $\dot{w}_{shaft}$ (kW)

E (in.) \ H (in.)	0.5	1.0	1.5	2.0	2.5	3.0	3.5	4.0	4.5	5.0	5.5	6.0	6.5	7.0	7.5	8.0	8.5	9.0	9.5	10.0
0.5	-	-	-	-	-	-	-	-	-	-	-	-	-	-	-	3	3	3	3	3
1.0	-	-	-	-	-	-	-	-	-	-	-	-	-	15	15	16	16	16	16	16
1.5	-	-	-	-	-	-	-	-	-	-	-	31	31	31	31	31	31	31	31	30
2.0	-	-	-	-	-	-	-	-	43	44	44	44	44	44	44	44	43	43	42	41
2.5	-	-	-	-	-	48	50	52	53	53	53	53	52	52	51	50	49	48	47	46
3.0	-	-	-	46	51	54	56	57	58	57	57	56	55	53	52	50	49	47	45	43
3.5	-	-	44	51	55	57	59	59	58	57	56	54	52	50	48	45	43	40	37	34
4.0	-	38	48	53	57	58	58	57	56	54	51	49	45	42	39	35	32	28	24	20
4.5	25	41	50	54	56	56	55	53	50	47	44	40	35	31	26	22	17	12	7	2
5.0	28	43	51	54	54	53	50	47	43	38	33	28	22	16	10	4	-	-	-	-
5.5	30	44	50	52	51	48	44	39	33	27	20	13	6	-	-	-	-	-	-	-
6.0	31	44	49	49	46	41	35	29	21	13	5	-	-	-	-	-	-	-	-	-
6.5	32	44	47	45	40	34	26	17	8	-	-	-	-	-	-	-	-	-	-	-
7.0	33	44	44	40	33	25	15	4	-	-	-	-	-	-	-	-	-	-	-	-
7.5	34	42	41	35	25	14	2	-	-	-	-	-	-	-	-	-	-	-	-	-
8.0	34	41	37	28	16	3	-	-	-	-	-	-	-	-	-	-	-	-	-	-
8.5	34	38	32	21	6	-	-	-	-	-	-	-	-	-	-	-	-	-	-	-
9.0	34	36	27	12	-	-	-	-	-	-	-	-	-	-	-	-	-	-	-	-
9.5	33	33	21	4	-	-	-	-	-	-	-	-	-	-	-	-	-	-	-	-
10.0	32	29	14	-	-	-	-	-	-	-	-	-	-	-	-	-	-	-	-	-

Equation 5 $$\dot{w}_{shaft} = \dot{V}_{cav.net} \cdot (P_2 - P_3)$$

The second byproduct of the PRE extracting fluid energy from the flow beside shaft power is a lower downstream fluid temperature due to the change in enthalpy.

Table 18: Study 1 State 3 Temperature T_3 (F)

E (in.) \ H (in.)	0.5	1.0	1.5	2.0	2.5	3.0	3.5	4.0	4.5	5.0	5.5	6.0	6.5	7.0	7.5	8.0	8.5	9.0	9.5	10.0
0.5	-	-	-	-	-	-	-	-	-	-	-	-	-	-	-	47.8	47.7	47.7	47.7	47.7
1.0	-	-	-	-	-	-	-	-	-	-	-	-	-	38.2	38.0	38.0	37.9	37.9	37.9	37.9
1.5	-	-	-	-	-	-	-	-	-	-	-	26.0	25.7	25.6	25.6	25.6	25.7	25.8	26.0	26.2
2.0	-	-	-	-	-	-	-	-	16.3	15.6	15.3	15.1	15.1	15.2	15.5	15.8	16.1	16.6	17.0	17.5
2.5	-	-	-	-	-	12.5	10.5	9.3	8.5	8.2	8.2	8.4	8.8	9.3	9.9	10.7	11.5	12.3	13.2	14.2
3.0	-	-	-	13.7	9.8	7.3	5.8	5.0	4.7	4.8	5.3	6.0	6.9	8.0	9.2	10.5	11.8	13.3	14.8	16.3
3.5	-	-	15.3	10.0	6.7	4.8	3.9	3.7	4.1	4.9	6.0	7.4	9.0	10.7	12.6	14.5	16.6	18.7	20.9	23.2
4.0	-	20.2	12.6	8.0	5.4	4.3	4.3	4.9	6.1	7.7	9.7	11.9	14.3	16.8	19.5	22.3	25.2	28.1	31.1	34.2
4.5	30.1	17.9	11.0	7.3	5.7	5.6	6.5	8.2	10.3	12.9	15.8	19.0	22.3	25.8	29.4	33.2	37.0	40.9	44.8	48.8
5.0	28.3	16.4	10.3	7.7	7.3	8.3	10.4	13.1	16.4	20.1	24.1	28.3	32.8	37.3	42.0	46.8	-	-	-	-
5.5	26.9	15.5	10.5	9.1	10.0	12.3	15.6	19.7	24.2	29.1	34.3	39.7	45.3	-	-	-	-	-	-	-
6.0	25.7	15.1	11.4	11.4	13.7	17.5	22.2	27.6	33.5	39.7	46.2	-	-	-	-	-	-	-	-	-
6.5	24.8	15.2	12.9	14.5	18.4	23.7	29.9	36.8	44.1	-	-	-	-	-	-	-	-	-	-	-
7.0	24.1	15.7	15.1	18.4	23.9	30.8	38.7	47.1	-	-	-	-	-	-	-	-	-	-	-	-
7.5	23.7	16.7	17.8	22.9	30.2	38.9	48.5	-	-	-	-	-	-	-	-	-	-	-	-	-
8.0	23.5	18.1	21.1	28.1	37.3	47.9	-	-	-	-	-	-	-	-	-	-	-	-	-	-
8.5	23.5	19.9	24.9	33.9	45.1	-	-	-	-	-	-	-	-	-	-	-	-	-	-	-
9.0	23.7	22.0	29.2	40.4	-	-	-	-	-	-	-	-	-	-	-	-	-	-	-	-
9.5	24.1	24.6	34.0	47.4	-	-	-	-	-	-	-	-	-	-	-	-	-	-	-	-
10.0	24.8	27.4	39.2	-	-	-	-	-	-	-	-	-	-	-	-	-	-	-	-	-

NIST REFPROP $T_3(P_3, h_3)$

Equation 6 $$h_3 = h_1 - \frac{\dot{w}_{shaft}}{\dot{m}_{tot}} \quad \text{From} \quad E_{system} = \frac{\dot{w}_{shaft}}{\dot{m}_{tot}(h_1 - h_{3,Isentropic})}$$

3.2 STUDY 2 – ENERGY RECOVERY SPEED OPTIMIZATION

Study 2 takes an arbitrary machine radius E (4 inches) and rotor height H (4 inches) and holds them constant while varying PRE angular velocity. An optimized solution is calculated showing the effects of expander speed on isentropic efficiency, also demonstrating how a single size machine can be optimized for different applications by varying machine speed. Note that the same calculation process is used in study 2 as from study 1, except in study 2 rotational frequency is variable and rotor geometry is held constant (see Figure 30)

Process Fluid	Methane	System Mass Flowrate	1 kg/s
Molecular Weight	16.04 kg/kmol	State 1 Pressure	1200 psi
Specific Gas Constant	518.27 kJ/kg°K	State 1 Temperature	100 °F
Machine Radius E	4.0 in.	State 1 Enthalpy (reference)	863.1 kJ/kg
Rotor Height H	4.0 in.	State 1 Entropy(reference)	4.3 kJ/kg°K
Tip Radius R_1	.125 in.	State 3 Pressure	200 psi
Rotor Gap Width G	.005 in.	State 3 Isentropic Enthalpy, $h_{3,Isentropic}$	658.2 kJ/kg

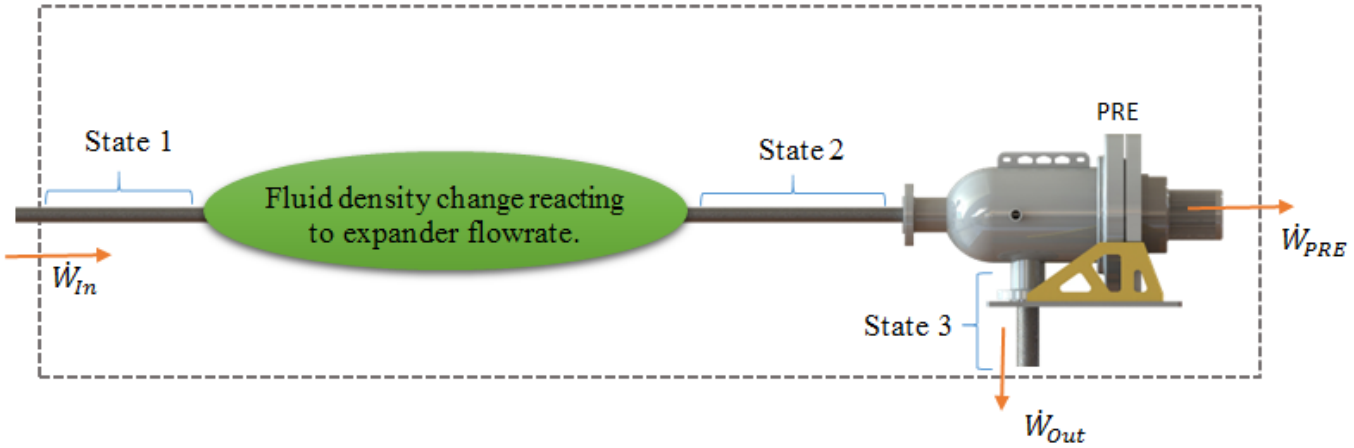

Table 19: Study 2 Isentropic Efficiency E_{system}

Speed	Cavity Flowrate		Cavity Pressure		Cavity Temperature		Cavity Density	Throat Properties							State 1-2 Enthalpy Loss	Leakage Mass Flowrate	Cavity Mass Flowrate	Total Mass	Isentropic Efficiency	Output Power
								Pressure		Temperature		Heat	Velocity	Density						
RPM	ACFM	m^3/s	psi	Mpa	F	K	kg/m³	psi	Mpa	F	K	Ratio	m/s	kg/m³	kj/kg	kg/s	kg/s	kg/s	%	kW
300	4.47	0.0021	1172.7	8.1	98.9	310.3	56.3	577	3.98	-35.2	235.8	1.63	446.6	38.83	2.1	0.881	0.12	1.000	6.9%	14.1
600	8.94	0.0042	1070.3	7.4	94.6	307.9	51.5	534	3.68	-30.8	238.2	1.58	442.4	34.81	10.4	0.783	0.22	1.000	12.4%	25.3
900	13.41	0.0063	978.7	6.7	90.6	305.7	47.2	493	3.40	-28.2	239.7	1.55	438.9	31.44	18.8	0.701	0.30	1.000	16.6%	34.0
1200	17.88	0.0084	898.5	6.2	86.9	303.7	43.4	457	3.15	-26.6	240.6	1.52	436.0	28.60	27.0	0.634	0.37	1.000	19.8%	40.6
1500	22.35	0.0105	828.7	5.7	83.7	301.9	40.1	424	2.92	-25.5	241.2	1.50	433.5	26.20	34.9	0.577	0.42	1.000	22.3%	45.7
1800	26.82	0.0127	768.0	5.3	80.8	300.2	37.2	395	2.72	-24.9	241.5	1.49	431.3	24.15	42.5	0.529	0.47	1.000	24.2%	49.6
2100	31.29	0.0148	714.9	4.9	78.2	298.8	34.6	369	2.55	-24.5	241.7	1.47	429.4	22.39	49.7	0.489	0.51	1.000	25.6%	52.4
2400	35.76	0.0169	668.3	4.6	75.8	297.5	32.4	346	2.39	-24.3	241.9	1.46	427.8	20.86	56.7	0.454	0.55	1.000	26.6%	54.5
2700	40.23	0.0190	627.1	4.3	73.8	296.3	30.4	326	2.25	-24.2	241.9	1.45	426.4	19.52	63.4	0.423	0.58	1.000	27.3%	55.9
3000	44.70	0.0211	590.5	4.1	71.9	295.3	28.6	308	2.12	-24.2	241.9	1.44	425.1	18.33	69.9	0.396	0.60	1.000	27.7%	56.8
3300	49.17	0.0232	557.8	3.8	70.2	294.4	27.0	292	2.01	-24.3	241.9	1.43	424.0	17.28	76.1	0.372	0.63	1.000	27.9%	57.2
3600	53.64	0.0253	528.4	3.6	68.6	293.5	25.6	277	1.91	-24.3	241.9	1.43	422.9	16.35	82.0	0.351	0.65	1.000	28.0%	57.3
3900	58.11	0.0274	502.0	3.5	67.2	292.7	24.3	263	1.82	-24.4	241.8	1.42	422.0	15.51	87.8	0.333	0.67	1.000	27.9%	57.1
4200	62.58	0.0295	478.0	3.3	65.9	292.0	23.2	251	1.73	-24.6	241.7	1.42	421.2	14.74	93.3	0.316	0.68	1.000	27.6%	56.6
4500	67.05	0.0316	456.1	3.1	64.7	291.3	22.1	240	1.66	-24.7	241.7	1.41	420.4	14.05	98.7	0.300	0.70	1.000	27.3%	55.9
4800	71.52	0.0338	436.1	3.0	63.6	290.7	21.1	230	1.59	-24.8	241.6	1.41	419.7	13.43	103.9	0.286	0.71	1.000	26.8%	55.0
5100	75.99	0.0359	417.8	2.9	62.6	290.2	20.3	221	1.52	-25.0	241.5	1.40	419.1	12.85	109.0	0.274	0.73	1.000	26.3%	53.9
5400	80.47	0.0380	401.0	2.8	61.7	289.7	19.4	212	1.46	-25.1	241.4	1.40	418.5	12.32	113.9	0.262	0.74	1.000	25.7%	52.6
5700	84.94	0.0401	385.4	2.7	60.8	289.2	18.7	204	1.41	-25.2	241.4	1.40	417.9	11.83	118.6	0.251	0.75	1.000	25.0%	51.2
6000	89.41	0.0422	371.0	2.6	60.0	288.7	18.0	196	1.35	-25.4	241.3	1.39	417.4	11.38	123.2	0.242	0.76	1.000	24.3%	49.7

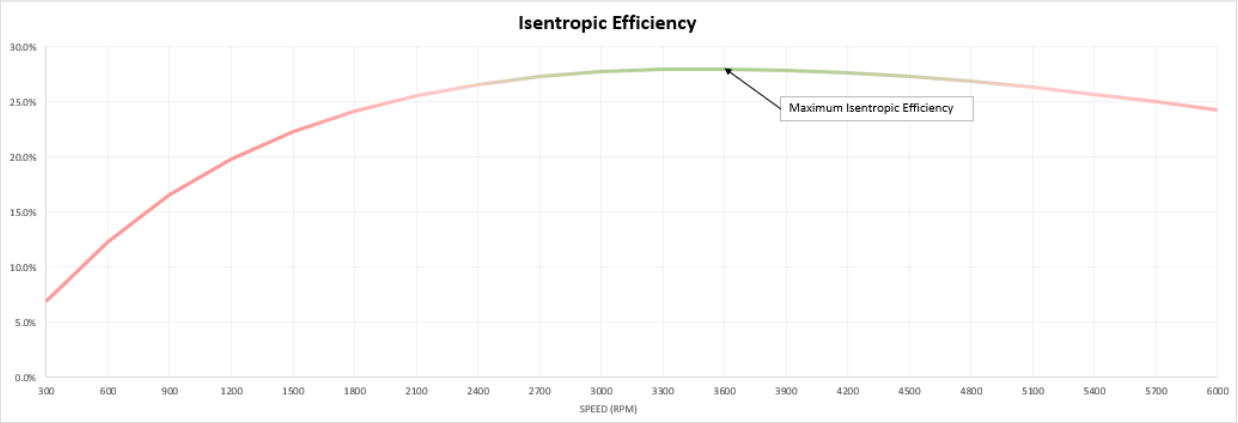

The same solver used in study 1 is used in study 2. PRE rotational speed is the independent variable, mass flowrate the objective variable, and state 2 cavity pressure is the changing variable in the iterative solver. Study 2 is simply a 1-dimensional analysis (rotation speed), while study 1 is a 2-dimensional analysis (machine radius E and rotor height H). For the application presented in study 2, a PRE with a rotational speed of 3600 RPM is optimal.

This 1-dimensional analysis shows the optimization the solver is working to accomplish. Note as speed increases so does State 1-2 enthalpy loss (a negative effect on isentropic efficiency), but leakage is reduced (a positive effect on isentropic efficiency). The dominance of these variables phase as speed varies generating an optimized isentropic efficiency.

3.3 STUDY 3 – TARGET POWER VARIABLE ROTOR SIZE

This study calculates equation 88 step by step to yield the isentropic efficiencies of 400 possible rotor height H and machine radius E combinations for a target power application.

The rotational frequency ƒ is held at a constant value typically found in industry, and other given parameters for this study are below. Study 3 demonstrates how rotor geometry influences isentropic efficiency and shows how to optimize a PRE when a constant rotational speed is required by the application. Figure 31 shows the calculation process for evaluating a target power process.

Process Fluid	Methane	State 1 Pressure	1200 psi
Molecular Weight	16.04 kg/kmol	State 1 Temperature	100 °F
Specific Gas Constant	518.27 kJ/kg°K	State 1 Enthalpy (reference)	863.1 kJ/kg
Expander Frequency	60 Hz	State 1 Entropy(reference)	4.3 kJ/kg°K
Tip Radius R_1	.125''	State 3 Pressure	200 psi
Rotor Gap Width G	.005''	State 3 Isentropic Enthalpy, $h_{3,Isentropic}$	658.2 kJ/kg
Target Power	30 kW		

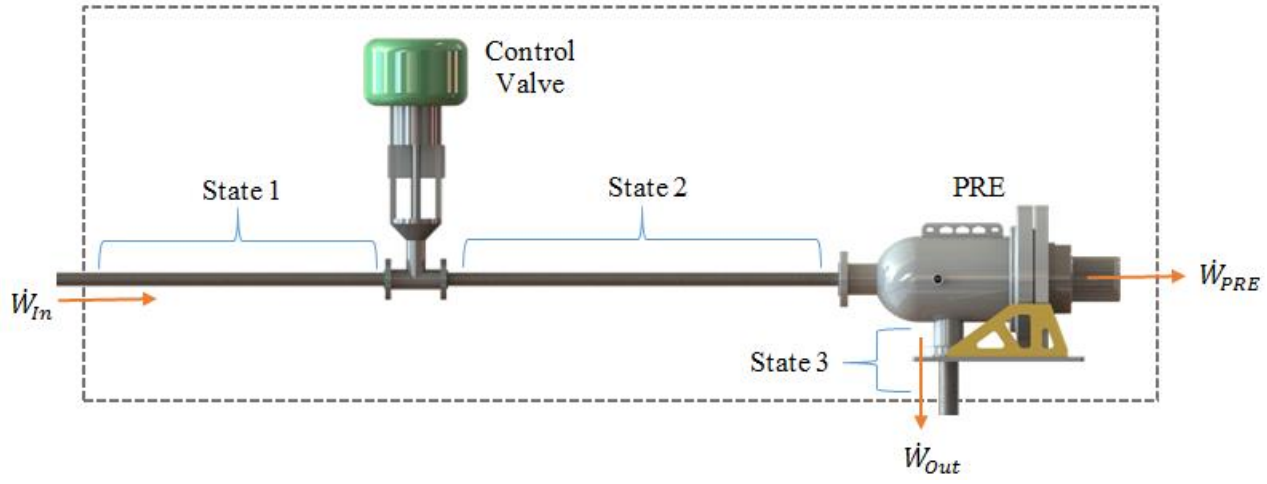

Figure 31 shows the calculation process for a target power application. Each step of this process is shown in study 1 below.

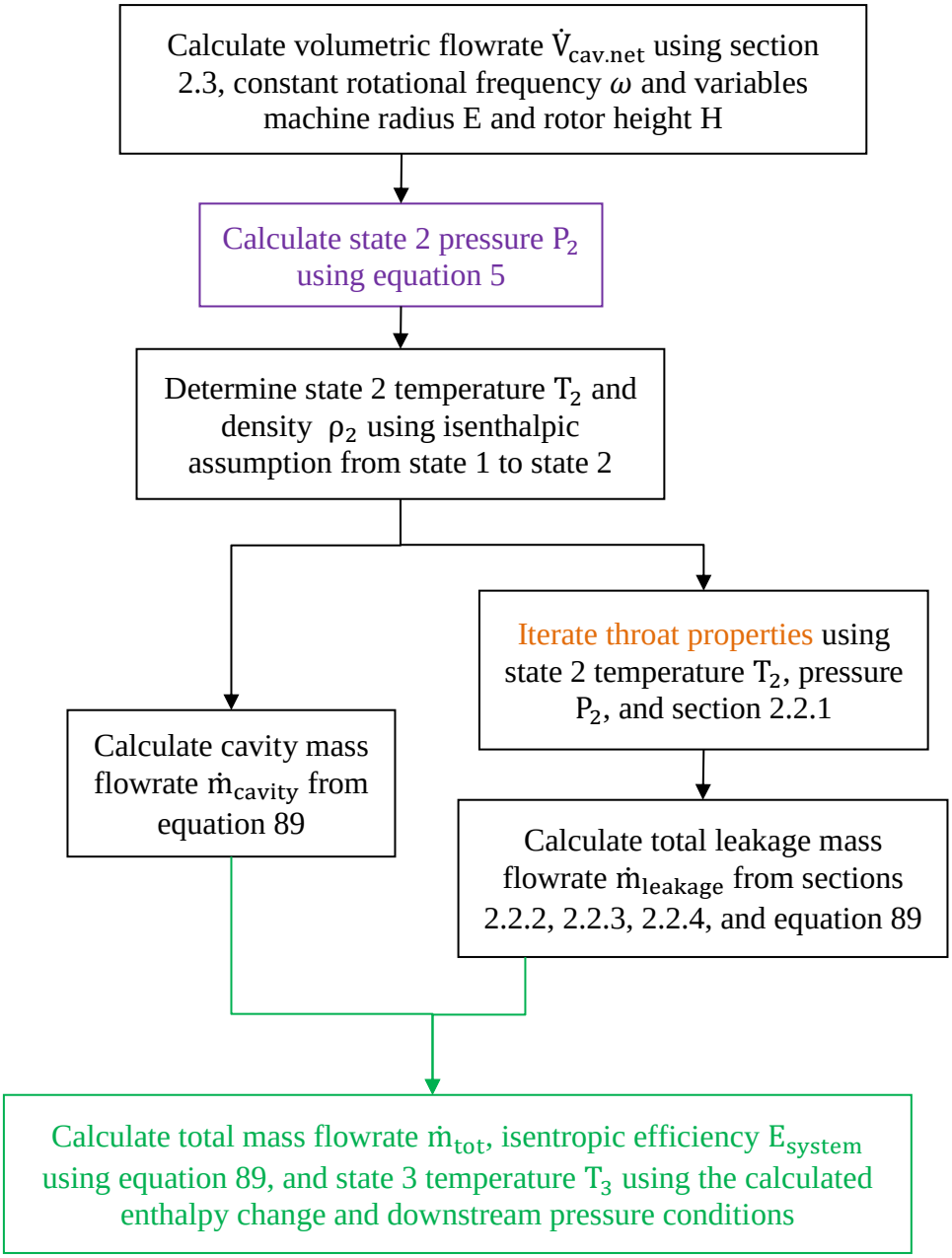

Figure 31: Study 3 Target Power Calculation Process

The primary focus when calculating equation 88 is determining state 2 pressure for each rotor size configuration (pressure inside the cavity). Since a target power application gives the required shaft power $\dot{w}_{shaft}$, state 2 pressure P_2 can be directly calculated from equation 5. This removes the need to iteratively solve state 2 pressure as in studies 1 and 2. The calculation process then follows Figure 31.

First, the cavity volumetric flowrate is calculated using the net cavity flowrate equation 84, and due to using a circular core, equation 22 is used to calculate core area. Note that machine radius E and rotor height H are given in inches.

Table 20: Study 3 Net Cavity Flowrate

$$\dot{V}_{cav.net}\left(\frac{ft.^3}{min.}\right)$$

	H (in.)																			
E (in.)	0.5	1.0	1.5	2.0	2.5	3.0	3.5	4.0	4.5	5.0	5.5	6.0	6.5	7.0	7.5	8.0	8.5	9.0	9.5	10.0
0.5	0.1	0.1	0.2	0.2	0.3	0.4	0.4	0.5	0.5	0.6	0.7	0.7	0.8	0.8	0.9	0.9	1.0	1.1	1.1	1.2
1.0	0.3	0.7	1.0	1.4	1.7	2.0	2.4	2.7	3.0	3.4	3.7	4.1	4.4	4.7	5.1	5.4	5.8	6.1	6.4	6.8
1.5	0.8	1.7	2.5	3.4	4.2	5.0	5.9	6.7	7.6	8.4	9.3	10.1	10.9	11.8	12.6	13.5	14.3	15.1	16.0	16.8
2.0	1.6	3.1	4.7	6.3	7.8	9.4	11.0	12.5	14.1	15.7	17.2	18.8	20.4	21.9	23.5	25.1	26.6	28.2	29.8	31.3
2.5	2.5	5.0	7.5	10.1	12.6	15.1	17.6	20.1	22.6	25.2	27.7	30.2	32.7	35.2	37.7	40.3	42.8	45.3	47.8	50.3
3.0	3.7	7.4	11.1	14.8	18.4	22.1	25.8	29.5	33.2	36.9	40.6	44.3	48.0	51.7	55.3	59.0	62.7	66.4	70.1	73.8
3.5	5.1	10.2	15.3	20.3	25.4	30.5	35.6	40.7	45.8	50.9	55.9	61.0	66.1	71.2	76.3	81.4	86.5	91.5	96.6	101.7
4.0	6.7	13.4	20.1	26.8	33.5	40.2	46.9	53.6	60.3	67.1	73.8	80.5	87.2	93.9	100.6	107.3	114.0	120.7	127.4	134.1
4.5	8.5	17.1	25.6	34.2	42.7	51.3	59.8	68.4	76.9	85.5	94.0	102.6	111.1	119.7	128.2	136.8	145.3	153.9	162.4	171.0
5.0	10.6	21.2	31.8	42.5	53.1	63.7	74.3	84.9	95.5	106.1	116.8	127.4	138.0	148.6	159.2	169.8	180.5	191.1	201.7	212.3
5.5	12.9	25.8	38.7	51.6	64.5	77.4	90.3	103.2	116.1	129.0	142.0	154.9	167.8	180.7	193.6	206.5	219.4	232.3	245.2	258.1
6.0	15.4	30.8	46.3	61.7	77.1	92.5	107.9	123.3	138.8	154.2	169.6	185.0	200.4	215.9	231.3	246.7	262.1	277.5	292.9	308.4
6.5	18.2	36.3	54.5	72.6	90.8	108.9	127.1	145.2	163.4	181.5	199.7	217.9	236.0	254.2	272.3	290.5	308.6	326.8	344.9	363.1
7.0	21.1	42.2	63.3	84.5	105.6	126.7	147.8	168.9	190.0	211.1	232.3	253.4	274.5	295.6	316.7	337.8	359.0	380.1	401.2	422.3
7.5	24.3	48.6	72.9	97.2	121.5	145.8	170.1	194.4	218.7	243.0	267.3	291.6	315.9	340.2	364.5	388.8	413.1	437.4	461.7	486.0
8.0	27.7	55.4	83.1	110.8	138.5	166.2	193.9	221.6	249.3	277.1	304.8	332.5	360.2	387.9	415.6	443.3	471.0	498.7	526.4	554.1
8.5	31.3	62.7	94.0	125.3	156.7	188.0	219.3	250.7	282.0	313.4	344.7	376.0	407.4	438.7	470.0	501.4	532.7	564.0	595.4	626.7
9.0	35.2	70.4	105.6	140.8	175.9	211.1	246.3	281.5	316.7	351.9	387.1	422.3	457.5	492.6	527.8	563.0	598.2	633.4	668.6	703.8
9.5	39.3	78.5	117.8	157.1	196.3	235.6	274.9	314.1	353.4	392.7	431.9	471.2	510.5	549.7	589.0	628.3	667.5	706.8	746.1	785.3
10.0	43.6	87.1	130.7	174.3	217.8	261.4	305.0	348.5	392.1	435.7	479.2	522.8	566.4	609.9	653.5	697.1	740.6	784.2	827.8	871.3

Equation 84 $$\dot{V}_{cav.net} = 2ʃH\left[(4-\pi)\left(\frac{E^2 - 2ER_1 + 3R_1^2}{4}\right) - A_{Core}\right]$$

Equation 22 $$A_{CylCore} = \pi R_1^2\left(1-\sqrt{2}\right)^2$$

Since a target power application gives the required shaft power, cavity pressure can be calculated using Table 20, equation 5, and solving for state 2 pressure. Dashes in the table indicate an impossible scenario where the rotor size combination would require a state 2 pressure greater than the state 1 pressure.

Table 21: Study 3 State 2 Pressure (cavity pressure)

$$P_2 \left(\frac{\text{lbs}}{\text{in.}^2}\right)$$

E (in.) \ H (in.)	0.5	1.0	1.5	2.0	2.5	3.0	3.5	4.0	4.5	5.0	5.5	6.0	6.5	7.0	7.5	8.0	8.5	9.0	9.5	10.0
0.5	-	-	-	-	-	-	-	-	-	-	-	-	-	-	-	-	-	-	-	-
1.0	-	-	-	-	-	-	-	-	-	-	-	-	-	-	-	-	-	-	-	-
1.5	-	-	-	-	-	-	-	-	-	-	1196	1113	1043	983	931	885	845	809	777	748
2.0	-	-	-	-	-	1180	1040	935	854	788	735	690	653	620	592	568	546	527	510	494
2.5	-	-	-	1116	933	811	723	658	607	566	533	505	482	462	444	429	415	404	393	383
3.0	-	-	1033	825	700	616	557	512	478	450	427	408	392	378	367	356	347	339	332	325
3.5	-	1106	804	653	563	502	459	427	401	381	365	351	339	329	321	313	307	301	295	291
4.0	-	887	658	544	475	429	396	372	353	337	325	315	306	298	292	286	281	276	272	269
4.5	-	739	559	470	416	380	354	335	320	308	298	290	283	277	272	267	263	260	257	254
5.0	1069	634	490	417	374	345	324	309	297	287	279	272	267	262	258	254	251	248	246	243
5.5	914	557	438	379	343	319	302	289	279	271	265	260	255	251	248	245	242	240	238	236
6.0	798	499	399	349	320	300	285	275	266	260	254	250	246	243	240	237	235	233	231	230
6.5	708	454	369	327	302	285	273	263	256	251	246	242	239	236	234	232	230	228	227	225
7.0	637	418	346	309	287	273	262	255	249	244	240	236	234	231	229	227	226	224	223	222
7.5	579	390	326	295	276	263	254	247	242	238	234	232	229	227	225	224	222	221	220	219
8.0	533	366	311	283	267	255	248	242	237	233	230	228	226	224	222	221	220	218	218	217
8.5	494	347	298	274	259	249	242	237	233	229	227	225	223	221	220	218	217	216	215	215
9.0	462	331	287	265	252	244	237	233	229	226	224	222	220	219	217	216	215	215	214	213
9.5	435	317	278	259	247	239	234	229	226	223	221	220	218	217	216	215	214	213	212	212
10.0	412	306	271	253	242	235	230	226	224	221	219	218	216	215	214	213	212	212	211	211

Equation 5 $\dot{w}_{shaft} = \dot{V}_{cav.net} \cdot (P_2 - P_3)$ Solved for P_2

Note the dark purple values in the above table require the lowest pressure drop across the control valve (state 1 to state 2). This would lead to the expectation that those machine sizes would yield the highest isentropic efficiency (lowest increase in entropy across the valve). These machine sizes will be compared with the final calculations.

State 2 temperature and density can be determined by assuming an isenthalpic process across the control valve. This determines that state 2 enthalpy is equal to state 1 enthalpy. Having two state variables, state 2 pressure from Table 21 and state 1 enthalpy, state 2 temperature and density are calculated using NIST REFPROP. State 2 temperature and density are required when determining leakage and cavity mass flowrates.

Table 22: Study 3 State 2 Temperature T_2 (°F)

E (in.) \ H (in.)	0.5	1.0	1.5	2.0	2.5	3.0	3.5	4.0	4.5	5.0	5.5	6.0	6.5	7.0	7.5	8.0	8.5	9.0	9.5	10.0
0.5	-	-	-	-	-	-	-	-	-	-	-	-	-	-	-	-	-	-	-	-
1.0	-	-	-	-	-	-	-	-	-	-	-	-	-	-	-	-	-	-	-	-
1.5	-	-	-	-	-	-	-	-	-	-	99.9	96.4	93.4	90.8	88.4	86.3	84.4	82.7	81.2	79.8
2.0	-	-	-	-	-	99.2	93.3	88.6	84.9	81.7	79.2	76.9	75.0	73.4	72.0	70.7	69.5	68.5	67.6	66.8
2.5	-	-	-	96.5	88.5	82.8	78.6	75.3	72.7	70.6	68.9	67.4	66.1	65.0	64.1	63.2	62.5	61.8	61.2	60.7
3.0	-	-	93.0	83.5	77.4	73.2	70.1	67.8	65.9	64.4	63.2	62.1	61.2	60.5	59.8	59.2	58.7	58.2	57.8	57.4
3.5	-	96.1	82.5	75.1	70.4	67.2	64.9	63.1	61.7	60.6	59.7	58.9	58.3	57.7	57.2	56.8	56.4	56.0	55.7	55.5
4.0	-	86.4	75.3	69.4	65.8	63.3	61.5	60.1	59.0	58.1	57.4	56.8	56.3	55.9	55.5	55.2	54.9	54.6	54.4	54.2
4.5	-	79.4	70.3	65.5	62.5	60.5	59.1	58.0	57.1	56.5	55.9	55.4	55.0	54.7	54.4	54.1	53.9	53.7	53.5	53.3
5.0	94.5	74.1	66.5	62.6	60.2	58.6	57.4	56.5	55.8	55.2	54.8	54.4	54.1	53.8	53.6	53.4	53.2	53.0	52.9	52.7
5.5	87.7	70.1	63.8	60.5	58.4	57.1	56.1	55.4	54.8	54.4	54.0	53.7	53.4	53.2	53.0	52.8	52.6	52.5	52.4	52.3
6.0	82.2	67.0	61.6	58.8	57.1	56.0	55.2	54.5	54.1	53.7	53.4	53.1	52.9	52.7	52.5	52.4	52.2	52.1	52.0	51.9
6.5	77.8	64.6	59.9	57.5	56.1	55.1	54.4	53.9	53.5	53.1	52.9	52.7	52.5	52.3	52.2	52.0	51.9	51.8	51.7	51.7
7.0	74.2	62.7	58.6	56.5	55.3	54.4	53.8	53.4	53.0	52.7	52.5	52.3	52.1	52.0	51.9	51.8	51.7	51.6	51.5	51.4
7.5	71.3	61.1	57.5	55.7	54.6	53.9	53.3	53.0	52.6	52.4	52.2	52.0	51.9	51.8	51.7	51.6	51.5	51.4	51.3	51.3
8.0	68.8	59.8	56.6	55.0	54.1	53.4	53.0	52.6	52.3	52.1	51.9	51.8	51.7	51.6	51.5	51.4	51.3	51.3	51.2	51.1
8.5	66.8	58.7	55.9	54.5	53.6	53.0	52.6	52.3	52.1	51.9	51.7	51.6	51.5	51.4	51.3	51.2	51.2	51.1	51.1	51.0
9.0	65.1	57.8	55.3	54.0	53.2	52.7	52.4	52.1	51.9	51.7	51.6	51.4	51.3	51.3	51.2	51.1	51.1	51.0	51.0	50.9
9.5	63.6	57.0	54.7	53.6	52.9	52.5	52.1	51.9	51.7	51.5	51.4	51.3	51.2	51.2	51.1	51.0	51.0	50.9	50.9	50.9
10.0	62.3	56.3	54.3	53.3	52.7	52.2	51.9	51.7	51.5	51.4	51.3	51.2	51.1	51.1	51.0	50.9	50.9	50.9	50.8	50.8

Table 23: Study 3 State 2 Density ρ_2 $\left(\frac{\text{kg}}{\text{m}^3}\right)$

E (in.) \ H (in.)	0.5	1.0	1.5	2.0	2.5	3.0	3.5	4.0	4.5	5.0	5.5	6.0	6.5	7.0	7.5	8.0	8.5	9.0	9.5	10.0
0.5	-	-	-	-	-	-	-	-	-	-	-	-	-	-	-	-	-	-	-	-
1.0	-	-	-	-	-	-	-	-	-	-	-	-	-	-	-	-	-	-	-	-
1.5	-	-	-	-	-	-	-	-	-	-	57.3	53.5	50.2	47.4	44.9	42.8	40.8	39.1	37.6	36.2
2.0	-	-	-	-	-	56.6	50.1	45.1	41.3	38.1	35.6	33.4	31.6	30.1	28.7	27.5	26.5	25.5	24.7	24.0
2.5	-	-	-	53.6	45.0	39.2	35.0	31.9	29.4	27.5	25.8	24.5	23.4	22.4	21.5	20.8	20.1	19.6	19.0	18.6
3.0	-	-	49.7	39.9	33.9	29.9	27.0	24.8	23.2	21.8	20.7	19.8	19.0	18.3	17.8	17.3	16.8	16.4	16.1	15.7
3.5	-	53.2	38.9	31.7	27.3	24.3	22.2	20.7	19.5	18.5	17.7	17.0	16.4	16.0	15.5	15.2	14.8	14.6	14.3	14.1
4.0	-	42.9	31.9	26.4	23.0	20.8	19.2	18.0	17.1	16.3	15.7	15.2	14.8	14.4	14.1	13.8	13.6	13.4	13.2	13.0
4.5	-	35.8	27.1	22.8	20.1	18.4	17.2	16.2	15.5	14.9	14.4	14.0	13.7	13.4	13.2	12.9	12.7	12.6	12.4	12.3
5.0	51.4	30.7	23.7	20.2	18.1	16.7	15.7	14.9	14.4	13.9	13.5	13.2	12.9	12.7	12.5	12.3	12.1	12.0	11.9	11.8
5.5	44.2	27.0	21.2	18.3	16.6	15.5	14.6	14.0	13.5	13.1	12.8	12.6	12.3	12.1	12.0	11.8	11.7	11.6	11.5	11.4
6.0	38.6	24.2	19.4	16.9	15.5	14.5	13.8	13.3	12.9	12.6	12.3	12.1	11.9	11.7	11.6	11.5	11.4	11.3	11.2	11.1
6.5	34.3	22.0	17.9	15.8	14.6	13.8	13.2	12.8	12.4	12.1	11.9	11.7	11.6	11.4	11.3	11.2	11.1	11.0	11.0	10.9
7.0	30.9	20.3	16.7	15.0	13.9	13.2	12.7	12.3	12.0	11.8	11.6	11.4	11.3	11.2	11.1	11.0	10.9	10.8	10.8	10.7
7.5	28.1	18.9	15.8	14.3	13.4	12.7	12.3	12.0	11.7	11.5	11.3	11.2	11.1	11.0	10.9	10.8	10.8	10.7	10.6	10.6
8.0	25.8	17.8	15.1	13.7	12.9	12.4	12.0	11.7	11.5	11.3	11.1	11.0	10.9	10.8	10.7	10.7	10.6	10.6	10.5	10.5
8.5	24.0	16.8	14.4	13.2	12.5	12.1	11.7	11.5	11.3	11.1	11.0	10.9	10.8	10.7	10.6	10.6	10.5	10.5	10.4	10.4
9.0	22.4	16.0	13.9	12.8	12.2	11.8	11.5	11.3	11.1	10.9	10.8	10.7	10.6	10.6	10.5	10.5	10.4	10.4	10.3	10.3
9.5	21.1	15.4	13.5	12.5	11.9	11.6	11.3	11.1	10.9	10.8	10.7	10.6	10.5	10.5	10.4	10.4	10.3	10.3	10.3	10.2
10.0	19.9	14.8	13.1	12.2	11.7	11.4	11.1	11.0	10.8	10.7	10.6	10.5	10.5	10.4	10.4	10.3	10.3	10.2	10.2	10.2

NIST REFPROP $T_2(P_2, h_1)$, isenthalpic

NIST REFPROP $\rho_2(P_2, T_2)$

Using Table 20 and Table 23, cavity mass flowrate can be calculated as mass flowrate is the product of density and volumetric flowrate (see equation 2).

Table 24: Study 3 Cavity Mass Flowrate $\dot{m}_{cav.net}\left(\frac{kg}{s}\right)$

E (in.) \ H (in.)	0.5	1.0	1.5	2.0	2.5	3.0	3.5	4.0	4.5	5.0	5.5	6.0	6.5	7.0	7.5	8.0	8.5	9.0	9.5	10.0
0.5	-	-	-	-	-	-	-	-	-	-	-	-	-	-	-	-	-	-	-	-
1.0	-	-	-	-	-	-	-	-	-	-	-	-	-	-	-	-	-	-	-	-
1.5	-	-	-	-	-	-	-	-	-	-	0.25	0.25	0.26	0.26	0.27	0.27	0.28	0.28	0.28	0.29
2.0	-	-	-	-	-	0.25	0.26	0.27	0.27	0.28	0.29	0.30	0.30	0.31	0.32	0.33	0.33	0.34	0.35	0.35
2.5	-	-	-	0.25	0.27	0.28	0.29	0.30	0.31	0.33	0.34	0.35	0.36	0.37	0.38	0.40	0.41	0.42	0.43	0.44
3.0	-	-	0.26	0.28	0.30	0.31	0.33	0.35	0.36	0.38	0.40	0.41	0.43	0.45	0.46	0.48	0.50	0.51	0.53	0.55
3.5	-	0.26	0.28	0.30	0.33	0.35	0.37	0.40	0.42	0.44	0.47	0.49	0.51	0.54	0.56	0.58	0.61	0.63	0.65	0.68
4.0	-	0.27	0.30	0.33	0.36	0.39	0.43	0.46	0.49	0.52	0.55	0.58	0.61	0.64	0.67	0.70	0.73	0.76	0.79	0.82
4.5	-	0.29	0.33	0.37	0.41	0.45	0.48	0.52	0.56	0.60	0.64	0.68	0.72	0.76	0.80	0.84	0.87	0.91	0.95	0.99
5.0	0.26	0.31	0.36	0.41	0.45	0.50	0.55	0.60	0.65	0.70	0.74	0.79	0.84	0.89	0.94	0.99	1.03	1.08	1.13	1.18
5.5	0.27	0.33	0.39	0.45	0.51	0.56	0.62	0.68	0.74	0.80	0.86	0.92	0.98	1.04	1.09	1.15	1.21	1.27	1.33	1.39
6.0	0.28	0.35	0.42	0.49	0.56	0.63	0.70	0.77	0.84	0.91	0.99	1.06	1.13	1.20	1.27	1.34	1.41	1.48	1.55	1.62
6.5	0.29	0.38	0.46	0.54	0.63	0.71	0.79	0.87	0.96	1.04	1.12	1.21	1.29	1.37	1.45	1.54	1.62	1.70	1.79	1.87
7.0	0.31	0.40	0.50	0.60	0.69	0.79	0.89	0.98	1.08	1.17	1.27	1.37	1.46	1.56	1.66	1.75	1.85	1.95	2.04	2.14
7.5	0.32	0.43	0.54	0.65	0.77	0.88	0.99	1.10	1.21	1.32	1.43	1.54	1.65	1.76	1.87	1.99	2.10	2.21	2.32	2.43
8.0	0.34	0.46	0.59	0.72	0.84	0.97	1.10	1.22	1.35	1.48	1.60	1.73	1.85	1.98	2.11	2.23	2.36	2.49	2.61	2.74
8.5	0.35	0.50	0.64	0.78	0.93	1.07	1.21	1.36	1.50	1.64	1.78	1.93	2.07	2.21	2.36	2.50	2.64	2.79	2.93	3.07
9.0	0.37	0.53	0.69	0.85	1.01	1.17	1.34	1.50	1.66	1.82	1.98	2.14	2.30	2.46	2.62	2.78	2.94	3.10	3.26	3.42
9.5	0.39	0.57	0.75	0.93	1.11	1.29	1.47	1.64	1.82	2.00	2.18	2.36	2.54	2.72	2.90	3.08	3.26	3.44	3.62	3.80
10.0	0.41	0.61	0.81	1.01	1.21	1.40	1.60	1.80	2.00	2.20	2.40	2.60	2.80	2.99	3.19	3.39	3.59	3.79	3.99	4.19

Equation 2 $\dot{m}_{cav.net} = \rho_2 \cdot \dot{V}_{cav.net}$

With cavity mass flowrate calculated, leakage flowrate is all that is required to determine the isentropic efficiencies. This is done by evaluating the fluid state at the leakage throat using equations 18 and 19 with and an iterative process with throat specific heat ratio. Note the red values in Table 26 indicate a throat pressure lower than the state 3 pressure and are not choked. This is for reference. See appendix B for details. Throat parameters are calculated as:

Equation 18 $$T_t = \frac{T_2}{1 + \frac{\gamma_t - 1}{2}}$$

Equation 19 $$P_t = \frac{P_2}{\left(1 + \frac{\gamma_t - 1}{2}\right)^{\frac{\gamma_t}{\gamma_t - 1}}}$$

NIST REFPROP $\gamma_t\,(T_t, P_t)$

Table 25: Study 3 Throat Temperature T_t (°F)

E (in.) \ H (in.)	0.5	1.0	1.5	2.0	2.5	3.0	3.5	4.0	4.5	5.0	5.5	6.0	6.5	7.0	7.5	8.0	8.5	9.0	9.5	10.0
0.5	-	-	-	-	-	-	-	-	-	-	-	-	-	-	-	-	-	-	-	-
1.0	-	-	-	-	-	-	-	-	-	-	-	-	-	-	-	-	-	-	-	-
1.5	-	-	-	-	-	-	-	-	-	-	-36.5	-32.5	-30.0	-28.3	-27.2	-26.3	-25.7	-25.3	-25.0	-24.7
2.0	-	-	-	-	-	-35.6	-29.9	-27.2	-25.9	-25.1	-24.6	-24.4	-24.3	-24.2	-24.2	-24.2	-24.3	-24.3	-24.4	-24.5
2.5	-	-	-	-32.6	-27.2	-25.3	-24.6	-24.3	-24.2	-24.2	-24.3	-24.4	-24.5	-24.7	-24.8	-24.9	-25.0	-25.1	-25.2	-25.3
3.0	-	-	-29.7	-25.5	-24.4	-24.2	-24.3	-24.4	-24.6	-24.7	-24.9	-25.0	-25.2	-25.3	-25.4	-25.5	-25.6	-25.7	-25.8	-25.9
3.5	-	-32.2	-25.2	-24.3	-24.3	-24.4	-24.7	-24.9	-25.1	-25.3	-25.4	-25.6	-25.7	-25.8	-25.9	-26.0	-26.1	-26.1	-26.2	-26.3
4.0	-	-26.4	-24.3	-24.3	-24.6	-24.9	-25.1	-25.4	-25.6	-25.7	-25.9	-26.0	-26.1	-26.2	-26.3	-26.3	-26.4	-26.5	-26.5	-26.6
4.5	-	-24.7	-24.3	-24.6	-25.0	-25.3	-25.5	-25.7	-25.9	-26.1	-26.2	-26.3	-26.4	-26.4	-26.5	-26.6	-26.6	-26.7	-26.7	-26.8
5.0	-30.8	-24.2	-24.5	-25.0	-25.3	-25.6	-25.9	-26.0	-26.2	-26.3	-26.4	-26.5	-26.6	-26.6	-26.7	-26.8	-26.8	-26.8	-26.9	-26.9
5.5	-26.8	-24.3	-24.8	-25.3	-25.7	-25.9	-26.1	-26.3	-26.4	-26.5	-26.6	-26.7	-26.7	-26.8	-26.8	-26.9	-26.9	-27.0	-27.0	-27.0
6.0	-25.2	-24.5	-25.1	-25.6	-25.9	-26.2	-26.3	-26.5	-26.6	-26.7	-26.7	-26.8	-26.9	-26.9	-27.0	-27.0	-27.0	-27.1	-27.1	-27.1
6.5	-24.5	-24.7	-25.4	-25.8	-26.1	-26.3	-26.5	-26.6	-26.7	-26.8	-26.9	-26.9	-27.0	-27.0	-27.0	-27.1	-27.1	-27.1	-27.1	-27.2
7.0	-24.2	-25.0	-25.6	-26.0	-26.3	-26.5	-26.6	-26.7	-26.8	-26.9	-27.0	-27.0	-27.0	-27.1	-27.1	-27.1	-27.2	-27.2	-27.2	-27.2
7.5	-24.2	-25.2	-25.8	-26.2	-26.5	-26.6	-26.8	-26.8	-26.9	-27.0	-27.0	-27.1	-27.1	-27.1	-27.2	-27.2	-27.2	-27.2	-27.2	-27.3
8.0	-24.3	-25.4	-26.0	-26.4	-26.6	-26.7	-26.8	-26.9	-27.0	-27.1	-27.1	-27.1	-27.2	-27.2	-27.2	-27.2	-27.3	-27.3	-27.3	-27.3
8.5	-24.5	-25.6	-26.2	-26.5	-26.7	-26.8	-26.9	-27.0	-27.1	-27.1	-27.1	-27.2	-27.2	-27.2	-27.3	-27.3	-27.3	-27.3	-27.3	-27.3
9.0	-24.7	-25.8	-26.3	-26.6	-26.8	-26.9	-27.0	-27.1	-27.1	-27.2	-27.2	-27.2	-27.2	-27.3	-27.3	-27.3	-27.3	-27.3	-27.3	-27.4
9.5	-24.8	-25.9	-26.4	-26.7	-26.9	-27.0	-27.0	-27.1	-27.2	-27.2	-27.2	-27.3	-27.3	-27.3	-27.3	-27.3	-27.3	-27.4	-27.4	-27.4
10.0	-25.0	-26.1	-26.5	-26.8	-26.9	-27.0	-27.1	-27.2	-27.2	-27.2	-27.3	-27.3	-27.3	-27.3	-27.3	-27.4	-27.4	-27.4	-27.4	-27.4

Table 26: Study 3 Throat Pressure P_t $\left(\frac{\text{lbs}}{\text{in.}^2}\right)$

E (in.) \ H (in.)	0.5	1.0	1.5	2.0	2.5	3.0	3.5	4.0	4.5	5.0	5.5	6.0	6.5	7.0	7.5	8.0	8.5	9.0	9.5	10.0
0.5	-	-	-	-	-	-	-	-	-	-	-	-	-	-	-	-	-	-	-	-
1.0	-	-	-	-	-	-	-	-	-	-	-	-	-	-	-	-	-	-	-	-
1.5	-	-	-	-	-	-	-	-	-	-	587	553	522	495	472	450	431	414	399	385
2.0	-	-	-	-	-	580	521	474	436	405	379	357	339	323	309	296	286	276	267	259
2.5	-	-	-	554	472	415	373	341	316	296	279	265	253	243	234	226	219	213	208	203
3.0	-	-	518	422	362	321	291	269	251	237	225	216	207	200	194	189	184	180	176	173
3.5	-	550	412	339	294	263	242	225	212	202	193	186	180	175	170	166	163	160	157	155
4.0	-	452	341	284	250	226	210	197	187	179	173	167	163	159	155	152	150	147	145	143
4.5	-	381	292	247	219	201	188	178	170	164	159	154	151	148	145	143	140	139	137	135
5.0	533	330	257	220	198	183	172	164	158	153	149	145	142	140	138	136	134	132	131	130
5.5	464	291	231	200	182	169	161	154	149	145	141	138	136	134	132	131	129	128	127	126
6.0	409	262	211	185	170	159	152	146	142	139	136	133	131	130	128	127	126	125	124	123
6.5	366	239	196	174	160	152	145	140	137	134	131	129	128	126	125	124	123	122	121	120
7.0	331	221	183	164	153	145	140	136	133	130	128	126	125	123	122	121	121	120	119	119
7.5	302	206	173	157	147	140	136	132	129	127	125	124	122	121	120	120	119	118	118	117
8.0	279	194	165	151	142	136	132	129	127	125	123	122	121	120	119	118	117	117	116	116
8.5	259	184	159	146	138	133	129	126	124	123	121	120	119	118	117	117	116	116	115	115
9.0	243	176	153	142	135	130	127	124	122	121	120	119	118	117	116	116	115	115	114	114
9.5	229	169	148	138	132	128	125	123	121	119	118	117	117	116	115	115	114	114	114	113
10.0	217	163	144	135	129	126	123	121	119	118	117	116	116	115	114	114	114	113	113	113

Table 27: Study 3 Throat Specific Heat Ratio γ_t

E (in.) \ H (in.)	0.5	1.0	1.5	2.0	2.5	3.0	3.5	4.0	4.5	5.0	5.5	6.0	6.5	7.0	7.5	8.0	8.5	9.0	9.5	10.0
0.5	-	-	-	-	-	-	-	-	-	-	-	-	-	-	-	-	-	-	-	-
1.0	-	-	-	-	-	-	-	-	-	-	-	-	-	-	-	-	-	-	-	-
1.5	-	-	-	-	-	-	-	-	-	-	1.64	1.60	1.57	1.55	1.53	1.52	1.51	1.50	1.49	1.48
2.0	-	-	-	-	-	1.64	1.57	1.54	1.51	1.49	1.48	1.47	1.46	1.45	1.44	1.44	1.43	1.43	1.42	1.42
2.5	-	-	-	1.60	1.53	1.50	1.47	1.46	1.45	1.44	1.43	1.42	1.42	1.41	1.41	1.41	1.40	1.40	1.40	1.40
3.0	-	-	1.57	1.50	1.47	1.45	1.43	1.42	1.42	1.41	1.40	1.40	1.40	1.39	1.39	1.39	1.39	1.39	1.39	1.38
3.5	-	1.60	1.50	1.46	1.43	1.42	1.41	1.40	1.40	1.40	1.39	1.39	1.39	1.38	1.38	1.38	1.38	1.38	1.38	1.38
4.0	-	1.52	1.46	1.43	1.42	1.41	1.40	1.39	1.39	1.39	1.38	1.38	1.38	1.38	1.38	1.38	1.38	1.37	1.37	1.37
4.5	-	1.48	1.43	1.41	1.40	1.40	1.39	1.39	1.38	1.38	1.38	1.38	1.38	1.37	1.37	1.37	1.37	1.37	1.37	1.37
5.0	1.58	1.45	1.42	1.40	1.39	1.39	1.38	1.38	1.38	1.38	1.37	1.37	1.37	1.37	1.37	1.37	1.37	1.37	1.37	1.37
5.5	1.53	1.43	1.41	1.39	1.39	1.38	1.38	1.38	1.37	1.37	1.37	1.37	1.37	1.37	1.37	1.37	1.37	1.37	1.37	1.37
6.0	1.49	1.42	1.40	1.39	1.38	1.38	1.38	1.37	1.37	1.37	1.37	1.37	1.37	1.37	1.37	1.37	1.37	1.37	1.37	1.37
6.5	1.47	1.41	1.39	1.38	1.38	1.38	1.37	1.37	1.37	1.37	1.37	1.37	1.37	1.37	1.37	1.37	1.37	1.37	1.36	1.36
7.0	1.45	1.40	1.39	1.38	1.38	1.37	1.37	1.37	1.37	1.37	1.37	1.37	1.37	1.37	1.37	1.36	1.36	1.36	1.36	1.36
7.5	1.44	1.40	1.38	1.38	1.37	1.37	1.37	1.37	1.37	1.37	1.37	1.37	1.37	1.36	1.36	1.36	1.36	1.36	1.36	1.36
8.0	1.43	1.39	1.38	1.38	1.37	1.37	1.37	1.37	1.37	1.37	1.37	1.36	1.36	1.36	1.36	1.36	1.36	1.36	1.36	1.36
8.5	1.42	1.39	1.38	1.37	1.37	1.37	1.37	1.37	1.37	1.37	1.36	1.36	1.36	1.36	1.36	1.36	1.36	1.36	1.36	1.36
9.0	1.41	1.39	1.38	1.37	1.37	1.37	1.37	1.37	1.37	1.36	1.36	1.36	1.36	1.36	1.36	1.36	1.36	1.36	1.36	1.36
9.5	1.41	1.38	1.37	1.37	1.37	1.37	1.37	1.37	1.36	1.36	1.36	1.36	1.36	1.36	1.36	1.36	1.36	1.36	1.36	1.36
10.0	1.40	1.38	1.37	1.37	1.37	1.37	1.37	1.36	1.36	1.36	1.36	1.36	1.36	1.36	1.36	1.36	1.36	1.36	1.36	1.36

The throat density and local speed of sound can be calculated using

Table 25, Table 26, and Table 27. These are used to calculate leakage mass flowrates.

Table 28: Study 3 Throat Density ρ_t $\left(\frac{kg}{m^3}\right)$

E (in.) \ H (in.)	0.5	1.0	1.5	2.0	2.5	3.0	3.5	4.0	4.5	5.0	5.5	6.0	6.5	7.0	7.5	8.0	8.5	9.0	9.5	10.0
0.5	-	-	-	-	-	-	-	-	-	-	-	-	-	-	-	-	-	-	-	-
1.0	-	-	-	-	-	-	-	-	-	-	-	-	-	-	-	-	-	-	-	-
1.5	-	-	-	-	-	-	-	-	-	-	39.81	36.46	33.79	31.59	29.73	28.13	26.75	25.53	24.45	23.49
2.0	-	-	-	-	-	39.15	33.69	29.89	27.05	24.83	23.05	21.58	20.34	19.29	18.39	17.60	16.91	16.30	15.75	15.26
2.5	-	-	-	36.56	29.80	25.58	22.67	20.52	18.87	17.56	16.49	15.61	14.87	14.23	13.68	13.20	12.78	12.40	12.07	11.76
3.0	-	-	33.41	26.06	21.89	19.17	17.26	15.84	14.73	13.86	13.14	12.55	12.05	11.62	11.25	10.92	10.64	10.38	10.16	9.95
3.5	-	36.19	25.37	20.36	17.44	15.51	14.14	13.13	12.34	11.71	11.19	10.76	10.40	10.09	9.82	9.59	9.38	9.20	9.04	8.89
4.0	-	28.22	20.53	16.84	14.65	13.21	12.18	11.41	10.82	10.34	9.95	9.63	9.36	9.12	8.92	8.74	8.59	8.45	8.32	8.21
4.5	-	23.19	17.34	14.48	12.78	11.66	10.86	10.26	9.79	9.42	9.12	8.86	8.65	8.47	8.31	8.17	8.05	7.94	7.84	7.75
5.0	34.74	19.75	15.11	12.83	11.47	10.57	9.92	9.44	9.07	8.77	8.53	8.32	8.15	8.00	7.88	7.76	7.67	7.58	7.50	7.43
5.5	29.16	17.27	13.49	11.62	10.51	9.77	9.24	8.85	8.54	8.29	8.09	7.93	7.79	7.66	7.56	7.47	7.39	7.32	7.25	7.19
6.0	25.16	15.41	12.27	10.71	9.79	9.17	8.73	8.40	8.14	7.93	7.77	7.63	7.51	7.41	7.32	7.24	7.18	7.12	7.06	7.01
6.5	22.15	13.99	11.33	10.01	9.23	8.70	8.33	8.05	7.83	7.66	7.51	7.40	7.30	7.21	7.14	7.07	7.01	6.96	6.92	6.88
7.0	19.83	12.87	10.59	9.46	8.79	8.34	8.01	7.77	7.59	7.44	7.32	7.21	7.13	7.05	6.99	6.93	6.88	6.84	6.80	6.77
7.5	17.98	11.97	10.00	9.02	8.43	8.04	7.76	7.55	7.39	7.26	7.16	7.07	6.99	6.93	6.87	6.82	6.78	6.74	6.71	6.68
8.0	16.49	11.24	9.52	8.66	8.14	7.80	7.56	7.37	7.23	7.12	7.02	6.95	6.88	6.83	6.78	6.73	6.70	6.66	6.63	6.61
8.5	15.26	10.64	9.12	8.36	7.91	7.60	7.39	7.23	7.10	7.00	6.92	6.85	6.79	6.74	6.70	6.66	6.63	6.60	6.57	6.55
9.0	14.24	10.14	8.79	8.11	7.71	7.44	7.25	7.10	6.99	6.90	6.83	6.77	6.71	6.67	6.63	6.60	6.57	6.54	6.52	6.50
9.5	13.38	9.72	8.51	7.90	7.54	7.30	7.13	7.00	6.90	6.82	6.75	6.70	6.65	6.61	6.58	6.55	6.52	6.50	6.47	6.46
10.0	12.66	9.36	8.27	7.72	7.40	7.18	7.02	6.91	6.82	6.74	6.69	6.64	6.59	6.56	6.53	6.50	6.48	6.46	6.44	6.42

NIST REFPROP $\rho_t\ (T_t, P_t)$

Table 29: Study 3 Throat Average Velocity $\widetilde{V}_t$ $\left(\frac{m}{s}\right)$

E (in.) \ H (in.)	0.5	1.0	1.5	2.0	2.5	3.0	3.5	4.0	4.5	5.0	5.5	6.0	6.5	7.0	7.5	8.0	8.5	9.0	9.5	10.0
0.5	-	-	-	-	-	-	-	-	-	-	-	-	-	-	-	-	-	-	-	-
1.0	-	-	-	-	-	-	-	-	-	-	-	-	-	-	-	-	-	-	-	-
1.5	-	-	-	-	-	-	-	-	-	-	447.6	444.1	441.3	439.0	437.1	435.5	434.0	432.8	431.6	430.6
2.0	-	-	-	-	-	446.9	441.2	437.3	434.3	432.0	430.1	428.6	427.3	426.1	425.2	424.3	423.5	422.9	422.3	421.7
2.5	-	-	-	444.2	437.2	432.8	429.7	427.5	425.7	424.3	423.1	422.1	421.3	420.6	420.0	419.4	419.0	418.6	418.2	417.8
3.0	-	-	440.9	433.3	428.9	426.0	423.9	422.4	421.2	420.2	419.4	418.7	418.2	417.7	417.2	416.9	416.6	416.3	416.0	415.8
3.5	-	443.8	432.6	427.3	424.1	422.0	420.5	419.4	418.5	417.8	417.2	416.7	416.3	415.9	415.6	415.4	415.1	414.9	414.7	414.6
4.0	-	435.6	427.5	423.5	421.1	419.5	418.3	417.4	416.8	416.2	415.8	415.4	415.1	414.8	414.6	414.4	414.2	414.0	413.9	413.8
4.5	-	430.3	424.0	420.9	419.0	417.7	416.8	416.1	415.6	415.2	414.8	414.5	414.3	414.1	413.9	413.7	413.6	413.5	413.3	413.2
5.0	442.3	426.6	421.6	419.0	417.5	416.5	415.7	415.2	414.8	414.4	414.1	413.9	413.7	413.5	413.4	413.3	413.1	413.0	412.9	412.9
5.5	436.5	423.9	419.8	417.7	416.4	415.6	415.0	414.5	414.1	413.9	413.6	413.4	413.3	413.1	413.0	412.9	412.8	412.7	412.7	412.6
6.0	432.4	421.9	418.4	416.6	415.6	414.9	414.4	414.0	413.7	413.4	413.3	413.1	413.0	412.8	412.7	412.6	412.6	412.5	412.4	412.4
6.5	429.2	420.3	417.3	415.8	414.9	414.3	413.9	413.6	413.3	413.1	413.0	412.8	412.7	412.6	412.5	412.4	412.4	412.3	412.3	412.2
7.0	426.7	419.1	416.5	415.2	414.4	413.9	413.5	413.3	413.0	412.9	412.7	412.6	412.5	412.4	412.3	412.3	412.2	412.2	412.1	412.1
7.5	424.7	418.1	415.8	414.7	414.0	413.6	413.2	413.0	412.8	412.7	412.5	412.4	412.4	412.3	412.2	412.2	412.1	412.1	412.0	412.0
8.0	423.1	417.2	415.3	414.3	413.7	413.3	413.0	412.8	412.6	412.5	412.4	412.3	412.2	412.2	412.1	412.1	412.0	412.0	411.9	411.9
8.5	421.7	416.6	414.8	413.9	413.4	413.1	412.8	412.6	412.5	412.4	412.3	412.2	412.1	412.1	412.0	412.0	411.9	411.9	411.9	411.8
9.0	420.6	416.0	414.4	413.7	413.2	412.9	412.6	412.5	412.3	412.2	412.2	412.1	412.0	412.0	411.9	411.9	411.9	411.8	411.8	411.8
9.5	419.7	415.5	414.1	413.4	413.0	412.7	412.5	412.4	412.2	412.1	412.1	412.0	412.0	411.9	411.9	411.8	411.8	411.8	411.7	411.7
10.0	418.8	415.1	413.8	413.2	412.8	412.6	412.4	412.3	412.1	412.1	412.0	411.9	411.9	411.8	411.8	411.8	411.7	411.7	411.7	411.7

Equation 16 $$\widetilde{V}_t = \sqrt{\gamma_t R_g T_t}$$

Next, the leak points cross sectional areas are calculated. Core leakage area using a cylindrical core is static as it is only dependent on R_1.

Table 30: Study 3 Core Leakage Area (cylindrical core)

$A_{CynLeakage}$ (in.^{2})

E (in.) \ H (in.)	0.5	1.0	1.5	2.0	2.5	3.0	3.5	4.0	4.5	5.0	5.5	6.0	6.5	7.0	7.5	8.0	8.5	9.0	9.5	10.0
0.5																				
1.0																				
1.5																				
2.0																				
2.5																				
3.0																				
3.5																				
4.0																				
4.5																				
5.0																				
5.5																				
6.0																				
6.5																				
7.0																				
7.5																				
8.0																				
8.5																				
9.0																				
9.5																				
10.0																				

$$.00499 \text{ in.}^2$$

Equation 25 $$A_{CynLeakage} = R_1^2\left[4 - \pi - \pi\left(1 - \sqrt{2}\right)^2\right] \cong .319R_1^2$$

Table 31: Study 3 Gap Leakage Area

A_{gap} (in.^{2})

E (in.) \ H (in.)	0.5	1.0	1.5	2.0	2.5	3.0	3.5	4.0	4.5	5.0	5.5	6.0	6.5	7.0	7.5	8.0	8.5	9.0	9.5	10.0
0.5	0.009	0.012	0.017	0.021	0.026	0.031	0.036	0.041	0.046	0.050	0.055	0.060	0.065	0.070	0.075	0.080	0.085	0.090	0.095	0.100
1.0	0.016	0.018	0.021	0.025	0.029	0.033	0.038	0.043	0.047	0.052	0.057	0.062	0.067	0.072	0.076	0.081	0.086	0.091	0.096	0.101
1.5	0.023	0.025	0.027	0.030	0.034	0.038	0.042	0.046	0.050	0.055	0.060	0.064	0.069	0.074	0.078	0.083	0.088	0.093	0.098	0.103
2.0	0.031	0.032	0.034	0.037	0.040	0.043	0.046	0.050	0.054	0.059	0.063	0.067	0.072	0.076	0.081	0.086	0.090	0.095	0.100	0.105
2.5	0.039	0.040	0.041	0.043	0.046	0.049	0.052	0.055	0.059	0.063	0.067	0.071	0.076	0.080	0.084	0.089	0.093	0.098	0.102	0.107
3.0	0.047	0.047	0.049	0.050	0.053	0.055	0.058	0.061	0.065	0.068	0.072	0.076	0.080	0.084	0.088	0.092	0.097	0.101	0.106	0.110
3.5	0.054	0.055	0.056	0.058	0.060	0.062	0.064	0.067	0.070	0.074	0.077	0.081	0.085	0.089	0.093	0.097	0.101	0.105	0.109	0.114
4.0	0.062	0.063	0.064	0.065	0.067	0.069	0.071	0.074	0.077	0.080	0.083	0.086	0.090	0.094	0.097	0.101	0.105	0.109	0.113	0.118
4.5	0.070	0.071	0.071	0.073	0.074	0.076	0.078	0.081	0.083	0.086	0.089	0.092	0.095	0.099	0.103	0.106	0.110	0.114	0.118	0.122
5.0	0.078	0.078	0.079	0.080	0.082	0.083	0.085	0.087	0.090	0.092	0.095	0.098	0.101	0.105	0.108	0.112	0.115	0.119	0.123	0.127
5.5	0.086	0.086	0.087	0.088	0.089	0.091	0.092	0.094	0.097	0.099	0.102	0.105	0.107	0.111	0.114	0.117	0.121	0.124	0.128	0.132
6.0	0.094	0.094	0.095	0.096	0.097	0.098	0.100	0.102	0.104	0.106	0.108	0.111	0.114	0.117	0.120	0.123	0.126	0.130	0.133	0.137
6.5	0.101	0.102	0.102	0.103	0.104	0.106	0.107	0.109	0.111	0.113	0.115	0.118	0.120	0.123	0.126	0.129	0.132	0.135	0.139	0.142
7.0	0.109	0.110	0.110	0.111	0.112	0.113	0.115	0.116	0.118	0.120	0.122	0.125	0.127	0.130	0.132	0.135	0.138	0.141	0.145	0.148
7.5	0.117	0.117	0.118	0.119	0.120	0.121	0.122	0.124	0.125	0.127	0.129	0.131	0.134	0.136	0.139	0.142	0.145	0.148	0.151	0.154
8.0	0.125	0.125	0.126	0.126	0.127	0.128	0.130	0.131	0.133	0.134	0.136	0.139	0.141	0.143	0.146	0.148	0.151	0.154	0.157	0.160
8.5	0.133	0.133	0.134	0.134	0.135	0.136	0.137	0.139	0.140	0.142	0.144	0.146	0.148	0.150	0.152	0.155	0.158	0.160	0.163	0.166
9.0	0.141	0.141	0.141	0.142	0.143	0.144	0.145	0.146	0.148	0.149	0.151	0.153	0.155	0.157	0.159	0.162	0.164	0.167	0.170	0.173
9.5	0.148	0.149	0.149	0.150	0.151	0.151	0.152	0.154	0.155	0.157	0.158	0.160	0.162	0.164	0.166	0.169	0.171	0.174	0.176	0.179
10.0	0.156	0.157	0.157	0.158	0.158	0.159	0.160	0.161	0.163	0.164	0.166	0.167	0.169	0.171	0.173	0.176	0.178	0.180	0.183	0.186

Equation 69 $$A_{gap} = 2G\sqrt{[\pi T_{helix} D]^2 + H^2}$$

Table 28, Table 29, Table 30, and Table 31 calculate total leakage mass flowrate.

Table 32: Study 3 Total Leakage Mass Flowrate $\dot{m}_{leak}$ $\left(\frac{kg}{s}\right)$

E (in.) \ H (in.)	0.5	1.0	1.5	2.0	2.5	3.0	3.5	4.0	4.5	5.0	5.5	6.0	6.5	7.0	7.5	8.0	8.5	9.0	9.5	10.0
0.5	-	-	-	-	-	-	-	-	-	-	-	-	-	-	-	-	-	-	-	-
1.0	-	-	-	-	-	-	-	-	-	-	-	-	-	-	-	-	-	-	-	-
1.5	-	-	-	-	-	-	-	-	-	-	0.742	0.722	0.711	0.703	0.699	0.697	0.696	0.697	0.699	0.702
2.0	-	-	-	-	-	0.540	0.494	0.467	0.450	0.440	0.434	0.432	0.431	0.432	0.434	0.437	0.440	0.445	0.450	0.455
2.5	-	-	-	0.506	0.427	0.384	0.358	0.342	0.333	0.327	0.325	0.324	0.325	0.328	0.331	0.335	0.339	0.344	0.350	0.356
3.0	-	-	0.510	0.404	0.349	0.317	0.298	0.286	0.279	0.275	0.273	0.274	0.276	0.278	0.282	0.286	0.291	0.296	0.302	0.307
3.5	-	0.622	0.433	0.352	0.308	0.283	0.267	0.257	0.251	0.248	0.248	0.248	0.250	0.253	0.257	0.261	0.266	0.271	0.276	0.282
4.0	-	0.538	0.390	0.323	0.286	0.264	0.250	0.242	0.237	0.235	0.235	0.236	0.238	0.241	0.244	0.248	0.253	0.258	0.263	0.269
4.5	-	0.487	0.363	0.305	0.274	0.255	0.243	0.235	0.231	0.229	0.229	0.230	0.232	0.235	0.238	0.243	0.247	0.252	0.257	0.263
5.0	0.822	0.453	0.346	0.296	0.268	0.251	0.240	0.234	0.230	0.228	0.228	0.229	0.231	0.234	0.237	0.241	0.246	0.250	0.255	0.261
5.5	0.745	0.430	0.336	0.291	0.266	0.251	0.241	0.235	0.232	0.231	0.231	0.232	0.233	0.236	0.239	0.243	0.247	0.252	0.256	0.262
6.0	0.692	0.415	0.330	0.290	0.267	0.253	0.244	0.239	0.236	0.235	0.235	0.236	0.238	0.240	0.243	0.247	0.251	0.255	0.260	0.265
6.5	0.653	0.405	0.328	0.291	0.270	0.257	0.249	0.245	0.242	0.241	0.241	0.242	0.243	0.246	0.249	0.252	0.256	0.260	0.265	0.269
7.0	0.624	0.399	0.328	0.294	0.275	0.263	0.256	0.251	0.249	0.248	0.248	0.249	0.250	0.253	0.256	0.259	0.262	0.266	0.271	0.275
7.5	0.601	0.395	0.330	0.298	0.281	0.270	0.263	0.259	0.257	0.256	0.256	0.257	0.258	0.260	0.263	0.266	0.270	0.274	0.278	0.282
8.0	0.585	0.394	0.333	0.304	0.288	0.277	0.271	0.267	0.265	0.264	0.264	0.265	0.267	0.269	0.271	0.274	0.278	0.281	0.285	0.290
8.5	0.572	0.395	0.338	0.311	0.295	0.286	0.280	0.276	0.274	0.273	0.273	0.274	0.276	0.278	0.280	0.283	0.286	0.290	0.294	0.298
9.0	0.563	0.397	0.344	0.318	0.304	0.295	0.289	0.286	0.284	0.283	0.283	0.284	0.285	0.287	0.290	0.292	0.295	0.299	0.302	0.306
9.5	0.556	0.400	0.350	0.326	0.312	0.304	0.299	0.295	0.294	0.293	0.293	0.294	0.295	0.297	0.299	0.302	0.305	0.308	0.312	0.315
10.0	0.552	0.405	0.357	0.335	0.322	0.314	0.309	0.306	0.304	0.303	0.303	0.304	0.305	0.307	0.309	0.312	0.315	0.318	0.321	0.325

Equation 2 $$\dot{m}_{leak} = \rho_t \cdot \dot{V}_{tot.leak} = \rho_t \tilde{V}_t \left(A_{gap} + A_{CynLeakage}\right)$$

Summing Table 24 and Table 32 yields the total mass flowrate through the PRE for each machine radius E and rotor height H combination.

Table 33: Study 3 Total PRE Mass Flowrate $\dot{m}_{tot}$ $\left(\frac{kg}{s}\right)$

E (in.) \ H (in.)	0.5	1.0	1.5	2.0	2.5	3.0	3.5	4.0	4.5	5.0	5.5	6.0	6.5	7.0	7.5	8.0	8.5	9.0	9.5	10.0
0.5	-	-	-	-	-	-	-	-	-	-	-	-	-	-	-	-	-	-	-	-
1.0	-	-	-	-	-	-	-	-	-	-	-	-	-	-	-	-	-	-	-	-
1.5	-	-	-	-	-	-	-	-	-	-	0.99	0.98	0.97	0.97	0.97	0.97	0.97	0.98	0.98	0.99
2.0	-	-	-	-	-	0.79	0.75	0.73	0.73	0.7	0.72	0.73	0.73	0.74	0.75	0.76	0.77	0.78	0.80	0.81
2.5	-	-	-	0.76	0.69	0.66	0.65	0.65	0.65	0.65	0.66	0.67	0.69	0.70	0.71	0.73	0.75	0.76	0.78	0.80
3.0	-	-	0.77	0.68	0.6	0.63	0.63	0.63	0.64	0.65	0.67	0.69	0.71	0.73	0.75	0.77	0.79	0.81	0.83	0.86
3.5	-	0.88	0.71	0.66	0.64	0.63	0.64	0.65	0.67	0.69	0.71	0.74	0.76	0.79	0.82	0.84	0.87	0.90	0.93	0.96
4.0	-	0.81	0.69	0.66	0.65	0.66	0.68	0.70	0.72	0.75	0.78	0.81	0.85	0.88	0.91	0.95	0.98	1.02	1.06	1.09
4.5	-	0.78	0.69	0.67	0.68	0.70	0.73	0.76	0.79	0.83	0.87	0.91	0.95	0.99	1.03	1.08	1.12	1.17	1.21	1.25
5.0	1.08	0.76	0.70	0.70	0.72	0.75	0.79	0.83	0.88	0.92	0.97	1.02	1.07	1.12	1.18	1.23	1.28	1.33	1.39	1.44
5.5	1.01	0.76	0.72	0.74	0.77	0.82	0.86	0.92	0.97	1.03	1.09	1.15	1.21	1.27	1.33	1.40	1.46	1.52	1.59	1.65
6.0	0.97	0.77	0.75	0.78	0.83	0.89	0.95	1.01	1.08	1.15	1.22	1.29	1.36	1.44	1.51	1.58	1.66	1.73	1.81	1.88
6.5	0.95	0.78	0.79	0.83	0.90	0.97	1.04	1.12	1.20	1.28	1.36	1.45	1.53	1.62	1.70	1.79	1.88	1.96	2.05	2.14
7.0	0.93	0.80	0.83	0.89	0.97	1.05	1.14	1.23	1.33	1.42	1.52	1.62	1.71	1.81	1.91	2.01	2.11	2.21	2.31	2.41
7.5	0.92	0.83	0.87	0.95	1.05	1.15	1.25	1.36	1.47	1.58	1.69	1.80	1.91	2.02	2.14	2.25	2.37	2.48	2.60	2.71
8.0	0.92	0.86	0.92	1.02	1.13	1.25	1.37	1.49	1.61	1.74	1.87	1.99	2.12	2.25	2.38	2.51	2.64	2.77	2.90	3.03
8.5	0.93	0.89	0.98	1.09	1.22	1.36	1.49	1.63	1.77	1.91	2.06	2.20	2.35	2.49	2.64	2.78	2.93	3.08	3.22	3.37
9.0	0.93	0.93	1.04	1.17	1.32	1.47	1.62	1.78	1.94	2.10	2.26	2.42	2.58	2.75	2.91	3.07	3.24	3.40	3.56	3.73
9.5	0.95	0.97	1.10	1.25	1.42	1.59	1.76	1.94	2.12	2.30	2.48	2.66	2.84	3.02	3.20	3.38	3.56	3.74	3.93	4.11
10.0	0.96	1.01	1.17	1.34	1.53	1.72	1.91	2.11	2.30	2.50	2.70	2.90	3.10	3.30	3.50	3.70	3.91	4.11	4.31	4.51

Equation 88 $$\dot{m}_{tot} = \dot{m}_{cavity} + \dot{m}_{leakage}$$

Mass efficiency as stated by equation 2 is shown in Table 34 using cavity mass flowrate from Table 24 and total mass flowrate from Table 33.

Table 34: Study 3 Mass Efficiency

E_{mass}

E (in.) \ H (in.)	0.5	1.0	1.5	2.0	2.5	3.0	3.5	4.0	4.5	5.0	5.5	6.0	6.5	7.0	7.5	8.0	8.5	9.0	9.5	10.0
0.5	-	-	-	-	-	-	-	-	-	-	-	-	-	-	-	-	-	-	-	-
1.0	-	-	-	-	-	-	-	-	-	-	-	-	-	-	-	-	-	-	-	-
1.5	-	-	-	-	-	-	-	-	-	-	25%	26%	27%	27%	28%	28%	28%	29%	29%	29%
2.0	-	-	-	-	-	32%	34%	36%	38%	39%	40%	41%	41%	42%	42%	43%	43%	43%	44%	44%
2.5	-	-	-	33%	38%	42%	45%	47%	49%	50%	51%	52%	53%	53%	54%	54%	55%	55%	55%	55%
3.0	-	-	34%	41%	46%	50%	53%	55%	57%	58%	59%	60%	61%	62%	62%	63%	63%	63%	64%	64%
3.5	-	29%	39%	46%	51%	55%	58%	61%	63%	64%	65%	66%	67%	68%	69%	69%	70%	70%	70%	71%
4.0	-	34%	44%	51%	56%	60%	63%	65%	67%	69%	70%	71%	72%	73%	73%	74%	74%	75%	75%	75%
4.5	-	37%	48%	55%	60%	64%	67%	69%	71%	72%	74%	75%	76%	76%	77%	78%	78%	78%	79%	79%
5.0	24%	40%	51%	58%	63%	67%	70%	72%	74%	75%	77%	78%	78%	79%	80%	80%	81%	81%	82%	82%
5.5	27%	43%	54%	61%	66%	69%	72%	74%	76%	78%	79%	80%	81%	81%	82%	83%	83%	83%	84%	84%
6.0	29%	46%	56%	63%	68%	71%	74%	76%	78%	80%	81%	82%	83%	83%	84%	84%	85%	85%	86%	86%
6.5	31%	48%	58%	65%	70%	73%	76%	78%	80%	81%	82%	83%	84%	85%	85%	86%	86%	87%	87%	87%
7.0	33%	50%	60%	67%	72%	75%	78%	80%	81%	83%	84%	85%	85%	86%	87%	87%	88%	88%	88%	89%
7.5	35%	52%	62%	69%	73%	76%	79%	81%	82%	84%	85%	86%	86%	87%	88%	88%	89%	89%	89%	90%
8.0	37%	54%	64%	70%	75%	78%	80%	82%	84%	85%	86%	87%	87%	88%	89%	89%	89%	90%	90%	90%
8.5	38%	56%	65%	72%	76%	79%	81%	83%	85%	86%	87%	88%	88%	89%	89%	90%	90%	91%	91%	91%
9.0	40%	57%	67%	73%	77%	80%	82%	84%	85%	87%	87%	88%	89%	90%	90%	90%	91%	91%	92%	92%
9.5	41%	59%	68%	74%	78%	81%	83%	85%	86%	87%	88%	89%	90%	90%	91%	91%	91%	92%	92%	92%
10.0	43%	60%	69%	75%	79%	82%	84%	86%	87%	88%	89%	90%	90%	91%	91%	92%	92%	92%	93%	93%

Equation 2 $$E_{mass} = \frac{\dot{m}_{cav.net}}{\dot{m}_{tot}}$$

Table 34 shows that as machine size increases, so does mass efficiency. Since mass efficiency is a measure of total mass being processed by the rotors, intuition might state that a larger machine size would produce a higher isentropic efficiency due to a larger percentage of the total mass flowrate being used. The definition of isentropic efficiency in equation 6 show how mass efficiency does not include all the variables required to assess isentropic efficiency.

Finally, the isentropic efficiency for the different PRE rotor combination can be calculated using equation 6 and the total mass flowrate in Table 33.

Table 35: Study 3 Isentropic Efficiency E_{system}

E (in.) \ H (in.)	0.5	1.0	1.5	2.0	2.5	3.0	3.5	4.0	4.5	5.0	5.5	6.0	6.5	7.0	7.5	8.0	8.5	9.0	9.5	10.0
0.5	-	-	-	-	-	-	-	-	-	-	-	-	-	-	-	-	-	-	-	-
1.0	-	-	-	-	-	-	-	-	-	-	-	-	-	-	-	-	-	-	-	-
1.5	-	-	-	-	-	-	-	-	-	-	14.8%	15.0%	15.1%	15.2%	15.2%	15.1%	15.1%	15.0%	14.9%	14.8%
2.0	-	-	-	-	-	18.5%	19.4%	20.0%	20.2%	20.3%	20.2%	20.1%	19.9%	19.7%	19.5%	19.2%	18.9%	18.7%	18.4%	18.1%
2.5	-	-	-	19.2%	21.1%	22.1%	22.6%	22.7%	22.6%	22.4%	22.1%	21.7%	21.3%	20.9%	20.5%	20.1%	19.6%	19.2%	18.8%	18.4%
3.0	-	-	19.0%	21.5%	22.7%	23.3%	23.4%	23.2%	22.8%	22.4%	21.9%	21.3%	20.7%	20.2%	19.6%	19.1%	18.6%	18.1%	17.6%	17.1%
3.5	-	16.7%	20.5%	22.3%	23.0%	23.1%	22.9%	22.4%	21.8%	21.2%	20.5%	19.8%	19.2%	18.5%	17.9%	17.4%	16.8%	16.3%	15.8%	15.3%
4.0	-	18.1%	21.2%	22.3%	22.5%	22.2%	21.7%	21.0%	20.2%	19.5%	18.7%	18.0%	17.3%	16.6%	16.0%	15.4%	14.9%	14.4%	13.9%	13.4%
4.5	-	18.9%	21.2%	21.8%	21.5%	20.9%	20.1%	19.3%	18.4%	17.6%	16.8%	16.1%	15.4%	14.8%	14.2%	13.6%	13.1%	12.6%	12.1%	11.7%
5.0	13.6%	19.2%	20.8%	20.9%	20.3%	19.5%	18.5%	17.6%	16.7%	15.8%	15.1%	14.3%	13.7%	13.0%	12.5%	11.9%	11.4%	11.0%	10.6%	10.2%
5.5	14.4%	19.3%	20.2%	19.8%	19.0%	18.0%	16.9%	16.0%	15.0%	14.2%	13.4%	12.7%	12.1%	11.5%	11.0%	10.5%	10.0%	9.6%	9.2%	8.9%
6.0	15.1%	19.1%	19.5%	18.7%	17.6%	16.5%	15.4%	14.5%	13.6%	12.7%	12.0%	11.3%	10.7%	10.2%	9.7%	9.2%	8.8%	8.5%	8.1%	7.8%
6.5	15.5%	18.7%	18.6%	17.6%	16.4%	15.2%	14.1%	13.1%	12.2%	11.4%	10.7%	10.1%	9.6%	9.1%	8.6%	8.2%	7.8%	7.5%	7.1%	6.9%
7.0	15.7%	18.2%	17.7%	16.4%	15.1%	13.9%	12.8%	11.9%	11.0%	10.3%	9.6%	9.1%	8.5%	8.1%	7.7%	7.3%	6.9%	6.6%	6.3%	6.1%
7.5	15.9%	17.7%	16.8%	15.4%	14.0%	12.8%	11.7%	10.8%	10.0%	9.3%	8.7%	8.1%	7.7%	7.2%	6.9%	6.5%	6.2%	5.9%	5.6%	5.4%
8.0	15.9%	17.1%	15.9%	14.3%	12.9%	11.7%	10.7%	9.8%	9.1%	8.4%	7.8%	7.3%	6.9%	6.5%	6.2%	5.8%	5.6%	5.3%	5.1%	4.8%
8.5	15.8%	16.4%	15.0%	13.4%	12.0%	10.8%	9.8%	9.0%	8.3%	7.6%	7.1%	6.7%	6.2%	5.9%	5.6%	5.3%	5.0%	4.8%	4.5%	4.3%
9.0	15.7%	15.8%	14.1%	12.5%	11.1%	10.0%	9.0%	8.2%	7.5%	7.0%	6.5%	6.0%	5.7%	5.3%	5.0%	4.8%	4.5%	4.3%	4.1%	3.9%
9.5	15.5%	15.1%	13.3%	11.7%	10.3%	9.2%	8.3%	7.5%	6.9%	6.4%	5.9%	5.5%	5.2%	4.9%	4.6%	4.3%	4.1%	3.9%	3.7%	3.6%
10.0	15.2%	14.4%	12.6%	10.9%	9.6%	8.5%	7.7%	6.9%	6.4%	5.9%	5.4%	5.0%	4.7%	4.4%	4.2%	4.0%	3.7%	3.6%	3.4%	3.2%

Equation 6 $$E_{system} = \frac{\dot{V}_{cav.net} \cdot (P_2 - P_3)}{\dot{m}_{tot}(h_1 - h_{3,Isentropic})} = \frac{\dot{w}_{shaft}}{\dot{m}_{tot}(h_1 - h_{3,Isentropic})}$$

NIST REFPROP $h_1(P_1, T_1)$

NIST REFPROP $h_{3,isentropic}(P_3, s_1)$

Table 35 is the calculated result of equation 88, which can be used to optimize a PRE with varying machine radius E and rotor height H in a target power application. It shows for study 3, a 3.5 inch by 3 inch rotor configuration yields the most efficient PRE design with the given application (~24%). It is important to reiterate that the presented PRE design does not incorporate a metering valve and runs “hydraulically”. Approximately 50% of the fluid energy in this application is accessible due to the absence of a meter.

The first byproduct of using a PRE is generated shaft power. Using equation 5, Table 20, and Table 21, shaft power generated is calculated in Table 36 showing iteration convergence.

Table 36: Study 3 Shaft Power $\dot{w}_{shaft}$ (kW)

E (in.) \ H (in.)	0.5	1.0	1.5	2.0	2.5	3.0	3.5	4.0	4.5	5.0	5.5	6.0	6.5	7.0	7.5	8.0	8.5	9.0	9.5	10.0
0.5	-	-	-	-	-	-	-	-	-	-	-	-	-	-	-	-	-	-	-	-
1.0	-	-	-	-	-	-	-	-	-	-	-	-	-	-	-	-	-	-	-	-
1.5	-	-	-	-	-	-	-	-	-	-	30	30	30	30	30	30	30	30	30	30
2.0	-	-	-	-	-	30	30	30	30	30	30	30	30	30	30	30	30	30	30	30
2.5	-	-	-	30	30	30	30	30	30	30	30	30	30	30	30	30	30	30	30	30
3.0	-	-	30	30	30	30	30	30	30	30	30	30	30	30	30	30	30	30	30	30
3.5	-	30	30	30	30	30	30	30	30	30	30	30	30	30	30	30	30	30	30	30
4.0	-	30	30	30	30	30	30	30	30	30	30	30	30	30	30	30	30	30	30	30
4.5	-	30	30	30	30	30	30	30	30	30	30	30	30	30	30	30	30	30	30	30
5.0	30	30	30	30	30	30	30	30	30	30	30	30	30	30	30	30	30	30	30	30
5.5	30	30	30	30	30	30	30	30	30	30	30	30	30	30	30	30	30	30	30	30
6.0	30	30	30	30	30	30	30	30	30	30	30	30	30	30	30	30	30	30	30	30
6.5	30	30	30	30	30	30	30	30	30	30	30	30	30	30	30	30	30	30	30	30
7.0	30	30	30	30	30	30	30	30	30	30	30	30	30	30	30	30	30	30	30	30
7.5	30	30	30	30	30	30	30	30	30	30	30	30	30	30	30	30	30	30	30	30
8.0	30	30	30	30	30	30	30	30	30	30	30	30	30	30	30	30	30	30	30	30
8.5	30	30	30	30	30	30	30	30	30	30	30	30	30	30	30	30	30	30	30	30
9.0	30	30	30	30	30	30	30	30	30	30	30	30	30	30	30	30	30	30	30	30
9.5	30	30	30	30	30	30	30	30	30	30	30	30	30	30	30	30	30	30	30	30
10.0	30	30	30	30	30	30	30	30	30	30	30	30	30	30	30	30	30	30	30	30

Equation 5 $$\dot{w}_{shaft} = \dot{V}_{cav.net} \cdot (P_2 - P_3)$$

The second byproduct of the PRE extracting fluid energy from the flow beside shaft power is a lower downstream fluid temperature (due to the change in enthalpy).

Table 37: Study 3 State 3 Temperature T_3 (F)

E (in.) \ H (in.)	0.5	1.0	1.5	2.0	2.5	3.0	3.5	4.0	4.5	5.0	5.5	6.0	6.5	7.0	7.5	8.0	8.5	9.0	9.5	10.0
0.5	-	-	-	-	-	-	-	-	-	-	-	-	-	-	-	-	-	-	-	-
1.0	-	-	-	-	-	-	-	-	-	-	-	-	-	-	-	-	-	-	-	-
1.5	-	-	-	-	-	-	-	-	-	-	26.3	26.0	25.8	25.7	25.7	25.7	25.8	25.9	26.1	26.3
2.0	-	-	-	-	-	20.3	18.7	17.9	17.5	17.4	17.5	17.7	18.0	18.3	18.7	19.1	19.6	20.0	20.5	20.9
2.5	-	-	-	19.1	16.1	14.5	13.7	13.5	13.6	13.9	14.4	15.0	15.7	16.3	17.0	17.7	18.4	19.1	19.8	20.5
3.0	-	-	19.4	15.4	13.4	12.5	12.4	12.7	13.3	14.0	14.8	15.7	16.6	17.5	18.4	19.3	20.2	21.0	21.8	22.5
3.5	-	23.2	17.0	14.1	12.9	12.8	13.2	14.0	14.9	15.9	17.0	18.1	19.2	20.2	21.2	22.1	23.0	23.9	24.7	25.5
4.0	-	20.9	16.0	14.1	13.8	14.2	15.1	16.3	17.5	18.7	19.9	21.1	22.2	23.3	24.3	25.2	26.1	27.0	27.8	28.5
4.5	-	19.6	15.9	15.0	15.4	16.4	17.6	19.0	20.4	21.7	23.0	24.2	25.3	26.3	27.3	28.2	29.1	29.9	30.6	31.3
5.0	28.3	19.1	16.5	16.4	17.3	18.7	20.2	21.7	23.2	24.6	25.8	27.0	28.1	29.1	30.0	30.9	31.7	32.4	33.1	33.8
5.5	26.8	19.0	17.5	18.1	19.5	21.1	22.8	24.4	25.9	27.2	28.5	29.6	30.6	31.6	32.4	33.2	34.0	34.6	35.3	35.8
6.0	25.8	19.3	18.7	19.9	21.7	23.5	25.2	26.8	28.3	29.6	30.8	31.9	32.8	33.7	34.5	35.2	35.9	36.5	37.1	37.6
6.5	25.2	19.9	20.1	21.8	23.7	25.7	27.4	29.0	30.4	31.7	32.8	33.8	34.7	35.5	36.3	37.0	37.6	38.1	38.6	39.1
7.0	24.8	20.7	21.6	23.6	25.7	27.7	29.4	31.0	32.4	33.5	34.6	35.5	36.4	37.1	37.8	38.4	39.0	39.5	39.9	40.4
7.5	24.6	21.6	23.1	25.4	27.6	29.5	31.3	32.7	34.0	35.2	36.2	37.0	37.8	38.5	39.1	39.7	40.2	40.6	41.1	41.4
8.0	24.5	22.6	24.6	27.0	29.3	31.2	32.9	34.3	35.5	36.6	37.5	38.3	39.0	39.7	40.2	40.7	41.2	41.6	42.0	42.4
8.5	24.6	23.6	26.0	28.5	30.8	32.7	34.3	35.7	36.8	37.8	38.7	39.4	40.1	40.7	41.2	41.7	42.1	42.5	42.8	43.2
9.0	24.9	24.7	27.4	30.0	32.2	34.1	35.6	36.9	38.0	38.9	39.7	40.4	41.0	41.6	42.0	42.5	42.9	43.2	43.5	43.8
9.5	25.2	25.8	28.6	31.3	33.5	35.3	36.8	38.0	39.0	39.9	40.6	41.3	41.8	42.3	42.8	43.2	43.5	43.9	44.1	44.4
10.0	25.6	26.8	29.9	32.5	34.7	36.4	37.8	39.0	39.9	40.7	41.4	42.0	42.5	43.0	43.4	43.8	44.1	44.4	44.7	44.9

NIST REFPROP $T_3(P_3, h_3)$

Equation 6 $$h_3 = h_1 - \frac{\dot{w}_{shaft}}{\dot{m}_{tot}} \quad \text{From} \quad E_{system} = \frac{\dot{w}_{shaft}}{\dot{m}_{tot}(h_1 - h_{3,Isentropic})}$$

3.4 STUDY 4 – TARGET POWER SPEED OPTIMIZATION

Study 4 takes an arbitrary machine radius E (4 inches) and rotor height H (4 inches) and holds them constant while varying PRE angular velocity. An optimized solution is calculated showing the effects of expander speed on isentropic efficiency, also demonstrating how a single size machine can be optimized for different situations by varying machine speed in a target power application.

Process Fluid	Methane	State 1 Pressure	1200 psi
Molecular Weight	16.04 kg/kmol	State 1 Temperature	100 °F
Specific Gas Constant	518.27 kJ/kg°K	State 1 Enthalpy (reference)	863.1 kJ/kg
Machine Radius E	4 in	State 1 Entropy(reference)	4.3 kJ/kg°K
Rotor Height H	4 in	State 3 Pressure	200 psi
Tip Radius R_1	.125''	State 3 Isentropic Enthalpy,	658.2 kJ/kg
Rotor Gap Width G	.005''	Target Power	30 kW

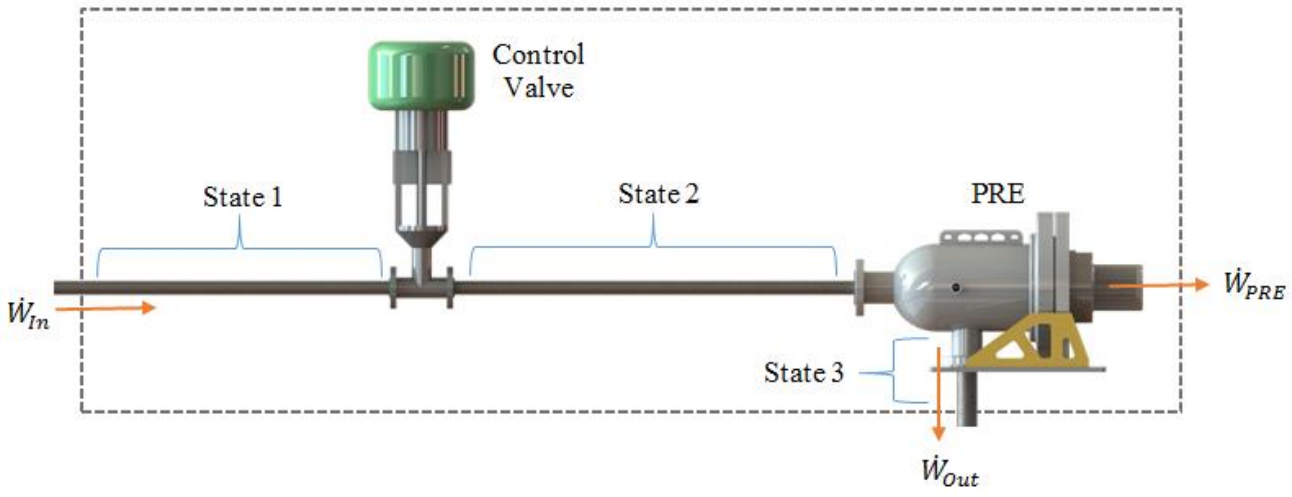

Table 38: Study 4 Isentropic Efficiency E_{system}

Angular Speed		Cavity Flowrate		Cavity Pressure		Cavity Temperature		Cavity Density	Total Throat Properties							State 1-2 Enthalpy Loss	Leakage Mass Flowrate	Cavity Mass Flowrate	Total Mass Flowrate	Isentropic Efficiency	Output Power
									Pressure		Temperature		Heat	Velocity	Density						
RPM	Hz	ACFM	m^3/s	psi	Mpa	F	K	kg/m³	psi	Mpa	F	K	Ratio	m/s	kg/m³	kj/kg	kg/s	kg/s	kg/s	%	kW
300	5	4.47	0.00	-	-	-	-	-	-	-	-	-	-	-	-	-	-	-	-	-	-
600	10	8.94	0.00	-	-	-	-	-	-	-	-	-	-	-	-	-	-	-	-	-	-
900	15	13.41	0.01	887.5	6.1	86.4	303.4	42.9	451.5	3.11	-26.4	240.7	1.52	435.6	28.22	28.2	0.625	0.27	0.896	16.3%	30.0
1200	20	17.88	0.01	715.6	4.9	78.2	298.8	34.7	369.5	2.55	-24.5	241.7	1.47	429.5	22.41	49.6	0.489	0.29	0.782	18.7%	30.0
1500	25	22.35	0.01	612.5	4.2	73.0	295.9	29.7	318.8	2.20	-24.2	241.9	1.45	425.9	19.04	65.9	0.412	0.31	0.725	20.2%	30.0
1800	30	26.82	0.01	543.7	3.7	69.4	293.9	26.4	284.5	1.96	-24.3	241.9	1.43	423.5	16.84	78.9	0.362	0.33	0.696	21.0%	30.0
2100	35	31.29	0.01	494.6	3.4	66.8	292.5	24.0	259.7	1.79	-24.5	241.8	1.42	421.8	15.27	89.4	0.327	0.35	0.682	21.5%	30.0
2400	40	35.76	0.02	457.8	3.2	64.8	291.4	22.2	241.0	1.66	-24.7	241.7	1.41	420.5	14.11	98.3	0.302	0.37	0.676	21.7%	30.0
2700	45	40.23	0.02	429.2	3.0	63.3	290.5	20.8	226.3	1.56	-24.9	241.6	1.41	419.5	13.21	105.8	0.282	0.39	0.677	21.6%	30.0
3000	50	44.70	0.02	406.2	2.8	62.0	289.8	19.7	214.6	1.48	-25.1	241.5	1.40	418.6	12.49	112.3	0.266	0.42	0.681	21.5%	30.0
3300	55	49.17	0.02	387.5	2.7	61.0	289.2	18.8	204.9	1.41	-25.2	241.4	1.40	418.0	11.90	118.0	0.253	0.44	0.689	21.3%	30.0
3600	60	53.64	0.03	371.9	2.6	60.1	288.8	18.0	196.9	1.36	-25.4	241.3	1.39	417.4	11.41	123.0	0.242	0.46	0.698	21.0%	30.0
3900	65	58.11	0.03	358.6	2.5	59.3	288.3	17.4	190.0	1.31	-25.5	241.2	1.39	417.0	11.00	127.4	0.233	0.48	0.710	20.6%	30.0
4200	70	62.58	0.03	347.3	2.4	58.7	288.0	16.8	184.2	1.27	-25.6	241.1	1.39	416.6	10.65	131.3	0.225	0.50	0.722	20.3%	30.0
4500	75	67.05	0.03	337.5	2.3	58.1	287.7	16.3	179.1	1.23	-25.7	241.1	1.39	416.2	10.34	134.9	0.219	0.52	0.736	19.9%	30.0
4800	80	71.52	0.03	328.9	2.3	57.7	287.4	15.9	174.6	1.20	-25.8	241.0	1.38	415.9	10.07	138.2	0.213	0.54	0.751	19.5%	30.0
5100	85	75.99	0.04	321.3	2.2	57.2	287.2	15.6	170.7	1.18	-25.9	241.0	1.38	415.6	9.84	141.1	0.208	0.56	0.766	19.1%	30.0
5400	90	80.47	0.04	314.6	2.2	56.8	286.9	15.2	167.1	1.15	-26.0	240.9	1.38	415.4	9.63	143.8	0.203	0.58	0.782	18.7%	30.0
5700	95	84.94	0.04	308.5	2.1	56.5	286.8	14.9	164.0	1.13	-26.0	240.9	1.38	415.2	9.44	146.3	0.199	0.60	0.798	18.3%	30.0
6000	100	89.41	0.04	303.1	2.1	56.2	286.6	14.7	161.2	1.11	-26.1	240.9	1.38	415.0	9.27	148.5	0.196	0.62	0.815	18.0%	30.0

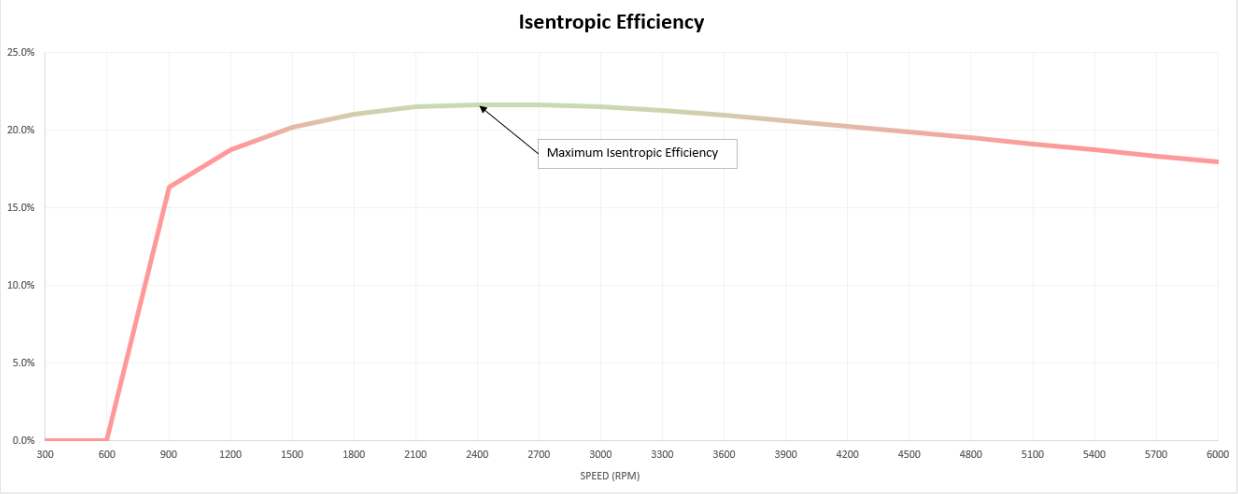

Again, the same solver is used in study 4 as was used in study 3. PRE rotational speed is the independent variable and shaft power $\dot{w}_{shaft}$ and state 2 cavity pressure P_2 dependent variables. Study 4 is simply a 1-dimensional analysis (rotation speed), while study 3 is a 2-dimensional analysis (machine radius E and rotor height H). For the application presented in study 4, a PRE with a rotational speed of 2400 RPM is optimal.

This 1-dimensional analysis shows the optimization being accomplished by analyzing the entire system. Note as speed increases so does State 1-2 enthalpy loss (a negative effect on isentropic efficiency), but leakage is reduced (a positive effect on isentropic efficiency). The dominance of these variables phase as speed varies generating an optimized isentropic efficiency.

3.5 STUDY 5 – TOTAL OPTIMIZATION

The final optimization occurs when both machine size and rotational speed are considered. Table 39 shows energy recovery and target power applications compared side by side. Equation 88 shows that PRE frequency ω is both in the denominator and numerator, and as PRE frequency increases, the leakage term becomes less dominant which increases overall efficiency. The solver confirms this as each case maximizes PRE rotational speed, then optimizes rotor size to maximize PRE isentropic efficiency.

This solver provides guidance when sizing a PRE for an application as it is immediately shown that PRE rotational frequency should be maximized. This is convenient as mating components often have speed limiting criteria that should be adhered to. After a maximum operating speed has been identified, the optimization processes found in studies 1 and 3 will configure the rotors size to yield the highest isentropic efficiency for that application.

Table 39 shows the optimized results when the solver was allowed a 1 to 10 inch rotor height H and a 1 to 10 inch machine radius E (uses the same parameters as studies 1 through 4). Two rotational speed ranges were allowed and presented below: 400 to 1800 RPM, and 400 to 3600 RPM (1800 and 3600 RPM being very common generator speeds). Note that rotational speed dominates isentropic efficiency and is maximized by the solver.

Table 39: Study 5 Isentropic Efficiency – Total Optimization

	Energy Recovery		Target Power	
RPM	3600	1800	3600	1800
E (in)	3.491	4.494	3.017	3.895
H (in)	3.766	4.877	3.260	4.242
Total Mass Flowrate (kg/s)	1.0	1.0	0.61	0.68
Isentropic Efficiency	28.8%	25.3%	23.8%	21.4%
Output Shaft Power (kW)	59.0	51.9	30.0	30.0
State 2 Pressure (psi)	676.5	583.5	572.1	537.8

CHAPTER 4: CONCLUSION

The planetary rotor expander has an optimized solution that is dependent on the application and system limitations. Case studies 1 through 5 look at the difference between an energy recovery and target power application. The requirements of achieving a specific power output and matching a system's mass flowrate call for different optimized machine sizes (yielding different isentropic efficiencies).

Studies 1 through 5 also show that each PRE's frequency has an optimized machine size (studies 1 and 3), and each machine size has an optimized rotational frequency (studies 2 and 4). Study 5 shows that when both machine size and rotational frequency are combined, the PRE with the highest isentropic efficiency for the application will have the highest allowed rotational frequency. This shows that to optimize a machine size for a specific application, the maximum rotational frequency needs to be assessed considering all auxiliary components (bearings, gear boxes, pulleys etc.). Once selected, the isentropic efficiency solver will drive the frequency to the maximum allowable, and then optimize the rotor size for highest efficiency.

An important note is that study 5 shows the difference of an optimized PRE operating at 3600 RPM versus 1800 RPM. Both speeds are common in power generation and rotating equipment. 3600 RPM poses possible challenges due to tip speeds and bearing limitations. Note, in Table 39, less than a 4% reduction in isentropic efficiency (~8 kW) occurs operating at 1800 RPM versus 3600 RPM and is a result of rotor size being allowed to adjust to the rotational frequency. This decrease in efficiency from 3600 to 1800 RPM makes it plausible that net isentropic efficiencies are negligibly altered due to the removal of power consuming auxiliary systems possibly required by a 3600 RPM expander (gear boxes, pulleys, oil pumps, etc.). These auxiliary requirements should be considered as higher rotational frequencies may require

additional equipment inducing more parasitic loss. This may produce net positive efficient PRE operating at slower speeds (depending on parasitic losses rotating at higher speeds).

This efficiency model contains some induced error requiring comment. Section 2.3 showed that equation 83 which is used to calculate cavity volume contains a average error is approximately 0.05%. This error is possibly caused by CAD tetrahedral approximation. Note that cavity volume is derived from a characteristic comparison to the sin-squared law. Cavity volume is proportionally related to isentropic efficiency, and thus so is this error. Error is also induced by using state 2 temperature and pressure as stagnation temperature pressure when calculating throat properties using equations 18 and 19 (see appendix A).

Future work for this model includes deriving a direct mathematical model of the cavity volume instead of deriving the model from the sin-squared law. This would reduce the induced error caused by the characteristic model currently used. Empirical validation also needs to be performed to prove out equation 88 and 89. When the one-to-one “hydraulic” configuration has been proven, a metering valve should be implemented to access the expansive energy within gaseous applications. This approximately doubles the isentropic efficiency if the pressure ratio is tuned correctly. The PRE efficiency model will need to be altered to include a variable cavity pressure as a cycle progresses to properly analyze a metered expander.

REFERENCES

[1] S. R. Turns, Thermal-Fluid Sciences An Integrated Approach, New York: Cambridge University Press, 2006, pp. 250, 525, 545-549, 885.

[2] A. Cleveland, "Turbo Expanders for Power Generation state of the Art Design Optimization (Pressure Pipeline Regulating Stations)," *The American Society of Mechanical Engineers,* Vols. 93-GT-244, p. 11, 1993.

[3] K. Nugent, "There's an art to picking the right turbo-expander technology for your project," HERA, 12 July 2017. [Online]. Available: https://www.hera.org.nz/picking-turbo-expander-technology/. [Accessed 22 December 2018].

[4] "Experimental investigation and optimal performance assessment of four volumetric expanders (scroll, screw, piston and roots) tested in a small-scale organic Rankine cycle system," *Elsevier ,* vol. Energy 165, pp. 1119-1127, 2018.

[5] T. K. E. I. Grzegorz Żywica∗, "Expanders for dispersed power generation: maintenance and diagnostics problems," *TRANSACTIONS OF THE INSTITUTE OF FLUID-FLOW MACHINERY,* vol. 131, p. 173–188, 2016.

[6] V. K. Avadhanula and C.-S. Lin, "ASME Journal of Engineering for Gas Turbines and Power," *Empirical Models for a Screw Expander Based on Experimental Data From Organic Rankine Cycle System Testing,* vol. 136, no. June, 2014.

[7] E. Casati, S. Vitale, M. P. Pini, G. Persico and C. Piero, "Centrifugal Turbines for Mini-Organic Rankine Cycle Power Systems," *ASME Journal of Engineering for Gas Turbines and Power,* vol. 136, no. December, 2014.

[8] L. A. Hawkins and L. Zhu, "Development of a 125 kW AMB Expander/Generator for Waste Heat Recovery," *ASME Journal of Engineering for Gas Turbines and Power,* vol. 133, no. July, 2011.

[9] M. S. Orosz, A. V. Mueller, B. J. Dechesne and H. F. Hemond, "Geometric Design of Scroll Expanders Optimized for Small Organic Rankine Cycles," *ASME Journal of Engineering for Gas Turbines and Power,* vol. 135, no. April, 2013.

[10] Z. Gnutek and P. Kolasin´ski, "The Application of Rotary Vane Expanders in Organic Rankine Cycle Systems—Thermodynamic Description and Experimental Results," *ASME Journal of Engineering for Gas Turbines and Power,* vol. 135, no. June, 2013.

[11] J. D. Anderson, Modern Compressable Flow With Historical Perspective, 3rd ed., New York: McGraw Hill Education (India) Private Limited, 2003, pp. 77-81.

[12] ANSI/ASME, *ASME MFC-14M–2003 Measurement Of Fluid Flow Using Small Bore Precision Orifice Meters,* The American Society of Mechanical Engineers, 2003.

[13] S. Whitmore, *Section 3.3.1 Injector Notes MAE 6530 Inctruction,* Logan: Dr. Stephen Whitmore, 2018.

[14] D. Jobson, "On the Flow of a Compressible Fluid through Orifices," in *Proceedings of the Institute of Mechanical Engineers,* Greenwhich, 1955.

[15] MIT, *Chapter 4: Flow in Pipes and Channels,* Massachusetts: Massachusetts Institue of Technology, 2018.

APPENDICES

A STAGNATION PRESSURE AND TEMPERATURE VERIFICATION

The following charts show the Mach speed inside the cavity for the different studies, and the ratio of the calculated state 2 pressure and the solved stagnation pressure. Generally, fluid speeds remain at or below Mach .3. This makes using incompressible analysis viable within the cavity, and up and downstream. Knowing the cavity fluid speeds, we can back calculate equations 18 and 19 to solve the stagnation pressure and temperatures. This verifies the assumption that state 2 pressure and temperature can be used as stagnation pressure and temperature inducing minimal error (~0 to 3% within the optimized region). The optimized region (or area of interest) can be found circled in red. Note that fluid speeds were calculated using mass flowrates evaluated at an area half of the maximum cavity cross sectional area. Due to the contours of the cavity, this is considered an average fluid speed, where fluid speed does vary greatly with position.

Study 1 Cavity Fluid Speed Verification

$Mach_2$

E (in.) \ H (in.)	0.5	1.0	1.5	2.0	2.5	3.0	3.5	4.0	4.5	5.0	5.5	6.0	6.5	7.0	7.5	8.0	8.5	9.0	9.5	10.0
0.5	-	-	-	-	-	-	-	-	-	-	-	-	-	-	-	0.02	0.02	0.02	0.02	0.02
1.0	-	-	-	-	-	-	-	-	-	-	-	-	-	0.04	0.04	0.04	0.05	0.05	0.05	0.06
1.5	-	-	-	-	-	-	-	-	-	-	-	0.05	0.06	0.06	0.06	0.07	0.07	0.08	0.08	0.09
2.0	-	-	-	-	-	-	-	-	0.05	0.06	0.06	0.07	0.08	0.08	0.09	0.10	0.10	0.11	0.12	0.12
2.5	-	-	-	-	-	0.04	0.05	0.06	0.07	0.08	0.08	0.09	0.10	0.11	0.12	0.12	0.13	0.14	0.15	0.16
3.0	-	-	-	0.04	0.04	0.05	0.06	0.07	0.08	0.09	0.10	0.11	0.12	0.13	0.14	0.15	0.16	0.17	0.18	0.19
3.5	-	-	0.03	0.04	0.05	0.06	0.08	0.09	0.10	0.11	0.12	0.13	0.15	0.16	0.17	0.18	0.19	0.20	0.22	0.23
4.0	-	0.02	0.04	0.05	0.06	0.08	0.09	0.10	0.12	0.13	0.14	0.16	0.17	0.18	0.20	0.21	0.22	0.24	0.25	0.26
4.5	0.01	0.03	0.04	0.06	0.07	0.09	0.10	0.12	0.13	0.15	0.16	0.18	0.19	0.21	0.22	0.24	0.25	0.27	0.28	0.30
5.0	0.02	0.03	0.05	0.06	0.08	0.10	0.11	0.13	0.15	0.16	0.18	0.20	0.22	0.23	0.25	0.27	-	-	-	-
5.5	0.02	0.03	0.05	0.07	0.09	0.11	0.13	0.14	0.16	0.18	0.20	0.22	0.24	-	-	-	-	-	-	-
6.0	0.02	0.04	0.06	0.08	0.10	0.12	0.14	0.16	0.18	0.20	0.22	-	-	-	-	-	-	-	-	-
6.5	0.02	0.04	0.06	0.09	0.11	0.13	0.15	0.17	0.20	-	-	-	-	-	-	-	-	-	-	-
7.0	0.02	0.05	0.07	0.09	0.12	0.14	0.16	0.19	-	-	-	-	-	-	-	-	-	-	-	-
7.5	0.02	0.05	0.07	0.10	0.13	0.15	0.18	-	-	-	-	-	-	-	-	-	-	-	-	-
8.0	0.03	0.05	0.08	0.11	0.13	0.16	-	-	-	-	-	-	-	-	-	-	-	-	-	-
8.5	0.03	0.06	0.08	0.11	0.14	-	-	-	-	-	-	-	-	-	-	-	-	-	-	-
9.0	0.03	0.06	0.09	0.12	-	-	-	-	-	-	-	-	-	-	-	-	-	-	-	-
9.5	0.03	0.06	0.10	0.13	-	-	-	-	-	-	-	-	-	-	-	-	-	-	-	-
10.0	0.03	0.07	0.10	-	-	-	-	-	-	-	-	-	-	-	-	-	-	-	-	-

$\frac{P_2}{P_0}$

E (in.) \ H (in.)	0.5	1.0	1.5	2.0	2.5	3.0	3.5	4.0	4.5	5.0	5.5	6.0	6.5	7.0	7.5	8.0	8.5	9.0	9.5	10.0
0.5	-	-	-	-	-	-	-	-	-	-	-	-	-	-	-	1.00	1.00	1.00	1.00	1.00
1.0	-	-	-	-	-	-	-	-	-	-	-	-	-	1.00	1.00	1.00	1.00	1.00	1.00	1.00
1.5	-	-	-	-	-	-	-	-	-	-	-	1.00	1.00	1.00	1.00	1.00	1.00	1.00	1.01	1.01
2.0	-	-	-	-	-	-	-	-	1.00	1.00	1.00	1.00	1.00	1.01	1.01	1.01	1.01	1.01	1.01	1.01
2.5	-	-	-	-	-	1.00	1.00	1.00	1.00	1.00	1.01	1.01	1.01	1.01	1.01	1.01	1.01	1.01	1.02	1.02
3.0	-	-	-	1.00	1.00	1.00	1.00	1.00	1.01	1.01	1.01	1.01	1.01	1.01	1.01	1.02	1.02	1.02	1.02	1.03
3.5	-	-	1.00	1.00	1.00	1.00	1.00	1.01	1.01	1.01	1.01	1.01	1.01	1.02	1.02	1.02	1.03	1.03	1.03	1.04
4.0	-	1.00	1.00	1.00	1.00	1.00	1.01	1.01	1.01	1.01	1.01	1.02	1.02	1.02	1.03	1.03	1.03	1.04	1.04	1.05
4.5	1.00	1.00	1.00	1.00	1.00	1.01	1.01	1.01	1.01	1.01	1.02	1.02	1.03	1.03	1.03	1.04	1.04	1.05	1.06	1.06
5.0	1.00	1.00	1.00	1.00	1.00	1.01	1.01	1.01	1.02	1.02	1.02	1.03	1.03	1.04	1.04	1.05	-	-	-	-
5.5	1.00	1.00	1.00	1.00	1.01	1.01	1.01	1.01	1.02	1.02	1.03	1.03	1.04	-	-	-	-	-	-	-
6.0	1.00	1.00	1.00	1.00	1.01	1.01	1.01	1.02	1.02	1.03	1.03	-	-	-	-	-	-	-	-	-
6.5	1.00	1.00	1.00	1.01	1.01	1.01	1.02	1.02	1.03	-	-	-	-	-	-	-	-	-	-	-
7.0	1.00	1.00	1.00	1.01	1.01	1.01	1.02	1.02	-	-	-	-	-	-	-	-	-	-	-	-
7.5	1.00	1.00	1.00	1.01	1.01	1.02	1.02	-	-	-	-	-	-	-	-	-	-	-	-	-
8.0	1.00	1.00	1.00	1.01	1.01	1.02	-	-	-	-	-	-	-	-	-	-	-	-	-	-
8.5	1.00	1.00	1.00	1.01	1.01	-	-	-	-	-	-	-	-	-	-	-	-	-	-	-
9.0	1.00	1.00	1.01	1.01	-	-	-	-	-	-	-	-	-	-	-	-	-	-	-	-
9.5	1.00	1.00	1.01	1.01	-	-	-	-	-	-	-	-	-	-	-	-	-	-	-	-
10.0	1.00	1.00	1.01	-	-	-	-	-	-	-	-	-	-	-	-	-	-	-	-	-

$\frac{T_2}{T_0}$

E (in.) \ H (in.)	0.5	1.0	1.5	2.0	2.5	3.0	3.5	4.0	4.5	5.0	5.5	6.0	6.5	7.0	7.5	8.0	8.5	9.0	9.5	10.0
0.5	-	-	-	-	-	-	-	-	-	-	-	-	-	-	-	1.00	1.00	1.00	1.00	1.00
1.0	-	-	-	-	-	-	-	-	-	-	-	-	-	1.00	1.00	1.00	1.00	1.00	1.00	1.00
1.5	-	-	-	-	-	-	-	-	-	-	-	1.00	1.00	1.00	1.00	1.00	1.00	1.00	1.00	1.00
2.0	-	-	-	-	-	-	-	-	1.00	1.00	1.00	1.00	1.00	1.00	1.00	1.00	1.00	1.00	1.00	1.00
2.5	-	-	-	-	-	1.00	1.00	1.00	1.00	1.00	1.00	1.00	1.00	1.00	1.00	1.00	1.00	1.00	1.00	1.01
3.0	-	-	-	1.00	1.00	1.00	1.00	1.00	1.00	1.00	1.00	1.00	1.00	1.00	1.00	1.00	1.01	1.01	1.01	1.01
3.5	-	-	1.00	1.00	1.00	1.00	1.00	1.00	1.00	1.00	1.00	1.00	1.00	1.00	1.01	1.01	1.01	1.01	1.01	1.01
4.0	-	1.00	1.00	1.00	1.00	1.00	1.00	1.00	1.00	1.00	1.00	1.00	1.01	1.01	1.01	1.01	1.01	1.01	1.01	1.01
4.5	1.00	1.00	1.00	1.00	1.00	1.00	1.00	1.00	1.00	1.00	1.01	1.01	1.01	1.01	1.01	1.01	1.01	1.01	1.01	1.02
5.0	1.00	1.00	1.00	1.00	1.00	1.00	1.00	1.00	1.00	1.01	1.01	1.01	1.01	1.01	1.01	1.01	-	-	-	-
5.5	1.00	1.00	1.00	1.00	1.00	1.00	1.00	1.00	1.00	1.01	1.01	1.01	1.01	-	-	-	-	-	-	-
6.0	1.00	1.00	1.00	1.00	1.00	1.00	1.00	1.00	1.01	1.01	1.01	-	-	-	-	-	-	-	-	-
6.5	1.00	1.00	1.00	1.00	1.00	1.00	1.00	1.01	1.01	-	-	-	-	-	-	-	-	-	-	-
7.0	1.00	1.00	1.00	1.00	1.00	1.00	1.00	1.01	-	-	-	-	-	-	-	-	-	-	-	-
7.5	1.00	1.00	1.00	1.00	1.00	1.00	1.01	-	-	-	-	-	-	-	-	-	-	-	-	-
8.0	1.00	1.00	1.00	1.00	1.00	1.00	-	-	-	-	-	-	-	-	-	-	-	-	-	-
8.5	1.00	1.00	1.00	1.00	1.00	-	-	-	-	-	-	-	-	-	-	-	-	-	-	-
9.0	1.00	1.00	1.00	1.00	-	-	-	-	-	-	-	-	-	-	-	-	-	-	-	-
9.5	1.00	1.00	1.00	1.00	-	-	-	-	-	-	-	-	-	-	-	-	-	-	-	-
10.0	1.00	1.00	1.00	-	-	-	-	-	-	-	-	-	-	-	-	-	-	-	-	-

Study 3 Cavity Fluid Speed Verification

$Mach_2$

E (in.) \ H (in.)	0.5	1.0	1.5	2.0	2.5	3.0	3.5	4.0	4.5	5.0	5.5	6.0	6.5	7.0	7.5	8.0	8.5	9.0	9.5	10.0
0.5	-	-	-	-	-	-	-	-	-	-	-	-	-	-	-	-	-	-	-	-
1.0	-	-	-	-	-	-	-	-	-	-	-	-	-	-	-	-	-	-	-	-
1.5	-	-	-	-	-	-	-	-	-	-	0.05	0.05	0.06	0.06	0.06	0.07	0.07	0.08	0.08	0.09
2.0	-	-	-	-	-	0.03	0.04	0.05	0.05	0.06	0.07	0.07	0.08	0.09	0.09	0.10	0.10	0.11	0.12	0.12
2.5	-	-	-	0.03	0.04	0.05	0.05	0.06	0.07	0.08	0.09	0.09	0.10	0.11	0.12	0.13	0.13	0.14	0.15	0.16
3.0	-	-	0.03	0.04	0.05	0.06	0.07	0.08	0.09	0.10	0.11	0.12	0.12	0.13	0.14	0.15	0.16	0.17	0.18	0.19
3.5	-	0.02	0.03	0.04	0.06	0.07	0.08	0.09	0.10	0.11	0.12	0.14	0.15	0.16	0.17	0.18	0.19	0.21	0.22	0.23
4.0	-	0.02	0.04	0.05	0.06	0.08	0.09	0.10	0.12	0.13	0.14	0.16	0.17	0.18	0.20	0.21	0.22	0.24	0.25	0.26
4.5	-	0.03	0.04	0.06	0.07	0.09	0.10	0.12	0.13	0.15	0.16	0.18	0.19	0.21	0.22	0.24	0.25	0.27	0.28	0.30
5.0	0.02	0.03	0.05	0.06	0.08	0.10	0.11	0.13	0.15	0.16	0.18	0.20	0.22	0.23	0.25	0.27	0.28	0.30	0.32	0.33
5.5	0.02	0.04	0.05	0.07	0.09	0.11	0.13	0.15	0.16	0.18	0.20	0.22	0.24	0.26	0.27	0.29	0.31	0.33	0.35	0.37
6.0	0.02	0.04	0.06	0.08	0.10	0.12	0.14	0.16	0.18	0.20	0.22	0.24	0.26	0.28	0.30	0.32	0.34	0.36	0.38	0.40
6.5	0.02	0.04	0.06	0.09	0.11	0.13	0.15	0.17	0.19	0.22	0.24	0.26	0.28	0.30	0.33	0.35	0.37	0.39	0.41	0.43
7.0	0.02	0.05	0.07	0.09	0.12	0.14	0.16	0.19	0.21	0.23	0.26	0.28	0.30	0.33	0.35	0.37	0.40	0.42	0.45	0.47
7.5	0.02	0.05	0.07	0.10	0.12	0.15	0.18	0.20	0.23	0.25	0.28	0.30	0.33	0.35	0.38	0.40	0.43	0.45	0.48	0.50
8.0	0.03	0.05	0.08	0.11	0.13	0.16	0.19	0.21	0.24	0.27	0.30	0.32	0.35	0.38	0.40	0.43	0.46	0.48	0.51	0.54
8.5	0.03	0.06	0.08	0.11	0.14	0.17	0.20	0.23	0.26	0.29	0.31	0.34	0.37	0.40	0.43	0.46	0.49	0.51	0.54	0.57
9.0	0.03	0.06	0.09	0.12	0.15	0.18	0.21	0.24	0.27	0.30	0.33	0.36	0.39	0.42	0.45	0.48	0.52	0.55	0.58	0.61
9.5	0.03	0.06	0.10	0.13	0.16	0.19	0.22	0.26	0.29	0.32	0.35	0.38	0.42	0.45	0.48	0.51	0.54	0.58	0.61	0.64
10.0	0.03	0.07	0.10	0.13	0.17	0.20	0.24	0.27	0.30	0.34	0.37	0.40	0.44	0.47	0.51	0.54	0.57	0.61	0.64	0.67

$\frac{P_2}{P_0}$

E (in.) \ H (in.)	0.5	1.0	1.5	2.0	2.5	3.0	3.5	4.0	4.5	5.0	5.5	6.0	6.5	7.0	7.5	8.0	8.5	9.0	9.5	10.0
0.5	-	-	-	-	-	-	-	-	-	-	-	-	-	-	-	-	-	-	-	-
1.0	-	-	-	-	-	-	-	-	-	-	-	-	-	-	-	-	-	-	-	-
1.5	-	-	-	-	-	-	-	-	-	-	1.00	1.00	1.00	1.00	1.00	1.00	1.00	1.00	1.01	1.01
2.0	-	-	-	-	-	1.00	1.00	1.00	1.00	1.00	1.00	1.00	1.00	1.01	1.01	1.01	1.01	1.01	1.01	1.01
2.5	-	-	-	1.00	1.00	1.00	1.00	1.00	1.00	1.00	1.01	1.01	1.01	1.01	1.01	1.01	1.01	1.01	1.02	1.02
3.0	-	-	1.00	1.00	1.00	1.00	1.00	1.00	1.01	1.01	1.01	1.01	1.01	1.01	1.01	1.02	1.02	1.02	1.02	1.03
3.5	-	1.00	1.00	1.00	1.00	1.00	1.00	1.01	1.01	1.01	1.01	1.01	1.02	1.02	1.02	1.02	1.03	1.03	1.03	1.04
4.0	-	1.00	1.00	1.00	1.00	1.00	1.01	1.01	1.01	1.01	1.01	1.02	1.02	1.02	1.03	1.03	1.03	1.04	1.04	1.05
4.5	-	1.00	1.00	1.00	1.00	1.01	1.01	1.01	1.01	1.02	1.02	1.02	1.03	1.03	1.03	1.04	1.04	1.05	1.06	1.06
5.0	1.00	1.00	1.00	1.00	1.00	1.01	1.01	1.01	1.02	1.02	1.02	1.03	1.03	1.04	1.04	1.05	1.06	1.06	1.07	1.08
5.5	1.00	1.00	1.00	1.00	1.01	1.01	1.01	1.01	1.02	1.02	1.03	1.03	1.04	1.05	1.05	1.06	1.07	1.08	1.08	1.09
6.0	1.00	1.00	1.00	1.00	1.01	1.01	1.01	1.02	1.02	1.03	1.03	1.04	1.05	1.05	1.06	1.07	1.08	1.09	1.10	1.11
6.5	1.00	1.00	1.00	1.01	1.01	1.01	1.02	1.02	1.03	1.03	1.04	1.05	1.06	1.06	1.07	1.08	1.10	1.11	1.12	1.13
7.0	1.00	1.00	1.00	1.01	1.01	1.01	1.02	1.02	1.03	1.04	1.05	1.05	1.06	1.08	1.09	1.10	1.11	1.13	1.14	1.16
7.5	1.00	1.00	1.00	1.01	1.01	1.02	1.02	1.03	1.04	1.04	1.05	1.06	1.07	1.09	1.10	1.11	1.13	1.15	1.16	1.18
8.0	1.00	1.00	1.00	1.01	1.01	1.02	1.02	1.03	1.04	1.05	1.06	1.07	1.09	1.10	1.11	1.13	1.15	1.17	1.19	1.21
8.5	1.00	1.00	1.00	1.01	1.01	1.02	1.03	1.04	1.05	1.06	1.07	1.08	1.10	1.11	1.13	1.15	1.17	1.19	1.22	1.24
9.0	1.00	1.00	1.01	1.01	1.02	1.02	1.03	1.04	1.05	1.06	1.08	1.09	1.11	1.13	1.15	1.17	1.19	1.22	1.24	1.27
9.5	1.00	1.00	1.01	1.01	1.02	1.03	1.03	1.05	1.06	1.07	1.09	1.10	1.12	1.14	1.17	1.19	1.22	1.24	1.28	1.31
10.0	1.00	1.00	1.01	1.01	1.02	1.03	1.04	1.05	1.06	1.08	1.10	1.12	1.14	1.16	1.18	1.21	1.24	1.27	1.31	1.35

$\frac{T_2}{T_0}$

E (in.) \ H (in.)	0.5	1.0	1.5	2.0	2.5	3.0	3.5	4.0	4.5	5.0	5.5	6.0	6.5	7.0	7.5	8.0	8.5	9.0	9.5	10.0
0.5	-	-	-	-	-	-	-	-	-	-	-	-	-	-	-	-	-	-	-	-
1.0	-	-	-	-	-	-	-	-	-	-	-	-	-	-	-	-	-	-	-	-
1.5	-	-	-	-	-	-	-	-	-	-	1.00	1.00	1.00	1.00	1.00	1.00	1.00	1.00	1.00	1.00
2.0	-	-	-	-	-	1.00	1.00	1.00	1.00	1.00	1.00	1.00	1.00	1.00	1.00	1.00	1.00	1.00	1.00	1.00
2.5	-	-	-	1.00	1.00	1.00	1.00	1.00	1.00	1.00	1.00	1.00	1.00	1.00	1.00	1.00	1.00	1.00	1.00	1.00
3.0	-	-	1.00	1.00	1.00	1.00	1.00	1.00	1.00	1.00	1.00	1.00	1.00	1.00	1.00	1.00	1.01	1.01	1.01	1.01
3.5	-	1.00	1.00	1.00	1.00	1.00	1.00	1.00	1.00	1.00	1.00	1.00	1.00	1.00	1.01	1.01	1.01	1.01	1.01	1.01
4.0	-	1.00	1.00	1.00	1.00	1.00	1.00	1.00	1.00	1.00	1.00	1.00	1.01	1.01	1.01	1.01	1.01	1.01	1.01	1.01
4.5	-	1.00	1.00	1.00	1.00	1.00	1.00	1.00	1.00	1.00	1.00	1.01	1.01	1.01	1.01	1.01	1.01	1.01	1.01	1.02
5.0	1.00	1.00	1.00	1.00	1.00	1.00	1.00	1.00	1.00	1.01	1.01	1.01	1.01	1.01	1.01	1.01	1.01	1.02	1.02	1.02
5.5	1.00	1.00	1.00	1.00	1.00	1.00	1.00	1.00	1.01	1.01	1.01	1.01	1.01	1.01	1.01	1.02	1.02	1.02	1.02	1.02
6.0	1.00	1.00	1.00	1.00	1.00	1.00	1.00	1.00	1.01	1.01	1.01	1.01	1.01	1.01	1.02	1.02	1.02	1.02	1.03	1.03
6.5	1.00	1.00	1.00	1.00	1.00	1.00	1.00	1.01	1.01	1.01	1.01	1.01	1.01	1.02	1.02	1.02	1.02	1.03	1.03	1.03
7.0	1.00	1.00	1.00	1.00	1.00	1.00	1.00	1.01	1.01	1.01	1.01	1.01	1.02	1.02	1.02	1.03	1.03	1.03	1.04	1.04
7.5	1.00	1.00	1.00	1.00	1.00	1.00	1.01	1.01	1.01	1.01	1.01	1.02	1.02	1.02	1.03	1.03	1.03	1.04	1.04	1.05
8.0	1.00	1.00	1.00	1.00	1.00	1.00	1.01	1.01	1.01	1.01	1.02	1.02	1.02	1.03	1.03	1.03	1.04	1.04	1.05	1.05
8.5	1.00	1.00	1.00	1.00	1.00	1.01	1.01	1.01	1.01	1.01	1.02	1.02	1.02	1.03	1.03	1.04	1.04	1.05	1.05	1.06
9.0	1.00	1.00	1.00	1.00	1.00	1.01	1.01	1.01	1.01	1.02	1.02	1.02	1.03	1.03	1.04	1.04	1.05	1.05	1.06	1.07
9.5	1.00	1.00	1.00	1.00	1.00	1.01	1.01	1.01	1.01	1.02	1.02	1.03	1.03	1.04	1.04	1.05	1.05	1.06	1.07	1.07
10.0	1.00	1.00	1.00	1.00	1.01	1.01	1.01	1.01	1.02	1.02	1.02	1.03	1.03	1.04	1.05	1.05	1.06	1.07	1.07	1.08

B LEAK POINT SUBCRITICAL FLOW

This appendix using case studies 3.1 and 3.3 to validate the theoretical accuracy of using choked flow the throat parameters for all rotor configurations. A subcritical flow analysis is inserted into the grid analysis where the throat parameters are not choked according to equation 17. It shows that a ~2% maximum error occurs using this assumption. However, this error is not in proximity to, and lower than, the identified optimized rotor configuration. This makes this error insignificant unless the choked/subcritical boundary is near the optimized solution.

The following shows the equations used for determining the incompressible parameters (which are used to calculate sub-critical compressible flow). Note that downstream diameter d is analogous to the throat and is determined by the throat hydraulic diameter equal to two times gap G. Also note that upstream diameter D is analogous to half of rotor diameter D from Figure 8 as "half" symbolizing a quasi-average dimension of the approach from the cavity to throat. Since rotor gap G is magnitudes smaller than the approach, this upstream diameter D factor ("half") could be as little as .01 with inconsequential affect.

ASME "STANDARD MODEL"

DIMENSIONS IN INCHES

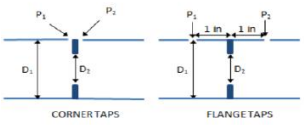

Corner tap:

$$C_v = \left[0.5991 + \frac{0.0044}{D} + \left(0.3155 + \frac{0.0175}{D}\right)\left(\left(\frac{d}{D}\right)^4 + 2\left(\frac{d}{D}\right)^{16}\right)\right]\sqrt{1-(d/D)^4} + \left[\frac{0.52}{D} - 0.192 + \left(16.48 - \frac{1.16}{D}\right)\left(\left(\frac{d}{D}\right)^4 + 4\left(\frac{d}{D}\right)^{16}\right)\right]\sqrt{\frac{1-(d/D)^4}{\mathrm{Re}_D}}$$

Simple orifice
***ASME MFC-14M-**

Flange tap:

$$C_v = \left[0.598 + 0.468\left(\left(\frac{d}{D}\right)^4 + 10\left(\frac{d}{D}\right)^{12}\right)\right]\sqrt{1-(d/D)^4} + \left(0.87 + 8.1\left(\frac{d}{D}\right)^4\right)\sqrt{\frac{1-(d/D)^4}{\mathrm{Re}_D}}$$

$$C_d \equiv \frac{C_v}{\left[1-\left(\frac{A_2}{A_1}\right)^2\right]^{\frac{1}{2}}} = \frac{C_v}{\left[1-\left(\frac{D_2}{D_1}\right)^4\right]^{\frac{1}{2}}} = \frac{C_v}{\sqrt{1-\beta^4}}$$

β - - > "*contraction ratio*" "*d/D*"

- **need to take area change into account**

The following shows the calculations of study 3.3 implementing sub-critical flow for non-chocked rotor configurations. First, the incompressible flow parameters are calculated:

Reynolds # state 2

E (in.) \ H (in.)	0.5	1.0	1.5	2.0	2.5	3.0	3.5	4.0	4.5	5.0	5.5	6.0	6.5	7.0	7.5	8.0	8.5	9.0	9.5	10.0
0.5	-	-	-	-	-	-	-	-	-	-	-	-	-	-	-	-	-	-	-	-
1.0	-	-	-	-	-	-	-	-	-	-	-	-	-	-	-	-	-	-	-	-
1.5	-	-	-	-	-	-	-	-	-	-	1.84E+06	1.90E+06	1.96E+06	2.02E+06	2.07E+06	2.12E+06	2.17E+06	2.22E+06	2.27E+06	2.32E+06
2.0	-	-	-	-	-	1.82E+06	1.93E+06	2.04E+06	2.13E+06	2.22E+06	2.30E+06	2.38E+06	2.46E+06	2.53E+06	2.61E+06	2.68E+06	2.75E+06	2.82E+06	2.89E+06	2.96E+06
2.5	-	-	-	1.85E+06	2.02E+06	2.17E+06	2.30E+06	2.42E+06	2.54E+06	2.66E+06	2.77E+06	2.89E+06	3.00E+06	3.11E+06	3.21E+06	3.32E+06	3.43E+06	3.53E+06	3.64E+06	3.74E+06
3.0	-	-	1.91E+06	2.13E+06	2.33E+06	2.51E+06	2.67E+06	2.84E+06	3.00E+06	3.16E+06	3.31E+06	3.47E+06	3.62E+06	3.77E+06	3.93E+06	4.08E+06	4.23E+06	4.38E+06	4.53E+06	4.68E+06
3.5	-	1.84E+06	2.15E+06	2.41E+06	2.65E+06	2.87E+06	3.09E+06	3.30E+06	3.51E+06	3.72E+06	3.93E+06	4.14E+06	4.35E+06	4.55E+06	4.76E+06	4.96E+06	5.17E+06	5.37E+06	5.58E+06	5.78E+06
4.0	-	2.04E+06	2.39E+06	2.70E+06	2.99E+06	3.27E+06	3.55E+06	3.83E+06	4.10E+06	4.37E+06	4.64E+06	4.91E+06	5.18E+06	5.45E+06	5.72E+06	5.99E+06	6.25E+06	6.52E+06	6.79E+06	7.06E+06
4.5	-	2.24E+06	2.64E+06	3.01E+06	3.37E+06	3.72E+06	4.07E+06	4.41E+06	4.76E+06	5.10E+06	5.44E+06	5.78E+06	6.13E+06	6.47E+06	6.81E+06	7.15E+06	7.49E+06	7.83E+06	8.17E+06	8.50E+06
5.0	1.86E+06	2.43E+06	2.91E+06	3.35E+06	3.79E+06	4.22E+06	4.64E+06	5.07E+06	5.49E+06	5.92E+06	6.34E+06	6.76E+06	7.18E+06	7.60E+06	8.02E+06	8.44E+06	8.86E+06	9.28E+06	9.70E+06	1.01E+07
5.5	2.00E+06	2.64E+06	3.19E+06	3.72E+06	4.24E+06	4.76E+06	5.28E+06	5.79E+06	6.30E+06	6.81E+06	7.33E+06	7.84E+06	8.35E+06	8.86E+06	9.37E+06	9.88E+06	1.04E+07	1.09E+07	1.14E+07	1.19E+07
6.0	2.14E+06	2.85E+06	3.50E+06	4.12E+06	4.74E+06	5.36E+06	5.97E+06	6.58E+06	7.19E+06	7.80E+06	8.41E+06	9.02E+06	9.63E+06	1.02E+07	1.08E+07	1.15E+07	1.21E+07	1.27E+07	1.33E+07	1.39E+07
6.5	2.28E+06	3.08E+06	3.83E+06	4.56E+06	5.28E+06	6.00E+06	6.72E+06	7.44E+06	8.15E+06	8.87E+06	9.59E+06	1.03E+07	1.10E+07	1.17E+07	1.24E+07	1.32E+07	1.39E+07	1.46E+07	1.53E+07	1.60E+07
7.0	2.42E+06	3.33E+06	4.18E+06	5.02E+06	5.86E+06	6.70E+06	7.53E+06	8.36E+06	9.20E+06	1.00E+07	1.09E+07	1.17E+07	1.25E+07	1.34E+07	1.42E+07	1.50E+07	1.58E+07	1.67E+07	1.75E+07	1.83E+07
7.5	2.56E+06	3.58E+06	4.56E+06	5.53E+06	6.49E+06	7.45E+06	8.40E+06	9.36E+06	1.03E+07	1.13E+07	1.22E+07	1.32E+07	1.41E+07	1.51E+07	1.60E+07	1.70E+07	1.80E+07	1.89E+07	1.99E+07	2.08E+07
8.0	2.71E+06	3.86E+06	4.96E+06	6.06E+06	7.15E+06	8.25E+06	9.34E+06	1.04E+07	1.15E+07	1.26E+07	1.37E+07	1.48E+07	1.59E+07	1.70E+07	1.80E+07	1.91E+07	2.02E+07	2.13E+07	2.24E+07	2.35E+07
8.5	2.86E+06	4.15E+06	5.39E+06	6.63E+06	7.86E+06	9.10E+06	1.03E+07	1.16E+07	1.28E+07	1.40E+07	1.53E+07	1.65E+07	1.77E+07	1.89E+07	2.02E+07	2.14E+07	2.26E+07	2.39E+07	2.51E+07	2.63E+07
9.0	3.02E+06	4.45E+06	5.85E+06	7.23E+06	8.62E+06	1.00E+07	1.14E+07	1.28E+07	1.41E+07	1.55E+07	1.69E+07	1.83E+07	1.97E+07	2.10E+07	2.24E+07	2.38E+07	2.52E+07	2.66E+07	2.79E+07	2.93E+07
9.5	3.19E+06	4.77E+06	6.33E+06	7.87E+06	9.41E+06	1.10E+07	1.25E+07	1.40E+07	1.56E+07	1.71E+07	1.87E+07	2.02E+07	2.17E+07	2.33E+07	2.48E+07	2.63E+07	2.79E+07	2.94E+07	3.10E+07	3.25E+07
10.0	3.37E+06	5.11E+06	6.83E+06	8.54E+06	1.03E+07	1.20E+07	1.37E+07	1.54E+07	1.71E+07	1.88E+07	2.05E+07	2.22E+07	2.39E+07	2.56E+07	2.73E+07	2.90E+07	3.07E+07	3.24E+07	3.42E+07	3.59E+07

Cv-Incompressable

E (in.) \ H (in.)	0.5	1.0	1.5	2.0	2.5	3.0	3.5	4.0	4.5	5.0	5.5	6.0	6.5	7.0	7.5	8.0	8.5	9.0	9.5	10.0
0.5	-	-	-	-	-	-	-	-	-	-	-	-	-	-	-	-	-	-	-	-
1.0	-	-	-	-	-	-	-	-	-	-	-	-	-	-	-	-	-	-	-	-
1.5	-	-	-	-	-	-	-	-	-	-	0.599	0.599	0.599	0.599	0.599	0.599	0.599	0.599	0.599	0.599
2.0	-	-	-	-	-	0.599	0.599	0.599	0.599	0.599	0.599	0.599	0.599	0.599	0.599	0.599	0.599	0.599	0.599	0.599
2.5	-	-	-	0.599	0.599	0.599	0.599	0.599	0.599	0.599	0.599	0.599	0.599	0.598	0.598	0.598	0.598	0.598	0.598	0.598
3.0	-	-	0.599	0.599	0.599	0.599	0.599	0.599	0.599	0.598	0.598	0.598	0.598	0.598	0.598	0.598	0.598	0.598	0.598	0.598
3.5	-	0.599	0.599	0.599	0.599	0.599	0.598	0.598	0.598	0.598	0.598	0.598	0.598	0.598	0.598	0.598	0.598	0.598	0.598	0.598
4.0	-	0.599	0.599	0.599	0.599	0.598	0.598	0.598	0.598	0.598	0.598	0.598	0.598	0.598	0.598	0.598	0.598	0.598	0.598	0.598
4.5	-	0.599	0.599	0.599	0.598	0.598	0.598	0.598	0.598	0.598	0.598	0.598	0.598	0.598	0.598	0.598	0.598	0.598	0.598	0.598
5.0	0.599	0.599	0.599	0.598	0.598	0.598	0.598	0.598	0.598	0.598	0.598	0.598	0.598	0.598	0.598	0.598	0.598	0.598	0.598	0.598
5.5	0.599	0.599	0.598	0.598	0.598	0.598	0.598	0.598	0.598	0.598	0.598	0.598	0.598	0.598	0.598	0.598	0.598	0.598	0.598	0.598
6.0	0.599	0.599	0.598	0.598	0.598	0.598	0.598	0.598	0.598	0.598	0.598	0.598	0.598	0.598	0.598	0.598	0.598	0.598	0.598	0.598
6.5	0.599	0.598	0.598	0.598	0.598	0.598	0.598	0.598	0.598	0.598	0.598	0.598	0.598	0.598	0.598	0.598	0.598	0.598	0.598	0.598
7.0	0.599	0.598	0.598	0.598	0.598	0.598	0.598	0.598	0.598	0.598	0.598	0.598	0.598	0.598	0.598	0.598	0.598	0.598	0.598	0.598
7.5	0.599	0.598	0.598	0.598	0.598	0.598	0.598	0.598	0.598	0.598	0.598	0.598	0.598	0.598	0.598	0.598	0.598	0.598	0.598	0.598
8.0	0.599	0.598	0.598	0.598	0.598	0.598	0.598	0.598	0.598	0.598	0.598	0.598	0.598	0.598	0.598	0.598	0.598	0.598	0.598	0.598
8.5	0.599	0.598	0.598	0.598	0.598	0.598	0.598	0.598	0.598	0.598	0.598	0.598	0.598	0.598	0.598	0.598	0.598	0.598	0.598	0.598
9.0	0.599	0.598	0.598	0.598	0.598	0.598	0.598	0.598	0.598	0.598	0.598	0.598	0.598	0.598	0.598	0.598	0.598	0.598	0.598	0.598
9.5	0.598	0.598	0.598	0.598	0.598	0.598	0.598	0.598	0.598	0.598	0.598	0.598	0.598	0.598	0.598	0.598	0.598	0.598	0.598	0.598
10.0	0.598	0.598	0.598	0.598	0.598	0.598	0.598	0.598	0.598	0.598	0.598	0.598	0.598	0.598	0.598	0.598	0.598	0.598	0.598	0.598

Cd-Incompressable

E (in.) \ H (in.)	0.5	1.0	1.5	2.0	2.5	3.0	3.5	4.0	4.5	5.0	5.5	6.0	6.5	7.0	7.5	8.0	8.5	9.0	9.5	10.0
0.5	-	-	-	-	-	-	-	-	-	-	-	-	-	-	-	-	-	-	-	-
1.0	-	-	-	-	-	-	-	-	-	-	-	-	-	-	-	-	-	-	-	-
1.5	-	-	-	-	-	-	-	-	-	-	0.599	0.599	0.599	0.599	0.599	0.599	0.599	0.599	0.599	0.599
2.0	-	-	-	-	-	0.599	0.599	0.599	0.599	0.599	0.599	0.599	0.599	0.599	0.599	0.599	0.599	0.599	0.599	0.599
2.5	-	-	-	0.599	0.599	0.599	0.599	0.599	0.599	0.599	0.599	0.599	0.599	0.598	0.598	0.598	0.598	0.598	0.598	0.598
3.0	-	-	0.599	0.599	0.599	0.599	0.599	0.599	0.599	0.598	0.598	0.598	0.598	0.598	0.598	0.598	0.598	0.598	0.598	0.598
3.5	-	0.599	0.599	0.599	0.599	0.599	0.598	0.598	0.598	0.598	0.598	0.598	0.598	0.598	0.598	0.598	0.598	0.598	0.598	0.598
4.0	-	0.599	0.599	0.599	0.599	0.598	0.598	0.598	0.598	0.598	0.598	0.598	0.598	0.598	0.598	0.598	0.598	0.598	0.598	0.598
4.5	-	0.599	0.599	0.599	0.598	0.598	0.598	0.598	0.598	0.598	0.598	0.598	0.598	0.598	0.598	0.598	0.598	0.598	0.598	0.598
5.0	0.599	0.599	0.599	0.598	0.598	0.598	0.598	0.598	0.598	0.598	0.598	0.598	0.598	0.598	0.598	0.598	0.598	0.598	0.598	0.598
5.5	0.599	0.599	0.598	0.598	0.598	0.598	0.598	0.598	0.598	0.598	0.598	0.598	0.598	0.598	0.598	0.598	0.598	0.598	0.598	0.598
6.0	0.599	0.599	0.598	0.598	0.598	0.598	0.598	0.598	0.598	0.598	0.598	0.598	0.598	0.598	0.598	0.598	0.598	0.598	0.598	0.598
6.5	0.599	0.598	0.598	0.598	0.598	0.598	0.598	0.598	0.598	0.598	0.598	0.598	0.598	0.598	0.598	0.598	0.598	0.598	0.598	0.598
7.0	0.599	0.598	0.598	0.598	0.598	0.598	0.598	0.598	0.598	0.598	0.598	0.598	0.598	0.598	0.598	0.598	0.598	0.598	0.598	0.598
7.5	0.599	0.598	0.598	0.598	0.598	0.598	0.598	0.598	0.598	0.598	0.598	0.598	0.598	0.598	0.598	0.598	0.598	0.598	0.598	0.598
8.0	0.599	0.598	0.598	0.598	0.598	0.598	0.598	0.598	0.598	0.598	0.598	0.598	0.598	0.598	0.598	0.598	0.598	0.598	0.598	0.598
8.5	0.599	0.598	0.598	0.598	0.598	0.598	0.598	0.598	0.598	0.598	0.598	0.598	0.598	0.598	0.598	0.598	0.598	0.598	0.598	0.598
9.0	0.599	0.598	0.598	0.598	0.598	0.598	0.598	0.598	0.598	0.598	0.598	0.598	0.598	0.598	0.598	0.598	0.598	0.598	0.598	0.598
9.5	0.598	0.598	0.598	0.598	0.598	0.598	0.598	0.598	0.598	0.598	0.598	0.598	0.598	0.598	0.598	0.598	0.598	0.598	0.598	0.598
10.0	0.598	0.598	0.598	0.598	0.598	0.598	0.598	0.598	0.598	0.598	0.598	0.598	0.598	0.598	0.598	0.598	0.598	0.598	0.598	0.598

Now using the incompressible flow parameters, the incompressible, subcritical flow mass flowrate through the throat can be calculated:

$$Subcritical\ Flow: \left(\frac{p}{P_0}\right) > \left(\frac{2}{\gamma+1}\right)^{\frac{\gamma}{\gamma-1}}$$

$$r = \frac{p}{P_0}$$

$$f = \frac{1}{\left(C_d\right)_{inc}} - \frac{1}{2\left(C_d\right)^2_{inc}}$$

$$K_n = \sqrt{\frac{2\gamma}{\gamma-1} \cdot r^{\frac{2}{\gamma}} \left[1 - r^{\frac{\gamma-1}{\gamma}}\right]}$$

$$C_d = \frac{1 - \sqrt{1 - f \cdot \left(2 \cdot r^{\frac{1}{\gamma}}\right)^2 \left(\frac{1-r}{K_n^{\,2}}\right)}}{2 \cdot f \cdot r^{\frac{1}{\gamma}}}$$

$$\rightarrow \dot{m} = K_n \cdot C_d \cdot A \cdot \sqrt{P_0 \cdot \rho_0}$$

Note here that P0 analogous to upstream pressure state 2 pressure P2, and P analogous to downstream state 3 pressure P3. Gama γ here is analogous to state 2 specific heat ratio γ2. Mdot equals the mass flowrate through the throat and A equals the total throat area (gap and core leakage areas).

Now calculates the subcritical flow parameters:

Cd - subcritical compressable

E (in.) \ H (in.)	0.5	1.0	1.5	2.0	2.5	3.0	3.5	4.0	4.5	5.0	5.5	6.0	6.5	7.0	7.5	8.0	8.5	9.0	9.5	10.0
0.5	-	-	-	-	-	-	-	-	-	-	-	-	-	-	-	-	-	-	-	-
1.0	-	-	-	-	-	-	-	-	-	-	-	-	-	-	-	-	-	-	-	-
1.5	-	-	-	-	-	-	-	-	-	-	1.105	1.077	1.052	1.030	1.010	0.992	0.976	0.961	0.947	0.934
2.0	-	-	-	-	-	1.100	1.051	1.012	0.979	0.952	0.928	0.907	0.888	0.872	0.858	0.845	0.833	0.822	0.813	0.804
2.5	-	-	-	1.078	1.011	0.961	0.922	0.891	0.865	0.844	0.826	0.810	0.796	0.784	0.774	0.764	0.756	0.748	0.741	0.735
3.0	-	-	1.049	0.967	0.911	0.870	0.839	0.814	0.794	0.777	0.763	0.751	0.741	0.732	0.724	0.717	0.710	0.705	0.700	0.695
3.5	-	1.075	0.959	0.889	0.842	0.808	0.783	0.763	0.747	0.734	0.723	0.713	0.705	0.698	0.692	0.687	0.682	0.677	0.673	0.670
4.0	-	0.993	0.891	0.832	0.792	0.764	0.744	0.727	0.714	0.704	0.695	0.687	0.681	0.676	0.671	0.666	0.663	0.659	0.656	0.653
4.5	-	0.930	0.840	0.789	0.756	0.733	0.715	0.702	0.691	0.683	0.675	0.669	0.664	0.660	0.656	0.652	0.649	0.647	0.644	0.642
5.0	1.062	0.879	0.801	0.757	0.729	0.709	0.694	0.683	0.674	0.667	0.661	0.656	0.652	0.648	0.645	0.642	0.640	0.637	0.635	0.634
5.5	1.004	0.839	0.770	0.732	0.708	0.691	0.678	0.669	0.661	0.655	0.650	0.646	0.643	0.640	0.637	0.635	0.632	0.631	0.629	0.627
6.0	0.956	0.806	0.745	0.712	0.691	0.677	0.666	0.658	0.652	0.646	0.642	0.639	0.636	0.633	0.631	0.629	0.627	0.625	0.624	0.623
6.5	0.915	0.780	0.726	0.696	0.678	0.665	0.656	0.649	0.644	0.639	0.636	0.633	0.630	0.628	0.626	0.624	0.623	0.621	0.620	0.619
7.0	0.881	0.758	0.709	0.684	0.667	0.656	0.648	0.642	0.638	0.634	0.631	0.628	0.626	0.624	0.622	0.621	0.619	0.618	0.617	0.616
7.5	0.851	0.739	0.696	0.673	0.659	0.649	0.642	0.637	0.633	0.629	0.626	0.624	0.622	0.620	0.619	0.618	0.617	0.616	0.615	0.614
8.0	0.826	0.724	0.685	0.664	0.652	0.643	0.637	0.632	0.628	0.625	0.623	0.621	0.619	0.618	0.616	0.615	0.614	0.613	0.613	0.612
8.5	0.804	0.710	0.675	0.657	0.646	0.638	0.632	0.628	0.625	0.622	0.620	0.618	0.617	0.616	0.614	0.613	0.612	0.612	0.611	0.610
9.0	0.785	0.699	0.667	0.651	0.641	0.634	0.629	0.625	0.622	0.620	0.618	0.616	0.615	0.614	0.613	0.612	0.611	0.610	0.610	0.609
9.5	0.768	0.690	0.661	0.646	0.636	0.630	0.626	0.622	0.620	0.618	0.616	0.614	0.613	0.612	0.611	0.610	0.610	0.609	0.608	0.608
10.0	0.753	0.681	0.655	0.641	0.633	0.627	0.623	0.620	0.618	0.616	0.614	0.613	0.612	0.611	0.610	0.609	0.608	0.608	0.607	0.607

mdot (kg/m^3) - subcritical compressable

E (in.) \ H (in.)	0.5	1.0	1.5	2.0	2.5	3.0	3.5	4.0	4.5	5.0	5.5	6.0	6.5	7.0	7.5	8.0	8.5	9.0	9.5	10.0
0.5	-	-	-	-	-	-	-	-	-	-	-	-	-	-	-	-	-	-	-	-
1.0	-	-	-	-	-	-	-	-	-	-	-	-	-	-	-	-	-	-	-	-
1.5	-	-	-	-	-	-	-	-	-	-	0.510	0.509	0.509	0.510	0.512	0.515	0.518	0.521	0.524	0.528
2.0	-	-	-	-	-	0.371	0.352	0.340	0.333	0.329	0.326	0.325	0.325	0.326	0.328	0.330	0.332	0.335	0.338	0.341
2.5	-	-	-	0.354	0.311	0.285	0.268	0.258	0.251	0.246	0.244	0.243	0.243	0.243	0.244	0.246	0.247	0.249	0.252	0.254
3.0	-	-	0.364	0.299	0.262	0.239	0.224	0.214	0.207	0.203	0.200	0.198	0.198	0.198	0.198	0.199	0.200	0.202	0.203	0.205
3.5	-	0.436	0.321	0.265	0.232	0.211	0.197	0.187	0.181	0.176	0.173	0.172	0.170	0.170	0.170	0.170	0.171	0.172	0.173	0.175
4.0	-	0.394	0.293	0.242	0.212	0.193	0.180	0.171	0.164	0.159	0.156	0.154	0.152	0.152	0.151	0.151	0.152	0.152	0.153	0.154
4.5	-	0.364	0.273	0.226	0.199	0.180	0.168	0.159	0.152	0.148	0.144	0.142	0.140	0.139	0.138	0.138	0.138	0.138	0.138	0.139
5.0	0.583	0.341	0.258	0.215	0.189	0.172	0.159	0.151	0.144	0.139	0.136	0.133	0.131	0.129	0.128	0.128	0.127	0.127	0.128	0.128
5.5	0.545	0.324	0.246	0.206	0.181	0.165	0.153	0.145	0.138	0.133	0.129	0.126	0.124	0.122	0.121	0.120	0.120	0.119	0.119	0.119
6.0	0.515	0.310	0.237	0.199	0.176	0.160	0.148	0.140	0.133	0.128	0.124	0.121	0.119	0.117	0.116	0.114	0.114	0.113	0.113	0.113
6.5	0.491	0.299	0.230	0.194	0.171	0.156	0.145	0.136	0.130	0.125	0.121	0.117	0.115	0.113	0.111	0.110	0.109	0.108	0.108	0.107
7.0	0.470	0.290	0.225	0.190	0.168	0.153	0.142	0.133	0.127	0.122	0.117	0.114	0.111	0.109	0.108	0.106	0.105	0.104	0.103	0.103
7.5	0.454	0.283	0.220	0.186	0.165	0.150	0.139	0.131	0.124	0.119	0.115	0.112	0.109	0.106	0.105	0.103	0.102	0.101	0.100	0.099
8.0	0.440	0.277	0.216	0.183	0.163	0.148	0.137	0.129	0.122	0.117	0.113	0.109	0.107	0.104	0.102	0.100	0.099	0.098	0.097	0.096
8.5	0.428	0.271	0.213	0.181	0.161	0.146	0.136	0.127	0.121	0.115	0.111	0.108	0.105	0.102	0.100	0.098	0.097	0.096	0.095	0.094
9.0	0.417	0.267	0.210	0.179	0.159	0.145	0.134	0.126	0.119	0.114	0.110	0.106	0.103	0.101	0.098	0.097	0.095	0.094	0.093	0.092
9.5	0.408	0.263	0.208	0.177	0.157	0.143	0.133	0.125	0.118	0.113	0.108	0.105	0.102	0.099	0.097	0.095	0.093	0.092	0.091	0.090
10.0	0.401	0.260	0.206	0.176	0.156	0.142	0.132	0.124	0.117	0.112	0.107	0.104	0.101	0.098	0.096	0.094	0.092	0.090	0.089	0.088

The above mass flowrate will be used as the total leakage mass flowrate when the rotor configuration yields a non-choked scenario. This will be reflected in the isentropic efficiency chart shown below. First, whether the rotor configurations are choked or not needs to be determined using equation 17.

Below show which rotor configurations are choked (1 = choked rotor configuration).

Choked Conditions

E (in.) \ H (in.)	0.5	1.0	1.5	2.0	2.5	3.0	3.5	4.0	4.5	5.0	5.5	6.0	6.5	7.0	7.5	8.0	8.5	9.0	9.5	10.0
0.5	-	-	-	-	-	-	-	-	-	-	-	-	-	-	-	-	-	-	-	-
1.0	-	-	-	-	-	-	-	-	-	-	-	-	-	-	-	-	-	-	-	-
1.5	-	-	-	-	-	-	-	-	-	-	1.0	1.0	1.0	1.0	1.0	1.0	1.0	1.0	1.0	1.0
2.0	-	-	-	-	-	1.0	1.0	1.0	1.0	1.0	1.0	1.0	1.0	1.0	1.0	1.0	1.0	1.0	1.0	1.0
2.5	-	-	-	1.0	1.0	1.0	1.0	1.0	1.0	1.0	1.0	1.0	1.0	1.0	1.0	1.0	1.0	1.0	1.0	1.0
3.0	-	-	1.0	1.0	1.0	1.0	1.0	1.0	1.0	1.0	1.0	1.0	1.0	1.0	0.0	0.0	0.0	0.0	0.0	0.0
3.5	-	1.0	1.0	1.0	1.0	1.0	1.0	1.0	1.0	1.0	0.0	0.0	0.0	0.0	0.0	0.0	0.0	0.0	0.0	0.0
4.0	-	1.0	1.0	1.0	1.0	1.0	1.0	0.0	0.0	0.0	0.0	0.0	0.0	0.0	0.0	0.0	0.0	0.0	0.0	0.0
4.5	-	1.0	1.0	1.0	1.0	1.0	0.0	0.0	0.0	0.0	0.0	0.0	0.0	0.0	0.0	0.0	0.0	0.0	0.0	0.0
5.0	1.0	1.0	1.0	1.0	0.0	0.0	0.0	0.0	0.0	0.0	0.0	0.0	0.0	0.0	0.0	0.0	0.0	0.0	0.0	0.0
5.5	1.0	1.0	1.0	1.0	0.0	0.0	0.0	0.0	0.0	0.0	0.0	0.0	0.0	0.0	0.0	0.0	0.0	0.0	0.0	0.0
6.0	1.0	1.0	1.0	0.0	0.0	0.0	0.0	0.0	0.0	0.0	0.0	0.0	0.0	0.0	0.0	0.0	0.0	0.0	0.0	0.0
6.5	1.0	1.0	0.0	0.0	0.0	0.0	0.0	0.0	0.0	0.0	0.0	0.0	0.0	0.0	0.0	0.0	0.0	0.0	0.0	0.0
7.0	1.0	1.0	0.0	0.0	0.0	0.0	0.0	0.0	0.0	0.0	0.0	0.0	0.0	0.0	0.0	0.0	0.0	0.0	0.0	0.0
7.5	1.0	1.0	0.0	0.0	0.0	0.0	0.0	0.0	0.0	0.0	0.0	0.0	0.0	0.0	0.0	0.0	0.0	0.0	0.0	0.0
8.0	1.0	0.0	0.0	0.0	0.0	0.0	0.0	0.0	0.0	0.0	0.0	0.0	0.0	0.0	0.0	0.0	0.0	0.0	0.0	0.0
8.5	1.0	0.0	0.0	0.0	0.0	0.0	0.0	0.0	0.0	0.0	0.0	0.0	0.0	0.0	0.0	0.0	0.0	0.0	0.0	0.0
9.0	1.0	0.0	0.0	0.0	0.0	0.0	0.0	0.0	0.0	0.0	0.0	0.0	0.0	0.0	0.0	0.0	0.0	0.0	0.0	0.0
9.5	1.0	0.0	0.0	0.0	0.0	0.0	0.0	0.0	0.0	0.0	0.0	0.0	0.0	0.0	0.0	0.0	0.0	0.0	0.0	0.0
10.0	1.0	0.0	0.0	0.0	0.0	0.0	0.0	0.0	0.0	0.0	0.0	0.0	0.0	0.0	0.0	0.0	0.0	0.0	0.0	0.0

Below shows isentropic efficiency assuming choked flow for ALL configurations:

E_system CHOKED ONLY

E (in.) \ H (in.)	0.5	1.0	1.5	2.0	2.5	3.0	3.5	4.0	4.5	5.0	5.5	6.0	6.5	7.0	7.5	8.0	8.5	9.0	9.5	10.0
0.5	-	-	-	-	-	-	-	-	-	-	-	-	-	-	-	-	-	-	-	-
1.0	-	-	-	-	-	-	-	-	-	-	-	-	-	-	-	-	-	-	-	-
1.5	-	-	-	-	-	-	-	-	-	-	14.8%	15.0%	15.1%	15.2%	15.2%	15.1%	15.1%	15.0%	14.9%	14.8%
2.0	-	-	-	-	-	18.6%	19.5%	20.0%	20.3%	20.3%	20.3%	20.1%	20.0%	19.7%	19.5%	19.2%	19.0%	18.7%	18.4%	18.1%
2.5	-	-	-	19.4%	21.2%	22.2%	22.6%	22.8%	22.7%	22.5%	22.2%	21.8%	21.4%	21.0%	20.5%	20.1%	19.7%	19.2%	18.8%	18.4%
3.0	-	-	19.1%	21.6%	22.8%	23.4%	**23.4%**	23.3%	22.9%	22.4%	21.9%	21.3%	20.8%	20.2%	19.7%	19.1%	18.6%	18.1%	17.6%	17.1%
3.5	-	16.8%	20.6%	22.4%	23.1%	23.2%	22.9%	22.5%	21.9%	21.2%	20.5%	19.9%	19.2%	18.6%	18.0%	17.4%	16.8%	16.3%	15.8%	15.3%
4.0	-	18.2%	21.2%	22.4%	22.6%	22.3%	21.7%	21.0%	20.3%	19.5%	18.7%	18.0%	17.3%	16.7%	16.0%	15.4%	14.9%	14.4%	13.9%	13.4%
4.5	-	19.0%	21.3%	21.8%	21.6%	21.0%	20.2%	19.3%	18.5%	17.7%	16.9%	16.1%	15.4%	14.8%	14.2%	13.6%	13.1%	12.6%	12.1%	11.7%
5.0	13.6%	19.3%	20.9%	21.0%	20.4%	19.5%	18.6%	17.6%	16.7%	15.9%	15.1%	14.3%	13.7%	13.0%	12.5%	11.9%	11.4%	11.0%	10.6%	10.2%
5.5	14.5%	19.4%	20.3%	19.9%	19.0%	18.0%	17.0%	16.0%	15.1%	14.2%	13.5%	12.8%	12.1%	11.5%	11.0%	10.5%	10.0%	9.6%	9.2%	8.9%
6.0	15.1%	19.1%	19.5%	18.8%	17.7%	16.5%	15.5%	14.5%	13.6%	12.7%	12.0%	11.3%	10.7%	10.2%	9.7%	9.3%	8.8%	8.5%	8.1%	7.8%
6.5	15.5%	18.8%	18.6%	17.6%	16.4%	15.2%	14.1%	13.1%	12.2%	11.4%	10.7%	10.1%	9.6%	9.1%	8.6%	8.2%	7.8%	7.5%	7.1%	6.9%
7.0	15.8%	18.3%	17.7%	16.5%	15.2%	13.9%	12.8%	11.9%	11.0%	10.3%	9.6%	9.1%	8.5%	8.1%	7.7%	7.3%	6.9%	6.6%	6.3%	6.1%
7.5	15.9%	17.7%	16.8%	15.4%	14.0%	12.8%	11.7%	10.8%	10.0%	9.3%	8.7%	8.1%	7.7%	7.2%	6.9%	6.5%	6.2%	5.9%	5.6%	5.4%
8.0	15.9%	17.1%	15.9%	14.4%	13.0%	11.8%	10.7%	9.8%	9.1%	8.4%	7.9%	7.3%	6.9%	6.5%	6.2%	5.8%	5.6%	5.3%	5.1%	4.8%
8.5	15.8%	16.4%	15.0%	13.4%	12.0%	10.8%	9.8%	9.0%	8.3%	7.7%	7.1%	6.7%	6.2%	5.9%	5.6%	5.3%	5.0%	4.8%	4.5%	4.3%
9.0	15.7%	15.8%	14.1%	12.5%	11.1%	10.0%	9.0%	8.2%	7.6%	7.0%	6.5%	6.0%	5.7%	5.3%	5.0%	4.8%	4.5%	4.3%	4.1%	3.9%
9.5	15.5%	15.1%	13.3%	11.7%	10.3%	9.2%	8.3%	7.6%	6.9%	6.4%	5.9%	5.5%	5.2%	4.9%	4.6%	4.3%	4.1%	3.9%	3.7%	3.6%
10.0	15.3%	14.5%	12.6%	10.9%	9.6%	8.5%	7.7%	7.0%	6.4%	5.9%	5.4%	5.0%	4.7%	4.4%	4.2%	4.0%	3.8%	3.6%	3.4%	3.2%

Below shows isentropic efficiency implementing choked and subcritical flow:

E_system CHOKED /SUBCRITICAL

E (in.) \ H (in.)	0.5	1.0	1.5	2.0	2.5	3.0	3.5	4.0	4.5	5.0	5.5	6.0	6.5	7.0	7.5	8.0	8.5	9.0	9.5	10.0
0.5	-	-	-	-	-	-	-	-	-	-	-	-	-	-	-	-	-	-	-	-
1.0	-	-	-	-	-	-	-	-	-	-	-	-	-	-	-	-	-	-	-	-
1.5	-	-	-	-	-	-	-	-	-	-	14.8%	15.0%	15.1%	15.2%	15.2%	15.1%	15.1%	15.0%	14.9%	14.8%
2.0	-	-	-	-	-	18.6%	19.5%	20.0%	20.3%	20.3%	20.3%	20.1%	20.0%	19.7%	19.5%	19.2%	19.0%	18.7%	18.4%	18.1%
2.5	-	-	-	19.4%	21.2%	22.2%	22.6%	22.8%	22.7%	22.5%	22.2%	21.8%	21.4%	21.0%	20.5%	20.1%	19.7%	19.2%	18.8%	18.4%
3.0	-	-	19.1%	21.6%	22.8%	23.4%	**23.4%**	23.3%	22.9%	22.4%	21.9%	21.3%	20.8%	20.2%	22.1%	21.5%	21.0%	20.4%	19.9%	19.4%
3.5	-	16.8%	20.6%	22.4%	23.1%	23.2%	22.9%	22.5%	21.9%	21.2%	22.9%	22.1%	21.4%	20.7%	20.1%	19.4%	18.8%	18.3%	17.7%	17.2%
4.0	-	18.2%	21.2%	22.4%	22.6%	22.3%	21.7%	23.4%	22.5%	21.6%	20.8%	20.0%	19.2%	18.5%	17.8%	17.2%	16.6%	16.0%	15.5%	15.0%
4.5	-	19.0%	21.3%	21.8%	21.6%	21.0%	22.4%	21.5%	20.5%	19.5%	18.7%	17.8%	17.1%	16.3%	15.7%	15.0%	14.5%	13.9%	13.4%	13.0%
5.0	13.6%	19.3%	20.9%	21.0%	22.8%	21.7%	20.6%	19.5%	18.5%	17.5%	16.6%	15.8%	15.1%	14.4%	13.7%	13.1%	12.6%	12.1%	11.6%	11.2%
5.5	14.5%	19.4%	20.3%	19.9%	21.3%	20.1%	18.9%	17.7%	16.7%	15.7%	14.8%	14.0%	13.3%	12.6%	12.0%	11.5%	11.0%	10.5%	10.1%	9.7%
6.0	15.1%	19.1%	19.5%	21.2%	19.8%	18.5%	17.2%	16.0%	15.0%	14.0%	13.2%	12.4%	11.8%	11.2%	10.6%	10.1%	9.6%	9.2%	8.8%	8.5%
6.5	15.5%	18.8%	21.2%	19.9%	18.4%	16.9%	15.6%	14.5%	13.5%	12.6%	11.8%	11.1%	10.4%	9.9%	9.4%	8.9%	8.5%	8.1%	7.7%	7.4%
7.0	15.8%	18.3%	20.2%	18.6%	17.0%	15.5%	14.3%	13.1%	12.2%	11.3%	10.5%	9.9%	9.3%	8.8%	8.3%	7.9%	7.5%	7.1%	6.8%	6.5%
7.5	15.9%	17.7%	19.2%	17.4%	15.7%	14.3%	13.0%	11.9%	11.0%	10.2%	9.5%	8.9%	8.3%	7.8%	7.4%	7.0%	6.7%	6.3%	6.1%	5.8%
8.0	15.9%	19.8%	18.2%	16.3%	14.6%	13.1%	11.9%	10.8%	10.0%	9.2%	8.5%	8.0%	7.5%	7.0%	6.6%	6.3%	6.0%	5.7%	5.4%	5.2%
8.5	15.8%	19.0%	17.2%	15.2%	13.5%	12.0%	10.9%	9.9%	9.0%	8.3%	7.7%	7.2%	6.7%	6.3%	6.0%	5.6%	5.3%	5.1%	4.8%	4.6%
9.0	15.7%	18.3%	16.2%	14.2%	12.5%	11.1%	10.0%	9.0%	8.2%	7.6%	7.0%	6.5%	6.1%	5.7%	5.4%	5.1%	4.8%	4.6%	4.4%	4.2%
9.5	15.5%	17.6%	15.3%	13.2%	11.6%	10.2%	9.2%	8.3%	7.5%	6.9%	6.4%	5.9%	5.5%	5.2%	4.9%	4.6%	4.4%	4.2%	4.0%	3.8%
10.0	15.3%	16.9%	14.4%	12.4%	10.8%	9.5%	8.4%	7.6%	6.9%	6.3%	5.8%	5.4%	5.1%	4.7%	4.5%	4.2%	4.0%	3.8%	3.6%	3.4%

Recall that the values in red indicate the highest 10% isentropic efficiency, and that the optimized rotor configuration stays the same. Below shows the deviation between the two analysis's (Esystsem CHOKED – Esystem CHOKED/SUBCRITICAL):

Difference between CHOKED ONLY and CHOKED/SUBCRITICAL analysis

E (in.) \ H (in.)	0.5	1.0	1.5	2.0	2.5	3.0	3.5	4.0	4.5	5.0	5.5	6.0	6.5	7.0	7.5	8.0	8.5	9.0	9.5	10.0
0.5	-	-	-	-	-	-	-	-	-	-	-	-	-	-	-	-	-	-	-	-
1.0	-	-	-	-	-	-	-	-	-	-	-	-	-	-	-	-	-	-	-	-
1.5	-	-	-	-	-	-	-	-	-	-	0.00%	0.00%	0.00%	0.00%	0.00%	0.00%	0.00%	0.00%	0.00%	0.00%
2.0	-	-	-	-	-	0.00%	0.00%	0.00%	0.00%	0.00%	0.00%	0.00%	0.00%	0.00%	0.00%	0.00%	0.00%	0.00%	0.00%	0.00%
2.5	-	-	-	0.00%	0.00%	0.00%	0.00%	0.00%	0.00%	0.00%	0.00%	0.00%	0.00%	0.00%	0.00%	0.00%	0.00%	0.00%	0.00%	0.00%
3.0	-	-	0.00%	0.00%	0.00%	0.00%	0.00%	0.00%	0.00%	0.00%	0.00%	0.00%	0.00%	0.00%	-2.46%	-2.43%	-2.39%	-2.36%	-2.34%	-2.31%
3.5	-	0.00%	0.00%	0.00%	0.00%	0.00%	0.00%	0.00%	0.00%	0.00%	-2.34%	-2.27%	-2.22%	-2.16%	-2.12%	-2.07%	-2.03%	-2.00%	-1.96%	-1.93%
4.0	-	0.00%	0.00%	0.00%	0.00%	0.00%	0.00%	-2.35%	-2.24%	-2.14%	-2.06%	-1.98%	-1.91%	-1.85%	-1.79%	-1.74%	-1.70%	-1.65%	-1.61%	-1.57%
4.5	-	0.00%	0.00%	0.00%	0.00%	0.00%	-2.27%	-2.13%	-2.00%	-1.90%	-1.80%	-1.72%	-1.64%	-1.57%	-1.51%	-1.45%	-1.40%	-1.35%	-1.31%	-1.27%
5.0	0.00%	0.00%	0.00%	0.00%	-2.45%	-2.25%	-2.07%	-1.92%	-1.79%	-1.67%	-1.57%	-1.48%	-1.40%	-1.33%	-1.26%	-1.21%	-1.15%	-1.11%	-1.07%	-1.03%
5.5	0.00%	0.00%	0.00%	0.00%	-2.29%	-2.08%	-1.89%	-1.73%	-1.59%	-1.47%	-1.36%	-1.27%	-1.19%	-1.12%	-1.06%	-1.00%	-0.95%	-0.91%	-0.87%	-0.83%
6.0	0.00%	0.00%	0.00%	-2.40%	-2.14%	-1.92%	-1.72%	-1.55%	-1.41%	-1.29%	-1.18%	-1.10%	-1.02%	-0.95%	-0.89%	-0.84%	-0.79%	-0.75%	-0.71%	-0.68%
6.5	0.00%	0.00%	-2.58%	-2.27%	-2.00%	-1.76%	-1.56%	-1.39%	-1.25%	-1.13%	-1.03%	-0.94%	-0.87%	-0.81%	-0.75%	-0.70%	-0.66%	-0.62%	-0.59%	-0.56%
7.0	0.00%	0.00%	-2.48%	-2.15%	-1.86%	-1.61%	-1.41%	-1.25%	-1.11%	-0.99%	-0.90%	-0.82%	-0.75%	-0.69%	-0.64%	-0.59%	-0.56%	-0.52%	-0.49%	-0.46%
7.5	0.00%	0.00%	-2.38%	-2.02%	-1.72%	-1.48%	-1.28%	-1.12%	-0.98%	-0.88%	-0.79%	-0.71%	-0.65%	-0.59%	-0.55%	-0.51%	-0.47%	-0.44%	-0.41%	-0.39%
8.0	0.00%	-2.67%	-2.28%	-1.90%	-1.60%	-1.35%	-1.15%	-1.00%	-0.87%	-0.77%	-0.69%	-0.62%	-0.56%	-0.51%	-0.47%	-0.43%	-0.40%	-0.37%	-0.35%	-0.33%
8.5	0.00%	-2.60%	-2.17%	-1.78%	-1.47%	-1.23%	-1.04%	-0.90%	-0.78%	-0.68%	-0.61%	-0.54%	-0.49%	-0.44%	-0.41%	-0.37%	-0.34%	-0.32%	-0.30%	-0.28%
9.0	0.00%	-2.53%	-2.07%	-1.67%	-1.36%	-1.13%	-0.94%	-0.80%	-0.69%	-0.61%	-0.54%	-0.48%	-0.43%	-0.39%	-0.35%	-0.32%	-0.30%	-0.28%	-0.26%	-0.24%
9.5	0.00%	-2.46%	-1.97%	-1.56%	-1.26%	-1.03%	-0.86%	-0.72%	-0.62%	-0.54%	-0.47%	-0.42%	-0.38%	-0.34%	-0.31%	-0.28%	-0.26%	-0.24%	-0.22%	-0.21%
10.0	0.00%	-2.39%	-1.87%	-1.46%	-1.16%	-0.94%	-0.78%	-0.65%	-0.56%	-0.48%	-0.42%	-0.37%	-0.33%	-0.30%	-0.27%	-0.25%	-0.23%	-0.21%	-0.19%	-0.18%

The maximum difference between the two computations are found at the choked/sub-critical boundary. This is where the pressure drop from state 1 to state 2 is smallest within the subcritical regime. However, as rotor size increases, state 1 to state 2 pressure drop increases dominating any increase in error induced by a choked flow assumption. As previously stated, the optimized solution has not changed validating the choked flow analysis for optimized rotor configurations.

An analysis of the more complicated energy recovery study 3.1 reveals similar results (note the two studies have the same pressure conditions):

Study 3.1 Choked Conditions

E (in.) \ H (in.)	0.5	10.5	20.5	30.5	40.5	50.5	60.5	70.5	80.5	90.5	100.5	110.5	120.5	130.5	140.5	150.5	160.5	170.5	180.5	190.5
0.5	-	-	-	-	-	-	-	-	-	-	-	-	-	-	-	1.0	1.0	1.0	1.0	1.0
10.5	-	-	-	-	-	-	-	-	-	-	-	-	-	1.0	1.0	1.0	1.0	1.0	1.0	1.0
20.5	-	-	-	-	-	-	-	-	-	-	-	1.0	1.0	1.0	1.0	1.0	1.0	1.0	1.0	1.0
30.5	-	-	-	-	-	-	-	-	1.0	1.0	1.0	1.0	1.0	1.0	1.0	1.0	1.0	1.0	1.0	1.0
40.5	-	-	-	-	-	1.0	1.0	1.0	1.0	1.0	1.0	1.0	1.0	1.0	1.0	1.0	1.0	1.0	1.0	1.0
50.5	-	-	-	1.0	1.0	1.0	1.0	1.0	1.0	1.0	1.0	1.0	1.0	1.0	1.0	1.0	1.0	1.0	1.0	1.0
60.5	-	-	1.0	1.0	1.0	1.0	1.0	1.0	1.0	1.0	1.0	1.0	1.0	1.0	1.0	0.0	0.0	0.0	0.0	0.0
70.5	-	1.0	1.0	1.0	1.0	1.0	1.0	1.0	1.0	1.0	1.0	1.0	0.0	0.0	0.0	0.0	0.0	0.0	0.0	0.0
80.5	1.0	1.0	1.0	1.0	1.0	1.0	1.0	1.0	1.0	0.0	0.0	0.0	0.0	0.0	0.0	0.0	0.0	0.0	0.0	0.0
90.5	1.0	1.0	1.0	1.0	1.0	1.0	1.0	0.0	0.0	0.0	0.0	0.0	0.0	0.0	0.0	0.0	-	-	-	-
100.5	1.0	1.0	1.0	1.0	1.0	1.0	0.0	0.0	0.0	0.0	0.0	0.0	0.0	-	-	-	-	-	-	-
110.5	1.0	1.0	1.0	1.0	1.0	0.0	0.0	0.0	0.0	0.0	0.0	-	-	-	-	-	-	-	-	-
120.5	1.0	1.0	1.0	1.0	0.0	0.0	0.0	0.0	0.0	-	-	-	-	-	-	-	-	-	-	-
130.5	1.0	1.0	1.0	0.0	0.0	0.0	0.0	0.0	-	-	-	-	-	-	-	-	-	-	-	-
140.5	1.0	1.0	0.0	0.0	0.0	0.0	0.0	-	-	-	-	-	-	-	-	-	-	-	-	-
150.5	1.0	1.0	0.0	0.0	0.0	0.0	-	-	-	-	-	-	-	-	-	-	-	-	-	-
160.5	1.0	1.0	0.0	0.0	0.0	-	-	-	-	-	-	-	-	-	-	-	-	-	-	-
170.5	1.0	0.0	0.0	0.0	-	-	-	-	-	-	-	-	-	-	-	-	-	-	-	-
180.5	1.0	0.0	0.0	0.0	-	-	-	-	-	-	-	-	-	-	-	-	-	-	-	-
190.5	1.0	0.0	0.0	-	-	-	-	-	-	-	-	-	-	-	-	-	-	-	-	-

Study 3.1 E_system CHOKED

E (in.) \ H (in.)	0.5	1.0	1.5	2.0	2.5	3.0	3.5	4.0	4.5	5.0	5.5	6.0	6.5	7.0	7.5	8.0	8.5	9.0	9.5	10.0
0.5	-	-	-	-	-	-	-	-	-	-	-	-	-	-	-	1.5%	1.5%	1.5%	1.5%	1.5%
1.0	-	-	-	-	-	-	-	-	-	-	-	-	-	7.5%	7.5%	7.6%	7.6%	7.6%	7.6%	7.6%
1.5	-	-	-	-	-	-	-	-	-	-	-	15.0%	15.2%	15.2%	15.2%	15.2%	15.2%	15.1%	15.0%	14.9%
2.0	-	-	-	-	-	-	-	-	21.0%	21.4%	21.7%	21.8%	21.7%	21.7%	21.5%	21.3%	21.1%	20.8%	20.5%	20.2%
2.5	-	-	-	-	-	23.4%	24.6%	25.4%	25.8%	26.0%	26.0%	25.9%	25.7%	25.3%	24.9%	24.5%	24.0%	23.4%	22.9%	22.3%
3.0	-	-	-	22.7%	25.1%	26.6%	27.6%	28.1%	28.2%	28.1%	27.8%	27.4%	26.8%	26.1%	25.4%	24.6%	23.7%	22.9%	21.9%	21.0%
3.5	-	-	21.7%	25.0%	27.0%	28.2%	28.7%	**28.8%**	28.6%	28.1%	27.4%	26.5%	25.5%	24.4%	23.3%	22.1%	20.8%	19.5%	18.1%	16.7%
4.0	-	18.7%	23.4%	26.2%	27.8%	28.5%	28.5%	28.1%	27.3%	26.3%	25.1%	23.7%	22.2%	20.7%	19.0%	17.3%	15.5%	13.7%	11.8%	9.9%
4.5	12.5%	20.0%	24.4%	26.6%	27.6%	27.6%	27.1%	26.1%	24.7%	23.1%	21.3%	19.3%	17.3%	15.1%	12.8%	10.5%	8.2%	5.7%	3.3%	0.8%
5.0	13.6%	21.0%	24.8%	26.4%	26.6%	25.9%	24.7%	23.0%	20.9%	18.6%	16.2%	13.5%	10.8%	8.0%	5.0%	2.1%	-	-	-	-
5.5	14.5%	21.6%	24.6%	25.5%	24.9%	23.5%	21.4%	18.9%	16.1%	13.1%	9.8%	6.5%	3.0%	-	-	-	-	-	-	-
6.0	15.2%	21.8%	24.1%	24.0%	22.6%	20.3%	17.4%	14.0%	10.4%	6.5%	2.4%	-	-	-	-	-	-	-	-	-
6.5	15.8%	21.7%	23.1%	22.1%	19.7%	16.4%	12.6%	8.3%	3.7%	-	-	-	-	-	-	-	-	-	-	-
7.0	16.2%	21.4%	21.8%	19.7%	16.3%	12.0%	7.1%	1.9%	-	-	-	-	-	-	-	-	-	-	-	-
7.5	16.5%	20.8%	20.1%	16.9%	12.4%	7.0%	1.0%	-	-	-	-	-	-	-	-	-	-	-	-	-
8.0	16.6%	19.9%	18.0%	13.7%	8.0%	1.4%	-	-	-	-	-	-	-	-	-	-	-	-	-	-
8.5	16.6%	18.8%	15.7%	10.1%	3.1%	-	-	-	-	-	-	-	-	-	-	-	-	-	-	-
9.0	16.4%	17.5%	13.0%	6.1%	-	-	-	-	-	-	-	-	-	-	-	-	-	-	-	-
9.5	16.2%	15.9%	10.1%	1.7%	-	-	-	-	-	-	-	-	-	-	-	-	-	-	-	-
10.0	15.8%	14.1%	6.8%	-	-	-	-	-	-	-	-	-	-	-	-	-	-	-	-	-

Study 3.1 E_system CHOKED/SUBCRITICAL

E (in.) \ H (in.)	0.5	1.0	1.5	2.0	2.5	3.0	3.5	4.0	4.5	5.0	5.5	6.0	6.5	7.0	7.5	8.0	8.5	9.0	9.5	10.0
0.5	-	-	-	-	-	-	-	-	-	-	-	-	-	-	-	1.5%	1.5%	1.5%	1.5%	1.5%
1.0	-	-	-	-	-	-	-	-	-	-	-	-	-	7.5%	7.5%	7.6%	7.6%	7.6%	7.6%	7.6%
1.5	-	-	-	-	-	-	-	-	-	-	-	15.0%	15.2%	15.2%	15.2%	15.2%	15.2%	15.1%	15.0%	14.9%
2.0	-	-	-	-	-	-	-	-	21.0%	21.4%	21.7%	21.8%	21.7%	21.7%	21.5%	21.3%	21.1%	20.8%	20.5%	20.2%
2.5	-	-	-	-	-	23.4%	24.6%	25.4%	25.8%	26.0%	26.0%	25.9%	25.7%	25.3%	24.9%	24.5%	24.0%	23.4%	22.9%	22.3%
3.0	-	-	-	22.7%	25.1%	26.6%	27.6%	28.1%	28.2%	28.1%	27.8%	27.4%	26.8%	26.1%	25.4%	24.6%	23.7%	22.9%	21.9%	21.0%
3.5	-	-	21.7%	25.0%	27.0%	28.2%	28.7%	**28.8%**	28.6%	28.1%	27.4%	26.5%	25.5%	24.4%	23.3%	24.3%	22.9%	21.6%	20.1%	18.7%
4.0	-	18.7%	23.4%	26.2%	27.8%	28.5%	28.5%	28.1%	27.3%	26.3%	25.1%	23.7%	24.3%	22.6%	20.9%	19.1%	17.2%	15.3%	13.3%	11.3%
4.5	12.5%	20.0%	24.4%	26.6%	27.6%	27.6%	27.1%	26.1%	24.7%	25.1%	23.2%	21.1%	19.0%	16.7%	14.3%	11.8%	9.3%	6.6%	3.9%	1.0%
5.0	13.6%	21.0%	24.8%	26.4%	26.6%	25.9%	24.7%	25.0%	22.8%	20.4%	17.8%	15.0%	12.0%	9.0%	5.8%	2.4%	-	-	-	-
5.5	14.5%	21.6%	24.6%	25.5%	24.9%	23.5%	23.4%	20.7%	17.7%	14.5%	11.0%	7.3%	3.5%	-	-	-	-	-	-	-
6.0	15.2%	21.8%	24.1%	24.0%	22.6%	22.3%	19.1%	15.5%	11.6%	7.4%	2.8%	-	-	-	-	-	-	-	-	-
6.5	15.8%	21.7%	23.1%	22.1%	21.8%	18.2%	14.1%	9.4%	4.3%	-	-	-	-	-	-	-	-	-	-	-
7.0	16.2%	21.4%	21.8%	22.0%	18.2%	13.5%	8.2%	2.2%	-	-	-	-	-	-	-	-	-	-	-	-
7.5	16.5%	20.8%	22.5%	19.0%	14.0%	8.1%	1.3%	-	-	-	-	-	-	-	-	-	-	-	-	-
8.0	16.6%	19.9%	20.4%	15.6%	9.2%	1.7%	-	-	-	-	-	-	-	-	-	-	-	-	-	-
8.5	16.6%	18.8%	17.9%	11.7%	3.8%	-	-	-	-	-	-	-	-	-	-	-	-	-	-	-
9.0	16.4%	20.0%	15.0%	7.2%	-	-	-	-	-	-	-	-	-	-	-	-	-	-	-	-
9.5	16.2%	18.4%	11.8%	2.2%	-	-	-	-	-	-	-	-	-	-	-	-	-	-	-	-
10.0	15.8%	16.5%	8.2%	-	-	-	-	-	-	-	-	-	-	-	-	-	-	-	-	-

The difference between the two computations yield a maximum ~2% at the boundary, and the optimized rotor configuration is unchanged. Below shows the difference between the choked only and choked/subcritical analysis.

Difference between CHOKED ONLY and CHOKED/SUBCRITICAL analysis

E (in.) \ H (in.)	0.5	9.5	18.5	27.5	36.5	45.5	54.5	63.5	72.5	81.5	90.5	99.5	108.5	117.5	126.5	135.5	144.5	153.5	162.5	171.5
0.5	-	-	-	-	-	-	-	-	-	-	-	-	-	-	-	0.00%	0.00%	0.00%	0.00%	0.00%
9.5	-	-	-	-	-	-	-	-	-	-	-	-	-	0.00%	0.00%	0.00%	0.00%	0.00%	0.00%	0.00%
18.5	-	-	-	-	-	-	-	-	-	-	-	0.00%	0.00%	0.00%	0.00%	0.00%	0.00%	0.00%	0.00%	0.00%
27.5	-	-	-	-	-	-	-	-	0.00%	0.00%	0.00%	0.00%	0.00%	0.00%	0.00%	0.00%	0.00%	0.00%	0.00%	0.00%
36.5	-	-	-	-	-	0.00%	0.00%	0.00%	0.00%	0.00%	0.00%	0.00%	0.00%	0.00%	0.00%	0.00%	0.00%	0.00%	0.00%	0.00%
45.5	-	-	-	0.00%	0.00%	0.00%	0.00%	0.00%	0.00%	0.00%	0.00%	0.00%	0.00%	0.00%	0.00%	0.00%	0.00%	0.00%	0.00%	0.00%
54.5	-	-	0.00%	0.00%	0.00%	0.00%	0.00%	0.00%	0.00%	0.00%	0.00%	0.00%	0.00%	0.00%	0.00%	-2.20%	-2.14%	-2.09%	-2.04%	-1.98%
63.5	-	0.00%	0.00%	0.00%	0.00%	0.00%	0.00%	0.00%	0.00%	0.00%	0.00%	0.00%	-2.04%	-1.96%	-1.89%	-1.81%	-1.72%	-1.62%	-1.51%	-1.37%
72.5	0.00%	0.00%	0.00%	0.00%	0.00%	0.00%	0.00%	0.00%	0.00%	-2.03%	-1.92%	-1.81%	-1.70%	-1.58%	-1.45%	-1.29%	-1.10%	-0.87%	-0.58%	-0.18%
81.5	0.00%	0.00%	0.00%	0.00%	0.00%	0.00%	0.00%	-2.06%	-1.90%	-1.76%	-1.61%	-1.44%	-1.26%	-1.03%	-0.74%	-0.36%	-	-	-	-
90.5	0.00%	0.00%	0.00%	0.00%	0.00%	0.00%	-2.01%	-1.82%	-1.63%	-1.42%	-1.17%	-0.87%	-0.48%	-	-	-	-	-	-	-
99.5	0.00%	0.00%	0.00%	0.00%	0.00%	-2.02%	-1.78%	-1.53%	-1.25%	-0.89%	-0.40%	-	-	-	-	-	-	-	-	-
108.5	0.00%	0.00%	0.00%	0.00%	-2.10%	-1.81%	-1.49%	-1.11%	-0.60%	-	-	-	-	-	-	-	-	-	-	-
117.5	0.00%	0.00%	0.00%	-2.24%	-1.90%	-1.52%	-1.04%	-0.35%	-	-	-	-	-	-	-	-	-	-	-	-
126.5	0.00%	0.00%	-2.47%	-2.08%	-1.64%	-1.08%	-0.22%	-	-	-	-	-	-	-	-	-	-	-	-	-
135.5	0.00%	0.00%	-2.34%	-1.87%	-1.26%	-0.31%	-	-	-	-	-	-	-	-	-	-	-	-	-	-
144.5	0.00%	0.00%	-2.20%	-1.58%	-0.64%	-	-	-	-	-	-	-	-	-	-	-	-	-	-	-
153.5	0.00%	-2.59%	-2.02%	-1.15%	-	-	-	-	-	-	-	-	-	-	-	-	-	-	-	-
162.5	0.00%	-2.49%	-1.76%	-0.43%	-	-	-	-	-	-	-	-	-	-	-	-	-	-	-	-
171.5	0.00%	-2.37%	-1.40%	-	-	-	-	-	-	-	-	-	-	-	-	-	-	-	-	-

C ROTOR RADIAL AREA

The following demonstrates how to calculate the radial area of a PRE rotor that is affected by a pressurized cavity. It is then possible to calculate the radial force on the rotor caused by the cavity pressure. This force is needed to calculate rotor bearing life and rotor deflection. This section creates a mathematical model so that radial area can be calculated for any rotor size.

Using CAD software, the radial area (at 180 degree position with the maximum cavity volume) can be drawn and calculated. Figures below show how using set points on the rotor, and then following the contours of the adjacent rotors, the radial area appears.

Points U, V, W, X, Y, and Z are key points used to find the geometric relationships with simpler geometry in order to formulate a mathematical model. The table shows the relationships of the key points and the known design variables.

The figure below shows the shape of the radial area affected by the cavity pressure. Line segments $\overset{\frown}{VX}$, $\overset{\frown}{WU}$, and $\overset{\frown}{YW}$ follow a non-consistent curvature due to the radial area being a projection onto a contour. For this reason, a mathematical description of these segments is complex.

Connecting the key points together with straight lines instead of following rotor contours produces a hexagon. Because of its symmetry, its area is the same as the hexagon. The positive area highlighted in blue is the same value as the negative area in which their mirroring position cancel each other out.

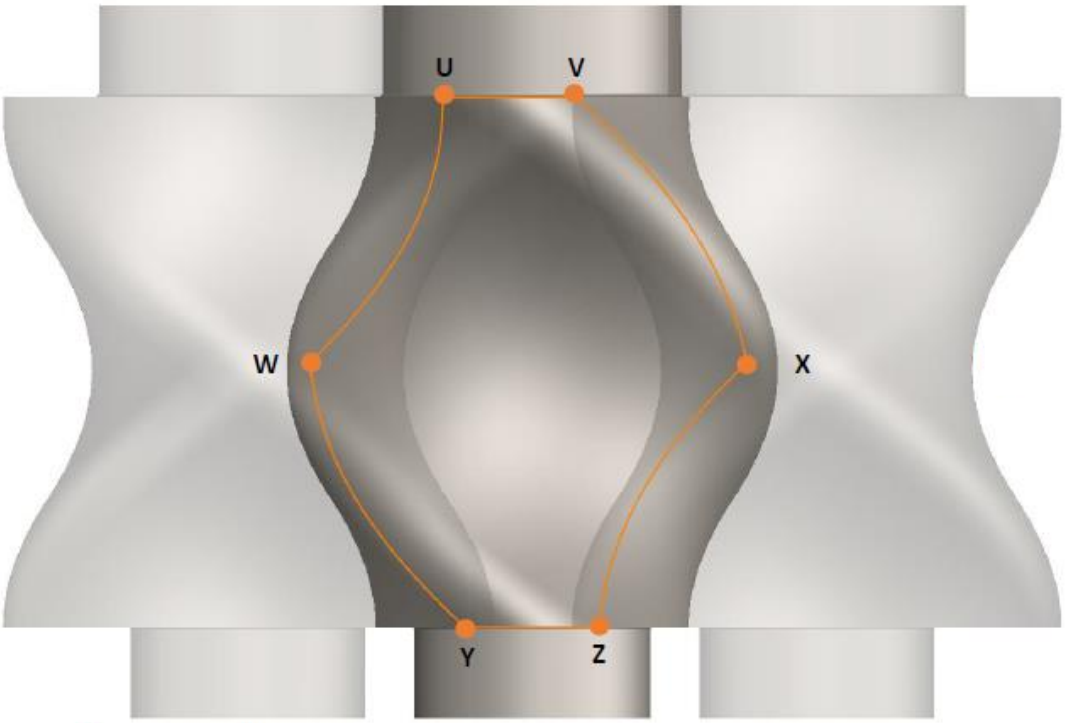

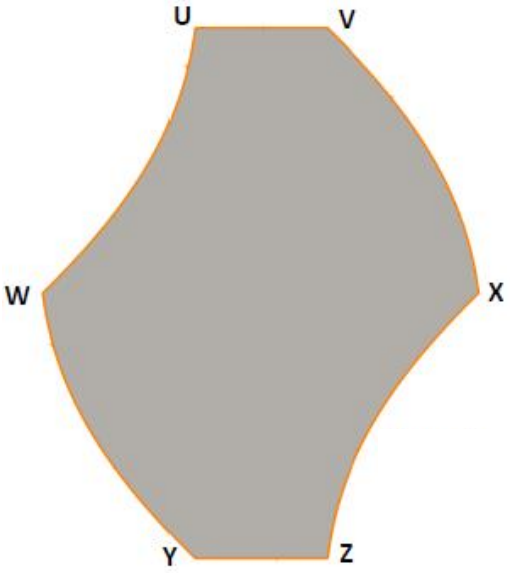

$\overline{UV}$ $\overline{ZY}$	The Junctions of R_1 and R_2 connected through R_2
$\overline{VX}$ $\overline{WU}$	The span from the head and tail of the rotor to the mid plane of the rotors. This segment follows the path of crossing from the outside R_1 Junction of the adjacent rotor to the inside R_1 junction.
$\overline{XZ}$ $\overline{YW}$	The span from the middle to the head and tail of the rotor. This segment follows the path of joining the inside R_1 junction of the adjacent rotor to head R_1 junction.

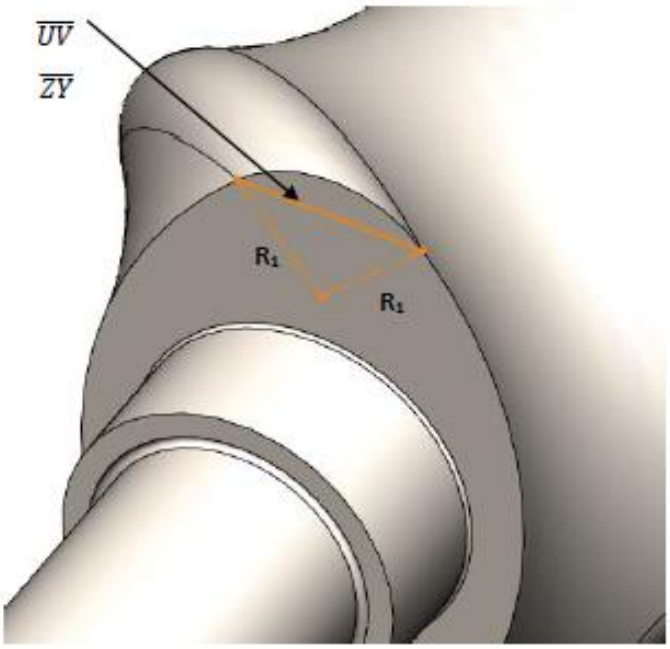
$\overline{UV}$
$\overline{ZY}$
R_1
R_1

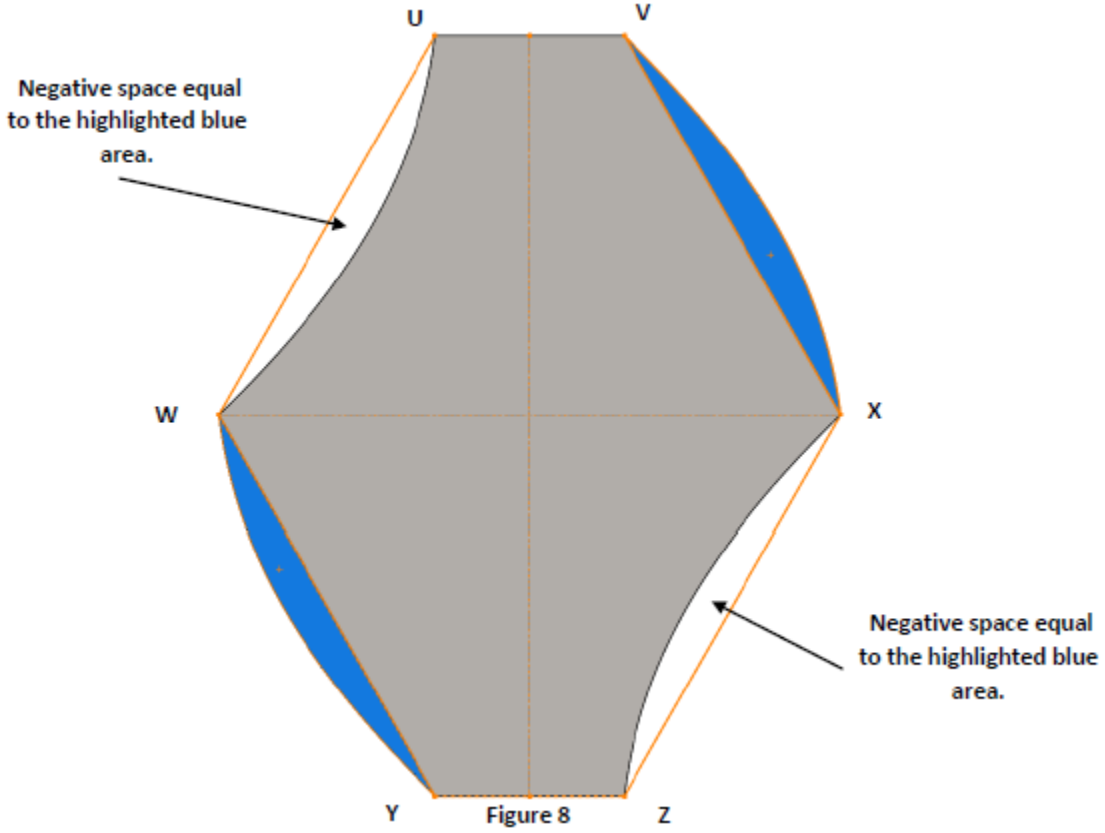
U
V
Negative space equal to the highlighted blue area.
W
X
Negative space equal to the highlighted blue area.
Y
Z

Figure 8

Calculating the area of this hexagon yields a mathematical model of the area. The area for this hexagon (derived from the area equation of 2 trapezoids) is:

$$A_{radial}=.5(J_1+J_2)$$

The figure below inserts these variables onto the hexagon created by figure 8. It is important to note that due to the inherent design of the PRE rotor, perfect symmetry can be assumed by mirroring both the horizontal and vertical axis.

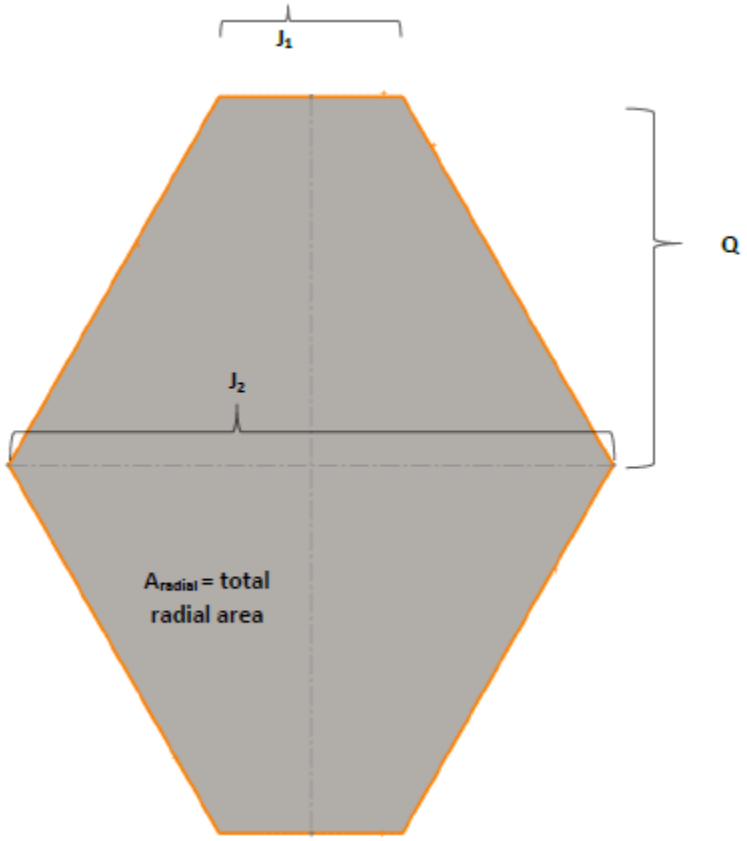

Mathematical Model:

Q is the axial distance from the head of the rotor to the mid plane.

$$Q = \frac{H}{2}$$

J_1 is equal to the hypotenuse length of the right angle triangle formed by the R_1 vectors

$$J_1 = \overline{UV} = \overline{ZY} = \sqrt{{R_1}^2 + {R_1}^2}$$

$$J_1 = R_1\sqrt{2}$$

The last variable J_2 is the distance between 2 same sided R_1 junctions measured on a cross-sectional plane. J_2 can be geometrically derived to be:

$$J_2 = 2[R_1 sin(45°) + S]$$

Finally, the total radial area can be calculated:

$$A_{radial} = \frac{H_{rtr}}{2}\{R_1\sqrt{2} + 2[R_1 sin(45°) + S]\}$$

All these variables can be described in terms of rotor height (H_{rtr}), machine radius (E), and the percentage of the machine radius that is the value of R_1 ($R_{\%}$=R_1/E). (NOTE: R_1 is a value that could replace $R_{\%}$ in terms of derivability. However, other design parameters like port and core size are optimized using $R_{\%}$ which is the more useful value). Making the substitutions for R_1 yield:

$$A_{radial} = \frac{H_{rtr}}{2}\{ER_{\%}\sqrt{2} + 2[ER_{\%} sin(45°) + S]\}$$

$$S = \sqrt{2}\left(\frac{L}{2} - R_1\right)$$

$$S = \sqrt{2}\left(\frac{L}{2} - ER_{\%}\right)$$

$$L = \frac{1}{\sqrt{2}}\left[E + R_1\left(\sqrt{2} - 1\right)\right]$$

$$L = \frac{1}{\sqrt{2}}\left[E + ER_{\%}\left(\sqrt{2} - 1\right)\right]$$

$$S = \sqrt{2}\left(\frac{\frac{1}{\sqrt{2}}\left[E + ER_{\%}\left(\sqrt{2} - 1\right)\right]}{2} - ER_{\%}\right)$$

Showing:

$$A_{radial} = \frac{H_{rtr}}{2}\left(ER_{\%}\sqrt{2} + 2\left[ER_{\%}\sin(45°) + \sqrt{2}\left(\frac{\frac{1}{\sqrt{2}}\left[E + ER_{\%}\left(\sqrt{2} - 1\right)\right]}{2} - ER_{\%}\right)\right]\right)$$

Simplified:

$$A_{radial} = H_{rtr}E\left(\frac{R_{\%}\sqrt{2}}{2} + \left[R_{\%}\sin(45°) + \left(\frac{\left[1 + R_{\%}\left(\sqrt{2} - 1\right)\right]}{2} - \sqrt{2}R_{\%}\right)\right]\right)$$

NOTE: it can be seen that the radial area is a linear relationship to rotor height as well as the machine radius.

Verification:

This section takes the radial area equation and substitutes the variables for real numbers. This will produce an area that is then compared to values given by SolidWorks CAD calculations.

$$H_{rtr} = 4''$$

$$E = 4''$$

$$R_{\%} = 17.76\% \text{ (optimized port size value)}$$

$$A_{radial} = (4\text{in.})(4\text{in.})\left(\frac{(.1776)\sqrt{2}}{2} + \left[(.1776)sin(45°) + \left(\frac{[1 + (.1776)(\sqrt{2} - 1)]}{2} - \sqrt{2}(.1776)\right)\right]\right)$$

$$A_{radial} = 16in.^2\,(.1256 + [.1256 + (.5368 - .2512)])$$

$$A_{radial} = 8.58\text{in.}^2$$

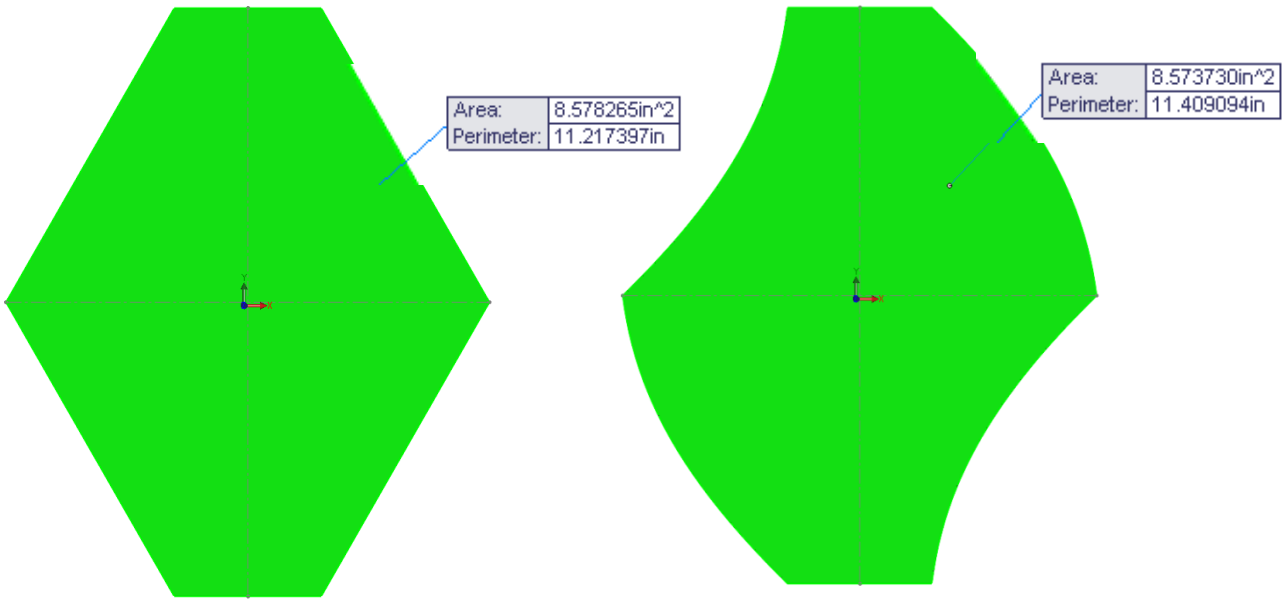

The area found in the radial equation shows to be within .01 in.^{2} of the area calculated by CAD Software in the figures above.

As previously mentioned, the rotor height and machine radius both linearly impact the area. Since the impact to the radial area (and thus radial bearing load) by the machine radius and height is equal, other design parameters should be used to choose rotor size. Some of these parameters could be cavity volume, application, or axial area where machine size increase axial area and rotor height does not.

The right hand side of the radial area equation pertains to the radius R_1. This cluster of terms can be renamed as the R_1 coefficient. Since one of the most important parameters when designing the R_1 is ports size (to allow for maximum flow), the $R_{\%}$ is optimized to allow for the largest ports. This creates a static $R_{\%}$ value that is the same for all size of rotors (See Manifold Design, June 2013). This is why the $R_{\%}$ is used in rotor equations instead of R_1.

$$A_{radial} = H_{rtr}E\underbrace{\left\{\frac{R_{\%}\sqrt{2}}{2} + \left[R_{\%}sin(45°) + \left(\frac{\left[1 + R_{\%}\left(\sqrt{2} - 1\right)\right]}{2} - \sqrt{2}R_{\%}\right)\right]\right\}}$$

R_1 Coefficient

The $R_{\%}$ that produces the largest ports has been calculated to be 17.76%. If it is decided to maximize port size and use this optimized $R_{\%}$, then the R_1 coefficient can be reduced to:

$$A_{radial} = H_{rtr}E\underbrace{(.5368)}$$

R_1 Coefficient (optimized port design)

Using a static $R_{\%}$ creates a very simple equation in calculating radial area.

If a different $R_{\%}$ is to be used, the graph shows that ranging from an $R_{\%}$ = 1-50%, the coefficient will only range from .5 to .6. The changes caused by using a different $R_{\%}$ are small in nature when compared to optimizing the $R_{\%}$ to other important parameters.

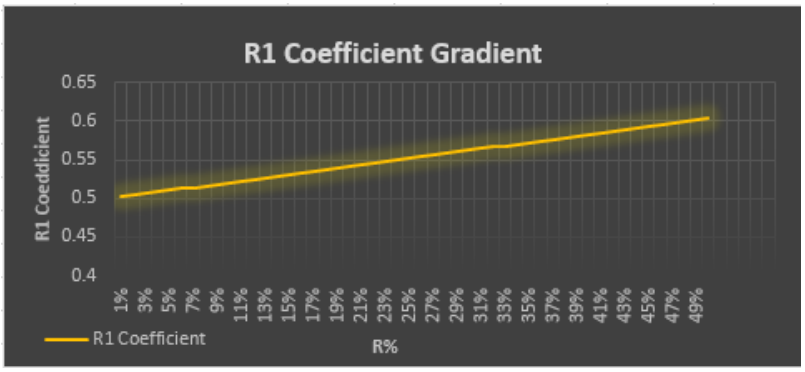

To illustrate the loading area during operation, see the figures below of a stress analysis performed on a 4 inch by inch rotor with a .7 inch R1 radius. The load applied is 1440 PSI and the rotor material of 4340 normalized steel. Max stress calculated = 43,000 psi:

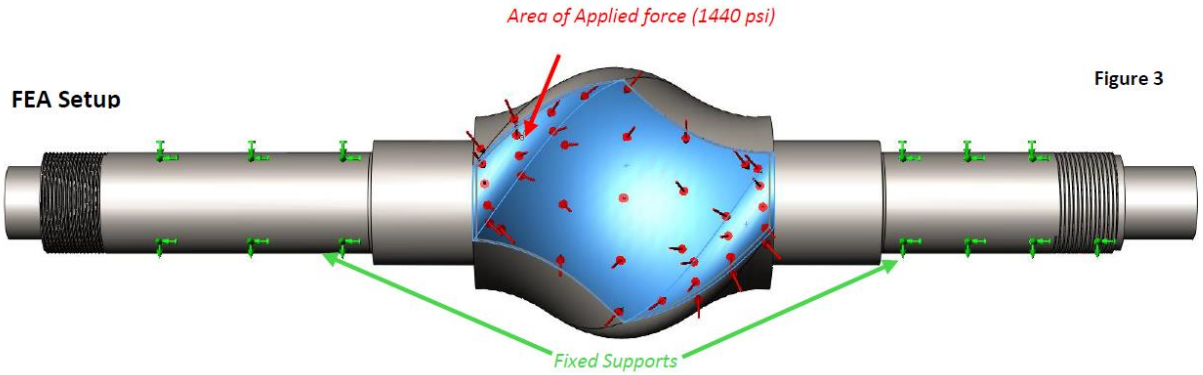

Figure 3

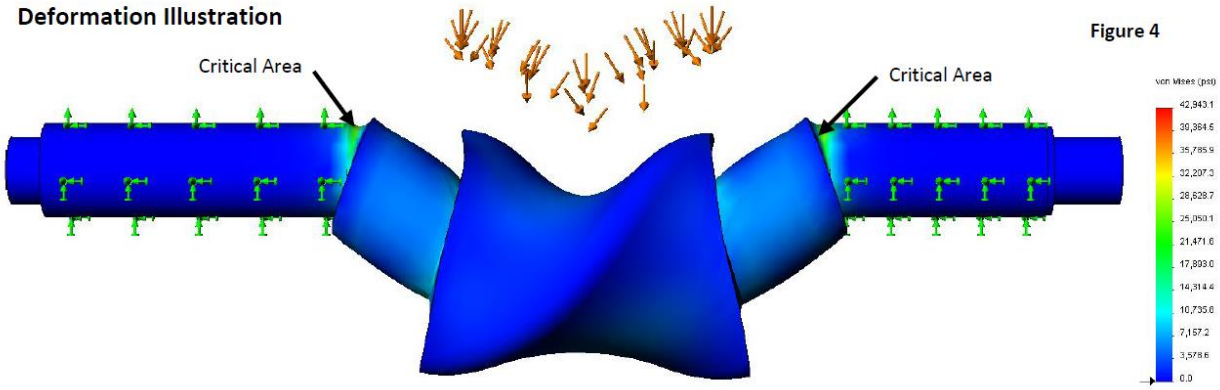

Figure 4

The follow illustration is a study of displacement of the rotors. This will affect leakage by increasing the rotor gap area during high loads.

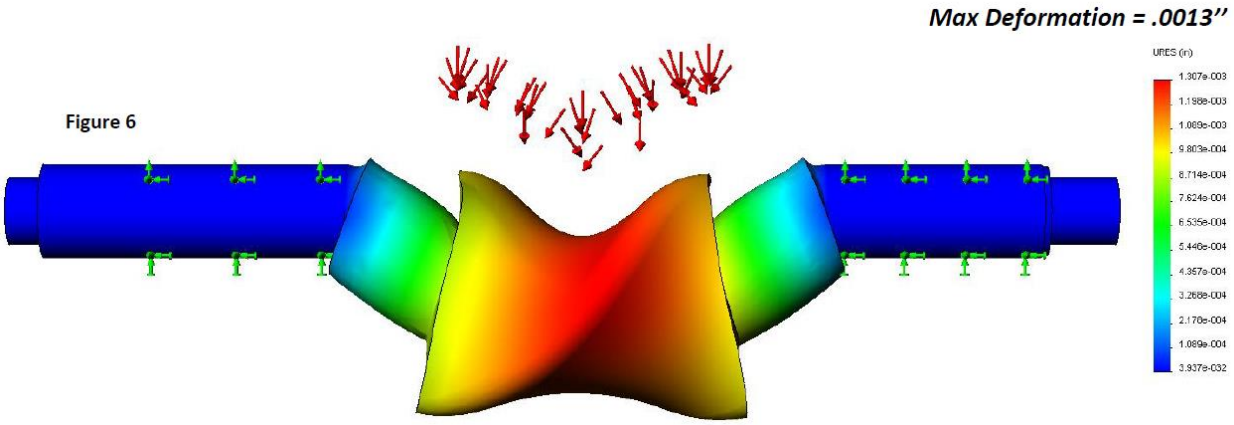

Figure 6

D MOLLIER CHART

Below is a Mollier chart which shows the relationship between an isenthalpic process (JT valve), isentropic process (no losses), and an expander operation. The values shown are of a possible configuration and possible expander efficiency.

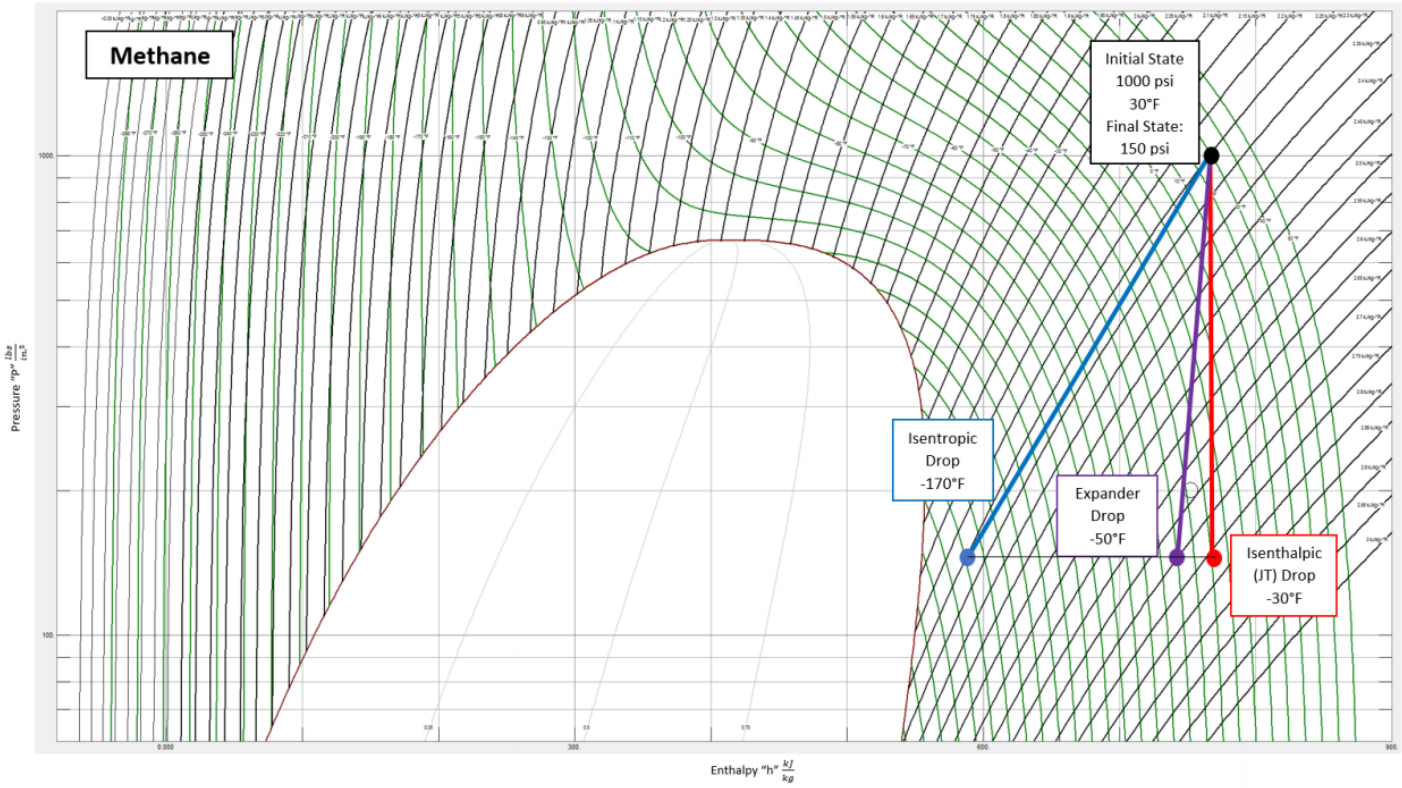

E PACKAGE DESIGN – NGL SKID (ENERGY RECOVERY)

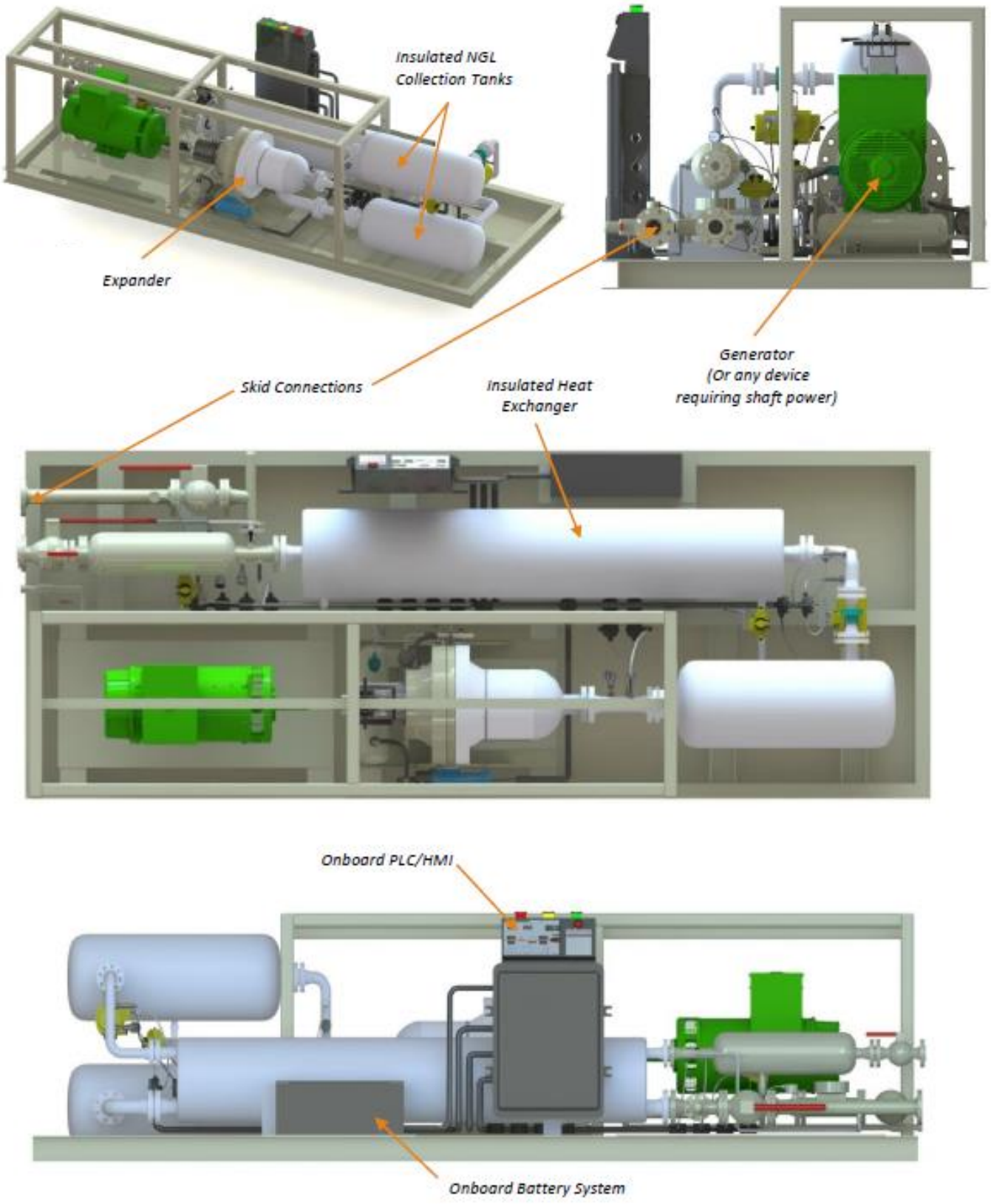

F PACKAGE DESIGN – POWER GENERATION SKID (TARGET POWER)

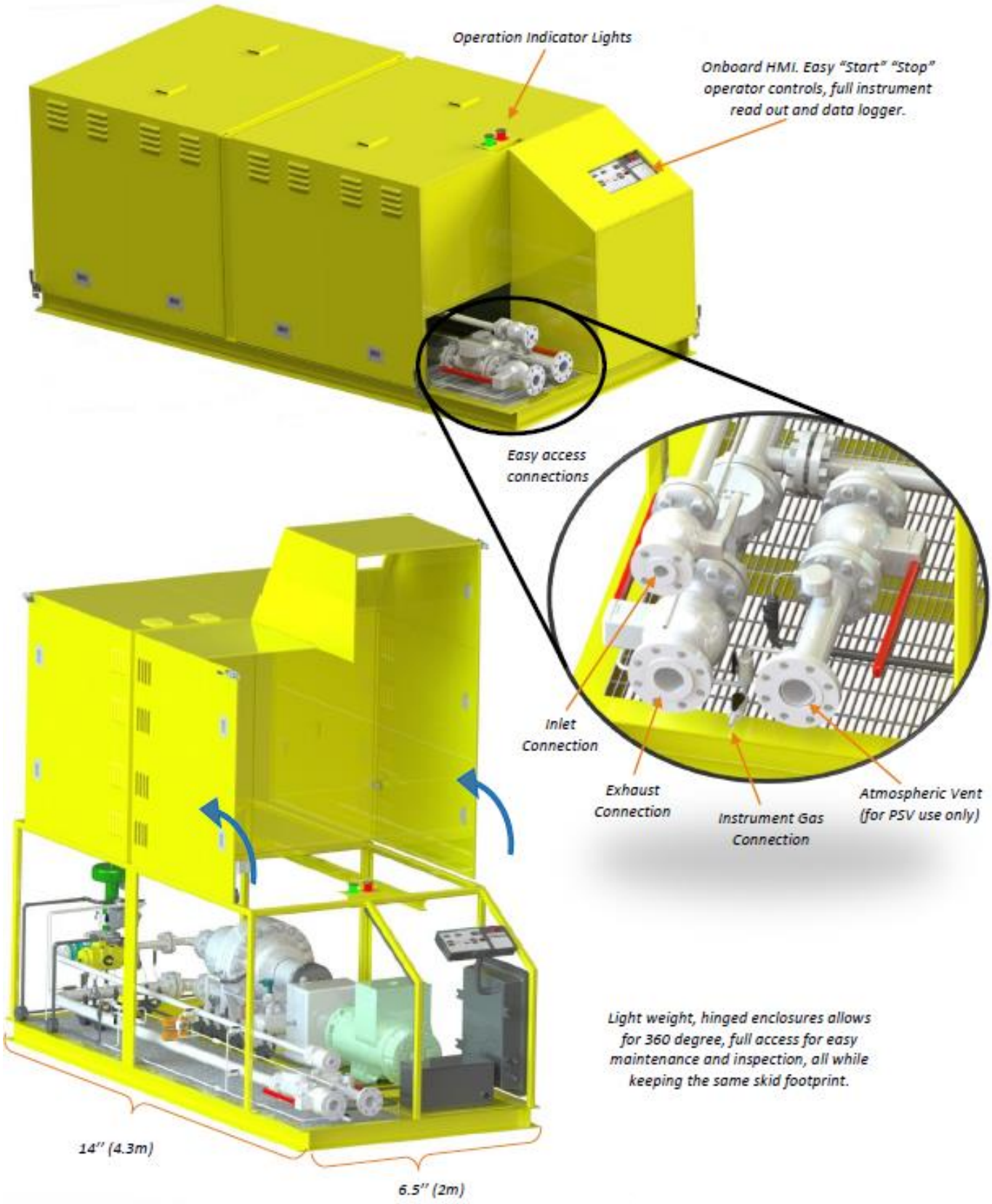

Employs 17 different sensors to monitor and regulate expander operation. Several redundancies are in place including automatic isolation valves, fail close flow control valve, and a pressure safety valve.

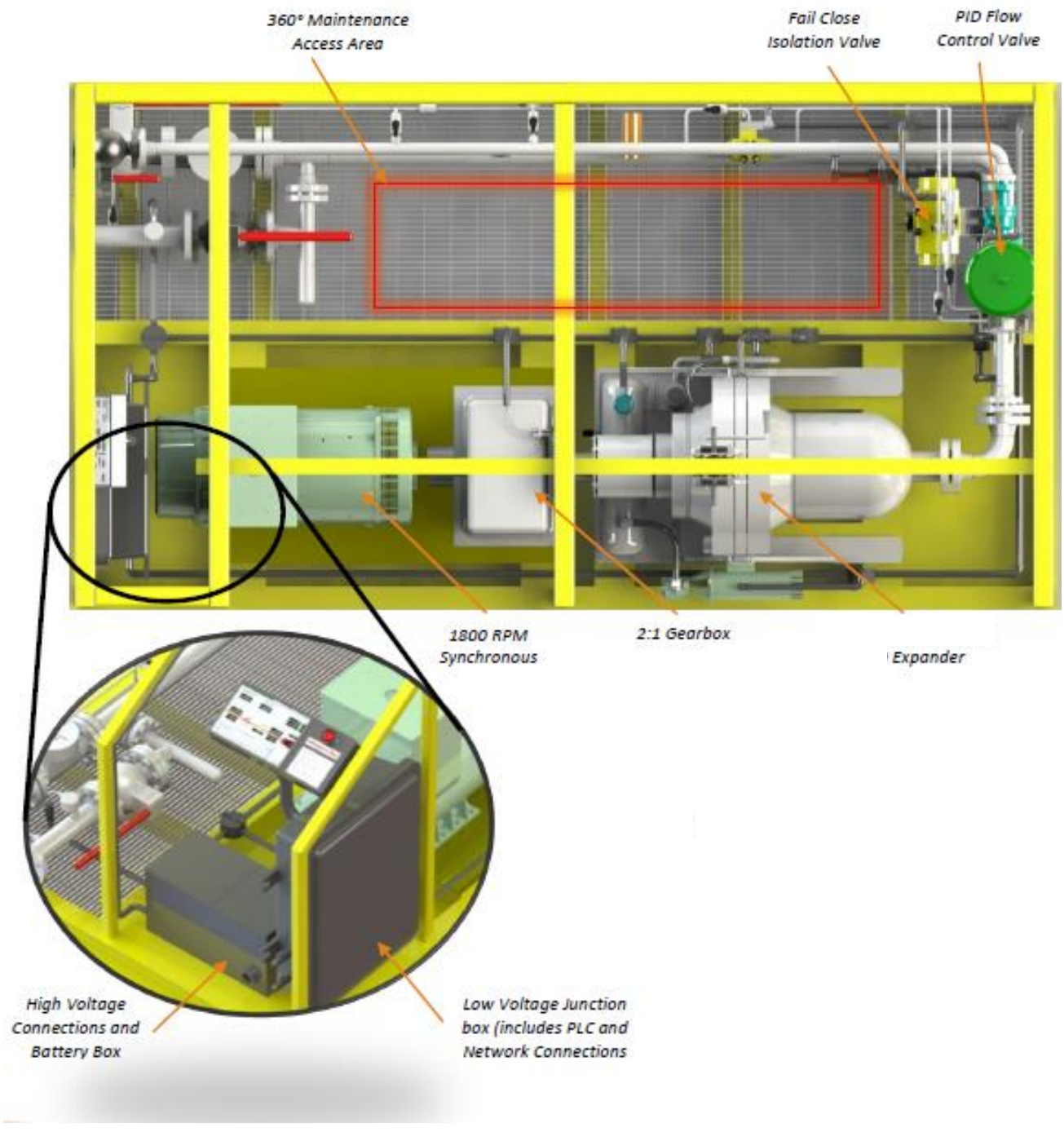

G GAP HELIX LENGTH DERIVATION

The base derivation of the length of a helix with a varying radius from the center axis is shown as with respect to position angle theta:

$$L_{helix}(\theta) = \sqrt{\left[R'_{helix}(\theta)\right]^2 + \left[R_{helix}(\theta)\right]^2 + H^2}$$

Starting with the vertex form of a parabola as the change in helix radius varies parabolically:

$$Y(x) = a(x-h)^2 + k$$

The variables are obtained by analyzing the rotor cross section geometry:

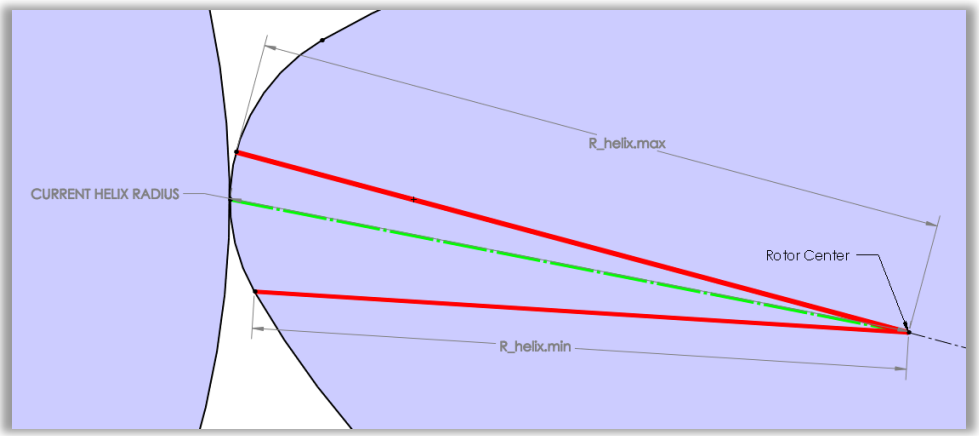

And the helix variation:

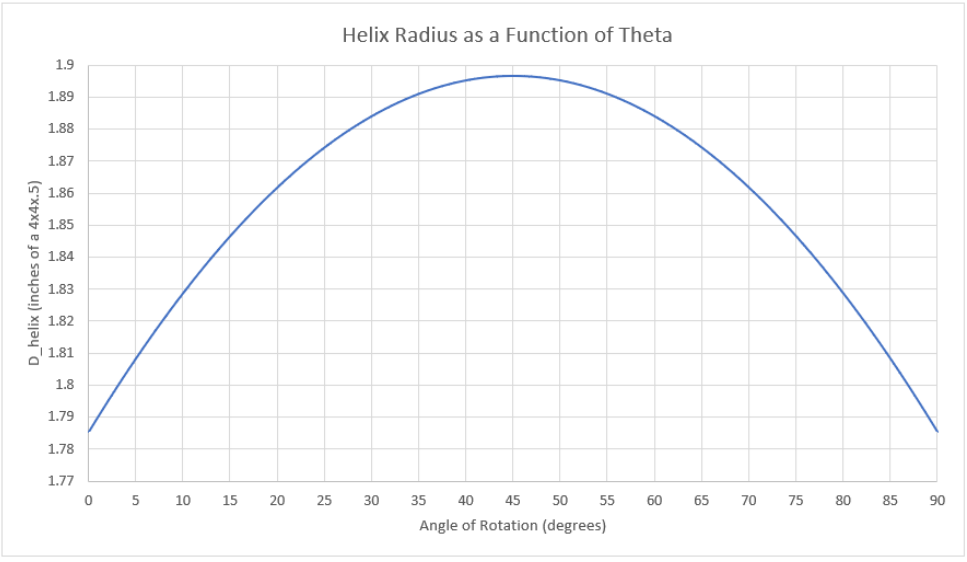

$$a = -\frac{\frac{D}{2} - R_{helix.min}}{{\theta_{max}}^2} \qquad h = \theta_{max} \qquad k = \frac{D}{2} - R_{helix.min}$$

Making:

$$R_{helix}(\theta) = -\frac{\frac{D}{2} - R_{helix.min}}{{\theta_{max}}^2}(\theta - \theta_{max})^2 + \left(\frac{D}{2} - R_{helix.min}\right) + R_{helix.min}$$

Where the end term $R_{helix.min}$ is the parabolic starting and ending position of R_{helix}.

Reduced:

$$R_{helix}(\theta) = -\frac{\frac{D}{2} - R_{helix.min}}{{\theta_{max}}^2}(\theta - \theta_{max})^2 + \frac{D}{2}$$

Expanded:

$$R_{helix}(\theta) = -\frac{\frac{D}{2} - R_{helix.min}}{{\theta_{max}}^2}\left(\theta^2 - 2\theta_{max}\theta + {\theta_{max}}^2\right) + \frac{D}{2}$$

The derivative of R_{helix}:

$${R_{helix}}'(\theta) = -2\theta\frac{\frac{D}{2} - R_{helix.min}}{{\theta_{max}}^2} + 2\theta_{max}\frac{\frac{D}{2} - R_{helix.min}}{{\theta_{max}}^2}$$

$${R_{helix}}'(\theta) = \frac{\theta(2R_{helix.min} - D)}{{\theta_{max}}^2} + \frac{D - 2R_{helix.min}}{\theta_{max}}$$

Substituting back into the helix length equation and including H in terms of theta:

$$h = H\frac{\theta}{\pi}$$

$$L_{helix}(\theta)$$

$$= \sqrt{\left[\frac{\theta(2R_{helix.min} - D)}{{\theta_{max}}^2} + \frac{D - 2R_{helix.min}}{\theta_{max}}\right]^2 + \left[-\frac{\frac{D}{2} - R_{helix.min}}{{\theta_{max}}^2}(\theta - \theta_{max})^2 + \frac{D}{2}\right]^2 + \left(H\frac{\theta}{\pi}\right)^2}$$

$$L_{helix}(\theta)$$

$$= \sqrt{\left(\frac{(2R_{helix.min} - D)}{\theta_{max}}\right)^2 \left[\frac{\theta}{\theta_{max}} + 1\right]^2 + \left[-\frac{\frac{D}{2} - R_{helix.min}}{{\theta_{max}}^2}(\theta - \theta_{max})^2 + \frac{D}{2}\right]^2 + \left(H\frac{\theta}{\pi}\right)^2}$$

Substituting for primary variables:

$$R_{helix.min} = \sqrt{\left(\frac{J_1}{2}\right)^2 + \left(\frac{J_2}{2}\right)^2} = \sqrt{\left(\frac{R_1\sqrt{2}}{2}\right)^2 + \left(\frac{E - R_1}{2}\right)^2}$$

$$D = E + R_1\left(1 - \sqrt{2}\right)$$

$$L_{helix}(\theta)$$

$$= \sqrt{\left(\frac{\left(2\sqrt{\left(\frac{R_1\sqrt{2}}{2}\right)^2 + \left(\frac{E - R_1}{2}\right)^2} - \left(E + R_1\left(1 - \sqrt{2}\right)\right)\right)}{\theta_{max}}\right)^2 \left(\frac{\theta}{\theta_{max}} + 1\right)^2 + \left[-\frac{\frac{E + R_1\left(1 - \sqrt{2}\right)}{2} - \sqrt{\left(\frac{R_1\sqrt{2}}{2}\right)^2 + \left(\frac{E - R_1}{2}\right)^2}}{{\theta_{max}}^2}(\theta - \theta_{max})^2 + \frac{D}{2}\right]^2 + \left(H\frac{\theta}{\pi}\right)^2}$$

In terms of time:

$$\theta(t) = 2\pi ft$$

$$L_{helix}(t)$$

$$= \sqrt{\left(\frac{\left(2\sqrt{\left(\frac{R_1\sqrt{2}}{2}\right)^2 + \left(\frac{E - R_1}{2}\right)^2} - \left(E + R_1\left(1 - \sqrt{2}\right)\right)\right)}{\theta_{max}}\right)^2 \left(\frac{2\pi ft}{\theta_{max}} + 1\right)^2 + \left[-\frac{\frac{E + R_1\left(1 - \sqrt{2}\right)}{2} - \sqrt{\left(\frac{R_1\sqrt{2}}{2}\right)^2 + \left(\frac{E - R_1}{2}\right)^2}}{{\theta_{max}}^2}(2\pi ft - \theta_{max})^2 + \frac{D}{2}\right]^2 + \left(H\frac{2\pi ft}{\pi}\right)^2}$$

$L_{helix}(t)$

$$= \sqrt{\left(\frac{\left(2\sqrt{\left(\frac{R_1\sqrt{2}}{2}\right)^2+\left(\frac{E-R_1}{2}\right)^2}-\left(E+R_1(1-\sqrt{2})\right)\right)}{\theta_{max}}\right)^2\left(\frac{2\pi f t}{\theta_{max}}+1\right)+\left[-\frac{\frac{E+R_1(1-\sqrt{2})}{2}-\sqrt{\left(\frac{R_1\sqrt{2}}{2}\right)^2+\left(\frac{E-R_1}{2}\right)^2}}{\theta_{max}{}^2}(2\pi f t-\theta_{max})^2+\frac{D}{2}\right]^2+(2Hft)^2}$$

$$c_1 = \left(\frac{\left(2\sqrt{\left(\frac{R_1\sqrt{2}}{2}\right)^2+\left(\frac{E-R_1}{2}\right)^2}-\left(E+R_1(1-\sqrt{2})\right)\right)}{\theta_{max}}\right)^2$$

$$c_2 = \frac{\frac{E+R_1(1-\sqrt{2})}{2}-\sqrt{\left(\frac{R_1\sqrt{2}}{2}\right)^2+\left(\frac{E-R_1}{2}\right)^2}}{\theta_{max}{}^2}$$

$$c_3 = \frac{2\pi f}{\theta_{max}}$$

$$c_4 = 2\pi f$$

$$c_5 = \frac{D}{2}$$

$$c_6 = 2Hf$$

$$L_{helix}(t) = \sqrt{c_1(c_3 t+1)^2+[-c_2(c_4 t-\theta_{max})^2+c_5]^2+c_6{}^2 t^2}$$

$$L_{helix}(t) = \sqrt{c_1 c_3{}^2 t^2+2c_1c_3 t+1+\left(-c_2c_4{}^2 t^2+2c_2c_4\theta_{max} t-c_2\theta_{max}{}^2+c_5\right)^2+c_6{}^2 t^2}$$

$L_{helix}(t)$ can be used to derive the gap area equation where the integrand is integrated in terms of time t.

Since the above equation for the helix length has certain complexities integrating into the rotor gap area equation and since it is shown that the radial variance of the helix is parabolic, an average helix diameter can be used. This is not a direct integration as the above helix length derivation, but is more accurate then assuming rotor diameter D as the helix diameter. This diameter requires the calculation of a minimum, maximum, and average radius from the rotor center to the dynamic location of the gap. The minimum radius $R_{helix.min}$ is measured from the rotor center to the R_1/R_2 junction and is calculated by:

$$R_{helix.min} = \sqrt{\left(\frac{J_1}{2}\right)^2 + \left(\frac{J_2}{2}\right)^2} = \sqrt{\left(\frac{R_1\sqrt{2}}{2}\right)^2 + \left(\frac{E - R_1}{2}\right)^2}.$$

The maximum helical radius $R_{helix.max}$ is simply the half the rotor diameter D:

$$R_{helix.max} = \frac{D}{2} = \frac{E + R_1\left(1 - \sqrt{2}\right)}{2}.$$

The average helical radius $R_{helix.avg}$ is the sum of two components. The first component is the minimum helix radius $R_{helix.min}$. The second component is the average distance the rotor gap radially travels as presented previously as gap behavior two. This gap's radial travel is parabolic in nature as confirmed by CAD, making the average distance traveled two thirds of the maximum radially traveled distance. In other words, the average helical radius $R_{helix.avg}$ is calculated by:

$$R_{helix.avg} = R_{helix.min} + \frac{2}{3}\left(R_{helix.max} - R_{helix.min}\right)$$

$$R_{helix.avg} = \sqrt{\left(\frac{R_1\sqrt{2}}{2}\right)^2 + \left(\frac{E - R_1}{2}\right)^2} + \frac{2}{3}\left(\frac{E + R_1\left(1 - \sqrt{2}\right)}{2} - \sqrt{\left(\frac{R_1\sqrt{2}}{2}\right)^2 + \left(\frac{E - R_1}{2}\right)^2}\right)$$

$$\mathrm{R}_{\mathrm{helix.avg}} = \frac{\sqrt{\frac{\mathrm{R}_1{}^2}{2} + \frac{(E - \mathrm{R}_1)^2}{4}} + E + \mathrm{R}_1\left(1 - \sqrt{2}\right)}{3}$$

The basic equation for the length of a helix $\mathrm{L}_{\mathrm{helix}}$ is used to evaluate the rotor gap area. This helix equation will use two times the average helix radius $\mathrm{R}_{\mathrm{helix.avg}}$ as the average helix diameter $D_{\mathrm{helix.avg}}$ (note that the notation $D_{\mathrm{helix.avg}}$ will be used in the derivation to make the derivations manageable):

$$D_{\mathrm{helix.avg}} = \frac{\sqrt{\frac{\mathrm{R}_1{}^2}{2} + \frac{(E - \mathrm{R}_1)^2}{4}} + E + \mathrm{R}_1\left(1 - \sqrt{2}\right)}{1.5}$$

$$\mathrm{L}_{\mathrm{helix}} = \sqrt{\left[\pi \mathrm{T}_{\mathrm{helix}}\left(D_{\mathrm{helix.avg}}\right)\right]^2 + \mathrm{H}^2} \quad .$$

Where:

$\mathrm{L}_{\mathrm{helix}}$ = total gap coil length

$\mathrm{T}_{\mathrm{helix}}$ = number of twists contained within rotor height H (.5 for the PRE)